THE UNIVERSITY OF HULL

The Synthesis of cationic porphyrins for use in Photodynamic Antimicrobial ChemoTherapy (PACT).

Being a Thesis submitted for the Degree of Doctor of Philosophy in the University of HULL

By

Claire Elizabeth Hall, MChem

April 2008.

Acknowledgements

I would firstly like to thank both Dr. Ross. W. Boyle and Dr. Tim. Paget for their supervision and encouragement during my PhD.

I would also like to thank the following people:

Cath Wadsworth, Dr Lesley Galbraith and Huguette Savoie for their help and support with the bacterial assays.

Dr Robert Hudson for donating compounds **97**, **98** and **99** for use in PACT screening.

Dr. Rob. Lewis for his help with the computational chemistry.

Dr Krysia Mazik for her help with the statistics and use of SPSS.

The Yorkshire Laser Centre and the Laser Trust Fund (Moghissi) charity for the funding they have given me over the last three years.

My lab colleagues both past and present and my friends and family for keeping me sane during the difficult times when nothing seemed to be working.

Abstract

Photodynamic therapy (PDT) has been widely used in recent years for the treatment of cancers. However the growing problem of drug resistance in bacteria has led to PDT being used to treat bacterial infections in a new type of therapy called Photodynamic Antimicrobial ChemoTherapy (PACT). In PACT a drug is administered and allowed to accumulate within the target molecules prior to irradiation with red light. This produces singlet oxygen and other reactive oxygen species which target multiple areas within the cell leading to a mode of therapy that is less susceptible to the emergence of bacterial resistance.

The development of an appropriate assay for use in PACT was undertaken, looking at various parameters which might affect cell kill. These parameters included incubation time, light dose (varying fluence and fractionating), drug concentration and methods of determining cell viability. The most important factor in achieving cell kill via a PDT effect was found to be the length of time with which the drug is allowed to incubate with the cells prior to irradiation. The optimum incubation time of bacterial cells with drug prior to irradiation was found to be 5 minutes.

Cationic photosensitizers are used in PACT due to their ability to interact with the negatively charged surface of the bacterial cell wall. Several different synthesis were attempted to produce multiply cationic porphyrins.

Initially the synthesis of four tetra cationic porphyrins bearing highly fluorinated side chains was attempted. Namely these were 5, 10, 15, 20-tetra-(4-*N*-(1H, 1H, 2H, 2H-perfluorohexyl)-pyridyl) porphyrin **(66)**, 5, 10, 15, 20-tetra-(4-*N*- (1H, 1H, 2H, 2H-perfluorododecyl)-pyridyl) porphyrin **(67)**, 5, 10, 15, 20-tetra-(4-(*N*-(1H, 1H, 2H, 2H-perfluorohexyl)-dimethylanilinium) porphyrin **(68)** and 5, 10, 15, 20-tetra-(4-(*N*-1H, 1H, 2H, 2H-perfluorododecyl)-dimethylanilinium) porphyrin **(69)**. However it was found that the alkyl iodides would not couple to the porphyrins, even under severe conditions. The

purification of reactions which had partially reacted, were found to be problematic due to the porphyrins sticking to silica.

The syntheses of several different octa cationic and dendritic porphyrins were attempted with varying degrees of success.

Amines at physiological pH are cationic and therefore it was decided to attempt the synthesis of 5, 10, 15, 20-tetra-(4-(aminomethyl)phenyl) porphyrin (**70**). Several different methods were used in the attempted synthesis, however all proved problematic.

It was decided to utilise parallel synthesis to produce a number of cationic photosensitizers. These were successfully synthesised and contain phosphorus, nitrogen or arsenic cations. The R groups surrounding the cations vary in 2 ways; either the aliphatic chain length varies from methyl to butyl or the aromatic vs. aliphatic character differs.

In total 11 compounds were synthesised and a further 3 were donated by Dr R Hudson to be screened *in-vitro* against both Gram negative and Gram positive bacteria in order to determine whether any structure activity relationships could be established.

The results of the bacterial assays for the compounds with phosphorus cations, showed that, with the exception of 5, 10, 15, 20-tetra-(4 ((trimethylphosphoniumyl)methyl) phenyl) porphyrin tetrabromide, PDT activity decreased as chain length increased. This was also found to be true in the case of the compounds with nitrogen cations, with the exception of both 5, 10, 15, 20-tetra-(4-((trimethylamino)methyl)phenyl)porphyrin tetrabromide (**92**) and 5, 10, 15, 20-tetra-(4-((triethylamino)methyl)phenyl)porphyrin tetrabromide (**82**), which gave no cell kill.

In general it was found that compounds with aromatic groups surrounding the cations have less activity than those with aliphatic groups. Differential activity was seen using the compounds synthesised and some idea of optimum structure derived, with 5, 10, 15,

20-tetra-(4-((tripropylphosphoniumyl)methyl)phenyl) porphyrin tetrabromide (**90**) and 5, 10, 15, 20-tetra-(4-((tripropylamino)methyl)phenyl) porphyrin tetrabromide (**93**) being the most active over a broad spectrum. Interestingly a difference was noted between the activities of *S. Aureus* and MRSA, possibly due to their different surface structures. Despite the limited range of compounds made, the results in this thesis show that porphyrins can be synthesised and optimized for use in PACT.

Abbreviations.

ABC	Adenosine triphosphate binding cassette
ANOVA	Analysis of Variance
ATP	Adenosine triphosphate
BMPP	5,10,15,20-Tetra (4-(bromomethyl)phenyl) porphyrin
BPD	Benzoporphyrin derivative
CCD	Charge-coupled device
CFU	Colony forming unit
CMBA	4-Chloromethylbenzaldehyde
CMPP	5,10,15,20-tetra (4-(chloromethyl) phenyl) porphyrin
DAP	Diaminopimelic acid
DCC	*N,N'*-Dicyclohexylcarbodiimide
DCM	Dichloromethane
DEAD	Diethylazodicarboxylate
DMF	*N,N*-Dimethylformamide
DNA	Deoxyribonucleic acid
EDTA	Ethylenediaminetetraacetic acid
ES	Electrospray ionisation
FDA	Food and Drug Administration
GAMESS	General Atomic and Molecular Electronic Structure System
GI	Gastro intestinal
GNB	Gram negative bacteria
GPB	Gram positive bacteria
HBTU	2-(1H-benzotriazol-1-yl)-1,1,3,3-tetramethyluronium hexafluorophosphate
HOBt	*N*-hydroxybenzotriazole
HpD	Haematoporphyrin Derivative
HPLC	High pressure liquid chromatography
HVD	Hydroxyethylvinyldeuteroporpyhrin
KDa	Kilodaltons

LB	Luria-Bertani
LD_{50}	Lethal dose for 50% of the population
LD_{90}	Lethal dose for 90% of the population
LED	Light emitting diode
LPS	Lipopolysaccharide
MALDI-TOF MS	Matrix-assisted laser desorption ionization-time of flight mass spectrometry
MATE	Multidrug and toxic compound extrusion family
MFS	Major facilitator superfamily
MIC	Minimum inhibitory concentration
MSSA	Methicillin-sensitive *Staphylococcus aureus*
MRSA	Methicillin-resistant *Staphylococcus aureus*
MTS	(3-(4,5-Dimethylthiazol-2-yl)-5-(3-carboxymethoxyphenyl)-2-(4-sulfophenyl)-2H-tetrazolium salt
MW	Molecular weight
NBS	*N*-bromosuccinimide
NMR	Nuclear magnetic resonance
PABA	*p*-Aminobenzoic acid
PACT	Photodynamic antimicrobial chemotherapy
PBP	Penicillin-binding protein
PBS	Phosphate-buffered saline
PDI	Photodynamic inactivation
PDT	Photodynamic therapy
PL	Poly-lysine
PMBN	Polymyxin B nonapeptide
PMS	Phenazine methosulfate
Pp	Protoporphyrin
PS	Photosensitizer
QSAR	Quantitative structure activity relationship
RBC	Red blood cell
RNA	Ribonucleic acid

RND	Resistance-nodulation-cell division family
SAR	Stucture activity relationship
SMR	Small multidrug resistance family
THF	Tetrahydrofuran
TLC	Thin layer chromatography
TMPyP	5,10,15,20-tetra-(4-N-methylpyridyl)porphyrin
UV	Ultra violet
VRE	Vancomycin-resistant *Enterococci*
VRSA	Vancomycin-resistant *Staphylococcus aureus*
VSV	Vesicular stomatis virus
χ^2	Chi-squared.

Contents

Chapter 1. Introduction 1

1.1. Aim 1

1.2. Bacteria 1

1.2.1. The problem of bacterial infection. 1

1.2.2. Classification. 2

1.2.3. Structure. 6

1.2.3.1. Capsule. 6

1.2.3.2. Cell Wall. 7

1.2.3.3. Outer membrane. 11

1.2.3.4. Bacterial physiology. 12

1.3. Antibacterial agents. 12

1.3.1. Introduction to antibacterial agents. 12

1.3.2. β-lactams. 13

1.3.3. Glycopeptides. 14

1.3.4. Sulfonamides. 15

1.3.5. Quinolones. 16

1.3.6. Tetracyclines. 16

1.4. Bacterial resistance to antibiotics. 17

1.4.1. Clinical importance. 17

1.4.2. Emerging resistance. 18

1.4.3. Mechanisms of resistance. 19

1.4.3.1. Enzymatic inactivation of the antibiotic. 19

1.4.3.2. Modification of the target (becoming insensitive). 21

1.4.3.3. Impermeability. 21

1.4.3.4. Efflux mechanism to pump out the antibiotic. 22

1.4.3.5. Enhanced production of the target to compensate. 24

1.4.3.6. By-pass of target using alternative insensitive route. 24

1.4.4. Self-promoted uptake. 24

1.4.5. Programmed cell death. 25

1.5. Porphyrins. **26**
1.5.1. Structure. 26
1.5.2. Excited states of porphyrins. 27
1.5.3. Synthesis of porphyrins. 28
1.6. Photodynamic therapy. **30**
1.7. Photodynamic Antimicrobial ChemoTherapy (PACT). **35**
1.7.1. Introduction to PACT. 35
1.7.2. Photosensitizers used in PACT. 37
1.7.2.1. Acridine. 37
1.7.2.2. Azines. 38
1.7.2.3. Porphyrins and phthalocyanines. 39
1.7.2.4. Poly-lysine conjugates. 49

Chapter 2. Photosensitizer synthesis. Tetracationic compounds. **54**
2.1. General synthetic routes to catonic porphyrins. **54**
2.1.1. Quaternisation of 5, 10, 15, 20-tetra-(4-*N*-methylpyridyl) porphyrin and 5, 10, 15, 20-tetra-(4-*N, N, N*-trimethyl-anilinium) porphyrin 54
2.1.2. Quaternisation of **22** using perfluorocarbon chains. 56
2.1.3. Attempted synthesis of 5, 10, 15, 20-tetra-(4-(aminomethyl) phenyl) porphyrin (**70**). 59
2.1.4. Alternative route to tetra-cationic porphyrins 61
2.2. Synthetic route used. **63**
2.3. Parallel synthesis vs step-wise synthesis. **66**
2.4. Library of compounds made. **67**

Chapter 3. Porphyrins with greater than 4 cationic charges. **70**
3.1. Octa-cationic porphyrins. **70**
3.1.1. Attempted synthesis of octa-cationic porphyrins 70
3.1.2. Retrosynthesis of an octa-cationic porphyrin 73
3.1.3. Octa-cationic compounds - synthesis attempted 77

3.2. Dendritic porphyrins. **78**
3.2.1. Dendrimers. 78
3.2.2. Porphyrin dendrimers 83
3.2.2.1. Target porphyrin dendrimers 83
3.2.2.2. Synthesis of porphyrin dendrimer **114**. 85
3.2.2.3. Synthesis of porphyrin dendrimer **135** 92
3.2.2.4. Synthesis of porphyrin dendrimer **143** 96

Chapter 4. Bacterial assay development. **99**
4.1. Bacterial assay **99**
4.1.1. Compound used for assay development. 99
4.1.2. Bacterial strains used. 99
4.1.3. Drug concentrations. 99
4.1.4. Overnight Culture preparation 100
4.1.5. Initial protocol followed. 100
4.1.6. Initial results. 100
4.2. Protocol optimisation. **102**
4.2.1. Higher drug concentrations. 102
4.2.2. Bacterial viability assay. 102
4.2.3. Possible problems with reading absorbance. 104
4.2.4. Varying fluence. 104
4.2.5. Alternative method for determining cell viability 106
4.2.6. Determining bacteriostatic vs. bacteriocidal activity. 106
4.2.7. Effects of washing cells. 107
4.2.8. Fractionating light dose. 107
4.2.9. Importance of incubation time. 109
4.3. Dose response curves. **110**
4.3.1. MRSA. 110
4.3.2. *E.coli* 111

Chapter 5. PACT results and discussion. **113**
5.1. Biological methods. **113**
5.1.1. General 113
5.1.1.1. Bacterial Cells 113
5.1.1.2. Assay Conditions 113
5.1.1.3. Assay Controls 113
5.1.1.4. Light Source 113
5.1.1.5. Reading Absorbances 114
5.1.2. Assay protocol. 114
5.2. Partition coefficients – method used. **114**
5.3. Statistics **115**
5.3.1. Data analysis methods 115
5.3.2. Statistical analysis 116
5.4. Structure activity relationships. **117**
5.4.1. The effect of chain length. 117
5.4.2. Aliphatic vs aromatic. 125
5.4.3. MRSA vs *S. aureus*. 132
5.4.4. *E. coli*. 134
5.4.5. Compound **17**. Arsenium cation. 138
5.5. Summary. **140**

Chapter 6. Experimental. **141**
6.1. General. **141**
6.2. Chemical synthesis. **142**

Appendix 1. Statistical Analysis Data

Appendix 2. Mulliken Charge calculation data

Chapter 1. Introduction.

1.1 Aim

Antibiotics have commonly been used to control bacterial infections, however in recent years resistance is becoming more of a problem. The aim of this project is to look at a new way to treat bacterial infections. Photodynamic antimicrobial chemotherapy (PACT) is one way in which this could be addressed. The production of singlet oxygen by porphyrins means that multiple sites within the microorganism could be targeted in order to overcome the bacteria's ability to develop resistance. This project concentrates on the synthesis of a library of cationic porphyrins substituted with either nitrogen or phosphorus-centred cationic groups. A bacterial assay has been developed for use in PACT and the compounds screened, using the optimised protocol, to test their potential for use in the photodynamic inactivation of bacteria.

1.2 Bacteria

1.2.1. The Problem of Bacterial Infection.

Although some bacteria are vital for our everyday health and well being they can also cause infection, and methods of eradicating them are needed. Burn victim's wounds are most commonly infected with bacteria such as *Staphylococcus aureus* (Gram positive bacteria), *Pseudomonas aeruginosa* and *Klebsiella* species (Gram negative bacteria). Once in the wounds the bacteria can spread and locally impede wound closure [1] or enter the vascular system. Sepsis and endotoxemia occur when bacterial infections overcome both antibacterial agents administered and the bodies' systemic immune responses. *S. aureus* can excrete several protein exotoxins which produce diverse systemic toxaemias, toxic shock syndrome toxin, and exfoliate toxin which causes scalded skin syndrome. The Gram negative bacteria produce strain-specific lipopolysaccharide endotoxins that can induce life-threatening endotoxic shock. Septicemia by any of these bacteria may be fatal [2].

1.2.2. Classification

There are two types of cells, eukaryotic and prokaryotic, and these differ greatly in size and structure. There are several groups of eukaryotic microorganisms and these include algae, fungi and protozoa, whilst bacteria are the only prokaryote. The major structural difference between eukaryotes and prokaryotes are their nuclear structures. The eukaryotic nucleus is bound by a nuclear membrane and contains several DNA molecules. In contrast to this the prokaryotic nuclear region has no membrane and is made up of a single DNA molecule. Table 1 shows the differences between prokaryotic cells and eukaryotic cells [3].

Eukaryotic cells	Prokaryotic cells
The chromosomes are enclosed within a sac-like, double-layered 'nuclear' membrane.	There is no nuclear membrane: Chromosomes are in direct contact with the cytoplasm.
Chromosome structure is complex; the DNA is usually associated with proteins called histones.	Chromosome structure is relatively simple.
Cell division involves mitosis or meiosis.	Mitosis and meiosis are not involved.
The cell wall, when present, includes structural compounds such as cellulose or chitin, but never peptidoglycan.	The cell wall, when present, usually contains peptidoglycan but never cellulose or chitin structural components.
Mitochondria are generally present; Chloroplasts occur in photosynthetic cells.	Mitochondria and chloroplasts are never present.
Cells contain ribosomes of two types; a larger type in the cytoplasm and a smaller type in the mitochondria and chloroplasts.	Cells contain ribosomes of only one size
Flagella, when present, have a complex structure.	Flagella, when present, have a relatively simple structure.

Table 1. The difference between eukaryotic cells and prokaryotic cells [3].

All bacteria, with a small number of exceptions, fall into one of two categories. These are either Gram-positive bacteria or Gram-negative bacteria and can be distinguished from each other using the Gram stain test. The Gram stain test involves the bacteria being mixed with a purple dye (crystal violet), washed with alcohol, and then mixed with a pink dye (safarin). The Gram negative bacteria lose the crystal violet and retain the safarin so turn pink, whereas the Gram positive bacteria retain the crystal violet so turn purple.

Bacterial species differ from one another in many ways. These include size, shape and structure. The smallest bacteria are 0.2μm (cells of *Chlamydia*) and the largest >600μm (*Epulopiscium fishelsoni*), although in general they are between 5 and 0.5μm. There are three main classes of bacterial shape and these are spherical – *cocci*, cylindrical or rod shaped – *bacilli* and helical – *spirochaetes*.

Bacteria can be classified through morphology, staining, cultural characteristics, biochemical reactions, antigenic structure and base composition (i.e. guanine to cytosine ratio of bacterial DNA). The most medically important genera are shown in tables 2 and 3, classified based on Gram's stain, morphology and aerobic or anaerobic growth [4].

Cocci	Aerobes or facultative anaerobes	Arranged in clusters	*Micrococcus*
			Staphylococcus
		Arranged in chains	*Streptococcus*
	Anaerobes	Arranged in clusters	*Peptococcus*
		Arranged in chains	*Peptostreptcoccus*
Bacilli	Aerobes or facultative anaerobes	Sporulating	*Bacillus*
		Non Sporulating	*Corynebacterium*
			Listeria
			Lactobacillus
			Nocardia
			Mycobacterium
	Anaerobes	Sporulating	*Clostridium*
		Non sporulating	*Actinomyces*

Table 2. Classification of some Gram positive bacteria [4].

Cocci	Aerobes	*Neisseria*	
	Anaerobes	*Veillonella*	
Bacilli	Aerobes	*Pseudomonas*	
	Aerobes or facultative anaerobes	*Salmonella*	*Enterobacteria*
		Shigella	
		Klebsiella	
		Proteus	
		Escherichia	
		Yersinia	
		Bordetella	*Parvobacteria*
		Haemophilus	
		Brucella	
		Pasteurella	
		Vibrio	
	Anaerobes	*Campylobacter*	
		Bacteroides	
		Fusobacterium	
Spirochaetes	Aerobes	*Leptospira*	
	Anaerobes	*Borrelia*	
		Treponema	

Table 3. Classification of some Gram negative bacteria [4].

1.2.3. Structure.

The general structure of a bacterium is shown in figure 1 [5].

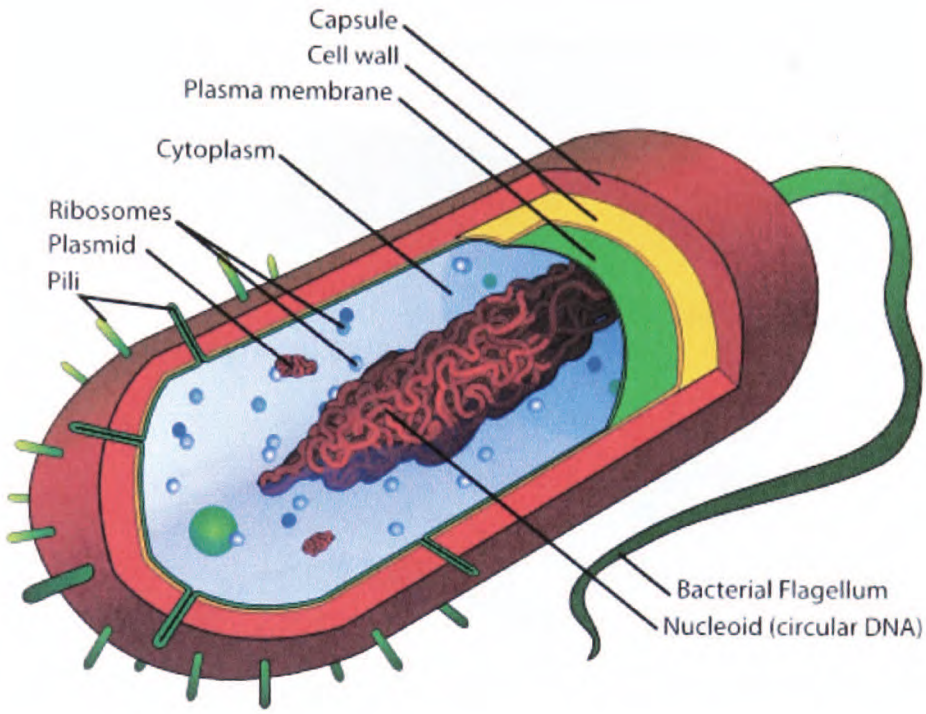

Figure 1. The generalised structure of a bacterium [5].

1.2.3.1. Capsule

The capsule or slime layer can be found on both Gram positive and Gram negative bacteria (i.e. *Streptococcus pneumoniae* and *Escherichia coli*). It is a layer of acidic polysaccharides usually composed of 2-3 sugars which are characteristic of the particular organism. The purpose of the capsule is to prevent the cell drying out and to protect against phagocytosis (engulfing) by larger organisms.

1.2.3.2. Cell Wall.

The function of the cell wall is to provide rigidity to the cell and protect against osmotic damage. The structure of the cell wall is different in Gram positive and Gram negative bacteria and this is the reason that they stain differently in the Gram stain test. Figures 2a, 2b and 2c show the structures of Gram positive and Gram negative cell walls.

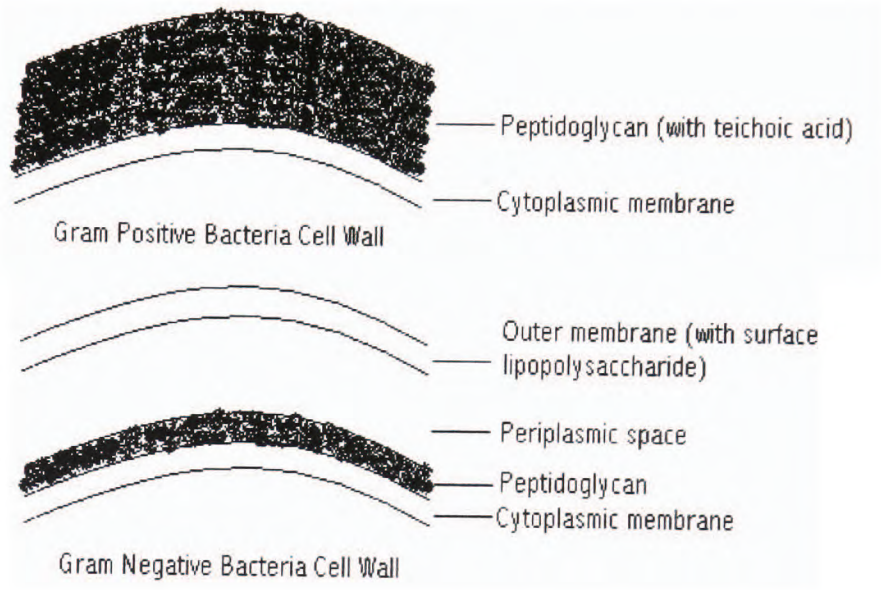

Figure 2a. The different structures of Gram positive and Gram negative cell walls.

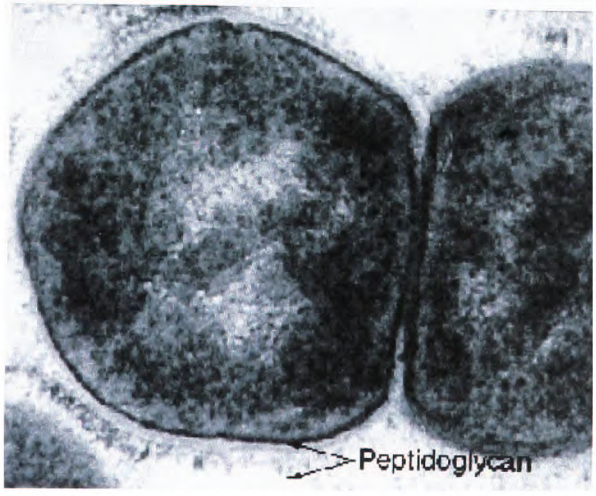

Figure 2b. Electron micrograph of Gram positive cell wall [6].

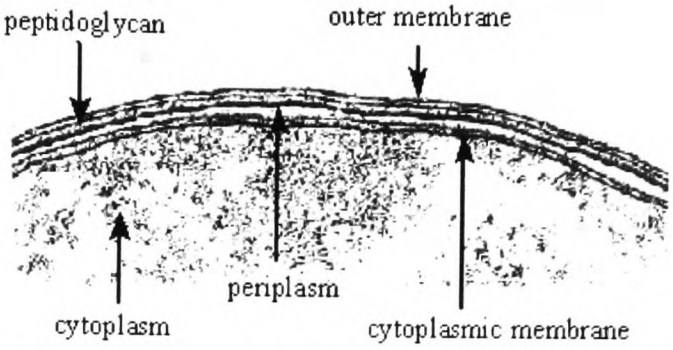

Figure 2c. Electron micrograph of Gram negative cell wall [6].

The Gram positive cell wall is usually between 15 and 50 nm thick and lies on the outside of the cell membrane. Approximately 50% of the cell wall is made up of peptidoglycan. Peptidoglycan is composed of two sugar derivatives (*N*-acetylglucosamine and *N*-acetylmuramic acid) and a small group of amino acids (L-alanine, D-alanine, D-glutamic acid and either lysine (GPB) or diaminopimelic acid (GNB)) to form a glycan tetrapeptide (see figure 3). These glycan chains are connected by peptide cross-links formed by the amino acids (see figure 4) and it is this cross linking that gives the peptidoglycan its strength [6]. In Gram positive bacteria the cross linkage is via a peptide inter-bridge whereas Gram negative cross links are by direct peptide link from the amine group of the diaminopimelic acid (DAP) to the carboxyl group of the terminal D-alanine (See figure 5). Gram positive bacteria have acidic polysaccharides attached to their cell walls called teichoic acids. Teichoic acids are negatively charged and are partly responsible for the negative charge of the cell surface.

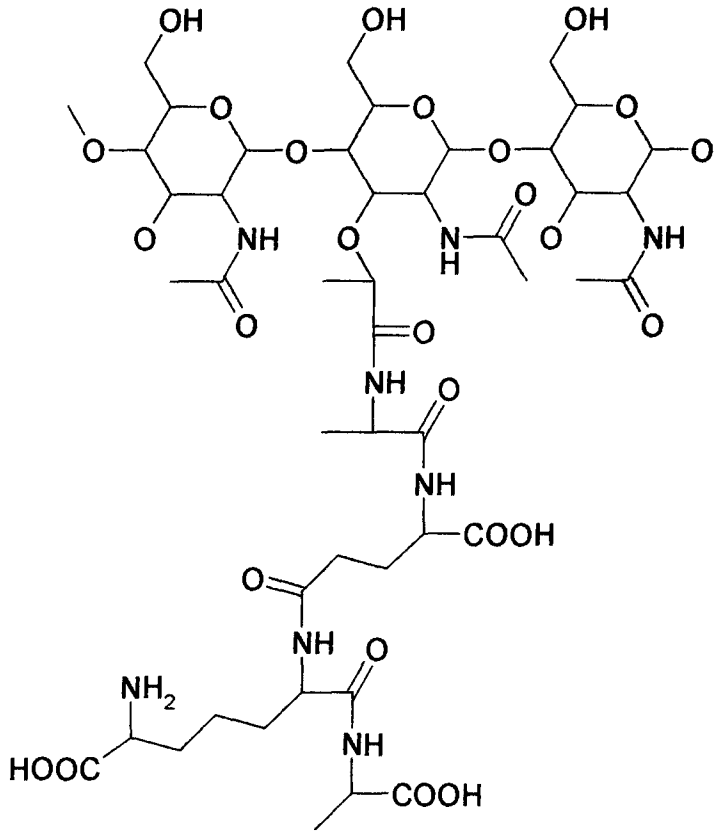

Figure 3. The glycan tetrapeptide.

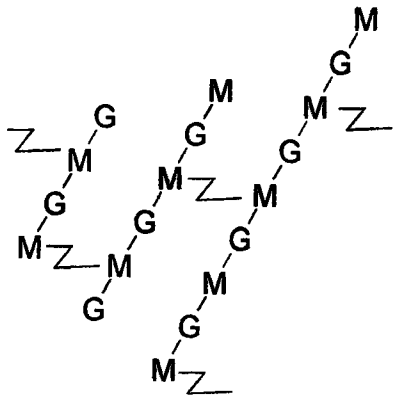

Z = peptide cross-links

M = *N*-acetylmuramic acid

G = *N*-acetylglucosamine

Figure 4. Overall structure of peptidoglycan showing cross linkages between glycan chains.

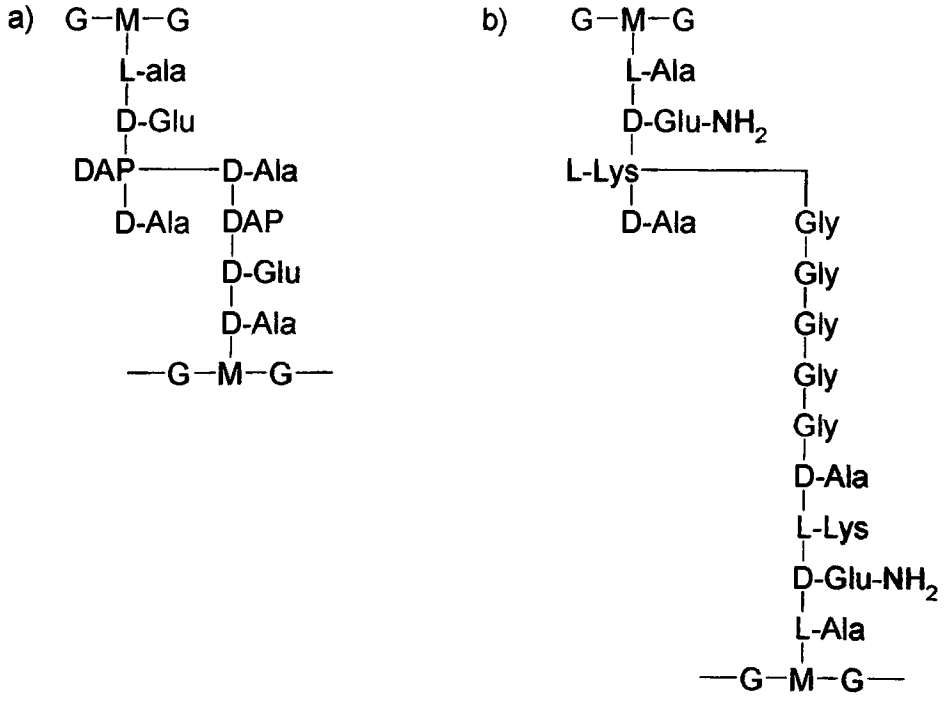

Figure 5. a) Direct interbridge in Gram negative bacteria. b) Glycine interbridge in Gram positive bacteria.

1.2.3.3 Outer membrane.

Unlike Gram positive bacteria, Gram negative bacteria are surrounded by an outer membrane. Embedded in the outer membrane are proteins called porins that facilitate transport across the membrane. The membrane is asymmetric and is made up of an inner phospholipid layer and an outer layer comprising lipopolysaccharide (LPS) molecules (see figure 6 [7]).

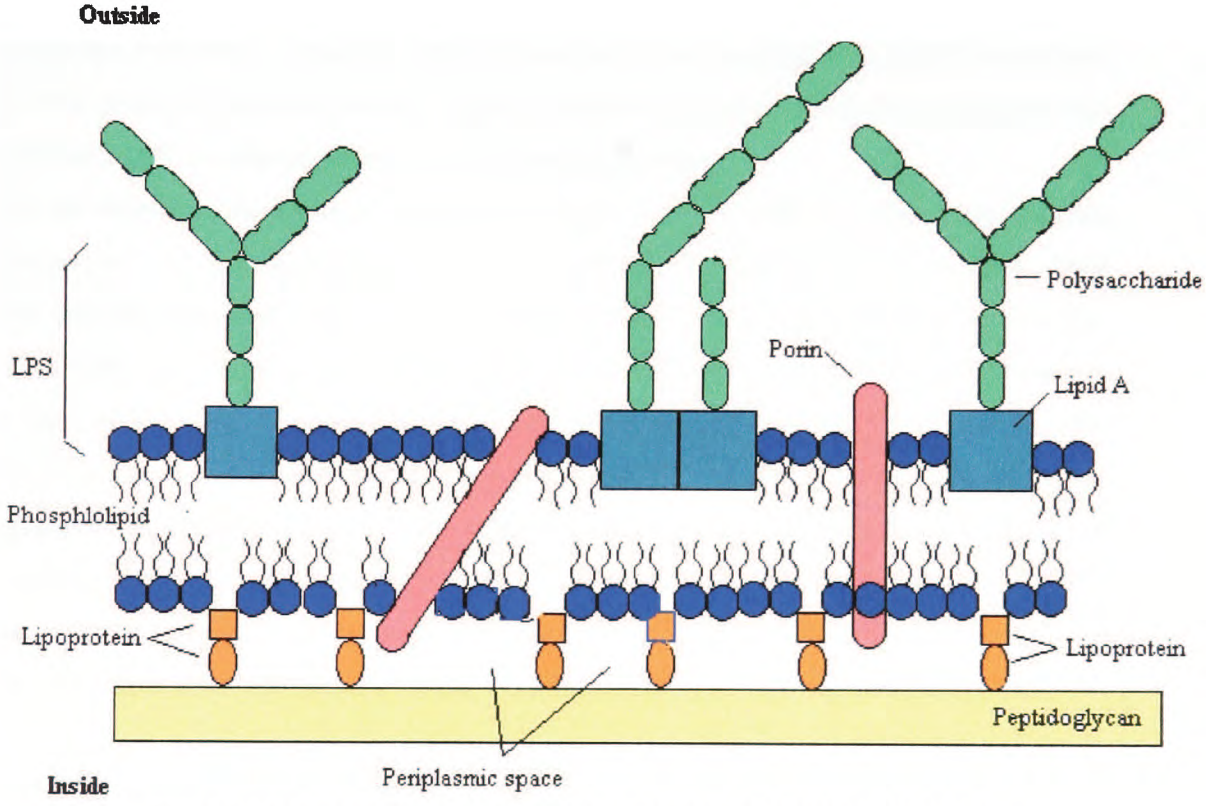

Figure 6. Diagram of a Gram negative bacterium outer membrane adapted from [7].

The lipid part of the LPS, called Lipid A, is comprised of fatty acids (caproic, lauric, myristic, palmitic and stearic acids) which are connected by an amide link to a disaccharide composed of *N*-acetylglucosamine. The LPS molecules associate with the phospholipids to form the outer layer of the outer membrane. The inner layer is 'anchored' to the peptidoglycan by lipoproteins.

The outer membrane acts as a permeability barrier. Small hydrophilic molecules do not pass through the LPS layer but instead they enter the cell via the porins.

1.2.3.4. Bacterial physiology.

The cytoplasmic membrane is made up of phospholipids and proteins and encloses the interior of the bacterium. It acts as an osmotic barrier and regulates the flow of materials in and out of the microorganism. It is also involved in electron transport and oxidative phosphorylation, energy production, motility and replication. Bacterial growth, metabolism and replication are carried out in the cytoplasm. The cytoplasm of bacteria is typically void of organelles except for ribosomes and some small membrane-bound structures (not always present). The chromosome is not encased in a nuclear membrane as it is in eukaryotic cells and is a single, continuous strand of DNA. Many bacteria also possess small circular elements of DNA termed plasmids.

On the outside of the bacterial cell are the flagella. Flagella (singular: flagellum) provide locomotion for the organism so it can move away from toxins or towards nutrients. They are hair-like structures that are helically shaped and comprised of protein subunits. Locomotion is brought about by rotation of the flagella in a propeller like movement. There are two main types of flagella and these are peritrichous flagella or polar flagella. Peritrichous flagella have flagellum surrounding the whole organism whereas polar flagella have flagellum located only at one end. Pili are also found on the outside of the bacteria. Pilli (singular: pillus) are hair-like projections, comprised of protein building blocks that emerge from the outside of the cell surface. They assist the bacteria in attachment to cells, surfaces and can also assist the transfer of DNA between bacteria.

1.3 Antibacterial agents.

1.3.1. Introduction to antibacterial agents.

The range of bacteria or other microorganisms affected by a certain antibacterial agent is called its spectrum of activity. If an antibacterial agent is active against both Gram positive bacteria and Gram negative bacteria then it is said to have a broad spectrum of activity whereas if it only works on one or the other then it is said to have a narrow spectrum of activity. A limited spectrum of activity is when the drug only acts on a single organism. To be clinically useful an antibiotic must have the following characteristics: it must have a broad spectrum of activity, it must be non toxic to the host, it must be non allergenic to the host, it must not eliminate the host's natural flora, it must reach the

infected part of the body, it must be inexpensive and easy to produce, it must be chemically stable and microbial resistance must be uncommon or unlikely to develop. Antibacterial agents can work in one of two ways and these are either bacteriocidal (bacteria-killing) or bacteriostactic (growth inhibiting).

1.3.2. β-lactams.

β-Lactam antibiotics include penicillins, cephalosporins, carbapenems, clavams and monobactams. The feature that they all have in common is a four-membered nitrogen containing ring called a β-lactam ring. Figure 7 shows the core structure of some common β-lactams.

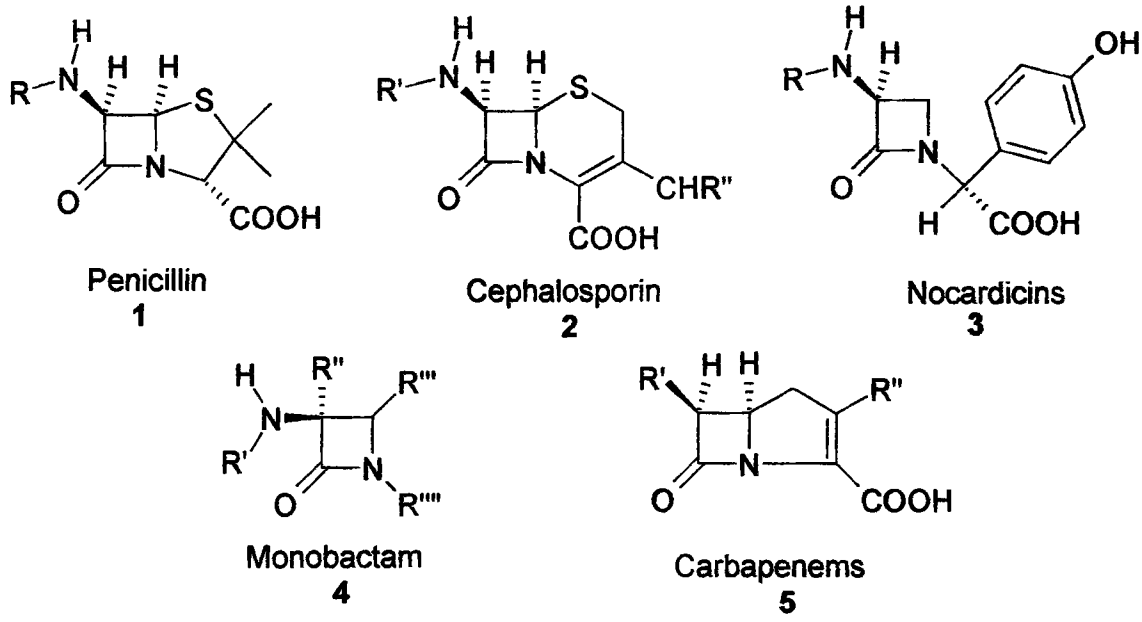

Figure 7. The generic structures of some common β-lactams.

The antibacterial effect of penicillin (**1**) was discovered by Alexander Fleming in 1929. β-Lactams are normally bacteriocidal however they require the bacteria to be growing in order to exert their toxicity. The different β-lactams vary in spectrum of activity, toxicity, stability, clearance rate, whether they can be orally taken or not, ability to cross the blood brain barrier and susceptibility to β-lactamases. However, despite all these differences, β-lactams have only one mode of action. Their mode of action is the inhibition of the final

stages of peptidoglycan biosynthesis and their activity is dependent on having an intact β-lactam ring. β-Lactams bind to the penicillin binding proteins (PBP's) found in the outer leaflet of the cell membrane and to do this they must penetrate the cell wall and operate in the periplasmic space. The periplasmic space is accessible in Gram positive bacteria but in Gram negative bacteria the drugs need to cross the bacterial cell membrane or pass through the porin channels. The 3-D structure of β-lactams resembles the D-alanyl-D-alanine end of the pentapeptide in peptidoglycan just before final assembly. The enzymes that normally work on the D-alanyl-D-alanine end of the pentapeptide are called transpeptidases and the β-lactams bind to the active sites of these enzymes, preventing the assembly of peptidoglycan. The β-lactam bond can also be hydrolysed by enzymes called β-lactamases.

1.3.3. Glycopeptides.

The most common glycopeptide is vancomycin (**6**), although teicoplanin is also now available. Vancomycin (see figure 9) was first isolated in 1956, and is thought of as the last line of defence against pathogenic bacteria. Like β-lactams, it inhibits the synthesis of peptidoglycan. However the mechanism by which it inhibits peptidoglycan synthesis is different to β-lactams. Vancomycin binds to the D-alanyl-D-alanine end of the peptidoglycan pentapeptide chain rather than the penicillin-binding enzyme. By doing this it blocks access to the active site of the enzyme. Vancomycin is often used to treat multiple resistant infections and is thought of as the antibiotic of last resort. However resistance to this has emerged over the years since it was introduced. Vancomycin-resistant enterococci (VRE) were first reported in the UK in 1988 [8] and the first isolation of vancomycin-resistant *Staphylococcus aureus* (VRSA) was in Japan in 1997 [9]. These discoveries mean that this antibiotic may in the future be less useful in the treatment of infections.

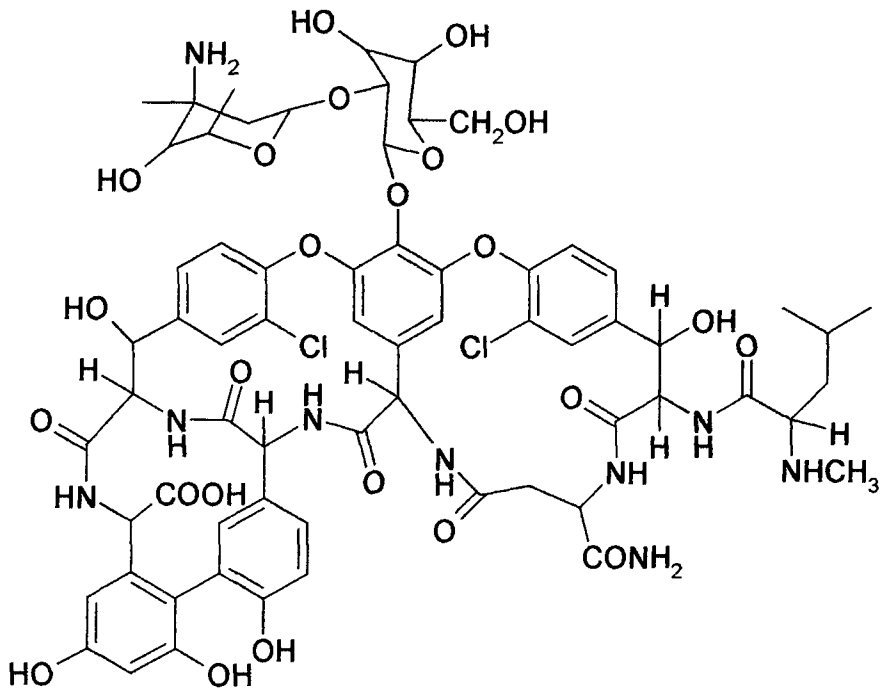

Figure 9. The structure of Vancomycin. **6**.

1.3.4. Sulfonamides.

In 1935 Domagk discovered a group of synthetic chemicals, known as sulfonamides, which exhibited broad antimicrobial activity. They are competitive inhibitors that act on the folic acid synthetic pathway [10]. Folic acid is a cofactor in the synthesis of purines, thymidine and methionine which are necessary for the synthesis of RNA, DNA and proteins. Sulfonamides are analogues of *p*-aminobenzoic acid **8** (see figure 10) and they competitively inhibit dihydropteroate synthetase which is the enzyme that condenses *p*-aminobenzoic acid with dihydropteroic acid in the early stages of folic acid synthesis.

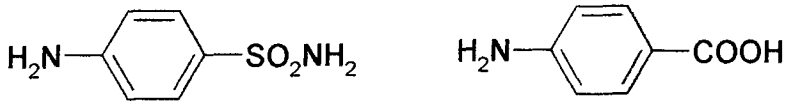

Sulfanilamide
7

p-Aminobenzoic acid
8

Figure 10. Comparison of the structures of sulfonamides and PABA.

Bacteria must synthesise folic acid however, mammalian cells uptake it as preformed folate. Despite this selectivity for bacteria over mammalian cells the sulfonamides have many side effects in the body including kidney damage due to sulfonamide crystals forming in acidic urine, allergic reactions such as rashes and drug induced fever, Stevens-Johnson syndrome (a rare, severe form of erythema multiforme), kernicterus (sulfonamides displace bilirubin from plasma protein binding sites), haemolytic anaemia, G.I. distress, nausea, vomiting, diarrhoea and photosensitivity [11].

1.3.5. Quinolones.

Quinolones are broad spectrum antibiotics that cause inhibition of the enzyme DNA gyrase. DNA gyrase is an enzyme involved in uncoiling supercoiled DNA prior to cell division. The prototype drug in this class was nalidixic acid (see figure 11) which was active against Gram negative bacteria. Many other analogues of this have been synthesised and it has been found that fluorination at the 6 position [i.e. in ciprofloxacin **10** (figure 11)] gives better activity against a broader spectrum of bacteria.

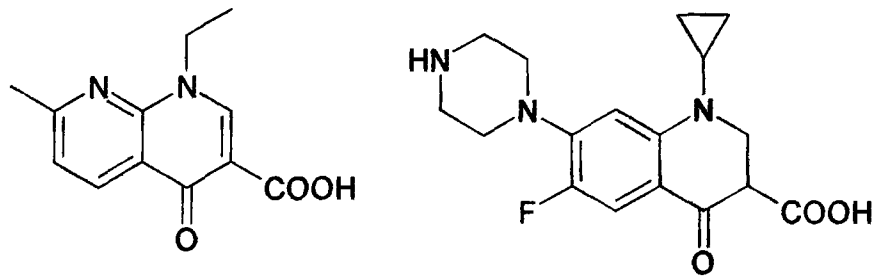

Nalidixic acid
9

Ciprofloxacin
10

Figure 11. The structures of nalidixic acid and ciprofloxacin.

1.3.6. Tetracyclines.

Tetracyclines have a broad spectrum of activity against a number of both Gram positive and Gram negative bacteria and are made up of four, fused C6 rings (see figure 12).

Tetracyclines are actively transported into bacterial cells where they act as protein synthesis inhibitors. They are bacteriostatic and prevent the binding of amino acyl-tRNA to the ribosome.

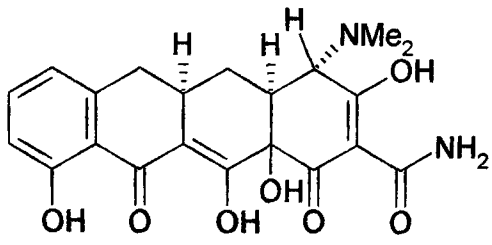

11

Figure 12. The structure of tetracycline.

All of the antibacterial agents have different modes of action although they share the fact that they are all targeted to a specific process and this means the bacteria are often able to find a way of combating their toxic effects.

1.4. Bacterial resistance to antibiotics.

1.4.1. Clinical importance.

Antimicrobial agents have reduced the threats posed by bacterial infections and have saved millions of lives since their introduction in the early part of the 20th century. Many serious infectious diseases have been brought under control and they have contributed in large part to increasing life expectancy. These gains however may be jeopardised by the emergence and spread of bacteria which are resistant to first line drugs. The emergence of resistance is most evident in the bacterial infections that contribute most to human disease. Some important examples of this are penicillin-resistant *Streptococcus pneumoniae*, vancomycin-resistant enterococci, methicillin-resistant *Staphylococcus aureus* (MRSA), multi-resistant *salmonellae* and multi-resistant *Mycobacterium tuberculosis* [12].

The consequences of the emergence of antibiotic resistance in bacteria are severe. Bacterial infections that fail to respond to treatment result in prolonged illness and greater risk of death. An infection that is not successfully treated allows for greater spread within the community. When first line treatments are no longer viable, second or third line treatments must be used however these are often more expensive and / or more toxic to

the patient. The major cause for concern however, is for organisms which are developing resistance to virtually all currently available drugs, necessitating the need for the development of drugs in which resistance will not occur (i.e. those that act on multiple targets).

There are a number of reasons why bacterial resistance is thought to have come about and these include the use and misuse of antimicrobial agents, increased use of invasive devices and procedures, a greater number of susceptible hosts, lapses in infection control practices leading to increased transmission of resistant organisms, and widespread use of antimicrobials in hospitals, for immunocompromised patients [13].

Most studies show a higher rate of resistance associated with noscomial pathogens, especially from intensive care units, than with community acquired organisms. Specific bacterial pathogens that are significant problems in hospitals today include MRSA, multidrug resistant Gram-negative bacilli, vancomycin-resistant enterococci (VRE) and oxacillin-resistant *S. aureus*.

1.4.2. Emerging resistance.

There are two general types of resistance and these are either intrinsic or acquired. Intrinsic resistance is inherent (chromosomal) whereas acquired resistance results from the alteration of the bacterial genome. This alteration of the genome can occur through one of two pathways, which are vertical evolution or horizontal evolution. Vertical evolution is thought to be linked to the selection of favourable mutations in a population and this gene is then passed on to the new cells. Horizontal evolution is by genetic transfer via plasmids which can occur through various mechanisms (see 1.4.3). Soon after each antibacterial agent was entered into clinical practice, resistance was reported by at least one organism (table 4) [14].

Agent for which resistance was observed	FDA approval	Resistance reported	Mechanism of resistance.
Penicillin G	1943	1940	Penicillinase production
Streptomycin	1947	1947	Mutation in ribosomal protein S12
Tetracycline	1952	1952	Efflux
Penicillin and tetracycline combination	1943 and 1952	1976-80	Plasmid coded broad spectrum β-lactamases and tetracycline efflux pump
Methicillin	1960	1961	MecA (Penicillin Binding Protein(PBP))
Nalidixic acid	1964	1966	Topoisomerase mutations
Gentamycin	1967	1969	Aminogylcoside modifying enzyme.

Table 4. Reported resistance to new agents following approval for clinical use and mechanisms of resistance.

1.4.3. Mechanisms of resistance.

1.4.3.1. Enzymatic inactivation of the antibiotic.

Resistance to β-lactams is common due to bacteria producing the β-lactamase enzyme. β-lactamase inactivates the drug by acting on the β-lactam ring. The overall reaction scheme for this is shown in scheme 1 and the mechanism of action is shown in scheme 2.

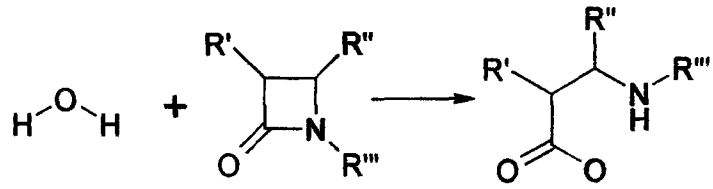

Scheme 1. The overall reaction scheme for β-lactamase action on the β-lactam ring.

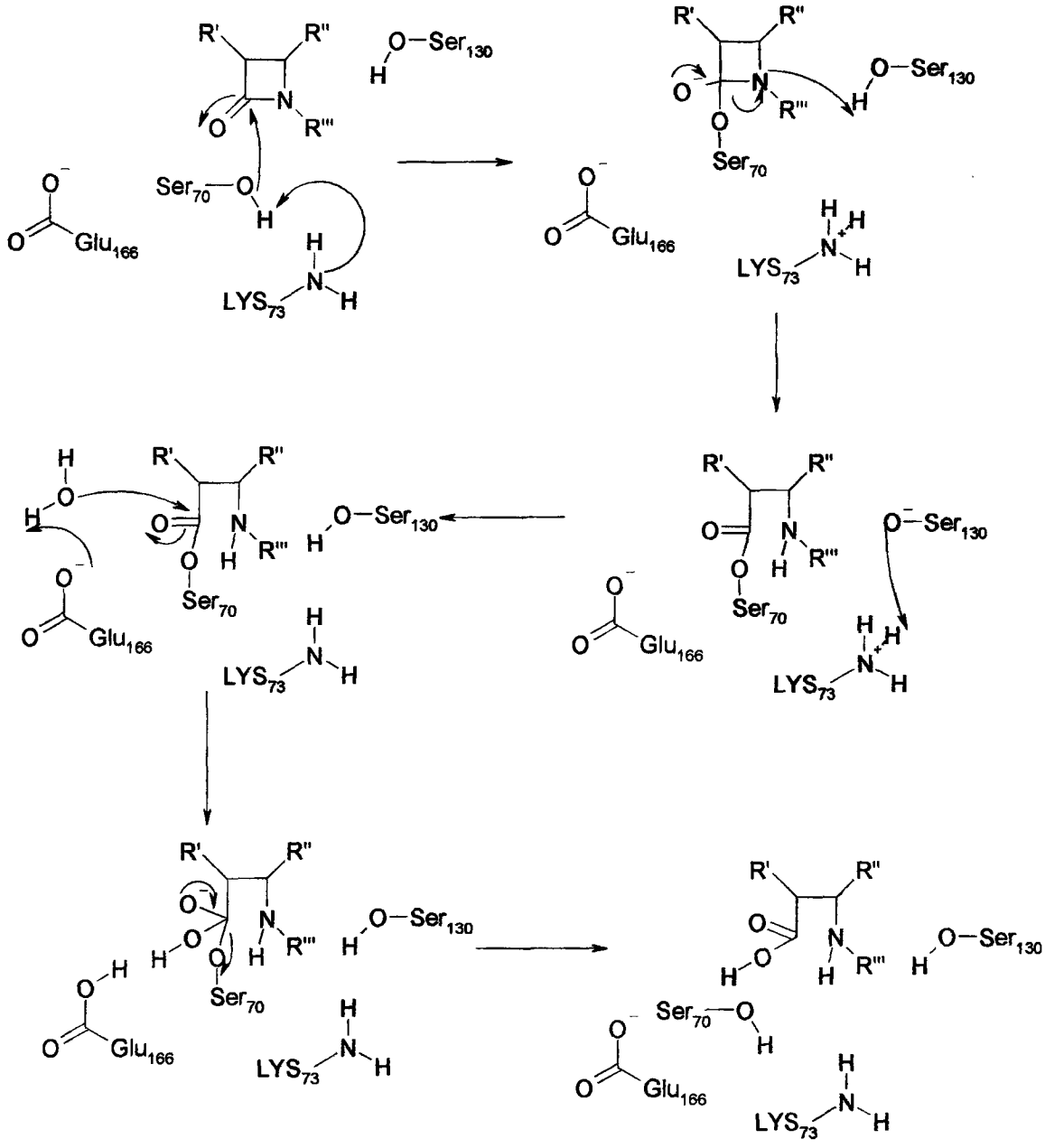

Scheme 2. Mechanism of β-lactamase action.

1.4.3.2. Modification of the target (becoming insensitive)

The most common mechanism of resistance to macrolides involves modification of the target site on the ribosome. This is achieved by methylation of an adenine residue in domain V of the 23S rRNA and it is carried out by a family of plasmid or transposon encoded M-methyltransferases [15].

Vancomycin resistance also occurs via modification of the target site. It targets the D-Ala-D-Ala termini of the UDP-N-acetylmuramyl-pentapeptide precursor of peptidoglycan. Resistance arises as a result of the synthesis of abnormal pentapeptide precursors which possess altered termini such as D-Ala-D-Lac or D-Ala-D-Ser and these have a lower affinity for vancomycin than D-Ala-D-Ala [15].

Another form of antibiotic resistance via modification of the target site has arisen with fluoroquinolones. This involves a mutation affecting the fluoroquinolone targets, the DNA gyrase and topoisomerase IV enzymes. Alterations can be made in either the GyrA or GyrB subunits of DNA gyrase. In Gram negative bacteria, the most common mutations in the GyrA subunit cause resistance through decreased drug affinity for the altered gyrase-DNA complex. The GyrB subunit modifications are less common and their effect on drug binding is not clear. Topoisomerase IV alterations due to mutations in ParC or ParE also occur in Gram negative bacteria but appear to be of less importance. The situation is reversed in Gram positive bacteria where the topoisomerase IV acts as the primary target over DNA gyrase.

1.4.3.3. Impermeability.

Antibiotics must be able to enter the cell in order to reach their intracellular targets. To enter the cell they must cross the Gram negative bacterial outer membrane. This, in part, explains why Gram negative bacteria are harder to kill than Gram positive bacteria. Acquired resistance to β-lactams in a number of Gram negative bacteria had been attributed to outer membrane changes that correlate with reduced permeability, however the outer membrane as a resistance mechanism is only significant in context of additional resistance mechanisms. A more general example of impermeability leading to resistance is found in biofilms [16]. A biofilm is a population of cells growing on a surface enclosed

in a polysaccharide matrix and, according to the National Institute of Health "more than 60% of all microbial infections are caused by biofilms" [16]. It is harder to kill bacterial cells in a biofilm than in planktonic populations. Although penetration of antibiotics into a biofilm may be important for some antibiotics this is unlikely to be the mechanism of resistance (persistence) for the majority of antibiotics.

Mutational impermeability is important in resistance to carbapenems and arises via the loss of OmpD, a porin that forms narrow transmembrane channels that are accessible to carbapenems but not other β-lactams [17].

The major porin from a wild type strain and a resistant strain of *Enterobacter aerogenes* were characterised and analysed. The findings showed that the OmpC / OmpF-like protein from the resistant stain had single-channel conductance 70% lower than the wild type, it was three times more selective for cations and had a lack of voltage sensitivity. These results indicated that the clinical strain was able to synthesise a modified porin that decreased the permeability of the outer membrane [18].

1.4.3.4. Efflux mechanism to pump out the antibiotic.

Tetracycline resistance, discovered in 1953, has arisen due to bacteria having an efflux mechanism which pumps the antibiotic out of the cell. Efflux proteins transport tetracycline molecules out of the cell, reducing the concentration of drug within the cell so that it is below the MIC for the inhibition of protein synthesis. The proteins are encoded by genes in bacteria called *tet* (from tetracycline) or *otr* (from oxytetracycline). The *tet* genes that encode efflux pumps, code for energy dependent membrane-associated proteins (46KDa in size) which export tetracycline out of the cell. See figure 13 for a diagram showing the structure of an efflux pump.

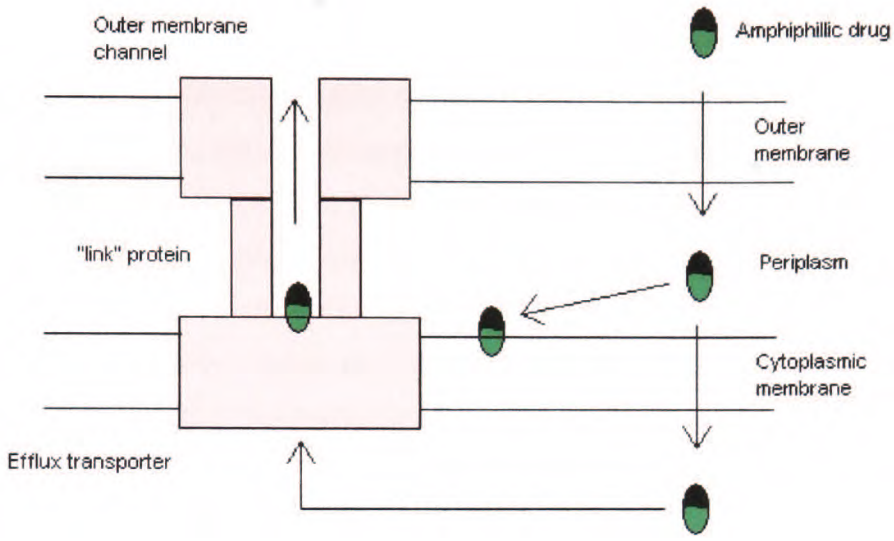

Figure 13. Diagram adapted from [4], shows efflux machinery used to pump tetracycline out of the bacterial cell in *P. aeruginosa*.

The mechanism by which the efflux pump works is by the active translocator 'catching' the drug in the cytoplasmic area. The efflux proteins then exchange a proton for a tetracycline cation complex against a concentration gradient. The bound molecule is transported out of the cell via a change in configuration of the protein and is then released into the surroundings [19]. Bacterial drug efflux pumps are classed into five families which are the major facilitator superfamily (MFS), the adenosine triphosphate (*A*TP)-binding cassette (ABC) superfamily, the small multidrug resistance (SMR) family, the resistance-nodulation-cell division (RND) superfamily and the multidrug and toxic compound extrusion (MATE) family [20]. Of these families the first two are very large whilst the others are smaller. Efflux pumps can be further classified into single component or multi component pumps. In most cases multidrug efflux pumps are chromosomally encoded and therefore not readily transferable between bacteria. However examples can be found in both Gram positive and Gram negative bacteria where the genes are on mobile elements.

1.4.3.5. Enhanced production of the target to compensate.

Glycopeptide antibiotics such as vancomycin inhibit cell wall synthesis by binding to the D-Ala-D-Ala end of the peptidoglycan precursors. However, vancomycin resistant *S.aureus* (VRSA) was first isolated in Japan in 1997. When compared to control stains these bacteria show a number of changes in their cell wall structures. Specifically, there is a two-fold increase in the thickness of the cell wall, there is an increased proportion of peptidoglycan stem peptides containing non-amidated glutamine residues and reduced peptidoglycan cross-linking [21]. The thicker cell wall with its multiple binding sites for vancomycin has been shown to trap antibiotic molecules, reducing the number of vancomycin molecules that reach the cytoplasmic membrane where the transglycosylase targets are located.

1.4.3.6. By-pass of target, using alternative insensitive route.

Bacteria can produce a new enzyme that is not inhibited by the antimicrobial. Trimethoprim-sulphamethoxazole resistance is due to bacteria that produce a new dihydrofolate reductase not inhibited by trimethoprim and a new dihydropteroate synthetase not susceptible to sulfonamides. These new enzymes are plasmid coded whereas the chromosomally determined enzyme is the target for sulphonamides [22]. The R-plasmid enzyme binds sulphonamides 10,000 times less tightly than the chromosomal enzyme while the K_m for the substrate, *p*-aminobenzoic acid, is the same for both enzymes.

1.4.4 Self promoted uptake

Self promoted uptake is a process by which cationic antimicrobial compounds can enter a bacterial cell. There is a high net negative charge on the outside of the bacterial cell wall which is partly neutralised by Mg^{2+} and Ca^{2+}. Polycationic drugs can interact with the divalent cation binding sites. They have a higher affinity for the site so either chelate or displace the divalent cations. In doing so the bulkiness of the polycation leads to a distortion of outer membrane structure. Gaps then appear in the membrane allowing the drug to diffuse into the cell.

1.4.5. Programmed cell death.

Bacteria live in colonies and when conditions become overcrowded or food is scarce some of the population commit suicide. This is done when a bacterial protein or peptide triggers a 'death signal' that causes the microbe to disintegrate. Many antibiotics are thought to exploit this signal and cause bacterial cell suicide. It has been shown that many bacterial species undergo programmed cell death [23]. In one of these, *Streptococcus pneumonia*, a sensor protein called VncS together with VncR form a suicide signalling pathway. VncR controls the amount of autolysin, which is an enzyme that hydrolyses components of a biological cell in which it is released. If VncS activity is triggered it chemically modifies VncR so that it releases autolysins to destroy the cell wall. The signal that stimulates VncS is a peptide of 27 amino acids called Pep. It is thought that antibiotics can increase the production of Pep until it reaches a concentration that the sensors can see, triggering the VncS-VncR-autolysin suicide pathway [24].

E. coli has also been shown to undergo programmed cell death when treated with antibiotics [25]. This occurs through a system called an "addiction module". An addiction module consists of a pair of genes, a stable toxin and an unstable antitoxin that prevents the lethal action of the toxin. The *E. coli mazEF* module consists of two adjacent genes called *mazE* and *mazF* and it has been found that this module has the properties of an addiction module. MazF is toxic and long lived whilst MazE is antitoxic and is a labile protein degraded *in-vivo* by the ATP dependent ClpPA serine protease. MazE and MazF interact with each other and are co-expressed. *E. coli* was treated with low concentrations of antibiotics known to inhibit transcription and / or translation. From this study it was found that the antibiotics can trigger mazEF-mediated cell death by reducing the levels of MazE.

University Library Hull

1.5. Porphyrins.

1.5.1. Structure.

Porphyrins are an important class of compound in biological systems and are central to the roles of photosynthesis, biological oxidation and reductions and the transport of oxygen by haemoglobin. Porphyrins are aromatic tetrapyrrolic macrocycles which follow Hückel's rule of $4n+2$ π electrons, where n = 4, 5 or 6. The structure and numbering of the porphyrin nucleus is shown in figure 14.

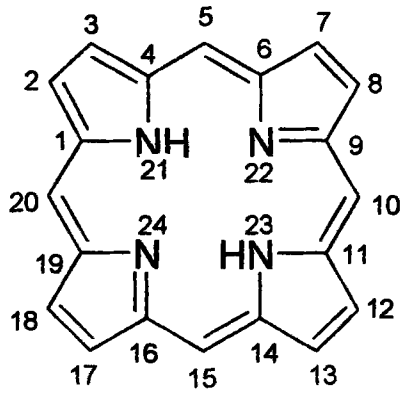

Figure 14. The porphyrin nucleus.

The porphyrin core is numbered from 1 to 20 where the 5, 10, 15 and 20 positions are known as the *meso* positions and the 2, 3, 7, 8, 12, 13, 17 and 18 positions are the β-positions. Porphyrins have a planar ring system which allows maximum overlap of the p orbitals. They are thermally stable and have an anisotropic ring current which is shown in a typical NMR spectrum. The inner protons on the nitrogen atoms are shielded by the ring current from the external magnetic field and so are found at the unusually low position of between -2 and -3 ppm. The outer protons on the backbone of the pyrrole rings, known as the β-protons, have a higher then usual resonance as they are deshielded by the ring current from the external magnetic field and appear between 8 and 9 ppm.

Porphyrins are tetradentate ligands which strongly chelate metal ions and this is an important property for haemoglobin in the transport and delivery of oxygen to cells. Porphyrins have four nitrogen atoms pointing to a central cavity of 2.01Å (from N to N).

Two of these nitrogen atoms exhibit pyridine character in that they are basic and protonate in acid to give mono- and di- cations whereas the other two have pyrrolic character in that they are acidic and deprotonate in base to give mono- and di- anions. Porphyrins are intensely coloured and absorb light in the visible part of the spectrum. Absorptions in the blue and green regions of the spectrum mean that porphyrins appear red. In the absorbance spectrum of tetraphenyl porphyrin, the largest band at ~ 400 nm is known as the Soret or B band and the smaller bands between ~500 nm and 650 nm are the Q bands. On metallation the Q bands collapse to leave two rather than four. This is due to an increase in symmetry of the molecule from D_{2h} to D_{4h}.

1.5.2. Excited states of porphyrins.

Porphyrins are photosensitizers which means they can absorb light and use it to perform chemical reactions. All photochemical reactions of porphyrins occur in their excited states and the generation and fates of these excited states can be explained using the Jablonski diagram shown in figure 15.

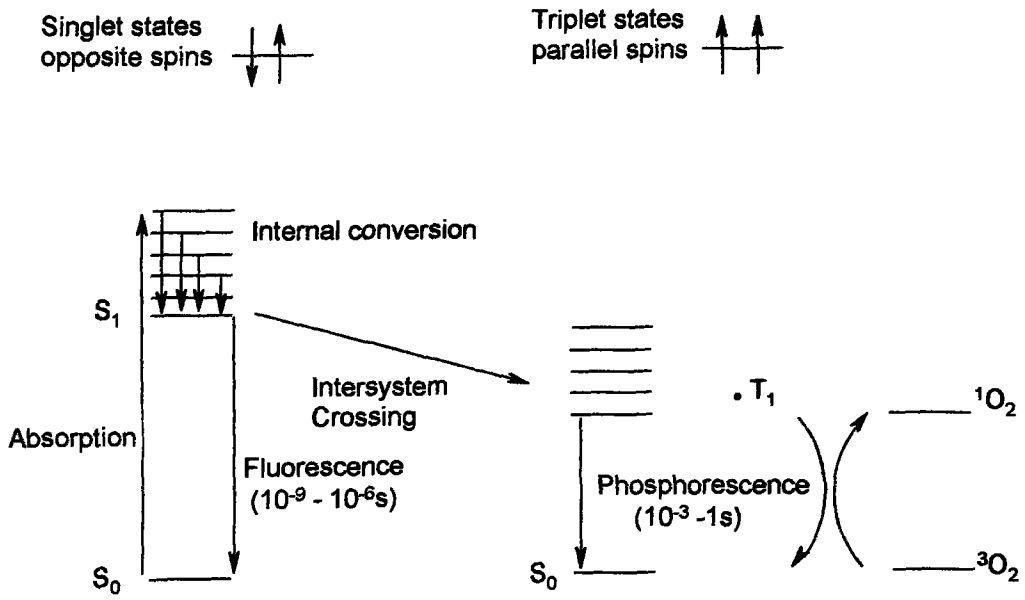

Figure 15. The Jablonski diagram showing the generation and fates of excited states.

Photosensitizers in their singlet ground state can absorb a photon of light and in doing so are excited to their singlet excited states. The singlet excited states of the photosensitizer

can then either undergo radiative decay back to the ground state, a process known as fluorescence, or it can undergo intersystem crossing (a radiationless crossing between different spin states) to the triplet excited state. The radiative decay from the triplet excited state to the singlet ground state is a spin forbidden process because it involves a net change of spin. Oxygen, unusually, has a triplet ground state and can react with the triplet excited state to produce ground state photosensitizer and singlet oxygen.

1.5.3. Synthesis of porphyrins.

5, 10, 15, 20-tetraphenyl porphyrin **(12)** was synthesised by Rothemund in 1936 for the first time. He reacted benzaldehyde **(13)** and pyrrole **(14)**, in pyridine, in a sealed bomb at 150 °C for 24 hours. However the yields were low and the conditions severe, so only a few substituted benzaldehydes could be made in this way. Adler and Longo altered these conditions by reacting benzaldehyde with pyrrole in propionic acid for 30 mins at reflux, in a system that was open to the air. Scheme 3 shows a typical reaction scheme for an Adler reaction. The milder conditions of the Adler-Longo reaction meant that many more substituents on the benzaldehydes can be converted to their corresponding porphyrins in yields of up to 20% and multigram quantities can be produced [26]. Unsymmetric porphyrins can also be made in this way by using two or three different benzaldehydes; however extensive column chromatography is needed in order to separate the products. If acid sensitive functional groups on the benzaldehyde are present, porphyrins can't be made in this way and this problem was addressed by Lindsey *et al* in 1987.

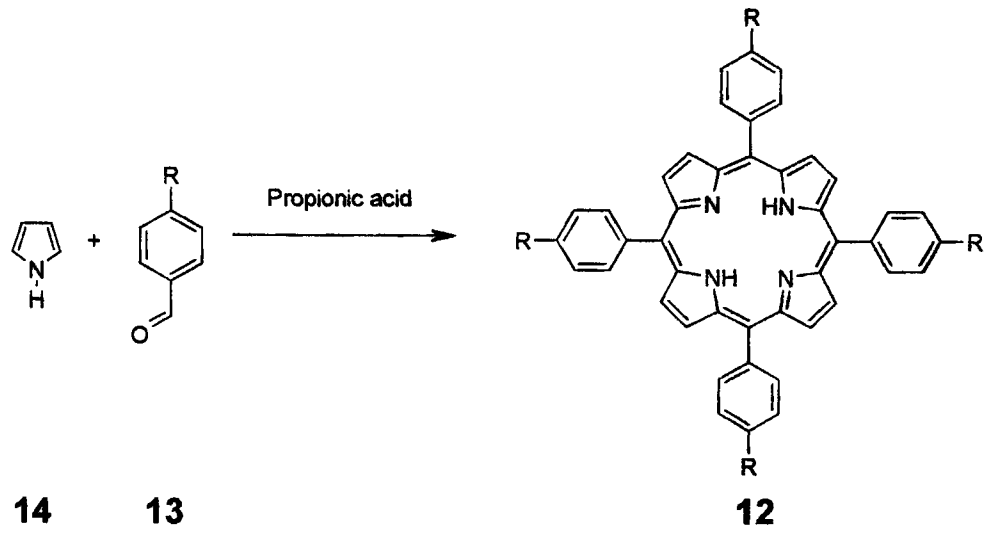

Scheme 3. A typical Adler reaction showing the condensation between pyrrole and a substituted benzaldehyde in propionic acid.

The Lindsey method relies on the formation of porphyrinogen as an intermediate in porphyrin synthesis [27]. Pyrrole and benzaldehyde form an equilibrium under mildly acidic conditions with tetraphenyl porphyrinogen (see scheme 4). After equilibrium has been reached a chemical oxidant is added to convert the porphyrinogen to the corresponding porphyrin. The advantages of this method are that it allows functional groups that are acid sensitive to be introduced, as well as allowing more facile purification and higher yields. However, higher dilution conditions are needed, in the order of 10^{-2}M, and this means it is not easily scaled up. In a typical Lindsey reaction equimolar concentrations of pyrrole and benzaldehyde are reacted with boron trifluoride at room temperature, under an inert atmosphere, for 1 hour in dichloromethane, using a water scavenger (triethyl orthoacetate). This is followed by addition of 2, 3, 5, 6-tetrachlorobenzoquinone, which is then refluxed for a further hour to produce the desired porphyrin.

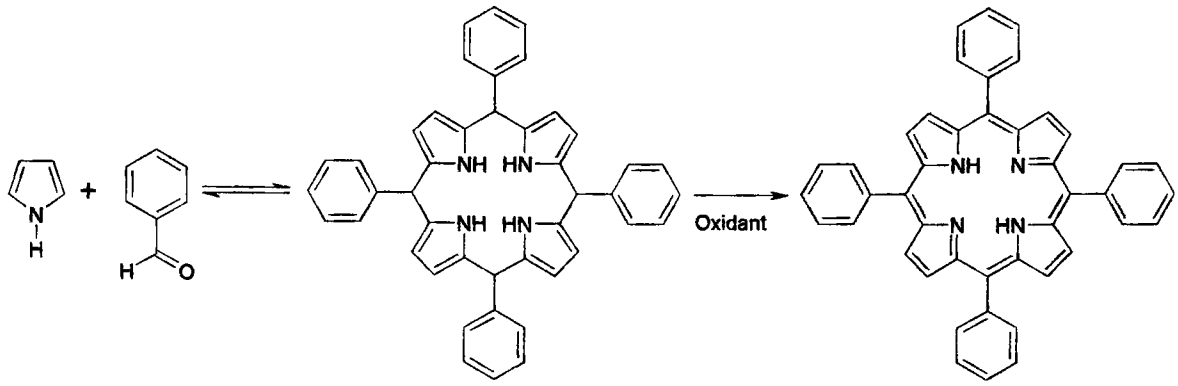

Scheme 4. Lindsey method. Equilibrium formed between pyrrole and benzaldehyde with porphyrinogen and then porphyrinogen oxidated to porphyrin.

1.6. Photodynamic therapy.

The photodynamic effect was demonstrated in 1913 when Meyer-Betz intravenously injected himself with 200 mg of haematoporphyrin. He subsequently exposed himself to light, which resulted in massive swelling and blistering. In 1970 Lipson and Schwartz found that a polymeric derivative of haematoporphyrin (HpD) was selectively taken up and retained by rapidly dividing cells and it was this observation that prompted investigations into the photodynamic therapy (PDT) of cancer. HpD is derived from acetylating haematoporphyrin (Hp) then neutralising it prior to alkaline hydrolysis. The resulting mixture contains haematoporphyrin, hydroxyethylvinyldeuteroporphyrin (HVD) and protoporphyrin (Pp), as well as a mixture of complex dimeric and oligomeric fractions containing ester, ether and carbon-carbon linkages of haematoporphyrin. HpD is ~ 45% monomeric/dimeric porphyrins and ~ 55% oligomeric material. This has been partly purified in Photofrin® to ~ 85% oligomeric material. Since the discovery of these compounds, the PDT of cancer has been well developed and compounds such as Photofrin® and Foscan® are regularly used in clinics for the treatment of cancers and many other second and third generation photosensitizers have been developed [28]. PDT, as shown in figure 16, involves the injection of a non-toxic dye called a photosensitizer (PS) into the patient. This PS must then selectively accumulate in the tumour site and, on

irradiation with red light, produce singlet oxygen and other reactive oxygen species which selectively destroy the tumour leaving the healthy patient.

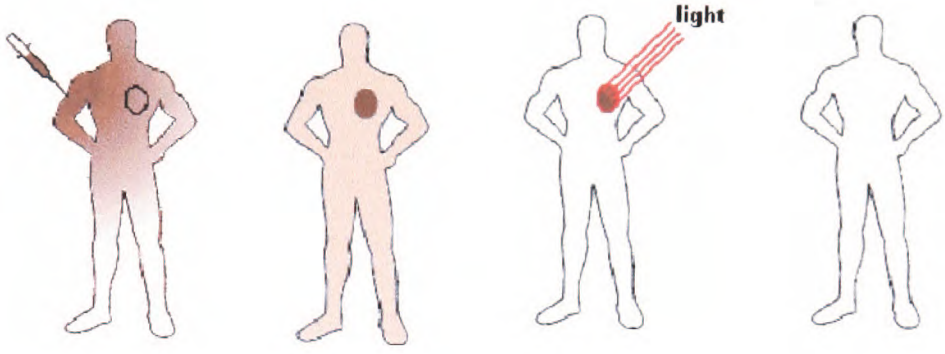

Figure 16. Photodynamic therapy of cancer. Involves injection of photosensitizer, localisation in tumour site and irradiation to produce singlet oxygen which leaves a healthy patient [29]

Although singlet oxygen is the main cytotoxic molecule produced by the photochemical excitation of the photosensitizer in the cells, other reactions can occur. The reactions of the excited photosensitizer can be classed into two types, type I reactions and type II reactions, and examples of both of these are given in figure 17 [30]. Type II reactions are characterised by dependence on oxygen concentration and include the production of singlet oxygen whereas type I reactions are characterised by dependence on target-substrate concentrations. In an anoxic environment, the excited photosensitizer can react with organic substrates (S) by electron exchange to produce an oxidised substrate (S^+) and a reduced PS (PS^-). In hypoxic conditions (low levels of oxygen) the reduced PS (PS^-) can react with oxygen (O_2) to form superoxide anions (O_2^-). This can then form the highly reactive hydroxyl radical ($^{\cdot}OH$).

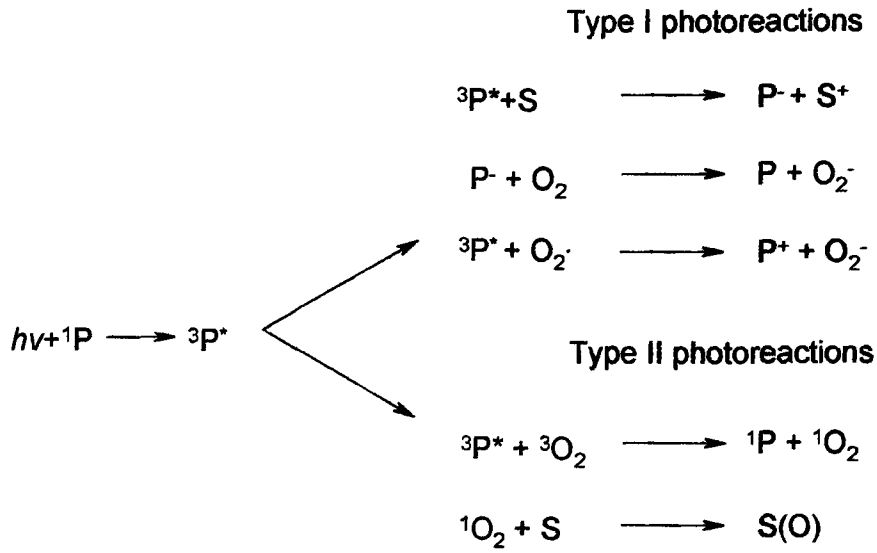

Figure 17. Photochemical reactions [30].

PDT relies on the production of singlet oxygen for its cidal effects and the production of singlet oxygen was discussed in section 1.5.2. Singlet oxygen can react with more than one target within a cell, as shown in figure 18, including DNA bases, proteins, and cholesterol found in cell membranes [31].

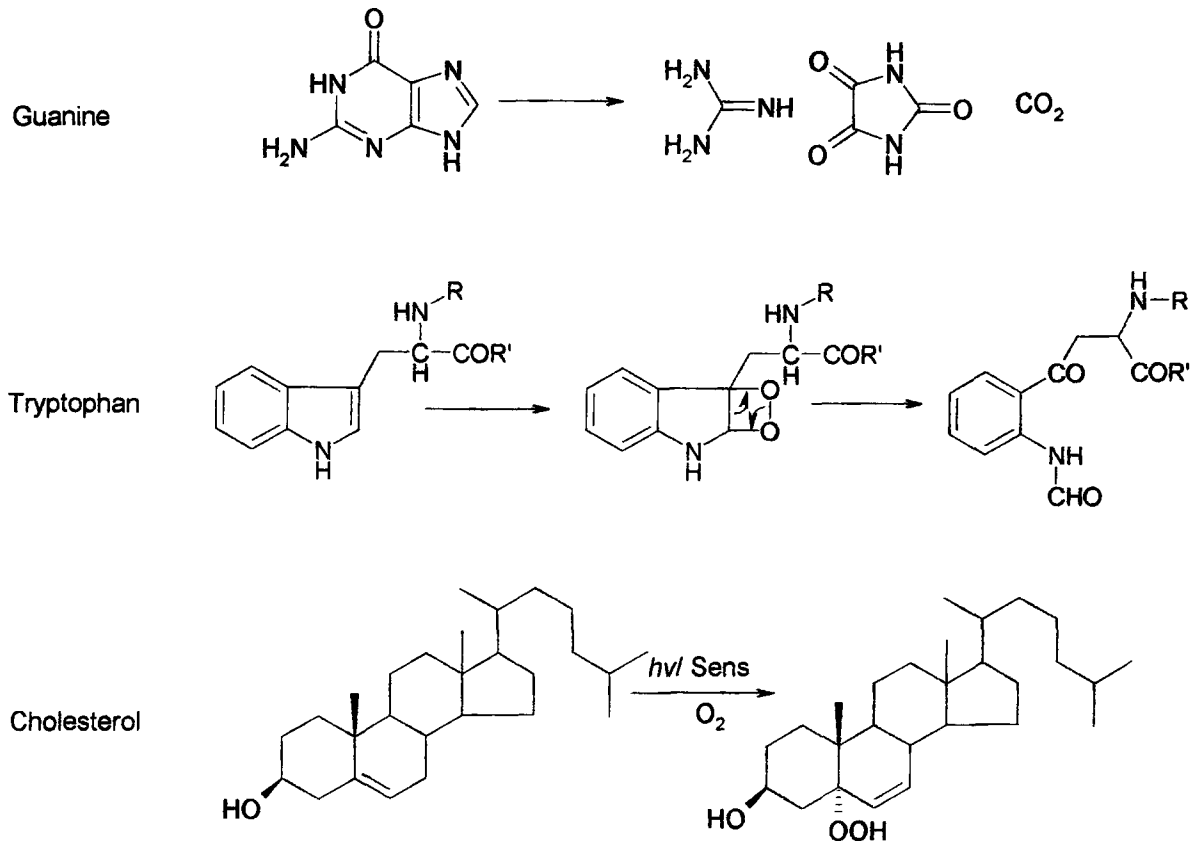

Figure 18. Targets for singlet oxygen reaction within a cell.

There are five factors which are necessary in order to produce a good PDT agent and these are:

1) Chemical purity
2) Minimal dark toxicity
3) Significant absorption at wavelengths that penetrate tissue deeply
4) High selectivity for target tissue
5) Rapid clearance from normal tissue.

Photofrin® fulfils these in that it has minimal dark toxicity and reasonable selectivity for target tissue. However it does not achieve chemical purity or significant absorption at wavelengths that penetrate tissue deeply and it is for this reason that it can not be used for deep-seated tumours and questions have arisen about the identity of its active

components. Tissue penetration is optimal with red light and this is shown pictorially in figures 19 and 20. Figure 19 shows the light absorption spectra of red blood cells overlaid with the light absorption spectra of a porphyrin based photosensitizer (a benzoporphyrin derivative, BPD). Red blood cells block the absorption of blue and green light though tissue and so the optimal wavelength to excite the porphyrin derivative is between 650-700 nm (red light).

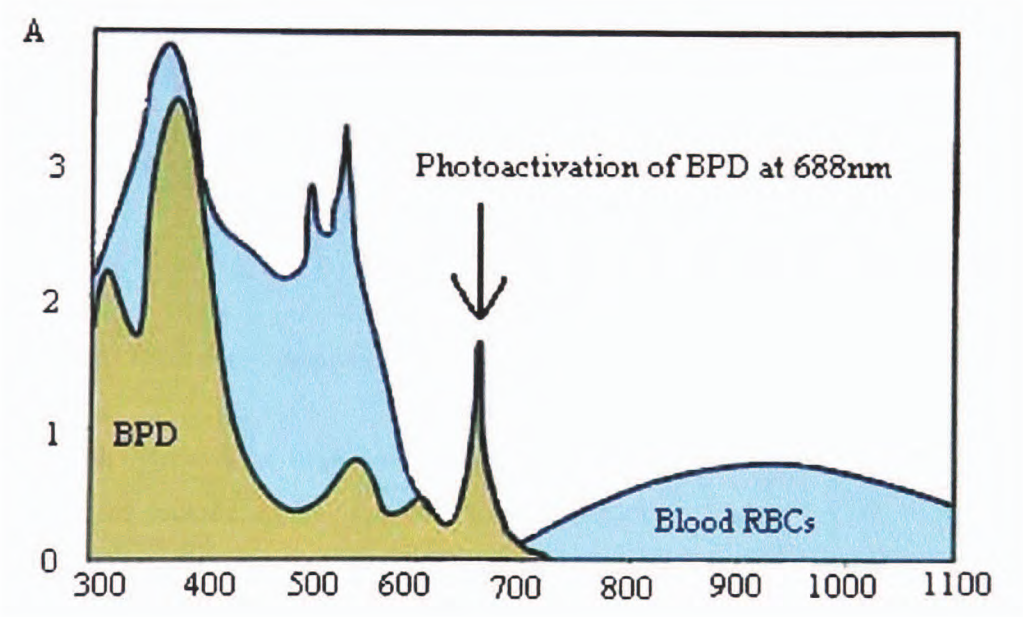

Figure 19. Light absorption spectra for red blood cells and a benzoporphyrin derivative (BPD) [32]

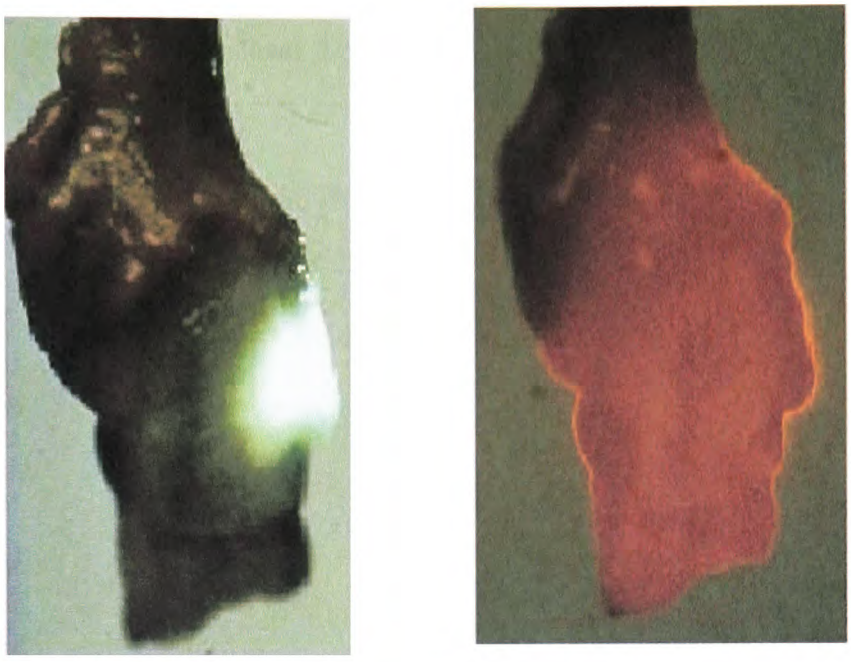

Figure 20. Light absorption through tissue is optimal with red light rather than white light [32]

Although red light must be used for PDT there are many types of light sources that can be used and these include argon / dye lasers, metal vapour lasers, KTP:YAG / dye lasers, diode lasers and other non laser light sources including light emitting diodes (LEDs) and these have been reviewed by Mang in some detail [33]. There are also many different types of photosensitizers in use for PDT as reviewed by Allison *et al* [34].

1.7. Photodynamic Antimicrobial ChemoTherapy (PACT).

1.7.1 Introduction to PACT.

PDT in cancer therapy is now well established and various groups have moved on to look at other areas to which the principles of PDT can be applied. Areas that have been looked at include age-related macular disease [35], inactivation of yeasts [36], inactivation of viruses [37], blood product disinfection [38], infected burn wounds [39] and ulcers

caused by bacteria. Photodynamic antimicrobial chemotherapy, or PACT, is potentially very useful in the treatment of chronic wounds or ulcers which are resistant to healing on their own or using conventional therapies, and this is a growing problem in the elderly (see figure 21).

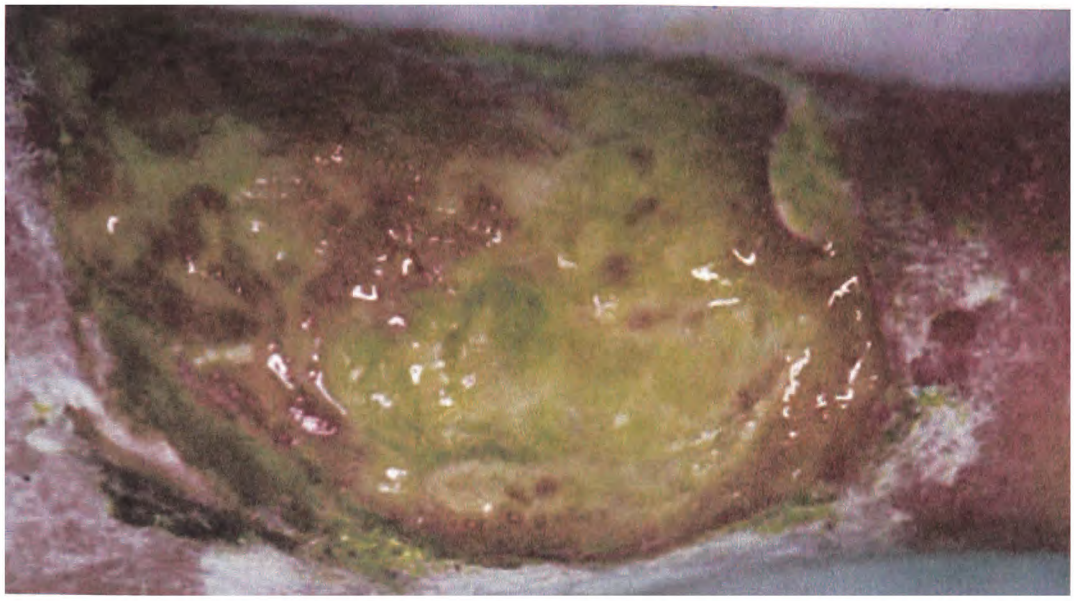

Figure 21. An example of an ulcer showing inflammation and immune response- this is likely to contain at least 10 different species of bacteria. [40].

The emergence of bacterial resistance to conventional antibiotics has left a gap in the market where new therapies are needed to cope with the demands of multiple drug resistant bacteria and the diseases that they cause. Many strains of bacteria are no longer susceptible to antibiotics due to the problem of developing resistance. PACT however is a therapy to which bacteria are less likely to build up a resistance to due to the nature of the singlet oxygen produced and the fact that it can attack multiple targets within the cell. The compounds can also potentially target anaerobic microorganisms through type I reactions. PACT is, however, limited to local, rather than systemic, infections because the body's natural flora needs to remain unaffected. There can also be problems with light delivery to internal sites, although deep-seated infections can now be treated due to the development of optical fibre technology.

1.7.2 Photosensitizers used in PACT.

There are a number of different types of photosensitizer that have been used in PACT and these include acridines, azines, macrocyclic photosensitizers such as porphyrins and phthalocyanines, naturally occurring sensitizers such as psoralens and polylysine conjugates attached to chlorins.

1.7.2.1 Acridine.

Adrien Albert, an Australian chemist worked with acridines **15** (shown in figure 22) and it was his work that lead to the understanding of their mode of action. He set the following parameters for antibacterial activity: 1) cationic ionization, 2) high levels of ionization at neutral pH and 3) planar molecular surface area $\geq 38 Å^2$. This hypothesis explained the activity against bacteria of many fused aromatic compounds.

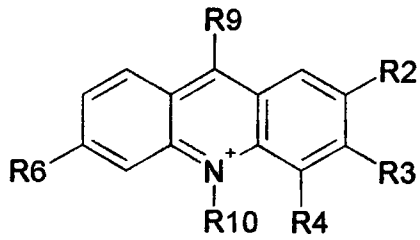

15

	R2	R3	R4	R6	R9	R10
Proflavin	H	NH_2	H	NH_2	H	H
Aminacrin	H	H	H	H	NH_2	H

Figure 22. Generic structure of acridines.

Albert showed that aminoacridines with electronic conjugation between the ring nitrogen and amino group were most active because of increased ionization of these compounds. Nucleic acids are the established sites of action of simple aminoacridine derivatives in bacteria. This is because, the planar area of the tricyclic acridine nucleus is ideally suited to intercalation between nucleotide base pairs in the helix and the positive charge aids targeting. DNA intercalation forms the basis of opposition to the use of acridines owing to the nucleic acid site of action resulting in positive mutagenicity testing *in-vitro*.

1.7.2.2 Azines

Figure 23 shows the generic structure of the azine photosensitizers with some specific examples [41]. The first synthetic antibacterial compounds were azine derivatives. They have a simple tricyclic skeleton. Methylene blue is an efficient nucleic acid intercalator and is relatively non-toxic to humans. It has been used for the inactivation of various pathogens contained in blood plasma and for the treatment of methaemoglobinaemia. Methylene blue and its related phenothiazinium structures are relatively easy to synthesize but are easily reduced to the neutral amine that is ineffective as a photosensitizer. The fact that the phenothiazine derivatives associate with nucleic acids suggests that the dyes would be more specific for pathogen reduction and cause less damage to red blood cells. However some of the phenothiazine is associated with red blood cells and the bound form of the dye is responsible for photo induced haemolysis. Photo treated red cells exhibit high rates of potassium efflux, which is indicative of membrane damage [42]. Small pores are produced which are permeable to ions but not haemoglobin. At ionic equilibrium, the internal osmotic pressure in ion permeable red cells is greater than the external osmotic pressure because haemoglobin contributes as an osmoticum. This imbalance in pressure leads to water influx, cell swelling and ultimately lysis.

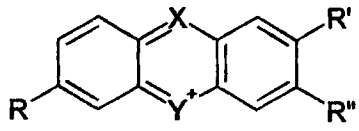

16

	R	R'	R''	X	Y	λ_{max}(nm)
Methylene blue	$N(CH_3)_2$	$N(CH_3)_2$	H	N	S	660
Toluidine blue O	$N(CH_3)_2$	NH_2	CH_3	N	S	625
Neutral red	$N(CH_3)_2$	NH_2	CH_3	N	NH	540
Proflavine	H_2N	NH_2	H	CH	NH	456
Acridine orange	$N(CH_3)_2$	$N(CH_3)_2$	H	CH	NH	492
Aminacrine	H	H	H	C-NH_2	NH	410
Ethacridine	H_2N	H	OC_2H_5	C-NH_2	NH	420

Figure 23. Azine photosensitizer structure with specific examples of some common azine based photosensitisers.

1.7.2.3. Porphyrins and Phthalocyanines.

Many groups have shown porphyrins to be efficient photosensitizers for use in PACT. While both naturally occurring and synthetic porphyrins can be used, the former are at a disadvantage due to similarities in their absorption spectra to endogenous porphyrins.

PACT studies by Orenstein *et al* showed that it was possible to kill *Staphylococcus aureus*, a Gram positive bacteria, using deuteroporphyrin [43] but Gram negative bacteria such as *Escherichia coli* and *Pseudomonas aeruginosa* could not be inhibited using deuteroporphyrin alone. Malik *et al* [44] overcame this problem by pre-treating the cells with either ethylenediaminetetraacetic acid (EDTA) or polymyxin B nonapeptide (PMBN). They found that cells pre-treated with EDTA lost up to 50% of their LPS into the medium due to an increased electrostatic repulsion between LPS molecules caused by the removal of the divalent cations. Cells pre-treated with PMBN did not cause the

release of LPS into the medium as with EDTA. The polycation bound tightly to the highly negatively charged surface and displaced the divalent cations. In doing so, they caused an expansion in the outer leaflet of the outer membrane which, in turn, caused the hydrophobic molecules to become less crystalline and allowed the partition of hydrophobic molecules from the external medium.

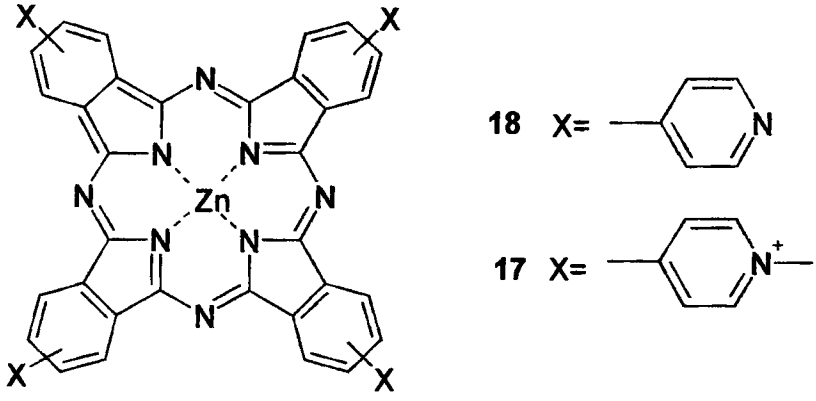

Figure 24. Zinc phthalocyanine used by Scalise *et al* [45] to inactivate *E.Coli*.

The use of phthalocyanines in PACT has been studied by several groups who have looked at the types of charge needed in order to inactivate bacteria. Scalise *et al* [45] synthesised a tetracationic zinc phthalocyanine derivative **17** (see figure 24) and compared this to the analogous non-charged phthalocyanine **18**. They found that it was possible to photoinactivate *E. coli* using the charged derivative (0.01% survival) but not the neutral one and that neither derivative produced any dark toxicity. A similar effect has been shown by Minnock *et al* [46] who tested the effect of different charges on the photoinactivation of Gram positive *Enterococcus seriolicida* and Gram negative *E. coli* and *P. aeruginosa* using the molecules shown in figure 25.

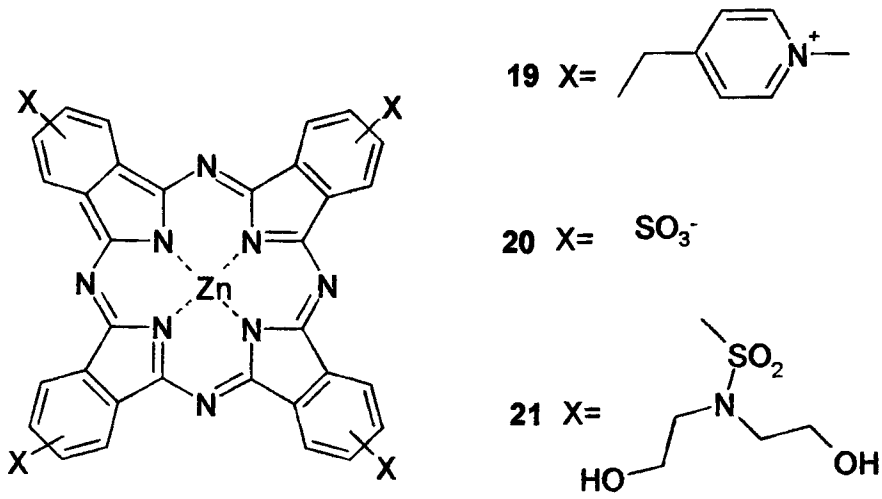

Figure 25. Cationic pyridinium phthalocyanine **19**, anionic tetra-sulphonated phthalocyanine **20** and neutral tetra-diethanolamine phthalocyanine **21**.

The results showed that the cationic compound could photoinactivate both Gram positive and Gram negative bacteria whilst the anionic and neutral molecules did not induce any appreciable decrease in cell survival.

Other studies, conducted using *meso* substituted porphyrins, have also shown that the molecules need to be cationic in order to photoinactivate both Gram positive and Gram negative bacteria. Several studies have been conducted using 5, 10, 15, 20–tetra-(4-N methylpyridyl) porphyrin **(22)** (TMPyP) shown in figure 26.

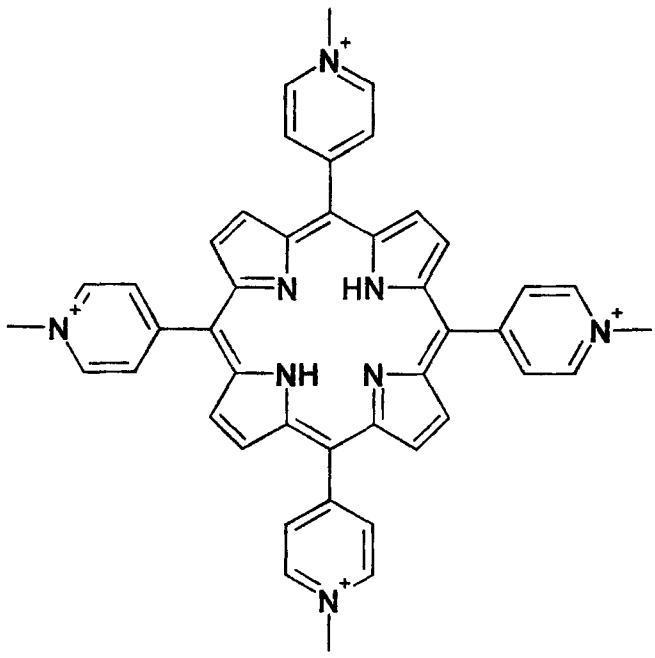

22

Figure 26. 5, 10, 15, 20–tetra (4-N-methylpyridyl) porphyrin **22** (TMPyP)

Nitzan and Ashkenazi [47] showed that **22** could be used to photoinactivate *E. coli* (Gram negative) and *A. baumannii* (Gram positive). Different light sources and different wavelengths were compared in this study. Using either red, green or blue light they found that green and red light needed a 8 to 16 or 20-fold higher light intensity, relative to blue light, for the total eradication of both bacteria at a concentration of 29.4 μmol/L. However despite their findings the use of blue light clinically would be irrelevant as it would have minimal transmission through tissue, conversely, the use of red light produces maximal tissue penetration and is more clinically relevant.

Merchat *et al* [48] compared the photodynamic activity of two cationic *meso*-substituted porphyrins, namely 5, 10, 15, 20-tetra (4-*N*-methyl-pyridyl) porphyrin tetraiodide **(22)** and 5, 10, 15, 20-tetra (4-*N, N, N*-trimethyl-anilinium) porphyrin **(23)** and compared their activity to the tetra anionic compound 5, 10, 15, 20-tetra(4-sulphonatophenyl) porphyrin **(24)** (Structures shown in figure 27). They found that the anionic compound had no appreciable photosensitizing activity against the Gram negative bacteria, but that all three compounds tested photo-inactivated Gram positive bacteria. The two cationic compounds

were both found to have good photosensitizing activity against Gram negative bacteria with no appreciable differences between the two compounds tested. Salmon-Divon *et al* [49] studied the mechanistic aspects of *E. coli* photo-inactivation using TMPyP. They suggested that TMPyP-dependent PDI of *E. coli* is primarily dependent on DNA damage rather than on protein or membrane malfunctions. However other authors have concluded that, although DNA damage does occur, it may not be the prime cause of bacterial cell death. The mechanisms of cell damage have been reviewed by Hamblin *et al* [50] who quoted studies using *Dinococcus radiodurans*, which is known to have a very efficient DNA repair mechanism and is easily killed by PDI, as a reason for DNA damage not being the prime cause of cell death. Instead they point the reader towards believing that damage to the cytoplasmic membrane is the main cause of bacterial cell death, quoting the alteration of cytoplasmic membrane proteins shown by Valduga *et al* and the disturbance of cell wall synthesis and appearance of a multilamellar structure near the septum of dividing cells, along with the loss of potassium ions from cells as reported by Salmon-Divon *et al* [49].

Several authors have started investigating the structure-activity relationships between various different cationic porphyrins [51, 52, 53, 54, 55]. Lazzeri *et al* [51] studied a series of asymmetrically *meso*-substituted cationic porphyrins shown in figure 28 and their activity against *E. coli*. They found that compounds **26** and **27** (Fig 29) produced ~ 5.5 log decrease in cell survival when treated with 10 μM solution whereas compound **25** gave ~ 4 log decrease and compound **28** (Fig 29) gave no significant decrease. From these results they concluded that the addition of the trifluoromethyl group made the molecule more amphiphilic and that it wasn't simply the cationic character that was important but the amphiphilic character also played a role in the PDI of Gram negative bacteria. Another study by the same authors [52] uses the compounds shown in figure 30.

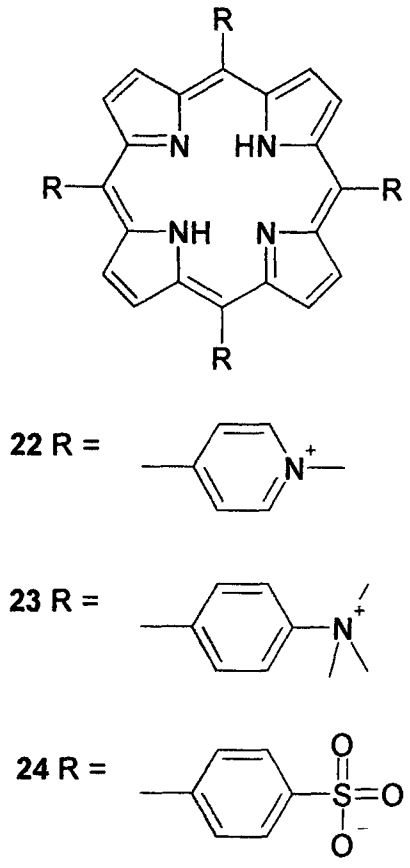

Figure 27. Structures of compounds used by Merchat *et al* [48] to compare photodynamic activity against Gram positive and Gram negative bacteria.

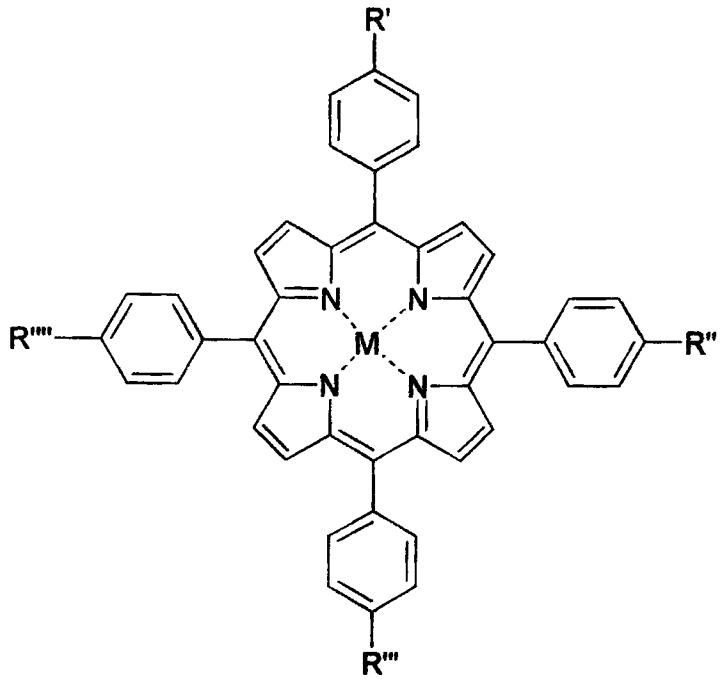

25 R' = R'' = $N^+(CH_3)_3I^-$ R''' = R'''' = CH_3 M = H_2

26 R' = R'' = R''' = $N^+(CH_3)_3I^-$ R'''' = CF_3 M = H_2

27 R' = R'' = R''' = $N^+(CH_3)_3I^-$ R'''' = CF_3 M = Pd(II)

28 R' = R'' = R''' = CH_3 R'''' = COOH M = H_2

Figure 28. Series of asymmetric porphyrins synthesised by Lazzeri *et al* [51] and tested against *E. coli*.

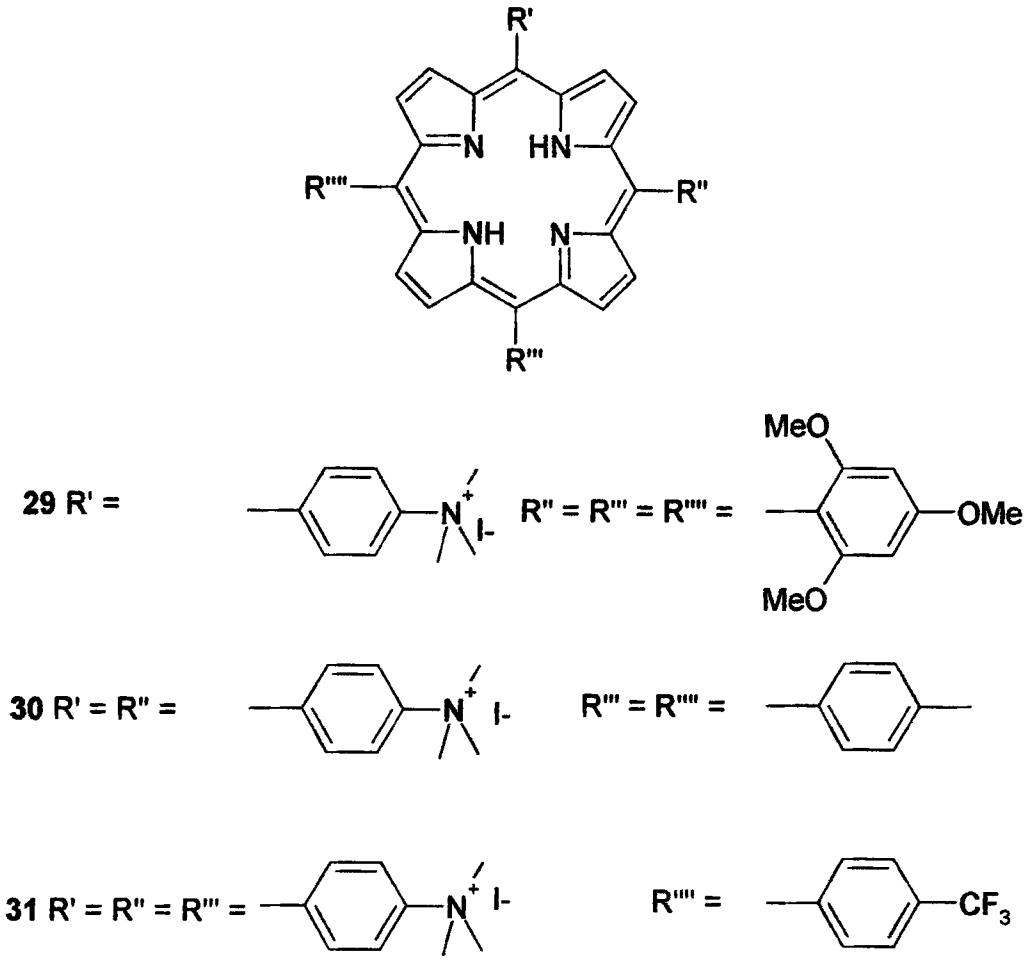

Figure 29. Series of porphyrins synthesised by Spesia *et al* [52] and tested against *E. coli*.

From these compounds it was found that the mono and di-cationic (**29** and **30**) compounds only photo-inactivated *E. coli* when the cells were irradiated without being washed, but that the tri-cationic porphyrin **31** gave promising results even with washing the cells prior to irradiation. The authors concluded from this, that photoinactivation of *E. coli* increases with increasing cationic charge.

Merchat *et al* [53] conducted a structure-activity relationship study using *Enterococcus seriolicida*, a Gram positive bacteria, *Vibrio anguillarum* and *E. coli*, both Gram negative bacteria. They used a series of mono-, di-, tri- and tetra-cationic porphyrins as shown in figure 30.

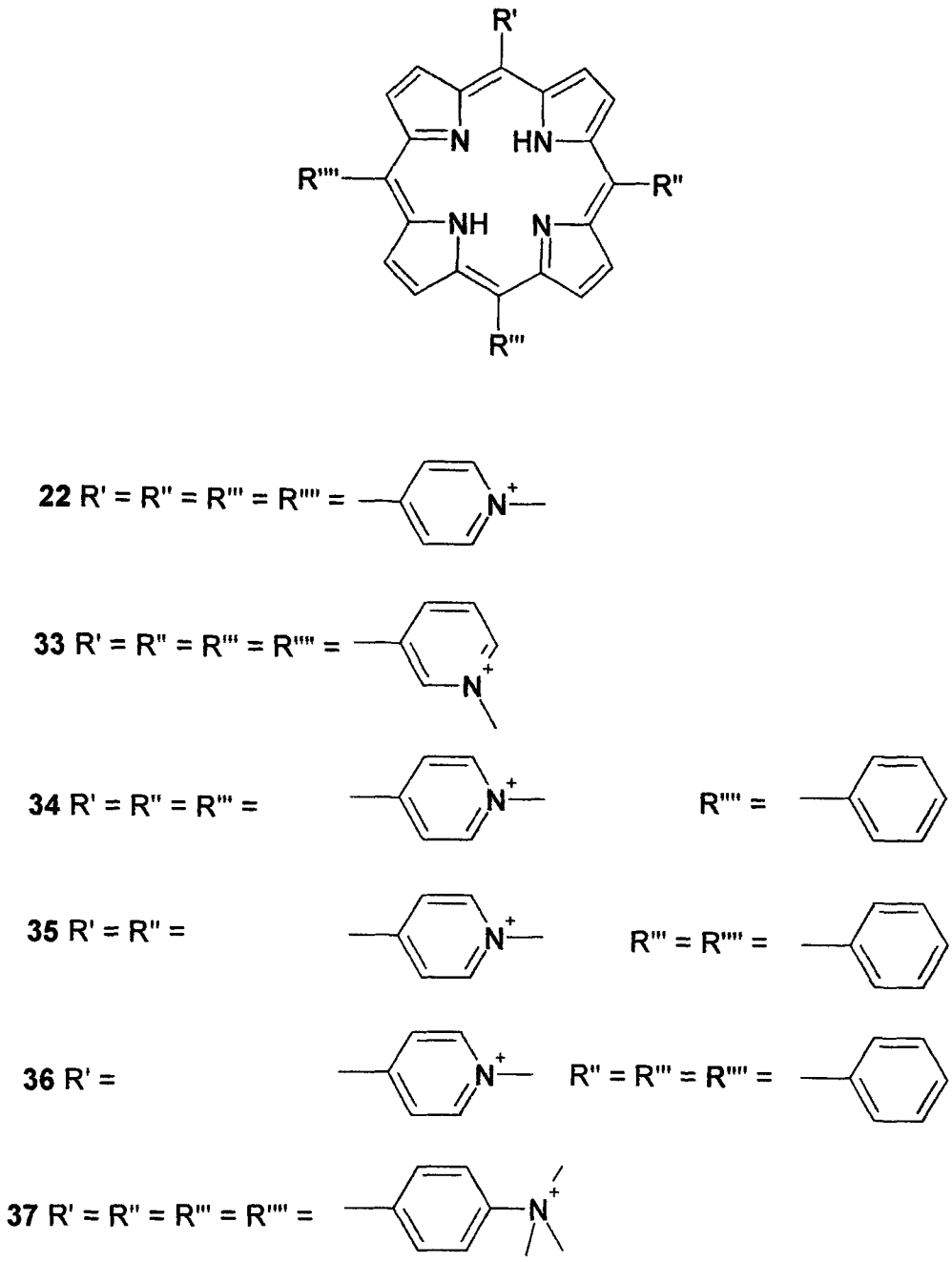

Figure 30. Series of porphyrins synthesised and assayed against *Enterococcus seriolicid, Vibrio anguillarum* and *E. coli* by Merchat *et al* [53].

Merchat *et al* [53] showed that all the porphyrins in figure 30 had a very similar affinity for Gram positive and Gram negative bacteria, which was reduced when the porphyrin was incorporated into liposomes prior to incubation. The tetra-cationic isomers (**22, 33,**

37) exhibited a nearly identical photosensitizing activity, both showing a ~ 4 log decrease in cell survival. This compared to ~ 6 - 7 log decrease for the tri- and di-cationic porphyrins (**34, 35**). The results from this study show that *meso*-substituted cationic porphyrins efficiently photosensitize the inactivation of both Gram positive and Gram negative bacteria, and this property appeared to be independent of the number or position of positive charges in the *meso* substituents. Merchat *et al* [53] proposed that the presence of one or more positively charged groups plays an essential role in orientating the photosensitizer toward sites which are critical for the stability of cell organisation and / or cell metabolism.

Reddi *et al* [54] conducted a structure activity relationship study looking at TMPyP **(22)** and its derivatives when one of the methyl groups are replace with longer carbon chains of C6, C10, C14, C18 and C22. These compounds were assayed against *E. coli* and *S. aureus* and the results are shown in table 5. It was found that the C10, C14 and C18 chains were the most efficient photosensitizers and the authors concluded that a limited increase in hydrophobicity of the photosensitizer enhances its affinity for bacterial cells.

Porphyrin	Concentration (μM)	Growth inhibition (%) *E.coli*	Growth inhibition (%) *S.aureus.*
22 TMPyP	8.3	29	96
38 C6	0.4	5	47
	8.3	99	-
39 C10	0.4	46	74
	0.8	96	-
40 C14	0.4	82	73
	0.8	100	-
41 C18	0.4	26	42
	0.8	58	59
42 C22	0.4	-	27
	0.8	3	70

Table 5. Percentage inhibition of growth for *E. coli* and *S. aureus*. Structure-activity relationship study by Reddi *et al* [54].

Trannoy *et al* [55] conducted a structure-activity relationship study in which they compared the cationic porphyrins as shown in figure 31 and they used these porphyrins to treat pathogens in red blood cells.

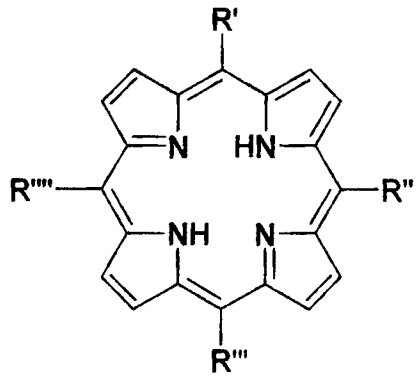

23 R' = R'' = R''' = R'''' =

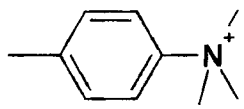

22 R' = R'' = R''' = R'''' =

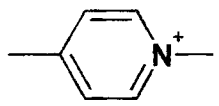

43 R' = R''' =

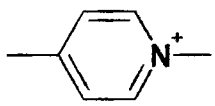

R'' = R'''' =

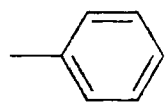

44 R' = R'' =

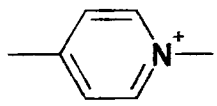

R''' = R'''' =

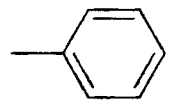

45 R'' = R''' = R'''' =

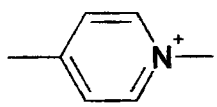

R' =

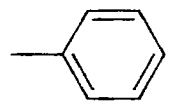

46 R' = R'' = R''' = R'''' =

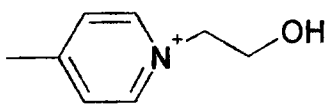

Figure 31. Structures synthesised and assayed [55]

They found that the mono-phenyl-tri-(*N*-methyl-4-pyridyl) porphyrin **45** was the best sensitizer against the vesicular stomatis virus (VSV).

1.7.2.4. Poly-lysine conjugates.

Tomé *et al* [56] have reported the synthesis of new conjugates of poly-L-lysine (PL) with either neutral or cationic *meso*-tetra-substituted porphyrins (see figure 32) and tested their activity against *S. aureus*, MRSA and *E. coli*. They found that the phototoxic effect was more pronounced in the presence of a polylysine moiety, because the polylysine chain can interact with the outer wall structure of Gram negative bacteria, thereby increasing its permeability. No dark toxicity was seen for either conjugate and both killed MRSA and *S. aureus* up to >6 log cell survival. The cationic compounds **48** and **49** (Fig 32) were the only ones to photo-inactivate the *E. coli* with a 4-5 log cell survival at a concentration of 1-5 μM.

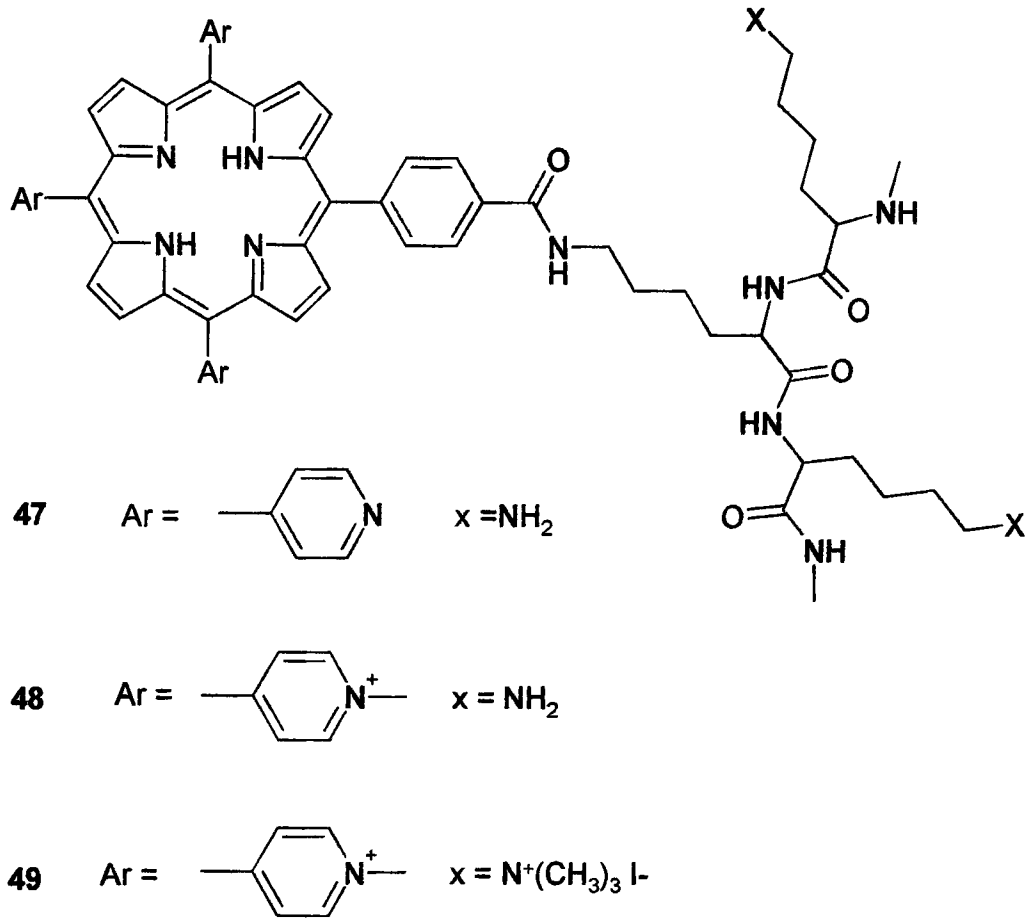

Figure 32. Poly lysine conjugates with either neutral or cationic charge.

Porphycenes are electronic isomers of porphyrins and Polo *et al* [57] have conjugated them to polylysine moieties of different chain lengths. The polylysine chains were either 1000-4000 MW (1-4 lysine monomers, average MW = 2900) or 15000-30000 (15-30 lysine monomers, average MW = 20700). Porphycene when neutral has no PDI effect but on binding to a polylysine chain, which is cationic at physiological pH, significant toxicity against Gram negative bacteria was reported. The 14-30 lysine chain exerted bacteriostatic action in the dark whereas the 1-4 polylysine (PL) chain showed no such effect. At a concentration of 1 μM both the 1-4 chain and the 15-30 chain gave significant photosensitivity, although *E. coli* was less susceptible than *S. aureus* and on increasing the concentration to 10 μM it was possible to achieve a 95% loss in cell viability for *E. coli.*

Soukos *et al* [58] have tested the hypothesis that polymeric conjugates between PL and C_{e6} **50** (see figure 33 for structures) selectively target bacteria for photodestruction. They varied the charge of the conjugates from cationic through neutral to anionic and investigated the selectivity they showed towards two oral bacteria and an oral epithelial cell line (HCPC-1). They found that conjugation of C_{e6} to PL promotes the uptake of C_{e6} by the bacteria and HCPC-1 cells and that the uptake is concentration-dependent. The bacteria tested were *P. gingivalis* and *A. viscosus* and they both showed the highest uptake for the cationic conjugate. HCPC-1 cells accumulated 30 to 100 times less C_{e6} from the cationic conjugate than the bacteria did. Photodynamic treatment showed no dark toxicity in either bacteria or the HPCL-1 cells at a concentration of 5 μM and the results for the photoinactivation are summarized in table 6. The mammalian cells will accumulate the C_{e6} conjugate **51**, as do the bacteria, however the former are spared due to the mammalian cells needing time to internalize the PS.

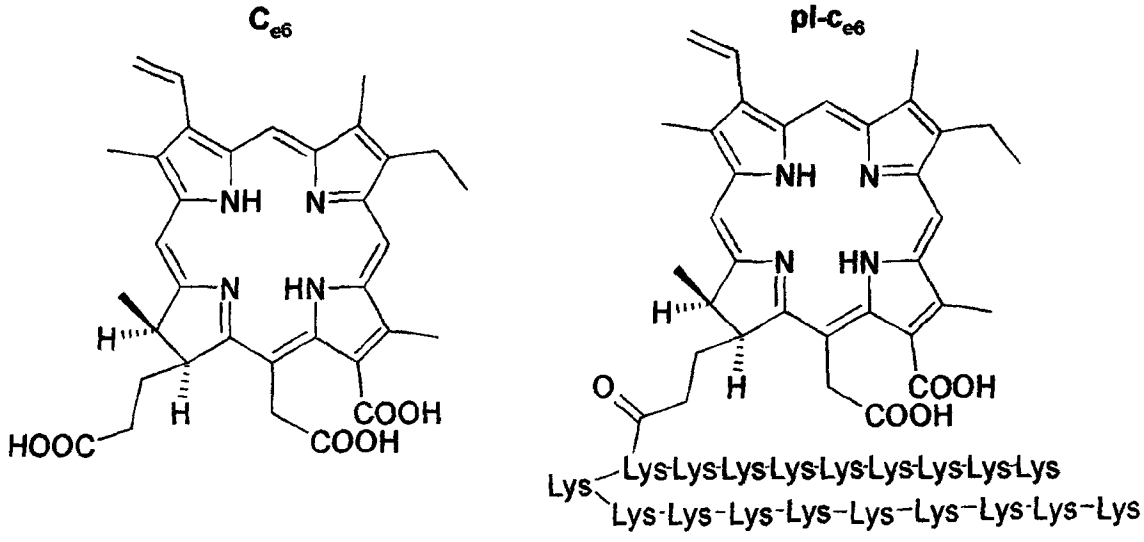

50 **51**

Figure 33. Structures of free chlorin and polylysine conjugate used by Soukos *et al* [58].

Photosenstitizer	% survival for organism or cell line.		
	P.gingivalis	*A.viscosus*	HCPC-1
Cationic conjugate	1.1 ± 0.9	< 0.01	102 ± 2.1
Anionic conjugate	23.9 ± 3.3	24.3 ± 3.4	127 ± 2.9
Neutral conjugate	9.3 ± 2.6	21.2 ± 1.5	108 ± 4.2
Free C_{e6}	39.6 ± 2.3	52.9 ± 5.9	126 ± 2.7
Mixture (PL and c_{e6})	8.1 ± 1.8	2 ± 0.1	100 ± 2.5

Table 6. Results of Soukos *et al* photoinactivation of *P. gingivalis, A. viscosus* and HCPC-1 cells [58].

Hamblin *et al* [59] developed this study to investigate the effects of PL chain lengths and Gram classification on the photodynamic inactivation of bacteria. They used two polylysine chain lengths of 8 and 37 lysines respectively and found that *S. aureus* and *E. coli* took up comparable amounts of the conjugates, but only *S. aureus* took up the free C_{e6} **50**. The photoinactivation of the Gram positive *S. aureus* was fluence dependent for the free C_{e6}, the 8 lysine conjugate and to a lesser extent with the 37 lysine conjugate. In contrast to this it was only the 37 lysine conjugate that inactivated the Gram negative *E.coli* at concentrations of 4μM, and much higher concentrations of 100 μM were needed for photoinactivation using the 8-lysine conjugate. Again in this study the incubation time was found to be important as the survival fraction after illumination decreased fairly sharply with increasing incubation time for both species.

Although compounds have been tested *in-vitro* for their ability to photoinactivate bacteria, very few studies have been completed *in-vivo*. Two *in-vivo* studies have been conducted by Hamblin *et al* [60] and Gad *et al* [61]. The first of these studies reports on the use of optical techniques to monitor and treat *Pseudomonas aeruginosa* wound infections in mice [60]. The PL-C_{e6} conjugate used in the *in-vitro* studies by the same authors [59, 60] was topically applied to a wound and this was followed by illumination with red light. The bacteria used were genetically engineered to emit bioluminescence which can be detected using an intensified charge-coupled device (CCD) camera. The mice used were all males of between 20 and 25g, their backs were shaved and they were anesthetized prior to surgery. Wounds were made down to, but not through the

panniculus carnosu so that there was no bleeding within the wound. 40 mice were used and they were split into 4 groups as follows: untreated controls (bacteria alone), bacteria plus light, bacteria plus conjugate and bacteria, light and conjugate. Because *Pseudomonas aeruginosa* is invasive, only the PDT-treated wounds could be monitored until healing occurred as all the control mice died of systemic sepsis whereas 90% of treated mice survived. PDT treatment produced a fluence dependent loss in bioluminescence until only a trace remained at a light dose of 240 J/cm^2. The second *in-vivo* study by Gad *et al* [61] involved the treatment of established bacterial infections in mice rather than treatment 30 minutes after infection as in the previous study. Although mice have been used as animal models of bacterial infection they are not particularly susceptible to developing established soft-tissue infections. In this study *S. aureus* were genetically modified to emit bioluminescence. The mice, again all male and weighing between 20 and 25g, were pre-treated with two doses of cyclophosphamide in order to create a temporary state of neutropenia which will allow the infection to take hold. A slight reduction in bacterial bioluminescense was observed after initial injection of the PL-C_{e6} conjugate and this was further reduced after 30 minutes incubation in the dark. On illumination there was a light dose dependent reduction in bioluminescense after each 40 J/cm^2 increment. After 160 J/cm^2 bioluminescense had decreased to the limit of detection and no re-growth of bacteria occurred.

The studies reported thus far in the literature have concentrated on a limited range of structures. It has been suggested that the amphiphilic character as well as the cationic character of porphyrins is important in the PDI of bacteria. A new route to cationic porphyrins is needed in which the amphiphilic character of the molecule can be altered relatively easily and this it should make it possible to produce a library of compounds which can be screened to assess the PDI of bacteria.

Chapter 2. Photosensitizer synthesis. Tetra-cationic compounds.

2.1. General synthetic routes to cationic porphyrins.

2.1.1. Quaternisation of 5, 10, 15, 20-tetra-(4-*N*-methylpyridyl) porphyrin and 5, 10, 15, 20-tetra-(4-*N*, *N*, *N*-trimethyl-anilinium) porphyrin.

The commercially available 5, 10, 15, 20-tetra-(4-*N*-methylpyridyl) porphyrin **22** and 5, 10, 15, 20-tetra-(4-*N*, *N*, *N*-trimethyl-anilinium) porphyrin **23** have been widely used in PACT studies and one reason for their popularity is that they can be synthesised relatively easily. The 5, 10, 15, 20-tetra-(4-*N*-methylpyridyl) porphyrin **22** is synthesised as shown in scheme 5. The first step in the synthesis is an Adler reaction, where pyridine-4-carboxaldehyde **52** and pyrrole **14** are refluxed in propionic acid for 30 minutes, then allowed to cool to room temperature. The precipitate is then filtered off and washed with methanol to afford 5, 10, 15, 20-tetra-(4-pyridyl) porphyrin **53** as a purple solid. The 5, 10, 15, 20-tetra-(4-pyridyl) porphyrin is then treated with methyl iodide to produce 5, 10, 15, 20-tetra-(4-*N*-methyl-pyridyl) porphyrin **22** as its tetra iodide salt.

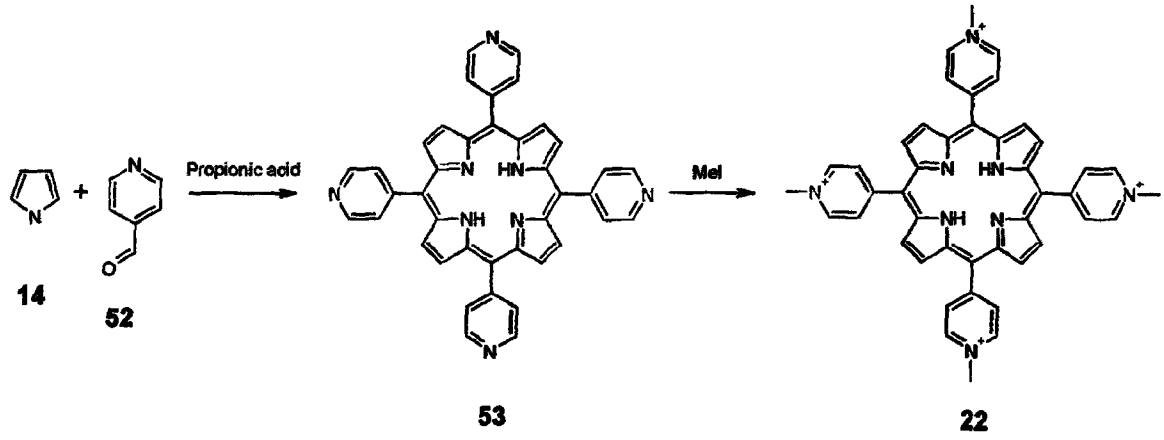

14 **52** **53** **22**

Scheme 5. Synthetic route to 5, 10, 15, 20-tetra-(4 -*N*-methyl-pyridyl) porphyrin **22**.

Similarly the 5, 10, 15, 20-tetra-(4-*N*, *N*, *N*-trimethyl-anilinium) porphyrin **23** (scheme 6) is made by means of an Adler reaction between 4-dimethylaminobenzaldehyde **54** with pyrrole, the product of which **55**, is then treated with methyl iodide to produce 5, 10, 15, 20-tetra-(4-*N*, *N*, *N*-trimethyl-anilinium) porphyrin **23**.

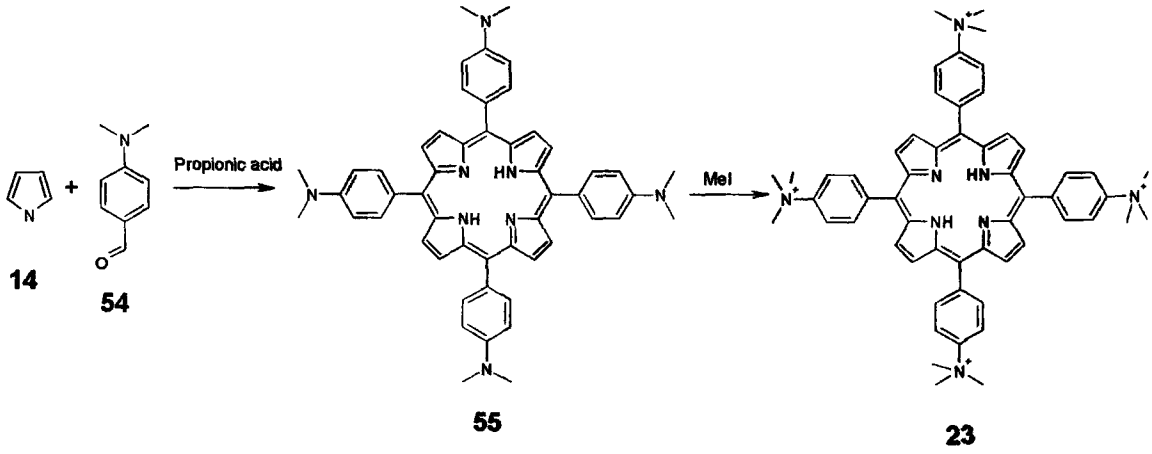

Scheme 6. Synthetic route to 5, 10, 15, 20-tetra-(4-N, N, N-trimethyl-anilinium) porphyrin.

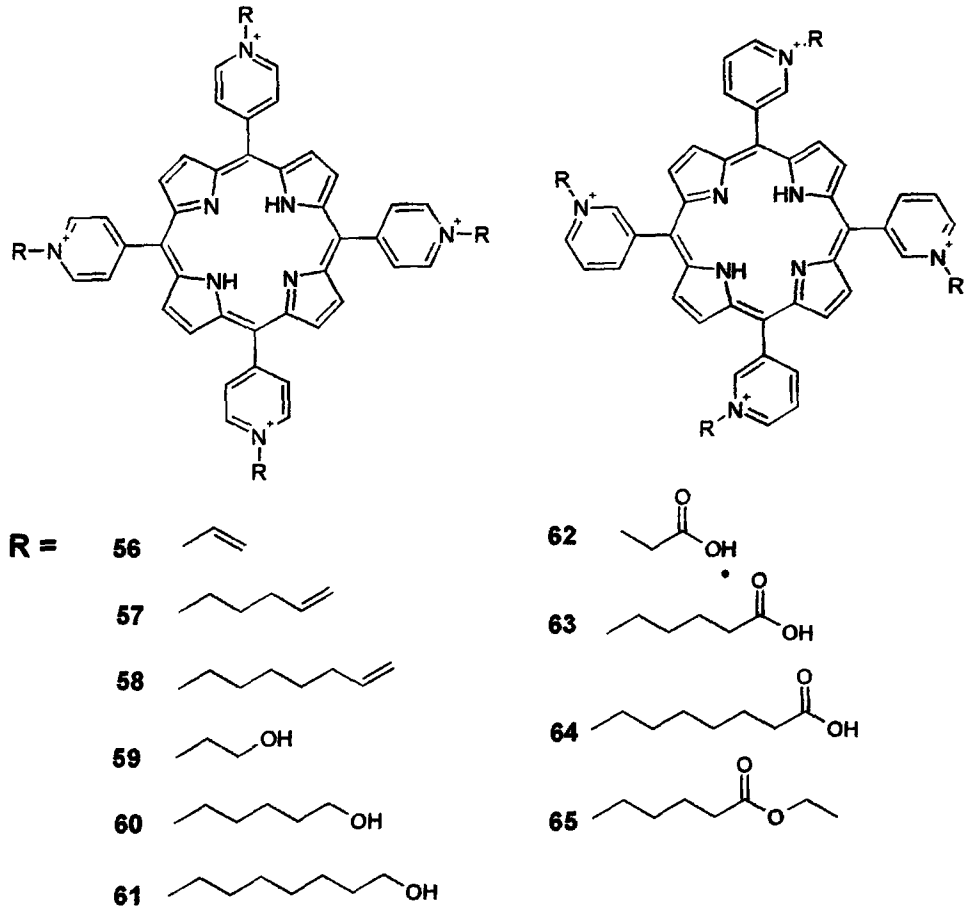

Figure 34. Compounds made by Dancil *et al* [62].

5, 10, 15, 20-tetra-(4-*N*-methyl-pyridyl) porphyrin has been derivatized by Dancil *et al* [62] in order to systematically determine the influence of *N*-alkyl chain length, *N*-alkyl chain functionality and peripheral charge distribution on the self-association of cationic porphyrins. A series of compounds were synthesised which are shown in figure 34. The general procedure for alkylation of 5, 10, 15, 20-tetra-(4-pyridyl) porphyrin **55** was to heat the starting porphyrin in DMF to 100°C and slowly add the alkylating agent, in this case alkyl bromides. The solution was then refluxed for 4 hours, cooled and the product collected by filtration.

2.1.2. Quaternisation of 22 using perfluorocarbon chains.

Perfluorocarbons (PFCs) have attracted much attention due to their unusual properties [63, 64, 65, 66]. PFCs can dissolve large volumes of respiratory and other non-polar gases and Lowe's review [67] gives examples of the uses which PFCs have found in medicine and cell biotechnology. The comparison of oxygen solubility in water (2.2 mmol/l) with that of oxygen solubility in PFCs (35-44 mmol/l) [67] suggested that this property could be used to enhance the effect of PDT. We hypothesised, that the addition of highly fluorinated groups, to cationic porphyrins, would increase oxygen concentration. On irradiation with red light, this would then yield an increased yield of singlet oxygen, and hence lower drug concentrations would be needed. We therefore decided to attempt the synthesis of molecules bearing highly fluorinated side chains. In order to achieve this analogues of the commercial compounds, 5, 10, 15, 20-tetra-(4-*N*, *N*, *N*-trimethyl-anilinium) porphyrin **(23)** and 5, 10, 15, 20-tetra-(4-pyridyl) porphyrin **(22)** were used. Namely, the syntheses of 5, 10, 15, 20-tetra-(4-*N*-(1H, 1H, 2H, 2H-perfluorohexyl)-pyridyl) porphyrin **(66)**, 5, 10, 15, 20-tetra-(4-*N*- (1H, 1H, 2H, 2H-perfluorododecyl)-pyridyl) porphyrin **(67)**, 5, 10, 15, 20-tetra-(4-(*N*-(1H, 1H, 2H, 2H-perfluorohexyl)-dimethylanilinium) porphyrin **(68)** and 5, 10, 15, 20-tetra-(4-(*N*-1H, 1H, 2H, 2H-perfluorododecyl)-dimethylanilinium) porphyrin **(69)** were attempted. The structures of these compounds are shown in figure 35. The synthesis followed the methods of Dancil *et al* [62], except that alkyl iodides were used rather than alkyl bromides. However the synthesis and purification of these molecules proved to be problematic.

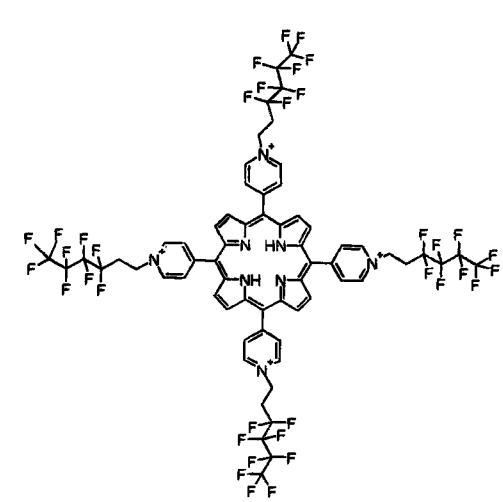

66

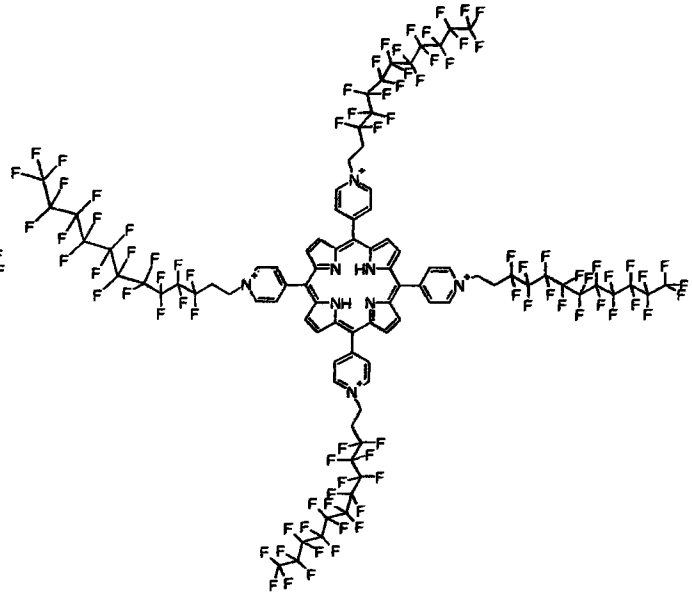

67

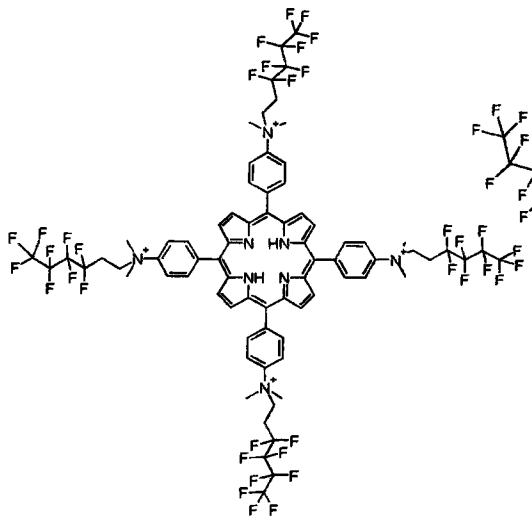

68

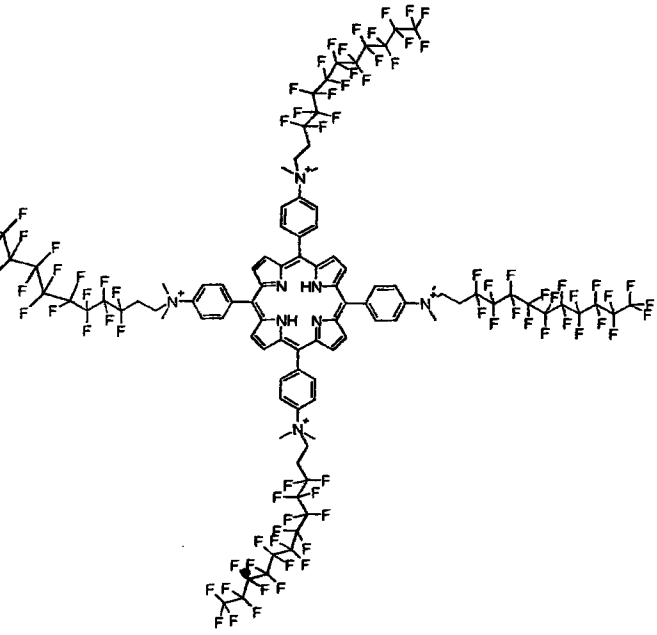

69

Figure 35. 5, 10, 15, 20-tetra-(4N- 1H, 1H, 2H, 2H-perfluorohexyl-pyridyl) porphyrin **(66)**, 5, 10, 15, 20-tetra-(4N- 1H, 1H, 2H, 2H-perfluorododecyl-pyridyl) porphyrin **(67)**, 5, 10, 15, 20-tetra-(4N- 1H, 1H, 2H, 2H-perfluorohexyl-anilinium)porphyrin **(68)**, 5, 10, 15, 20-tetra-(4N- 1H, 1H, 2H, 2H-perfluorododecyl-anilinium)porphyrin **(69)**.

It was found that under the conditions used by Dancil *et al* [62] no change was seen from the starting material even on refluxing for up to 3 days. Thin layer chromatography (TLC) in 90/10/0.5 chloroform: methanol: 25% NH_3 in H_2O indicated that a cationic product was formed which was not a porphyrin. It was deduced that the iodoperfluorohexane and iodoperfluorododecane were reacting with decomposition products of the solvent, dimethylformamide (DMF), instead of the nitrogen atoms on the porphyrins. Dioxane was used instead of DMF but again no change was seen from the starting materials, possibly due to the boiling point of dioxane lowering the reaction temperature. Purification of the compounds, from a reaction which had gone partly to completion, was problematic due to the porphyrins sticking to the amberlite ion exchange resin.

Tjahjono *et al* [68, 69] have synthesised octa-cationic porphyrins bearing diazonium rings, as shown in figure 36, and these were used to study their interaction with calf thymus DNA. They were synthesised via an Adler reaction between either 1-methylimidazole-2-carboxaldehyde or 1-methylpyrazole-4-carboxaldehyde and pyrrole, followed by quaternisation with methyl iodide.

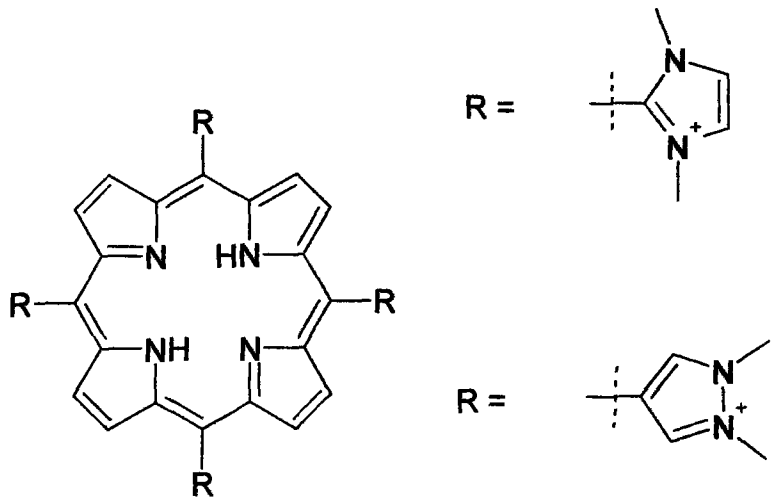

Figure 36. Tjahjono's octa-cationic porphyrins bearing diazonium rings.

These porphyrins were then metallated with Mn^{III}, Ni^{II}, Cu^{II} or Zn^{II} and it was found that the nickel and copper porphyrins intercalated into the 5'GC3' step of ctDNA, in which

the 2 positively charged *N, N*-dimethylpyrazolium rings were located in the major groove and the 2 others were located in the minor groove. The manganese porphyrin was bound edge-on at the 5'TA3' step of the minor groove of ctDNA and the zinc porphyrin was bound face-on at the 5'TA3' step of the major groove of ctDNA

2.1.3. Attempted synthesis of 5, 10, 15, 20-tetra (4-(aminomethyl) phenyl) porphyrin (70).

Amines at physiological pH are cationic and therefore photosensitizers with multiple amine groups can be used in PACT. It was decided to attempt the synthesis of the 5, 10, 15, 20-tetra-(4-(aminomethyl)phenyl) porphyrin **(70)**, shown in figure 37.

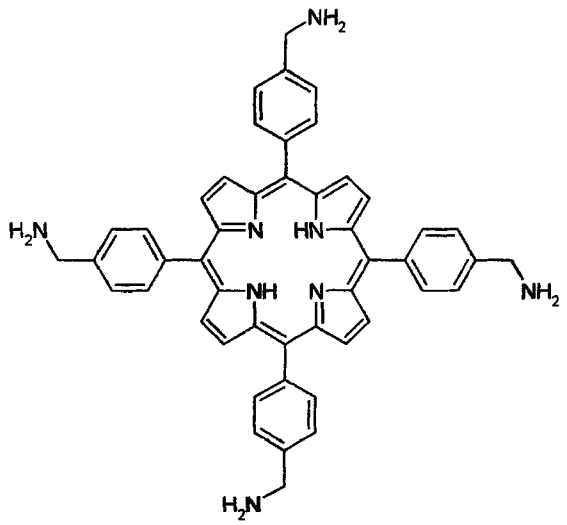

70

Figure 37. 5, 10, 15, 20-tetra-(4-(aminomethyl)phenyl) porphyrin.

It has been reported that the aminomethyl groups can be synthesised by the reduction of a nitrile group [71, 72, 73, 74, 75]. 5, 10, 15, 20-tetra-(4-cyanophenyl) porphyrin **(71)** was synthesised via an Adler reaction between 4-cyanobenzaldehyde **(72)** and pyrrole **(14)** in propionic acid. Several attempts were then made to reduce the nitrile groups although all these attempts proved fruitless. 5, 10, 15, 20-tetra-(4-cyanophenyl) porphyrin **(71)** was stirred with lithium aluminium hydride in THF in the dark for 4 days, but no change was seen relative to the starting material by TLC. Reduction using borane-THF complex was

attempted by refluxing **71** with this reagent for 18 hours, but no porphyrin was left in the reaction mixture after this time as determined by UV-visible spectroscopy. It was concluded that the borane-THF complex had attacked the macrocycle. Milder conditions of stirring the reaction at room temperature were attempted, but no change was seen from the starting materials. Finally, reduction of the nitrile groups was attempted by hydrogenation using palladium on carbon catalyst in THF / EtOH (3:1). The reaction was carried out at 40 psi overnight with shaking but again there was no change from the starting material and the majority of the porphyrin stuck to the palladium carbon catalyst. Zhang and Lippard [76] have employed the Gabriel synthesis on porphyrins to convert bromomethyl groups into aminomethyl groups. Brunner and Schellerer [74] have also used a modified version of this reaction in order to produce the phthalimide group via a Mitsunobu methodology [77] using triphenylphosphine, potassium phthalimide and diethyl azodicarboxylate (DEAD). The advantage of this method is that it has one less step in the synthetic route to the amine. It bypasses the bromination of the hydroxymethyl groups prior to conversion to phthalimido groups. It was decided to attempt a modified Gabriel synthesis [78] from 5, 10, 15, 20-tetra-(4-(hydroxymethyl)phenyl) porphyrin **(73)** using DEAD, PPh_3, and potassium phthalimide, in order to produce 5, 10, 15, 20-tetra-(4-(phthalimidomethyl)phenyl) porphyrin **(74)**, as shown in figure 38. **74** was successfully made in a 54% yield, and so the hydrolysis of 5, 10, 15, 20-tetra-(4-(phthalimidomethyl)phenyl) porphyrin was attempted, using NaOH and HCl, as described by Lavallee *et al* [79]. However the hydrolysis proved problematic. The reaction did not go to completion, by TLC, and purification proved problematic due to the solubility's of both compounds in aqueous work up (both stick to silica / alumina and so column not possible).

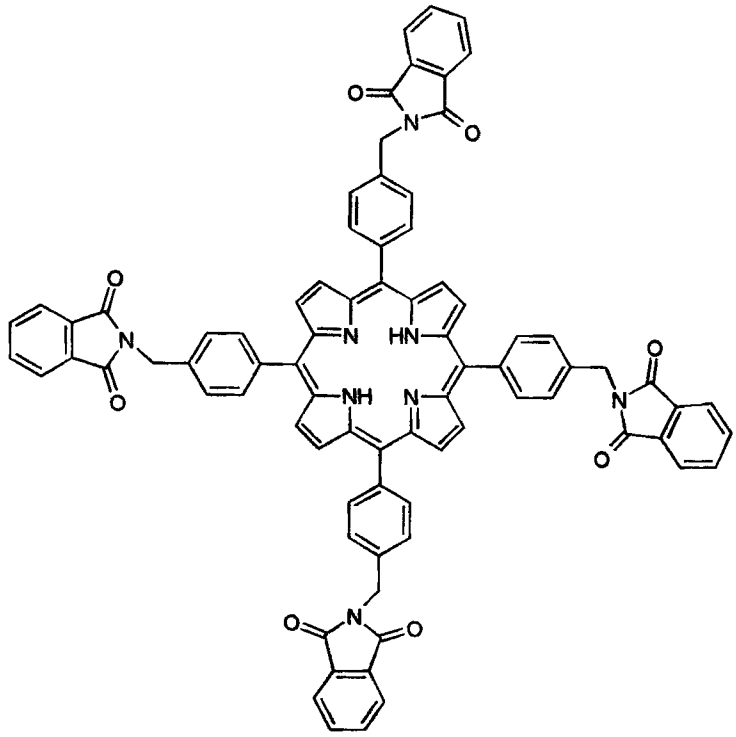

74

Figure 38. 5, 10, 15, 20-tetra-(4-(phthalimidomethyl)phenyl) porphyrin

2.1.4. Alternative route to tetra-cationic porphyrins.

Cationic porphyrins are usually derived from 5, 10, 15, 20-tetra-(4-pyridyl) porphyrin or 5, 10, 15, 20-tetra-(4-aminophenyl) porphyrin and in using these types of compounds the nitrogen atoms are already attached to the porphyrin precursor prior to quaternisation to cationic centres. This methodology limits the number and type of cationic compounds that can be made to the amount of halo-alkanes that are available. Ideally what is needed is a synthetic route that can be manipulated in order to give as diverse a range of cationic centres as possible with the minimal amount of steps involved in the synthesis. One such route was developed by Jin *el al* [80, 81]. They produced water soluble cationic porphyrins containing different phosphonium and ammonium cations derived from one precursor, namely, 5, 10, 15, 20-tetra-(4-(chloromethyl)-phenyl) porphyrin **(80).** Initially they had to make the starting benzaldehyde, 4-chloromethylbenzaldehyde **(79),** as shown in Scheme 8. This was achieved by protection of the aldehyde as an acetal, reduction of the methyl ester group to the hydroxyl group, chlorination, and finally deprotection of the

acetal to give the desired aldehyde. **79** was then reacted with pyrrole under Lindsey conditions to afford **80** in a 47% yield. **80** was reacted with either excess triphenylphosphine or triethylamine in DMF to produce the compounds shown in figure 39.

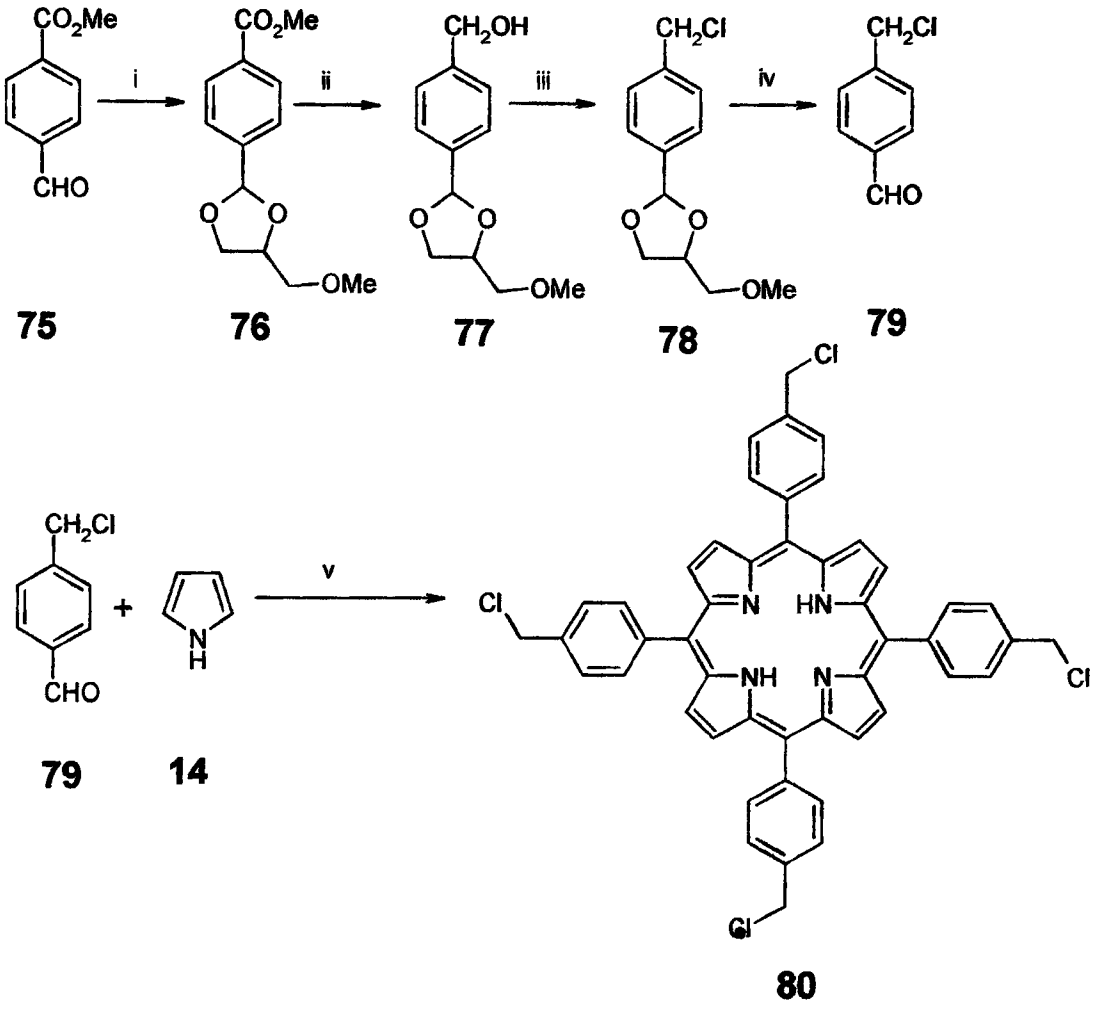

Scheme 8. Synthetic routes to **79** and **80** [80, 81]. i) glycidyl methyl ether (excess), tetrabutylammonium bromide (cat.), 80°C,3 days; ii) a. $LiAlH_4$ in THF, 70°C, 16hrs b. $NH_4Cl_{(aq)}$; iii) PPh_3, CCl_4, reflux, 3hrs iv) EtOH, 2M HCl room temp, 1 hr; v) a. BF_3-Et_2O, $CHCl_3$, room temp, 1hr. b. chroranil, NH_3, $CHCl_3$, reflux, 1hr.

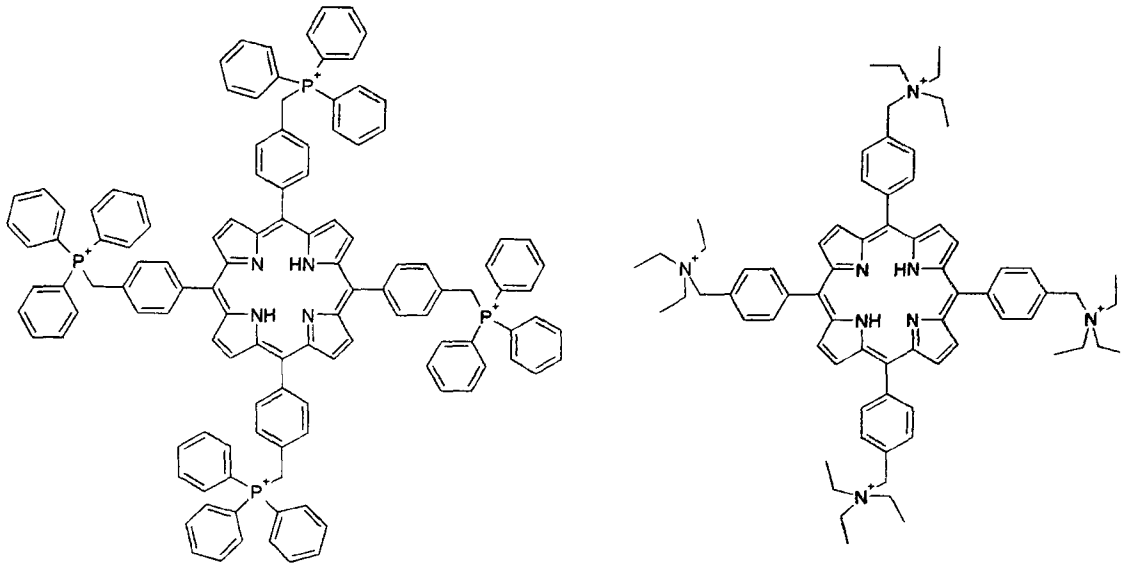

81 82

Figure 39. The structures of **81** and **82** [80, 81].

2.2. Synthetic route used.

Although some structure-activity relationship studies are available in the literature most have been conducted on commercially available porphyrins. A new series of compounds have been synthesised to study the effect of lipophilicity, aromatic vs aliphatic groups around the cation, and whether the analogous phosphorous cations show significant differences in photo-inactivating bacteria compared with their nitrogen analogues.

The synthetic route devised by Jin *et al* [80] has been adapted to allow a parallel synthesis, from one intermediate compound, in which numerous compounds can be made simultaneously and their structure-activity relationships compared *in-vitro*. The retrosynthetic analysis is shown in figure 40 and the synthetic route chosen for use, is shown in Scheme 9. Retrosynthetic analysis showed two possible routes to the intermediate compound 5, 10, 15, 20-tetra-(4-(bromomethyl)phenyl) porphyrin **(83)**. Retrosynthetic route 1 shows a two step method where 5, 10, 15, 20-tetra-(4-methylphenyl) porphyrin **(84)** is synthesised via an Adler reaction from pyrrole **(14)** and 4-methyl benzaldehyde **(85)**. Bromination of 5, 10, 15, 20-tetra-(4-methylphenyl) porphyrin **(84)** would then afford the desired intermediate. Bromination reactions using

NBS and a radical initiator have been used for this however the β-positions could also be brominated, and this would result in extensive chromatography in order to isolate the desired compound. Although retrosynthetic route 2 has more steps than route 1 they are widely used and afford high yields hence this was the chosen route to **83**. The initial step in the synthesis was an Adler reaction between 4-formyl-benzoate **(86)** and pyrrole **(14)**. The 5, 10, 15, 20-tetra-(4-(carboxymethyl)phenyl) porphyrin **(87)** was then reduced using $LiAlH_4$ in dry THF to 5, 10, 15, 20-tetra-(4-(hydroxymethyl)phenyl) porphyrin **(73)**. Bromination, using PBr_3 in dioxane, gave the intermediate compound 5, 10, 15, 20-tetra-(4-(bromomethyl)phenyl) porphyrin **(83)**. It was decided to use **83** rather than **80** because the bromide ion is a better leaving group than the chloride ion, and hence reactions should be more facile and an increased number of compounds could be made for the library. **83** was spilt into batches and the parallel synthesis of cationic porphyrins was conducted by heating **83** in DMF and adding the appropriate phosphine, amine or arsine. Purification of final compounds was achieved by precipitation between methanol and diethyl ether followed by microfiltration.

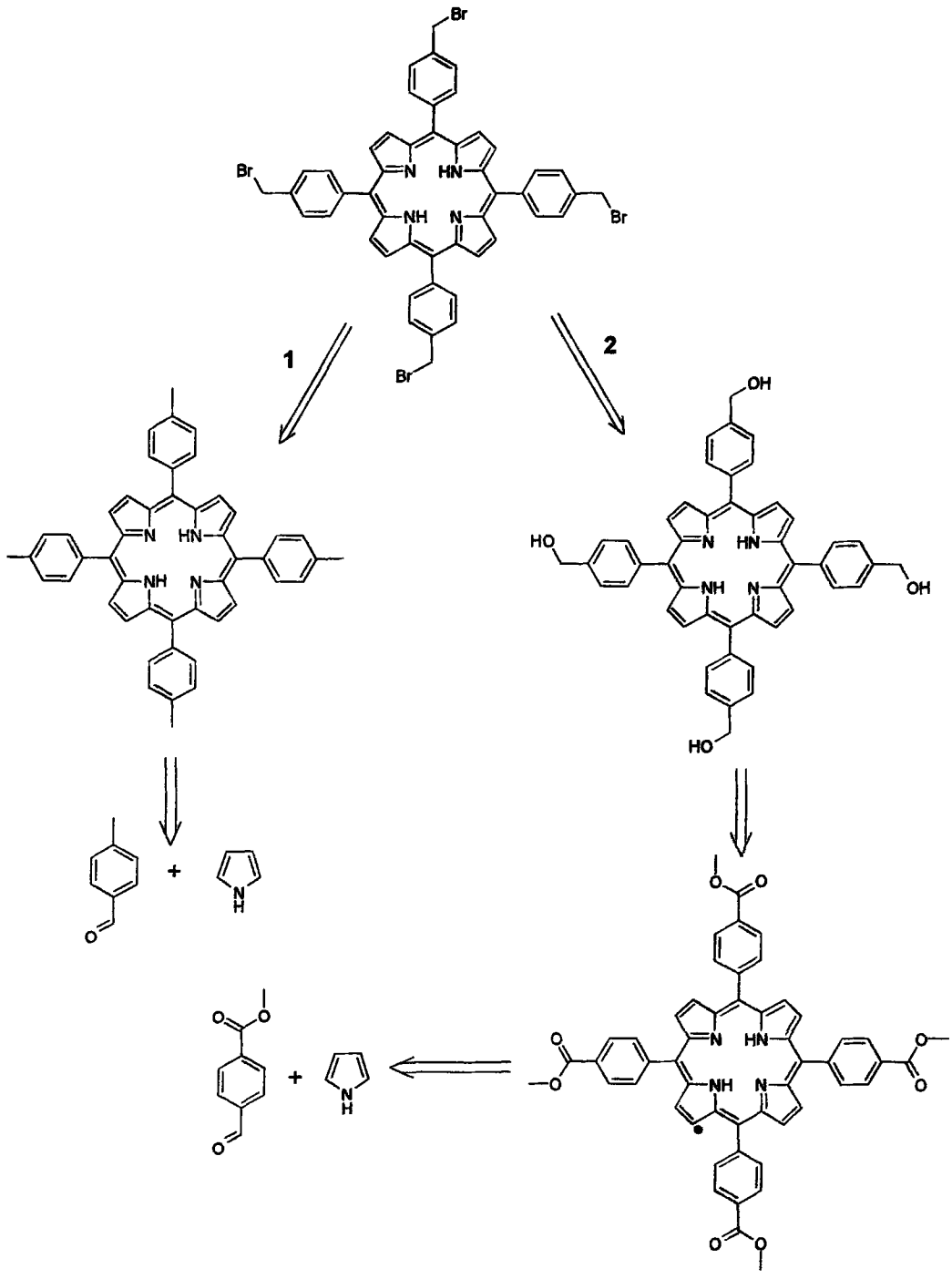

Figure 40. Retrosynthetic analysis of 5, 10, 15, 20-tetra-(4-(bromomethyl)phenyl) porphyrin **(83)**.

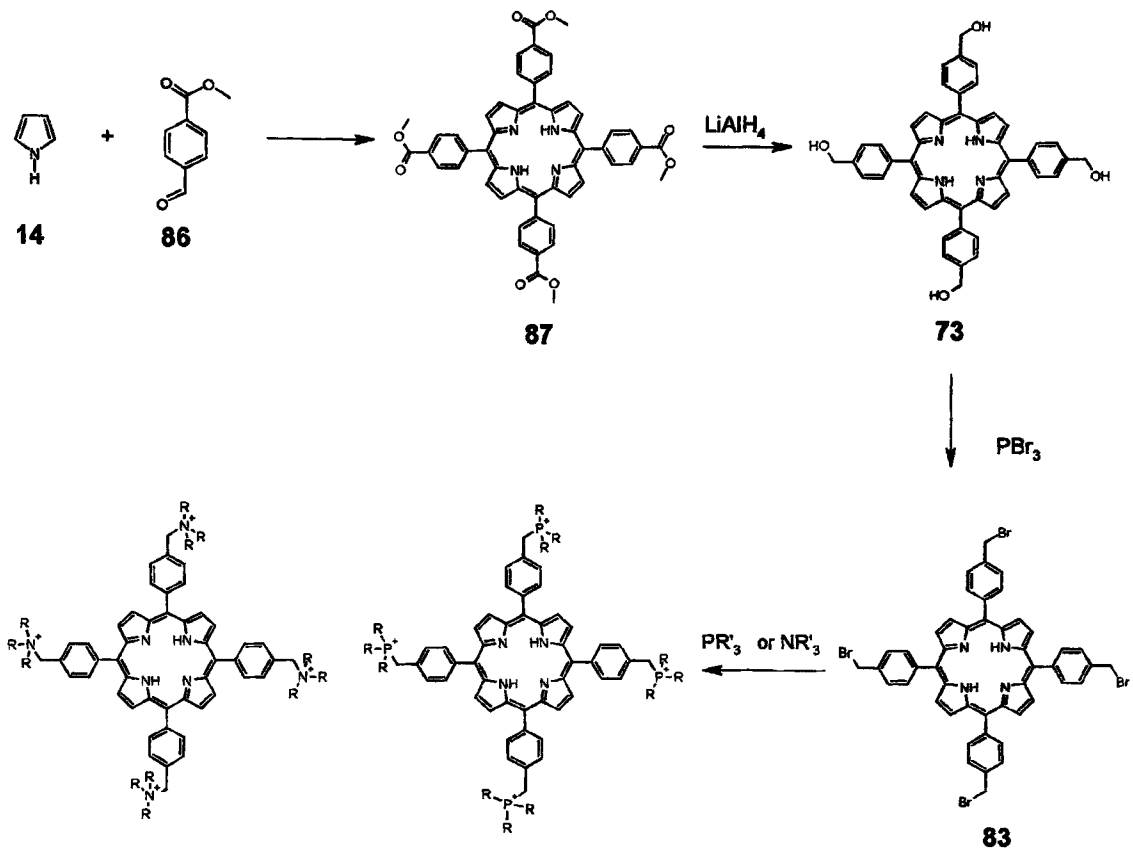

Scheme 9. Synthetic route used for the library of cationic porphyrins.

2.3. Parallel synthesis vs step-wise synthesis.

It was decided to use a parallel synthesis rather than a stepwise synthesis in order to minimise the amount of reaction steps needed and hence to improve the yield. The intermediate 5, 10, 15, 20-tetra-(4-(bromomethyl) phenyl) porphyrin was produced and was subsequently split into batches for the parallel production of the final library of compounds.

2.4. Library of compounds made.

Figure 41 shows the combinatorial library of compounds made for use in PACT.

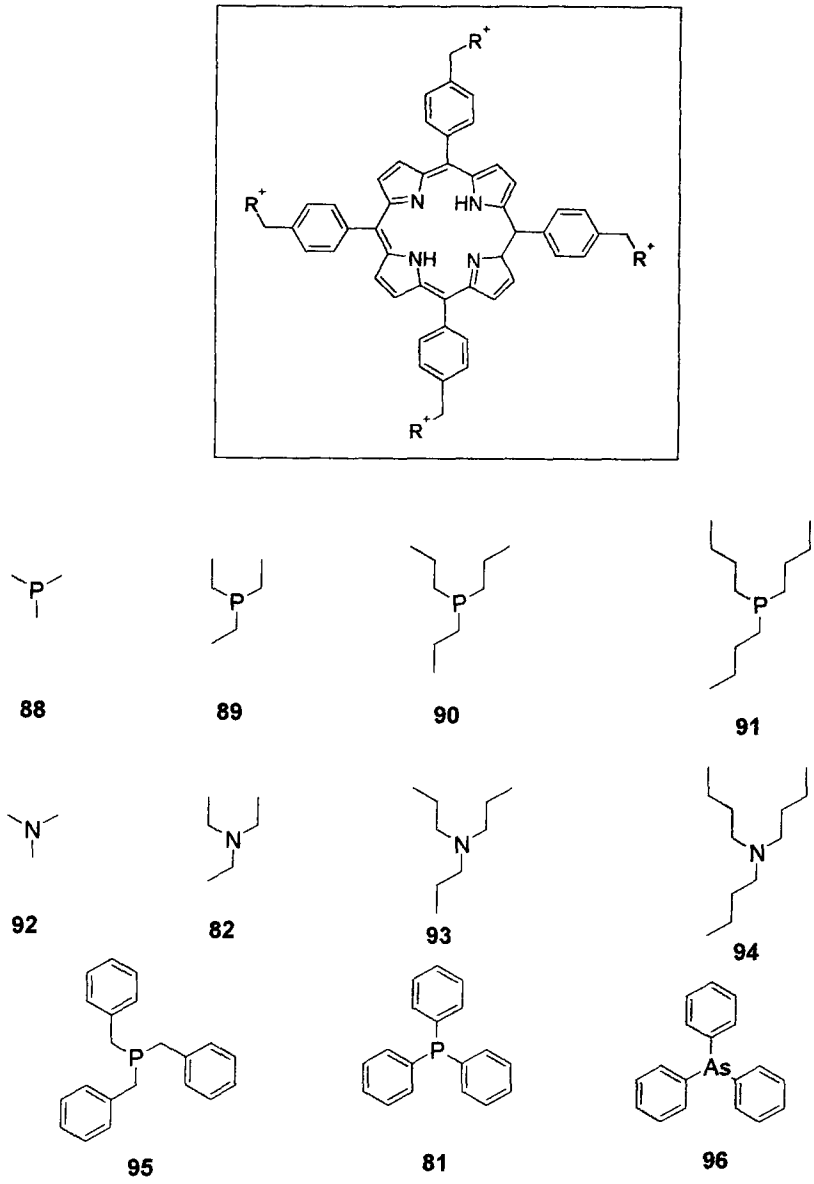

Figure 41. Library of compounds made for use in PACT (all counter ions are Br^-).

series of cationic compounds have been made for use in PACT. An additional three ɔmpounds were provided by Dr. R. Hudson and are shown in figure 42. Compounds **97** ıd **99** have cationic charges, although the groups surrounding the cationic centres differ. ɔmpound **98** however, I believe to be the neutral compound shown in figure 43, hence it

may not have any biological activity. The electrospray mass spectrum of compound **98** shows a lone peak at 1065.0 (M^+) which suggests that the compound is not charged, due to the lack of any (M^{4+}), $(M + Br)^{3+}$, or $(M + 2Br)^{2+}$ peaks shown for all of the other tetra cationic porphyrins.

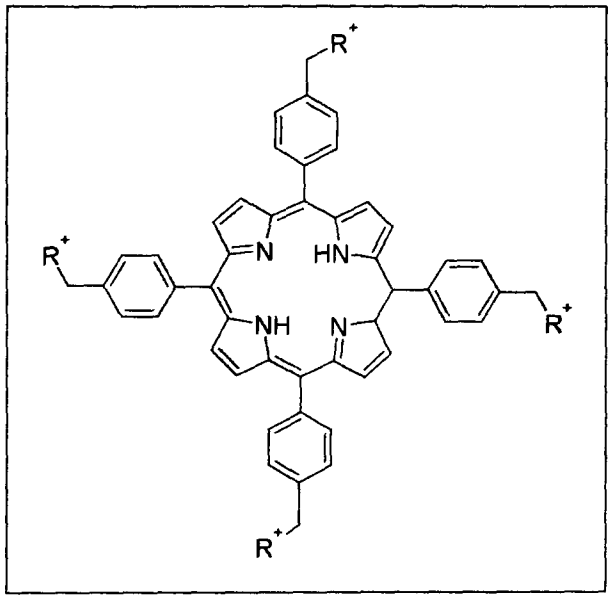

97 R = 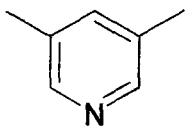

98 R = 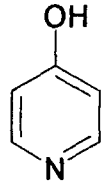

99 R = 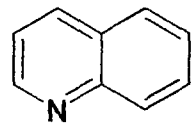

Figure 42 Compounds supplied by Dr. R. Hudson for use in PACT.

was now possible to compare the structure-activity relationships for the PDI of bacteria om nitrogen, phosphorous and arsenic cations and analyse these using standard ualitative Structure Activity Relationship (QSAR) methods.

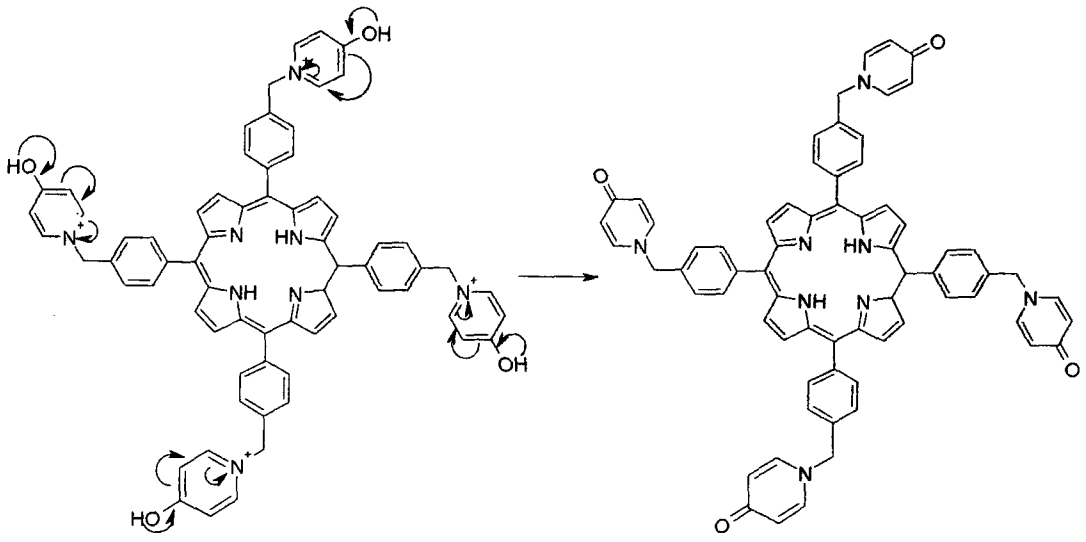

Figure 43. Alternative structure of compound **98**.

Chapter 3. Compounds with greater than 4 cationic charges.

Cationic porphyrins have been utilised for PACT, the most studied being 5,10 15, 20-tetra-(4-*N*-methylpyridyl) porphyrin **22** or related compounds derived from this porphyrin core. Spesia *et al* [52] showed that the PDI of *E. coli* increases with increasing positive charge, using compounds with between 1 and 4 cationic charges. To explore this hypothesis further it was decided to investigate the use of photosensitizers with greater than four cationic charges. This would then allow for the comparison of bacterial PDI for both the octa- and tetra-cationic compounds.

3.1. Octa-cationic porphyrins.

3.1.1. Attempted synthesis of octa-cationic porphyrins.

Marzilli *et al* [82] have synthesised an octa-cationic porphyrin, **100**, for use in DNA binding studies, as shown in figure 44.

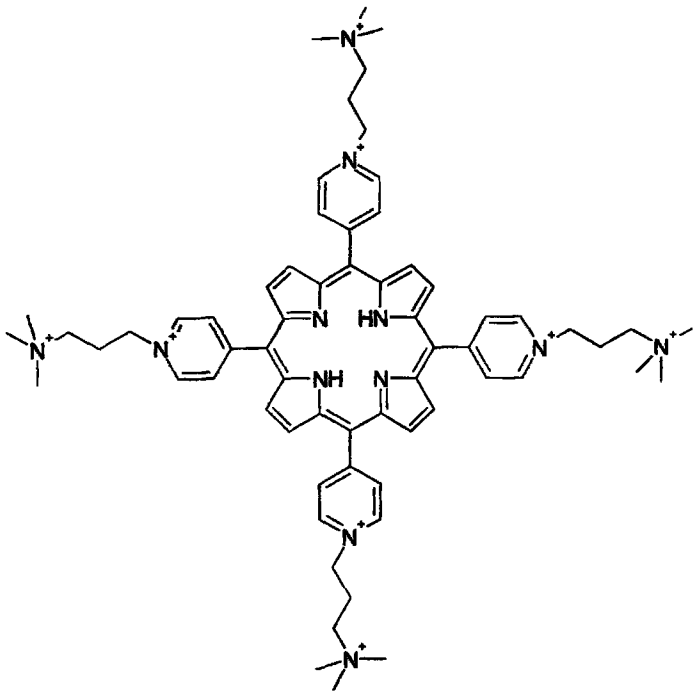

100

Figure 44. **100** made by Marzilli *et al* for use in DNA binding studies [82]

Schneider *et al* [83] have also examined DNA interactions of porphyrins bearing ammonium side chains. They investigated cationic ammonium groups spaced at a distance from the macrocycle (scheme 10) rather than close to it as with 5, 10, 15, 20-tetra-(4-*N*-methylpyridyl) porphyrin and 5, 10, 15, 20-tetra-(4-*N*, *N*, *N*-trimethyl-anilinium) porphyrins.

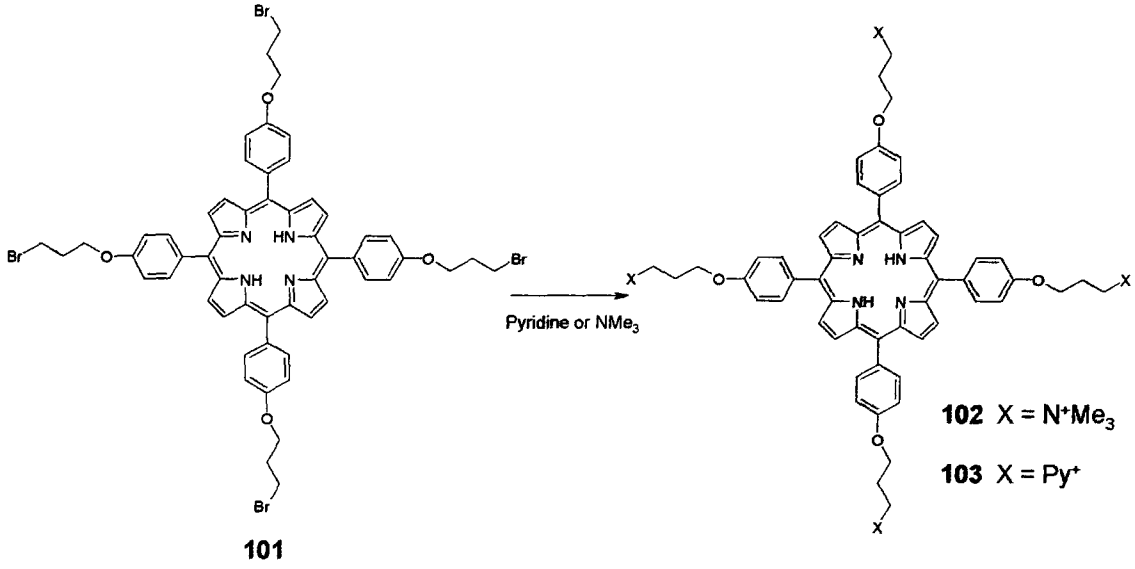

101

Scheme 10. Synthesis of compounds with cationic charge at a distance from the macrocycle [83].

Although the compounds shown in scheme 10 and figure 45 are not octa-cationic porphyrins, the methodology was adapted to produce octa-cationic compounds.

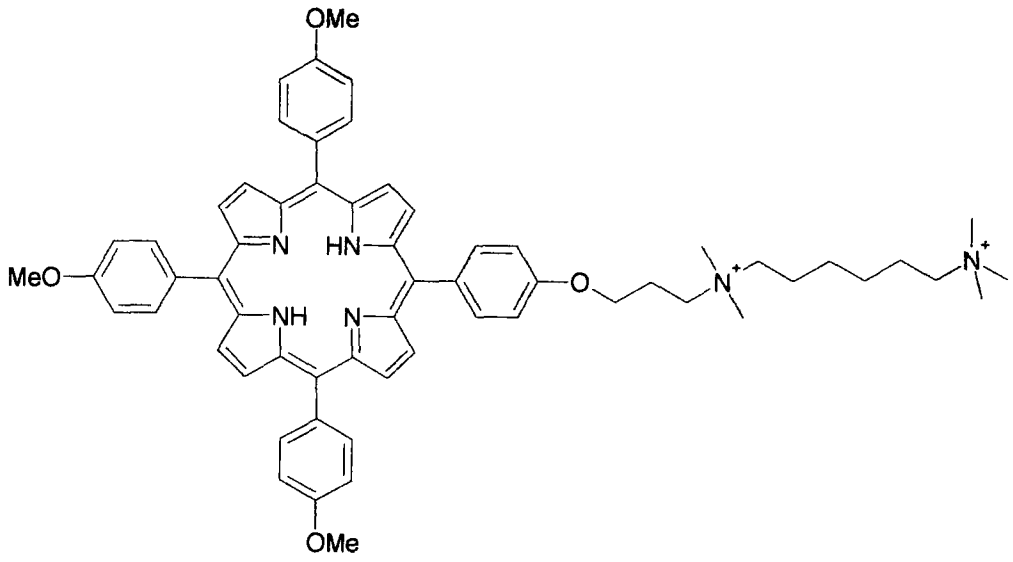

104

Figure 45. Compound **104** made by Schneider *et al* [83] which could be adapted to produce an octa-cationic compound for use in PACT.

In an attempt to produce an octa-cationic porphyrin, the following synthesis was performed (shown in figure 46):

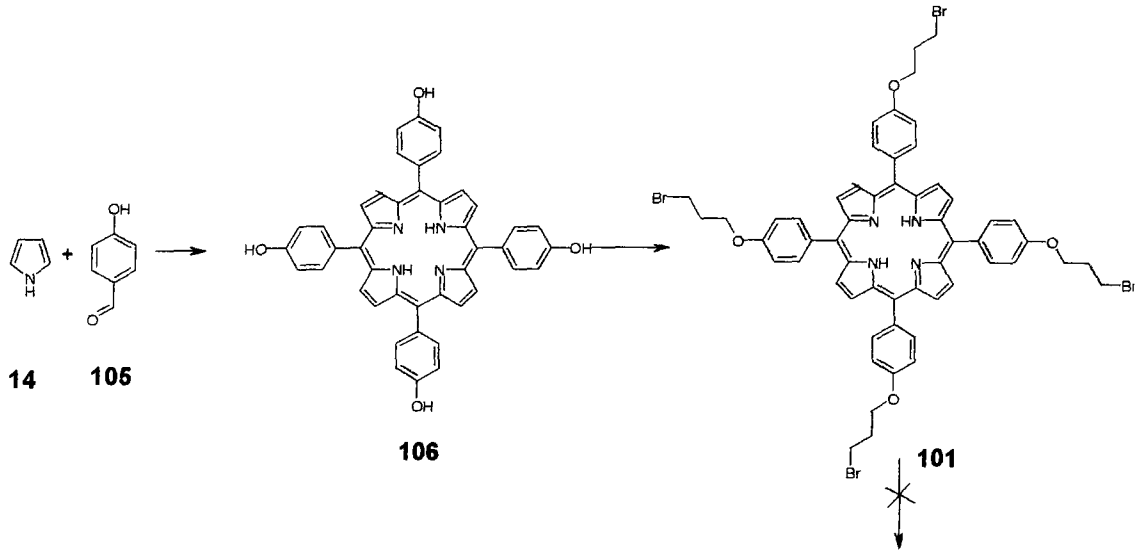

Figure 46. Synthetic route to 5, 10, 15, 20-tetra-(4-(3-bromopropoxy)phenyl) porphyrin **101**. Quaternisation to produce octa-cationic compound was unsuccessful.

The first step in the synthesis was an Adler reaction, producing 5, 10, 15, 20-tetra-(4-hydroxyphenyl) porphyrin **(106)**, from 4-hydroxybenzaldehyde **(105)** and pyrrole. This was then converted to 5, 10, 15, 20-tetra-(4-(3-bromopropoxy)phenyl) porphyrin **(101)** by the method reported by Momenteau *et al* [83]. Namely 5, 10, 15, 20-tetra-(4-hydroxyphenyl) porphyrin was dissolved in dry dioxane with potassium carbonate. The reaction was heated to 100°C and 1, 3-dibromopropane was added drop wise. The reaction was stirred at 100°C for 4 days and allowed to cool to room temperature. It was then filtered and the filtrate evaporated *in-vacuo*. Quaternization was then attempted using *N, N, N', N'*-tetramethylethylene diamine **(107)** or *N, N, N', N'*-tetramethyl-*p*-phenylene diamine **(108)**. The Quaternization, however, proved problematic. It was found that the diamine reacted with the 5, 10, 15, 20-tetra-(4-(3-bromopropoxy)phenyl) porphyrin, to form a cross-linked polymer, rather than the desired product. To overcome this problem methyl iodide was added slowly to a solution of ice cold chloroform. *N, N, N', N'*-tetramethylethylene diamine was added in a 1:1 ratio. This ratio was used to attempt to quaternize one of the amine functionalities whilst leaving the other free for further reaction, as described by Schneider *et al* [82]. Unfortunately TLC revealed that both ends were quaternized simultaneously, leaving the reaction mixture with either doubly quaternized amine or doubly free amines (shown in scheme 11).

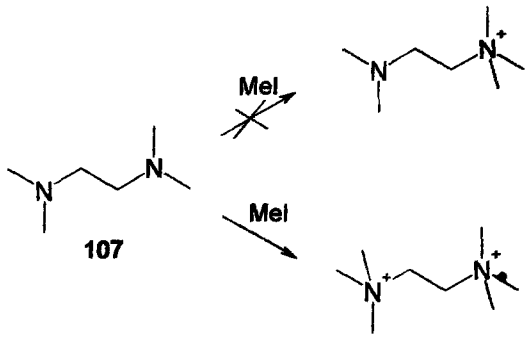

Scheme 11. Quaternization with methyl iodide resulted in di-quaternized product rather than mono-quaternized product.

3.1.2. Retrosynthesis of an octa-cationic porphyrin

Figures 47 and 48 show the retrosynthetic analysis of the octa-cationic 5, 10, 15, 20-tetra-(4-(dimethylamino-ethyl-trimethylamino)methylphenyl) porphyrin **(108)**. Route 1

was chosen as the preferred synthetic route due to the complications involved in quaternizing one end of the diamine without quaternizing the other as shown in scheme 11. The synthetic route used for the synthesis is shown in scheme 12.

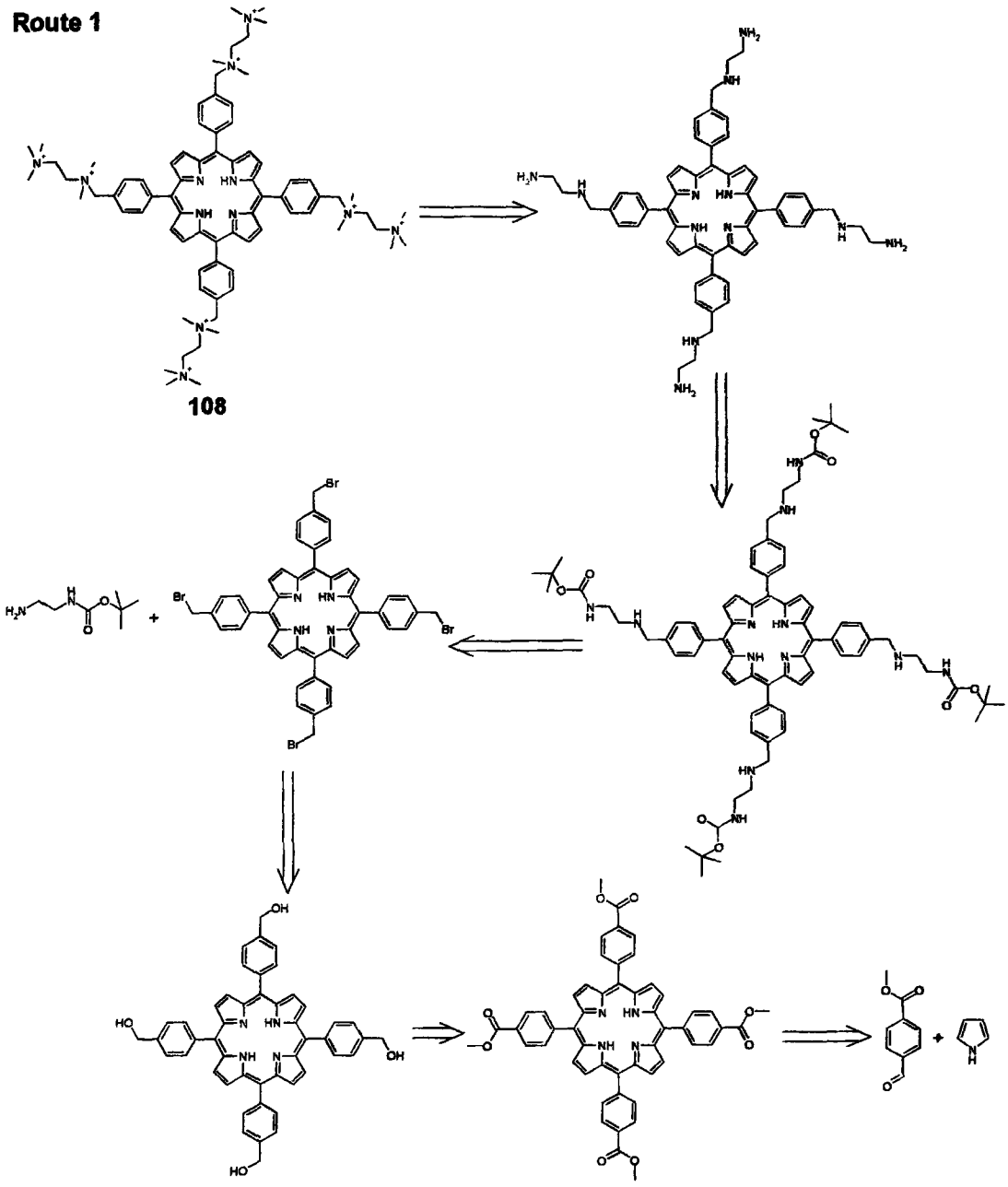

Figure 47. Route 1. Retrosynthetic analysis of 5, 10, 15, 20-tetra-(4-(dimethylamino-ethyl-trimethylamino)methylphenyl) porphyrin **(108)**.

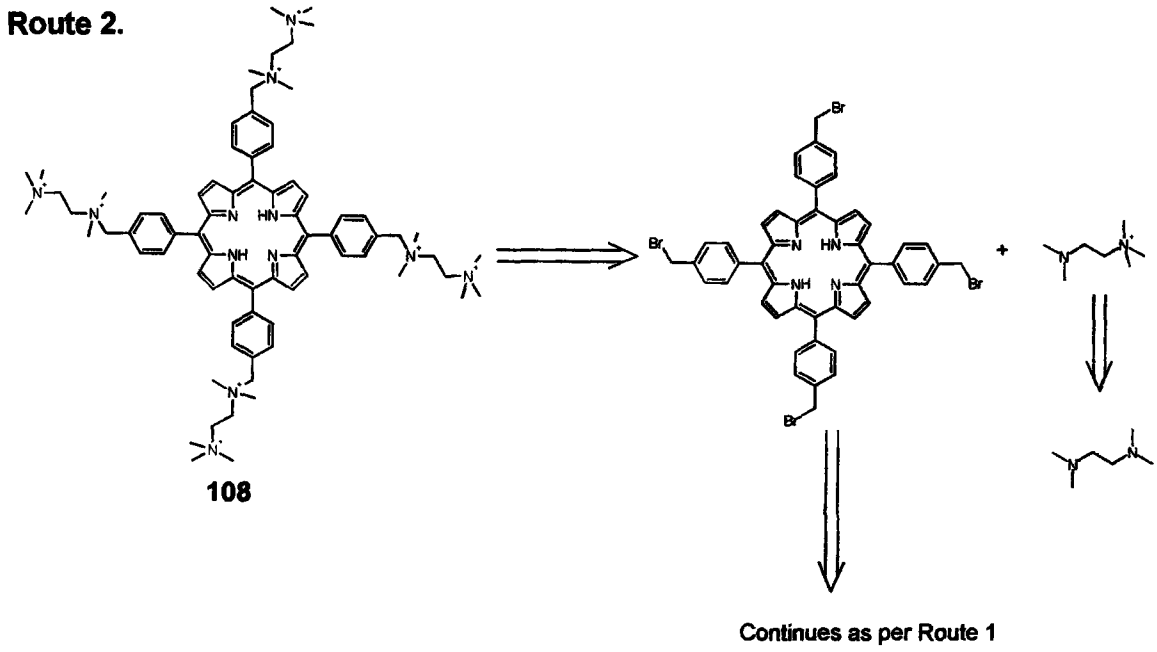

Figure 48. Route 2. Retrosynthetic analysis of 5, 10, 15, 20-tetra-(4-(dimethylamino-ethyl-trimethylamino)methylphenyl) porphyrin (**108**).

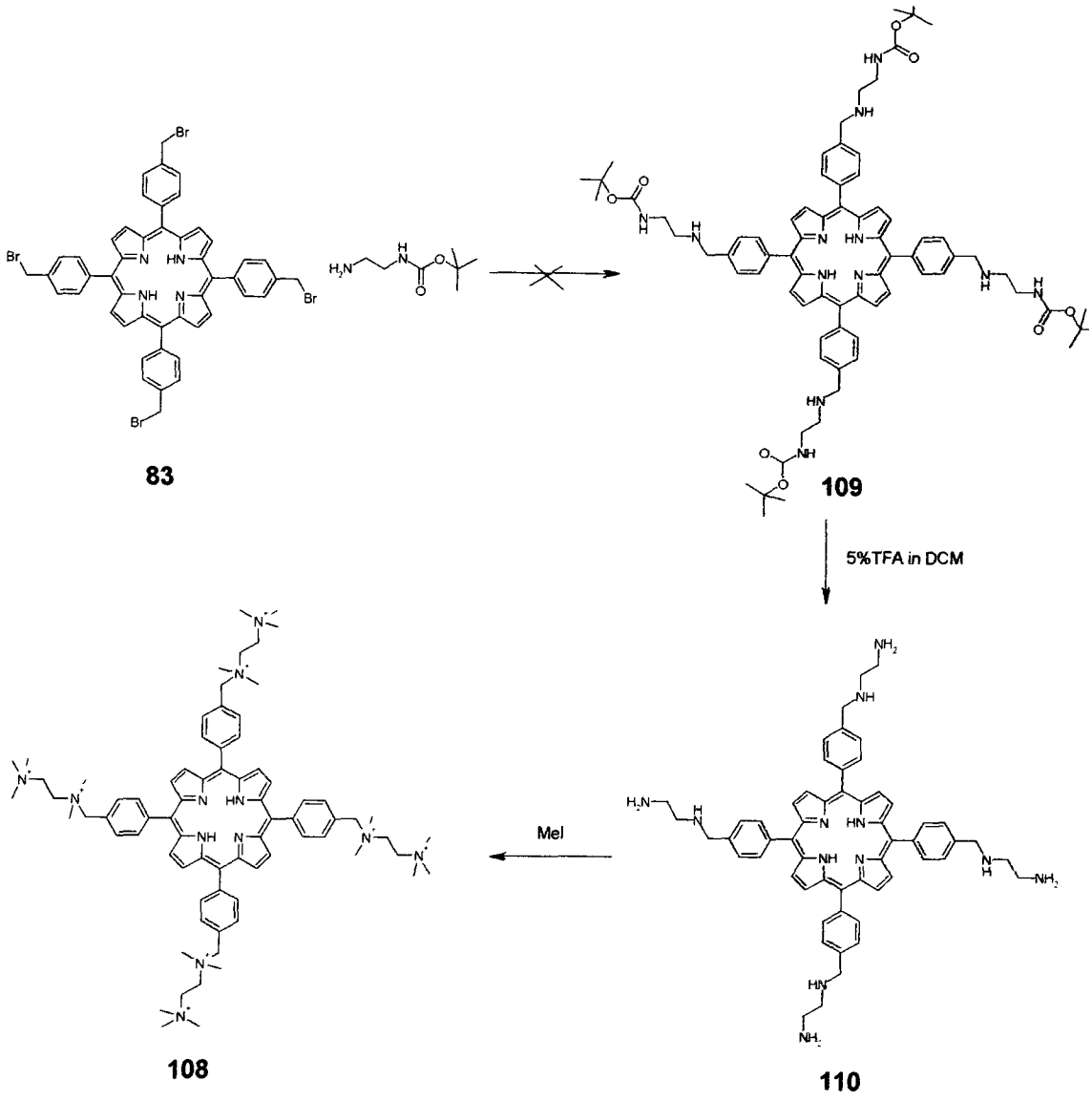

Scheme 12. Synthetic route used for octa-cationic porphyrin.

3.1.3. Octa-cationic compounds - synthesis attempted.

Synthesis of a series of octa-cationic compounds for screening against bacteria was attempted as shown in figure 49. They vary in chain length between the nitrogen atoms, namely C2, C3 and C6.

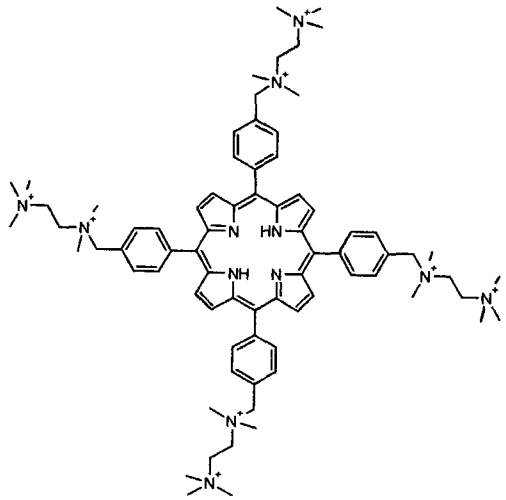

108

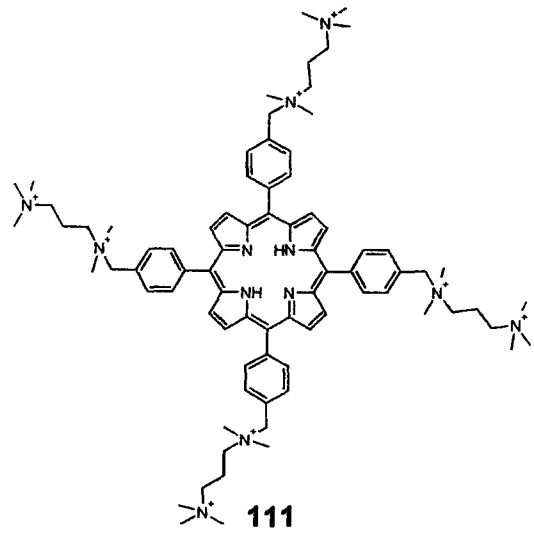

111

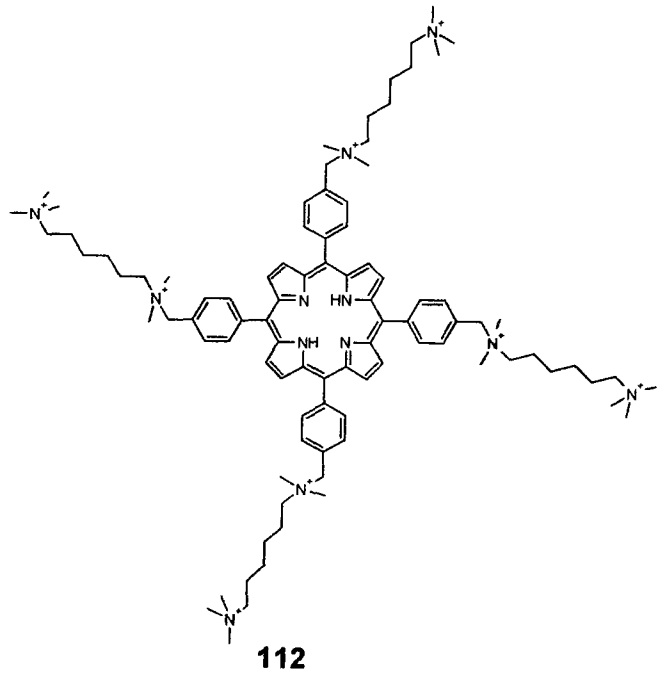

112

Figure 49. Octa-cationic compounds made for use in PACT.

The intermediate 5, 10, 15, 20-tetra-(4-(bromomethyl)phenyl) porphyrin **(83)** was reacted with a Boc-protected diamine, purchased from Aldrich, then deprotected using 5%TFA in DCM. The resulting octa-amine porphyrin **(113)** was purified by dialysis and quaternization was attempted. However problems arose on quaternization of the amino

groups with methyl iodide because the reaction did not go to completion, even on heating, and hence purification proved problematic.

3.2. Dendritic porphyrins.

3.2.1. Dendrimers.

Dendrimers are monodisperse macromolecules with a regular and highly branched three dimensional architecture. They are produced in an iterative sequence of reaction steps leading to higher generations. The first example of a dendrimer was produced by Vögtle. There are two ways to make dendrimers, by divergent or convergent synthesis. In divergent synthesis the dendrimer is grown from the core in a stepwise manner and many reactions are performed on a single molecule as shown in figure 50.

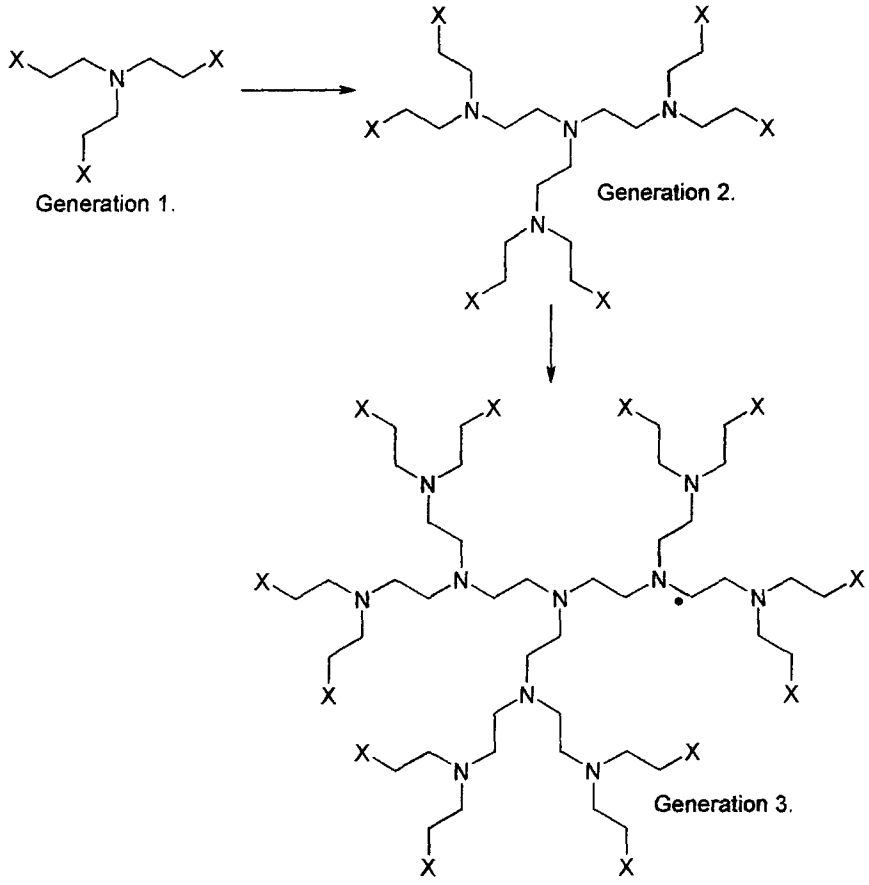

Figure 50. Example of divergent dendrimer synthesis.

The opposite of divergent synthesis is convergent synthesis, in which the molecule is synthesised from the periphery, in towards the core. This method allows a lower number of reaction sites per step and is shown in figure 51.

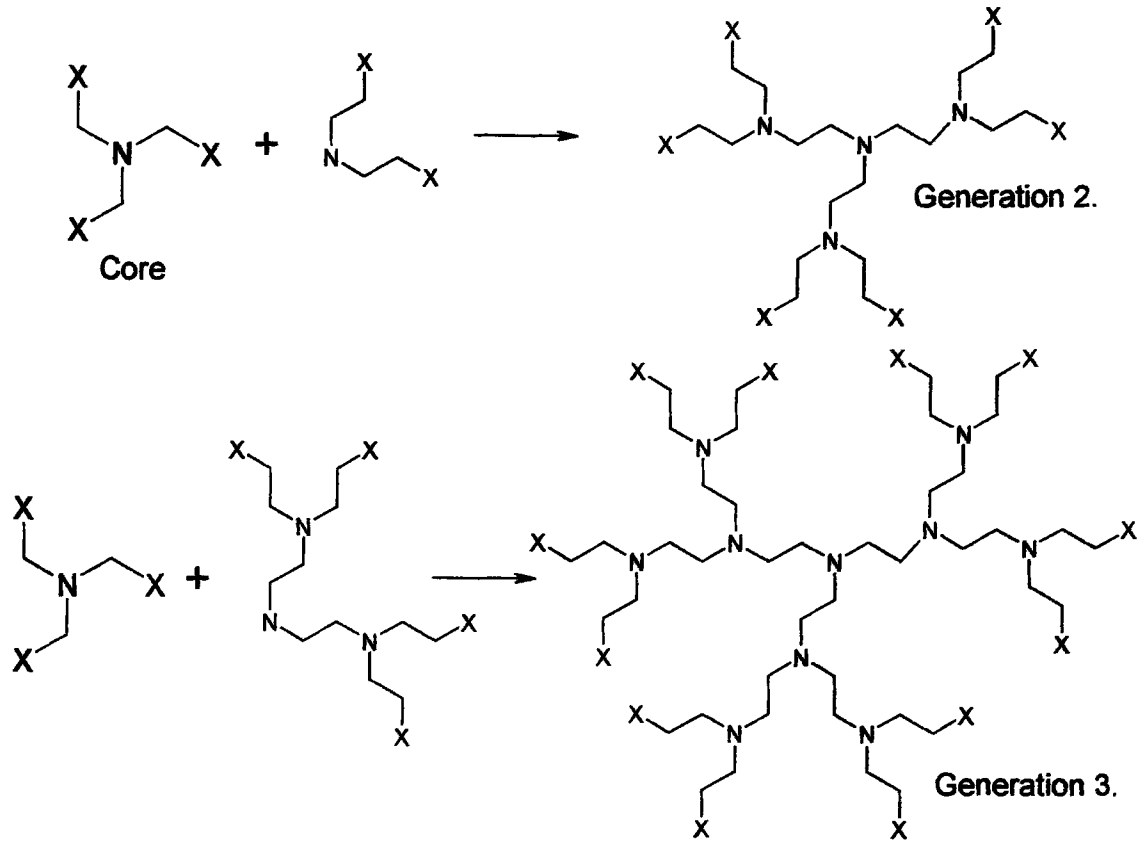

Figure 51. Convergent dendrimer synthesis.

Buhleir et al [84] reported the first dendritic structure to be synthesised via a divergent synthesis in 1978. They treated a primary amine with acrylonitrile in a conjugate addition reaction to form the desired dinitrile (scheme 13). This was then reduced by using cobalt (II) chloride hexahydrate and sodium borohydride, in methanol, to produce the diamine. The process was then repeated in order to generate the hepta-amine. However, more recent repetition of the reduction conditions, have proven them to be unreliable and diisobutyl aluminium hydride [85] or hydrogenation using Raney nickel on cobalt catalyst [86] have been used in its place.

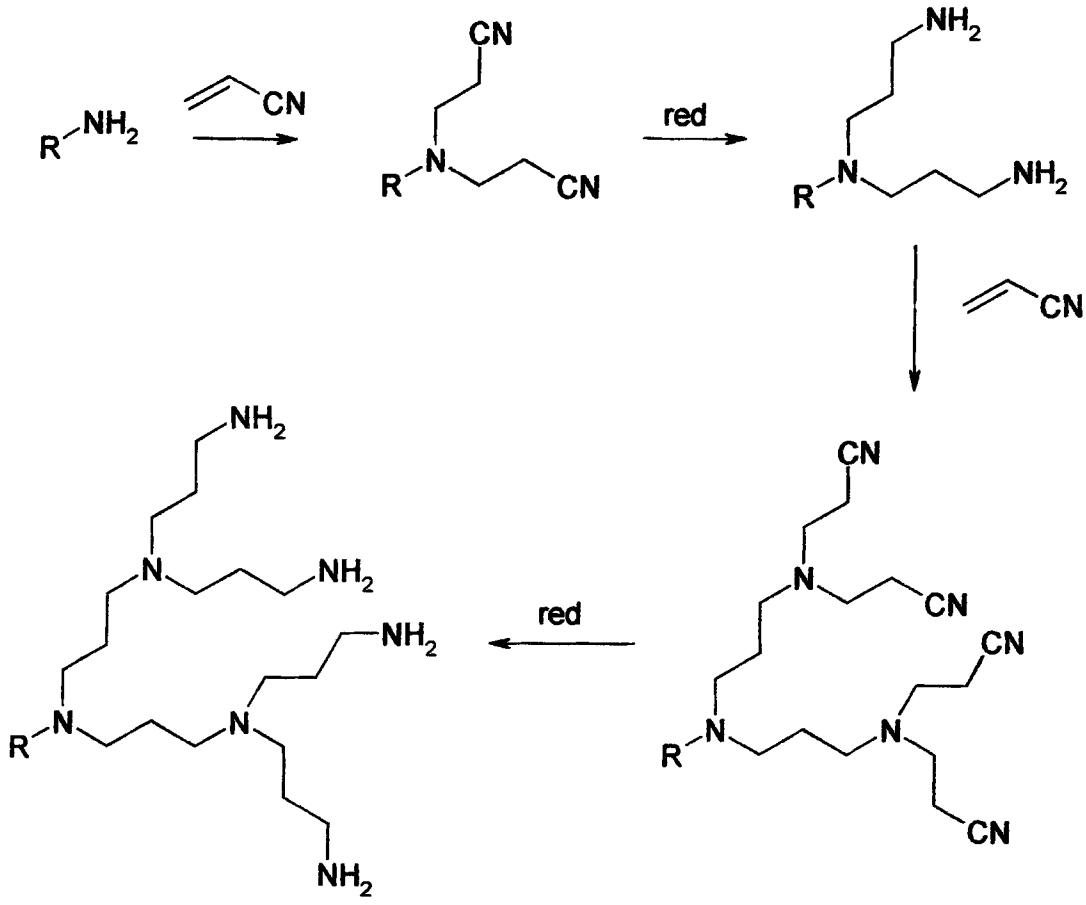

Scheme 13. Vögtle *et al*'s divergent synthesis to a hepta-amine.

Shortly after the report of Vögtle *et al* [87], came another from Denkewalter in 1981 [88]. He reported the first divergent preparation of dendritic polypeptides using the protected amino acid *N*, *N*'-bis(tert-butoxycarbonyl)-L-lysine as a building block (scheme 14).

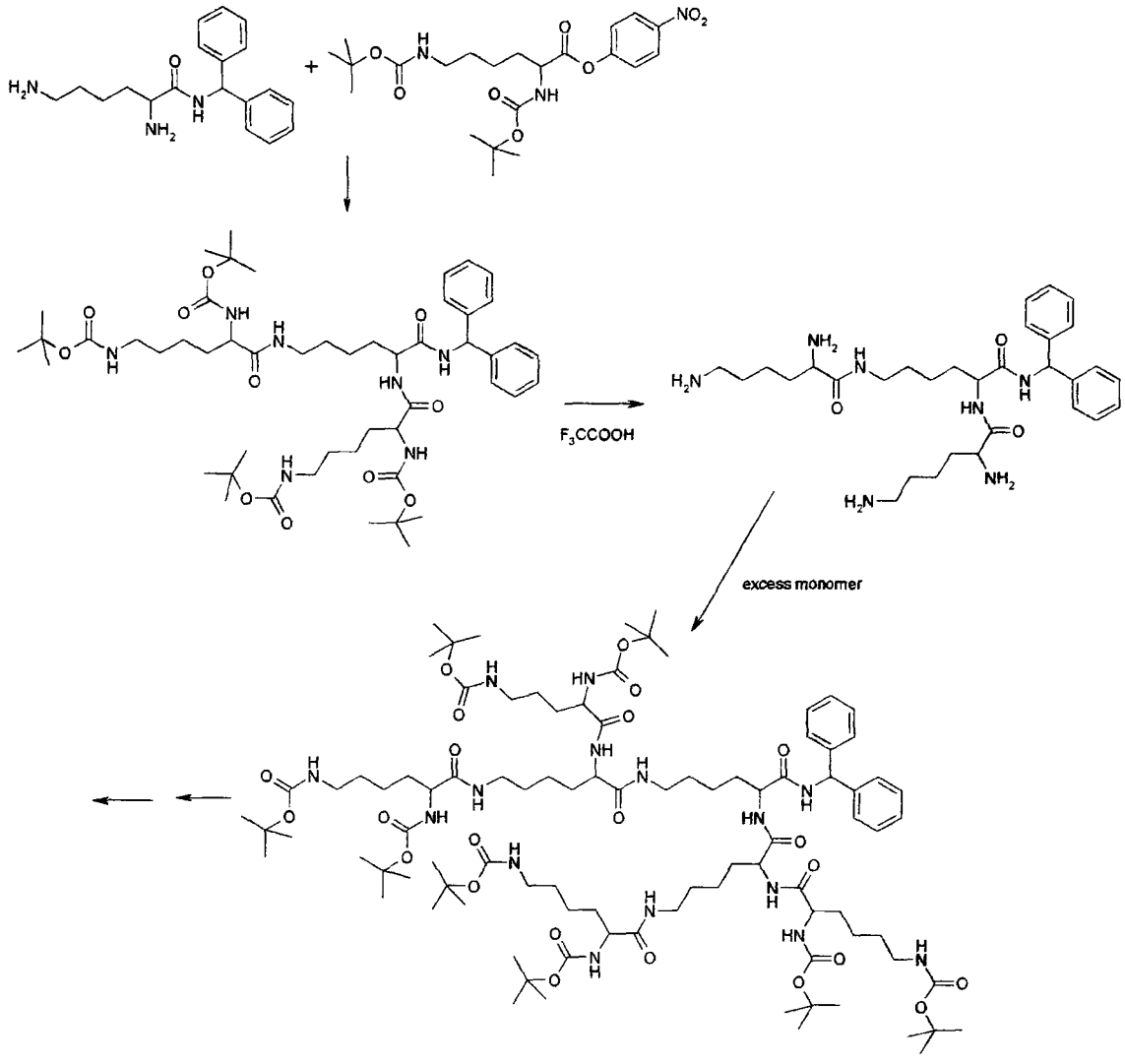

Scheme 14. Denkewalter's divergent synthesis of dendritic polypeptides [88].

Since then many other dendrimers have been reported with multiple generations and they have been utilised for a wide range of purposes including drug delivery, energy/ light harvesting, ion sensing, catalysis, information storage, immuno-diagnostic agents, lubricants, diagnostic reagents, vaccines against bacteria, viruses, parasites, modification of gene expression and PDT [89, 90, 91].

3.2.2. Porphyrin dendrimers.

Examples of porphyrin dendrimers exist and porphyrin dendrimers with cationic charges on the periphery are of particular interest for use in PACT as they are single, discrete, molecules with a known molecular weight. Another reason for interest in cationic dendrimers is that the number of cationic charges increases per generation and hence it would be possible to find the optimum amount of cationic charge needed for use in the PDI of Gram negative and Gram positive bacteria.

3.2.2.1. Target porphyrin dendrimers.

Three target porphyrin dendrimers were identified which bore cationic charges on the periphery and the synthesis was undertaken with varying degrees of success. The structures of the first generation compounds are shown in figures 52, 53 and 54.

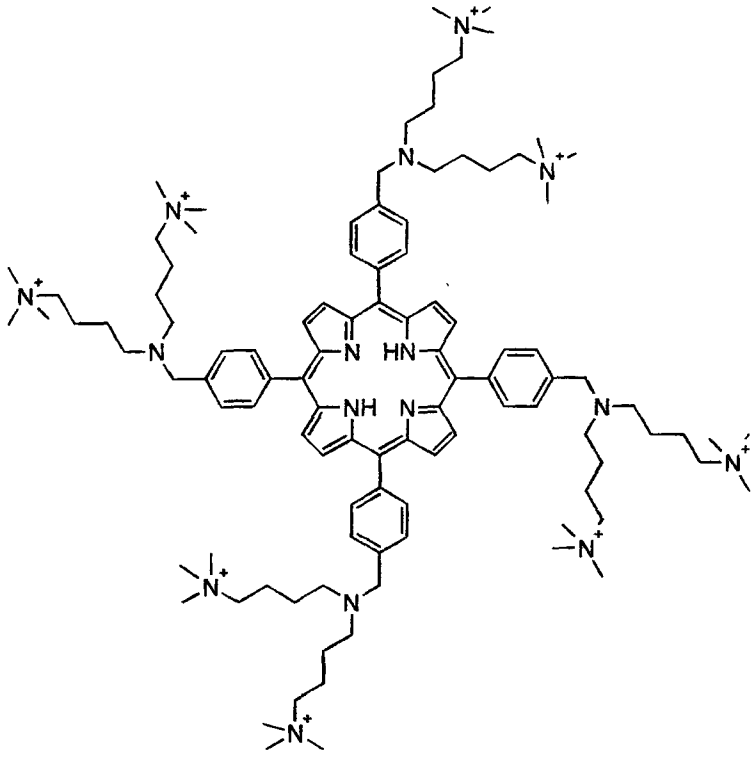

114

Figure 52. Porphyrin dendrimer (**114**).

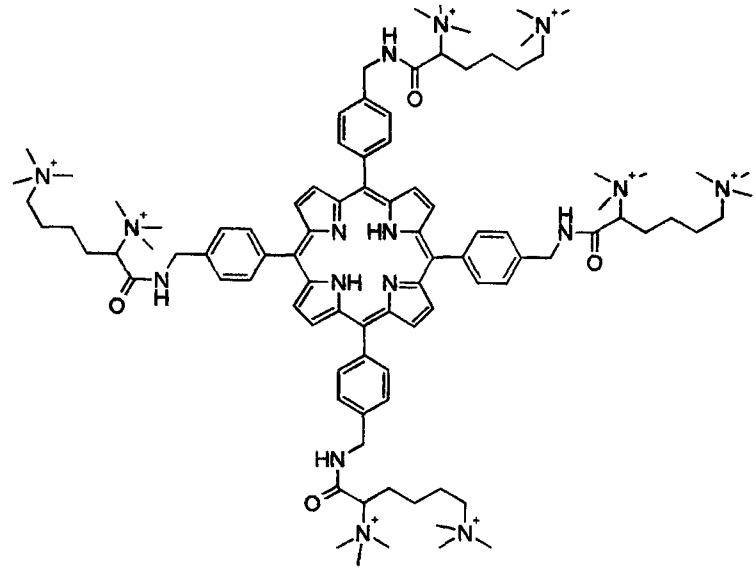

115

Figure 53. Porphyrin dendrimer (**135**).

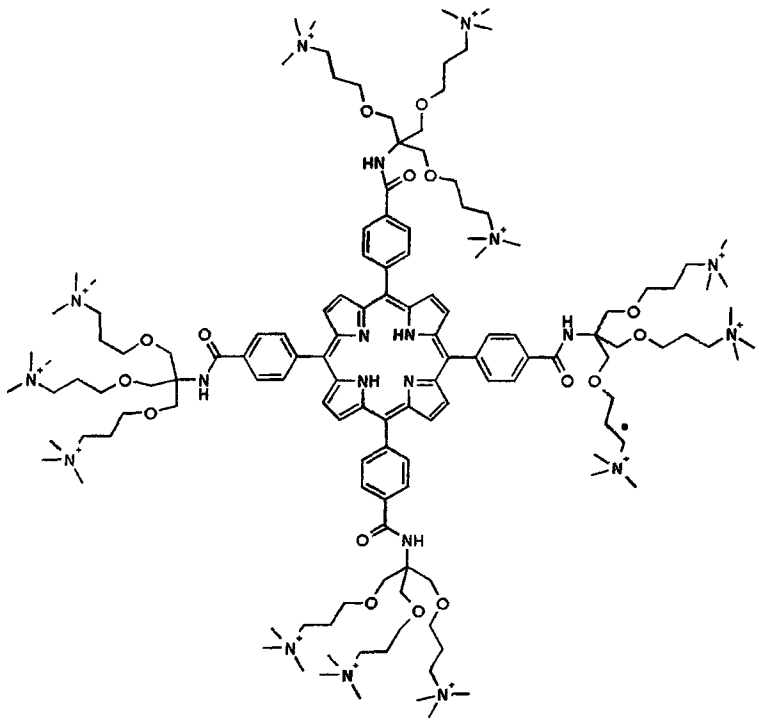

116

Figure 54. Porphyrin dendrimer (**143**).

3.2.2.2. Synthesis of porphyrin dendrimer 114.

Retrosynthesis of porphyrin dendrimer **114** showed a number of different routes, to this compound, the first of these is shown in figure 55.

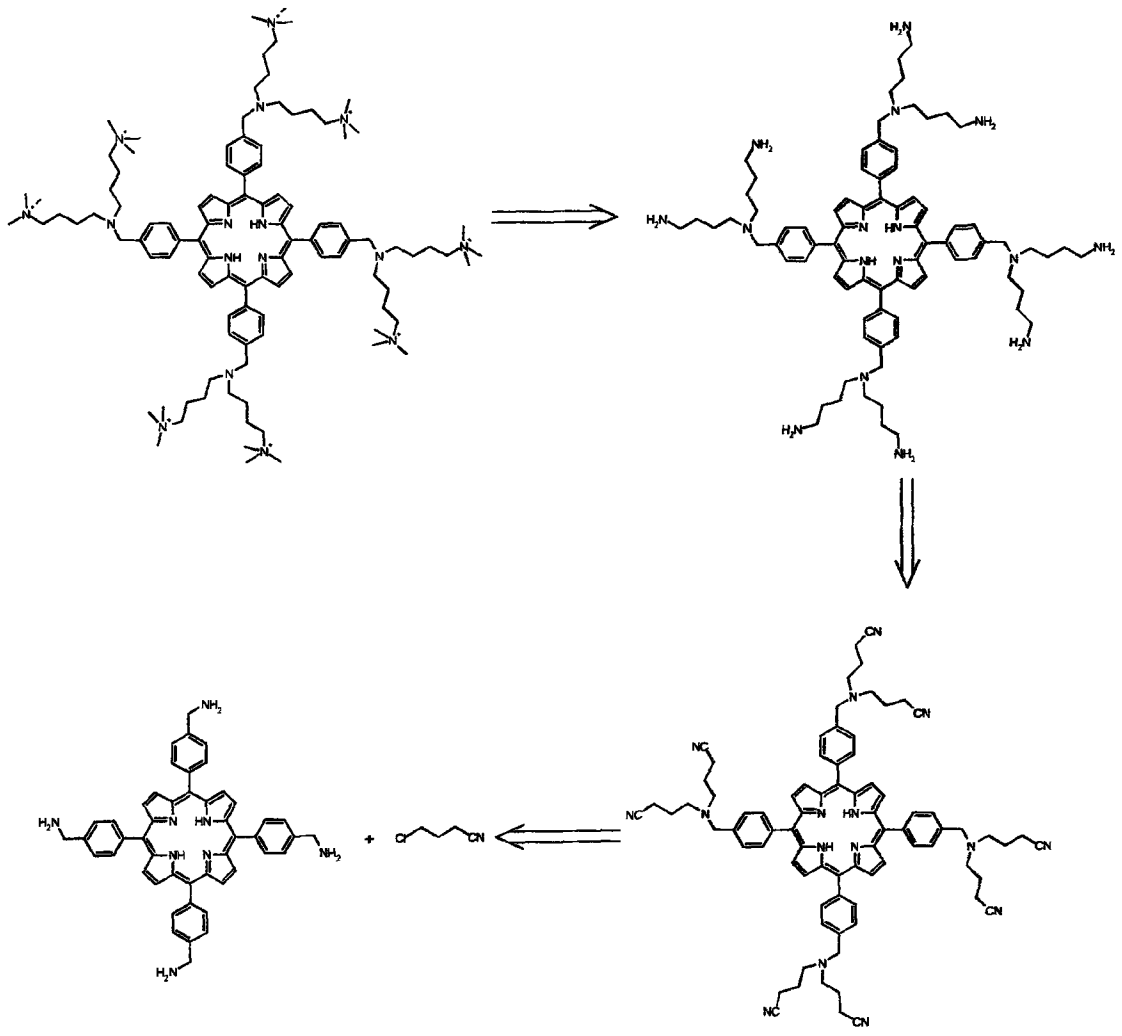

Figure 55. Retrosynthesis of porphyrin dendrimer **114**.

The synthetic route used for the attempted synthesis of porphyrin dendrimer **114** is shown in scheme 15.

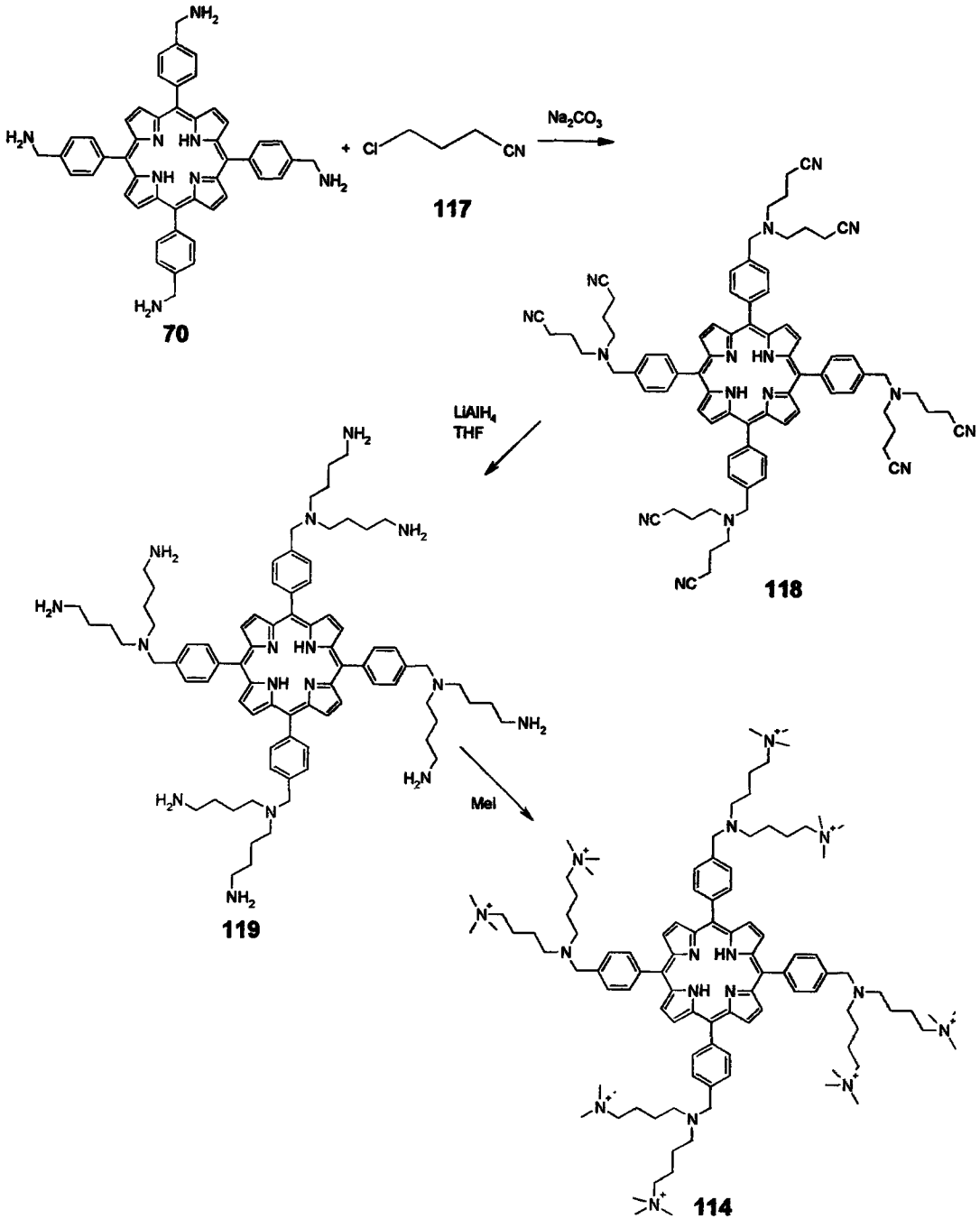

Scheme 15. Synthetic route to porphyrin dendrimer **114**.

Prior to synthesising this compound using the porphyrin core, it was decided to test the methodology using benzylamine, as shown in scheme 16. The reaction yielded the mono-substituted product **121**, with a small fraction of di-substituted product **122**. It was

therefore decided not to attempt this synthetic route using the porphyrin, due to the possibility of multiple products occurring. This would cause problems with purification and extensive purification would be needed, resulting in low yields.

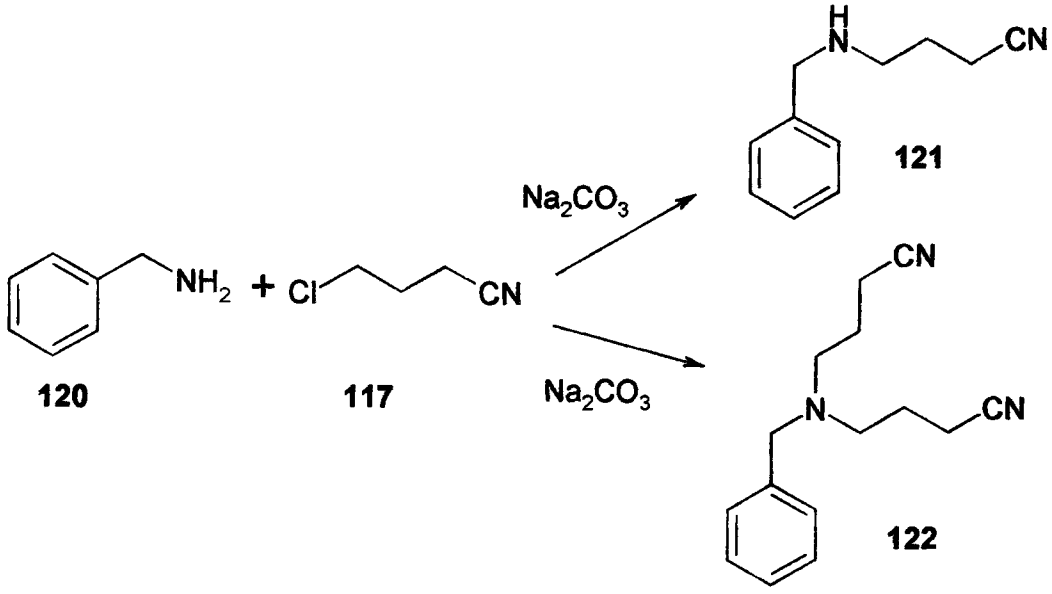

Scheme 16. Synthesis attempted using benzylamine instead of the porphyrin core to test the feasibility of the reaction.

The retrosynthesis of an analogous compound **(123)**, with one less carbon atom in the alkyl chain, was attempted. This is shown in figure 56.

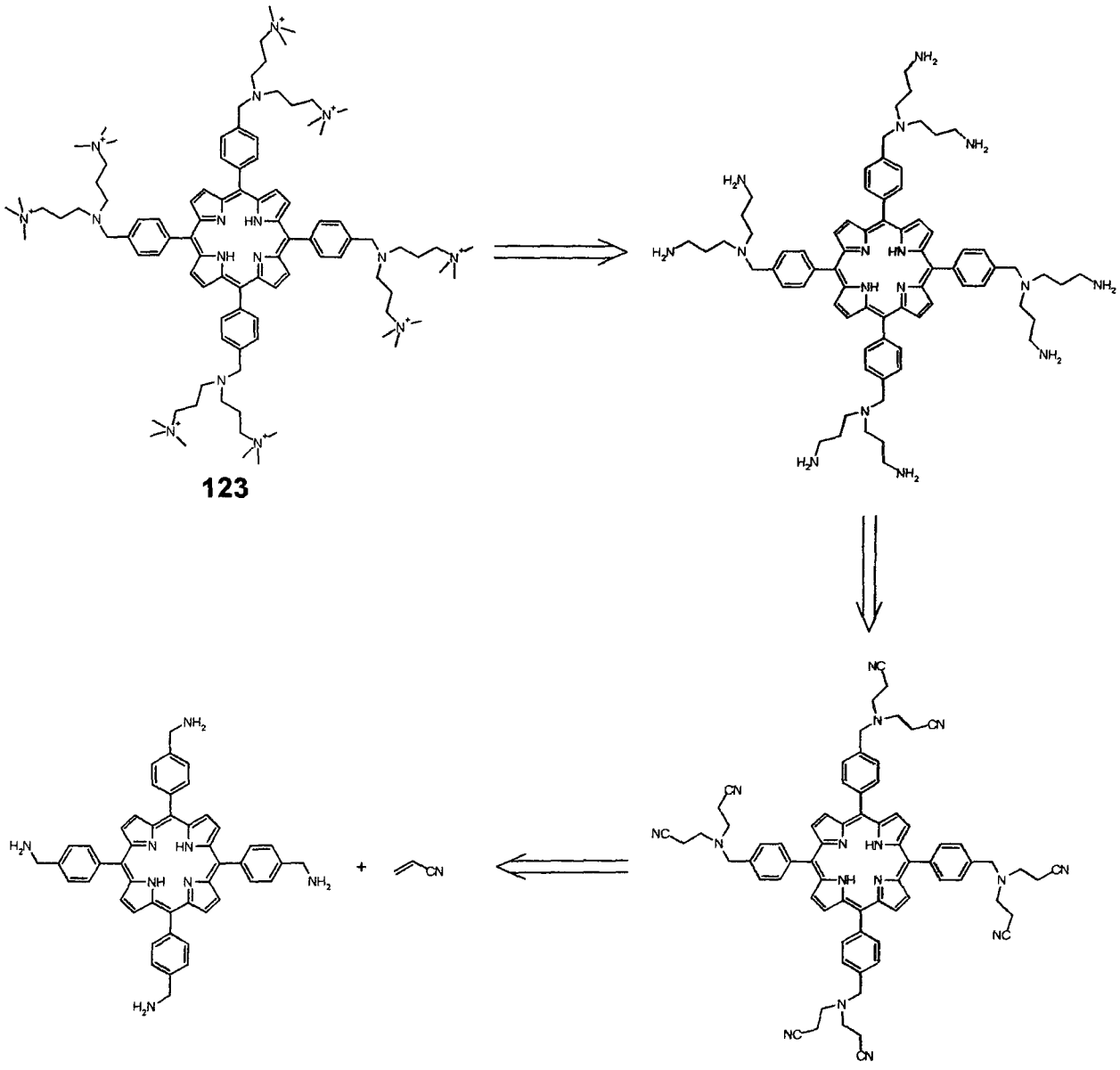

Figure 56. Retrosynthesis using analogous compound, porphyrin dendrimer **(123)**.

The synthetic route followed is shown in scheme 17. Again, the synthetic route was tested prior to using the porphyrin, and this is shown in scheme 18.

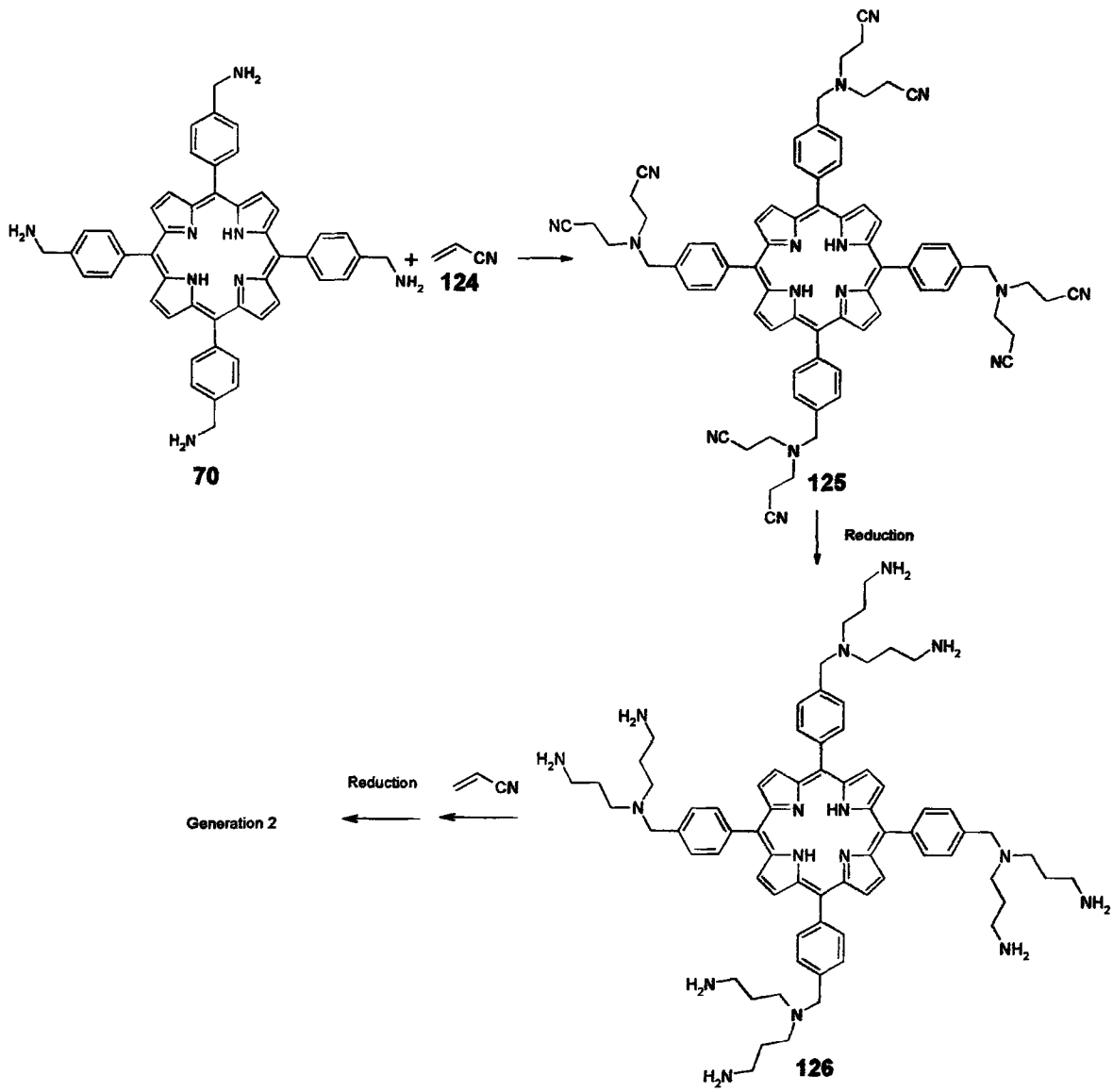

Scheme 17. Synthetic route to porphyrin dendrimer **123**.

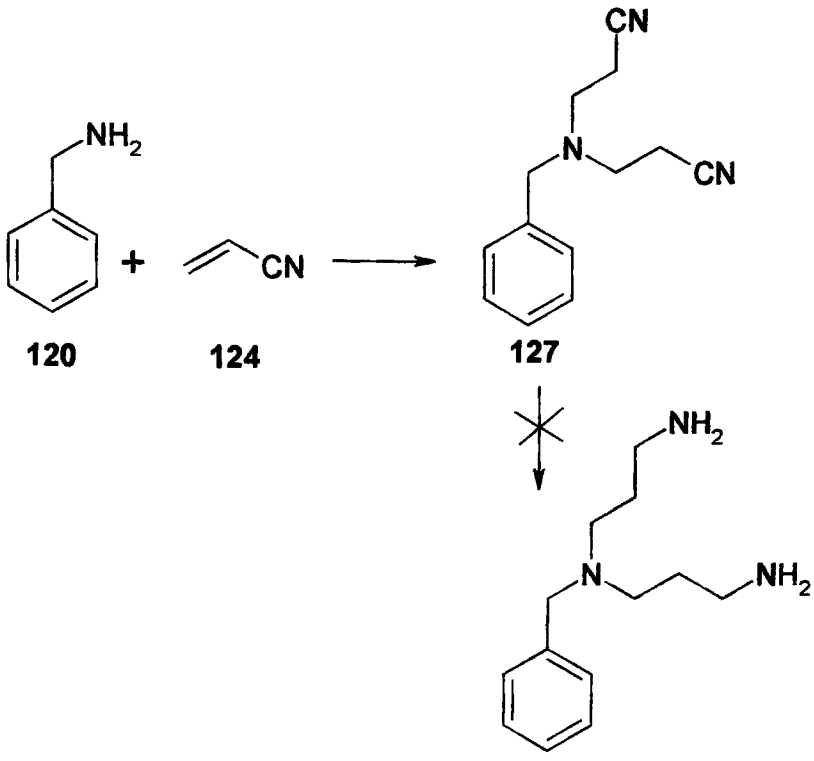

Scheme18. Synthetic route used for test reaction.

The main problem which occurred using this route was that the reduction of the nitrile groups to amino groups did not work despite using several methods. The methods attempted included $LiAlH_4$, borane-THF complex and hydrogenation with palladium on carbon. It was therefore decided to look at an alternative route, where the reduction of the nitrile group was not required. The retrosynthesis of this is shown in figure 57.

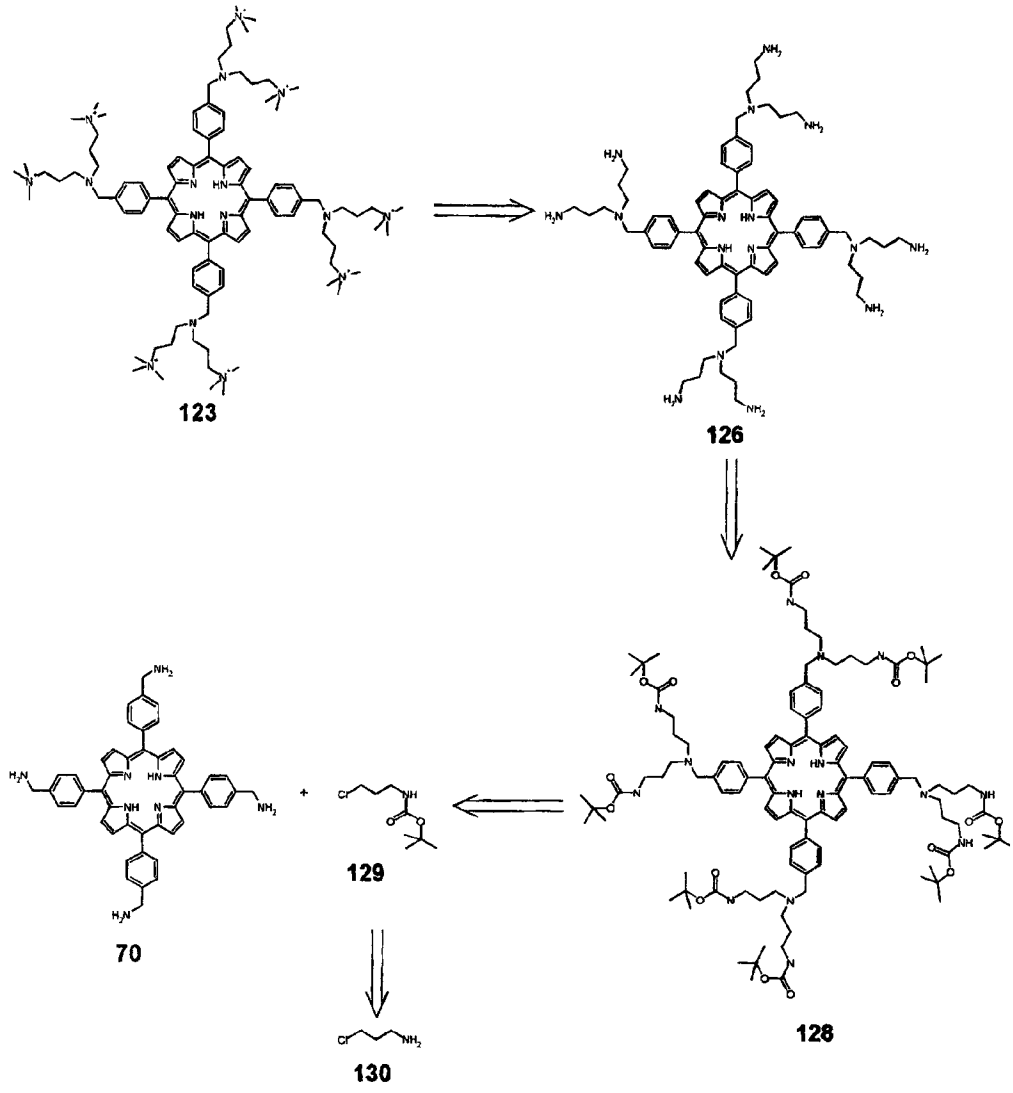

Figure 57. Retrosynthesis of **123**.

The methodology for the synthetic route was again, tested using benzylamine instead of the porphyrin core. The synthetic route used is shown in scheme 19.

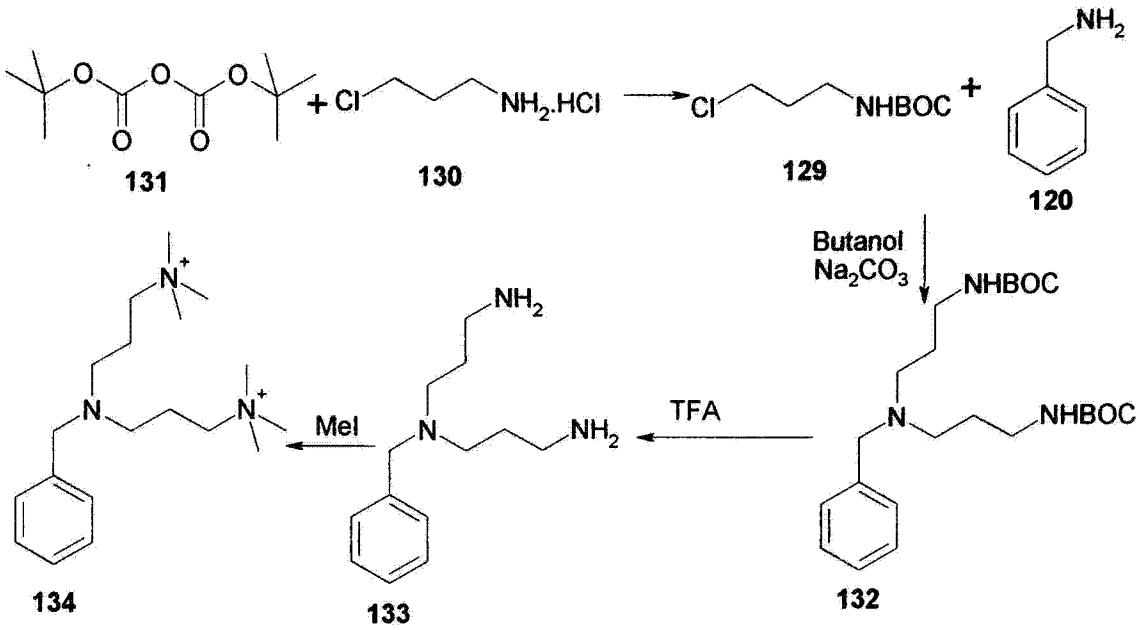

Scheme 19.

Firstly, chloropropylamine hydrochloride **(130)** was Boc-protected using the method described by Kohl *et al* [91]. Namely, chloropropylamine hydrochloride and di-tert-butyldicarbonate **(131)** were dissolved in THF/Water (50/50 v/v) and the pH was adjusted to 8.5 with 4% aqueous NaOH, the reaction was then stirred overnight. The solution was acidified to pH 2 using 0.1M HCl and the product extracted into chloroform. The product **129** was reacted with benzylamine in the presence of base, deprotected and quaternized using methyl iodide. However this was not attempted on a porphyrin due to problems encountered synthesising 5, 10, 15, 20-tetra-(4-(aminomethyl)phenyl) porphyrin **(70)**.

3.2.2.3. Synthesis of porphyrin dendrimer 135.

Hamblin *et al* [59] have shown that polylysine conjugated to a chlorin e6 molecule is active against bacteria. However polylysine is not a single discrete molecule, as is desirable for a good PDT agent. It was thus decided to attempt the synthesis of a porphyrin dendrimer containing a known number of lysine units and hence with a known molecular weight. The retrosynthesis of this and the synthetic route are shown in figure 58 and scheme 20 respectively.

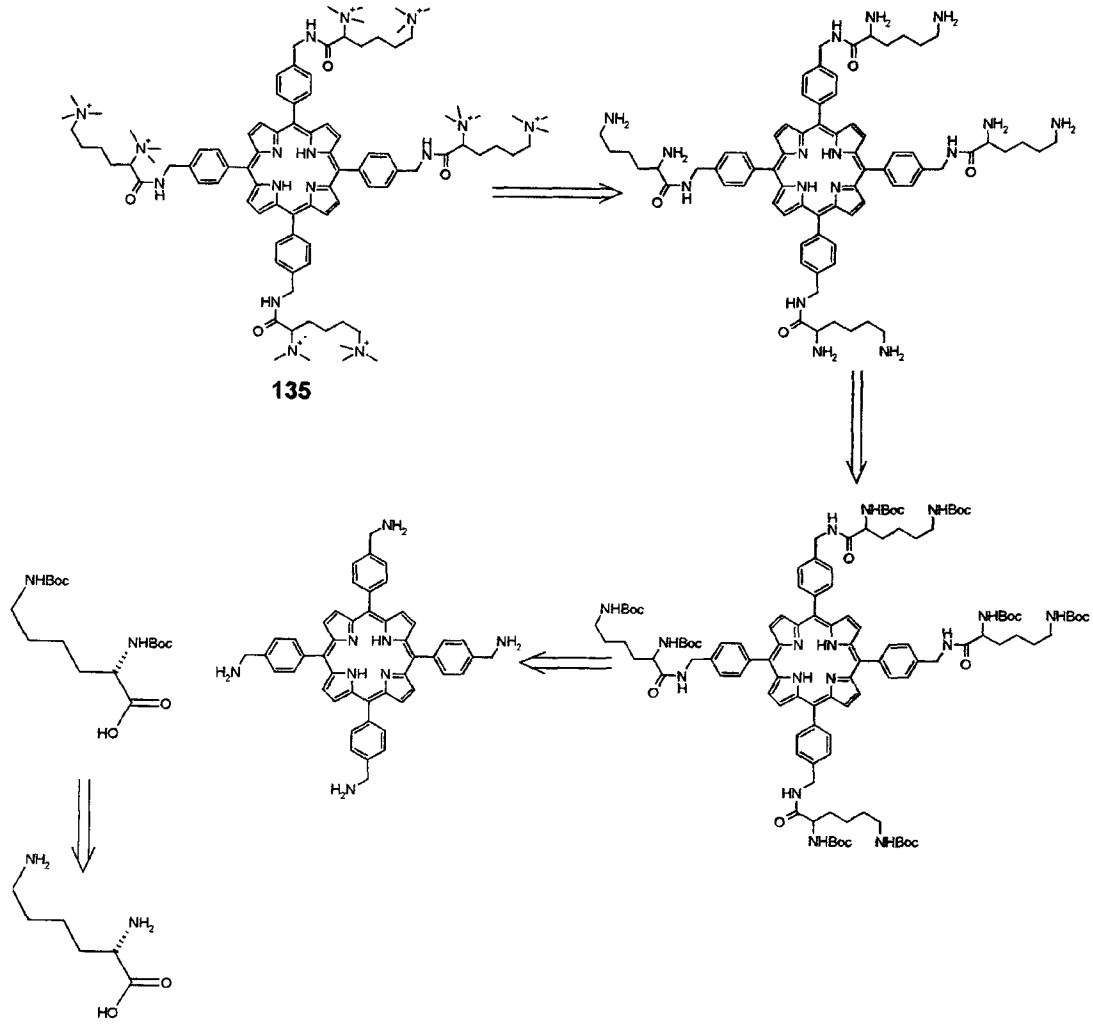

Figure 58. Retrosynthesis of porphyrin dendrimer **135**.

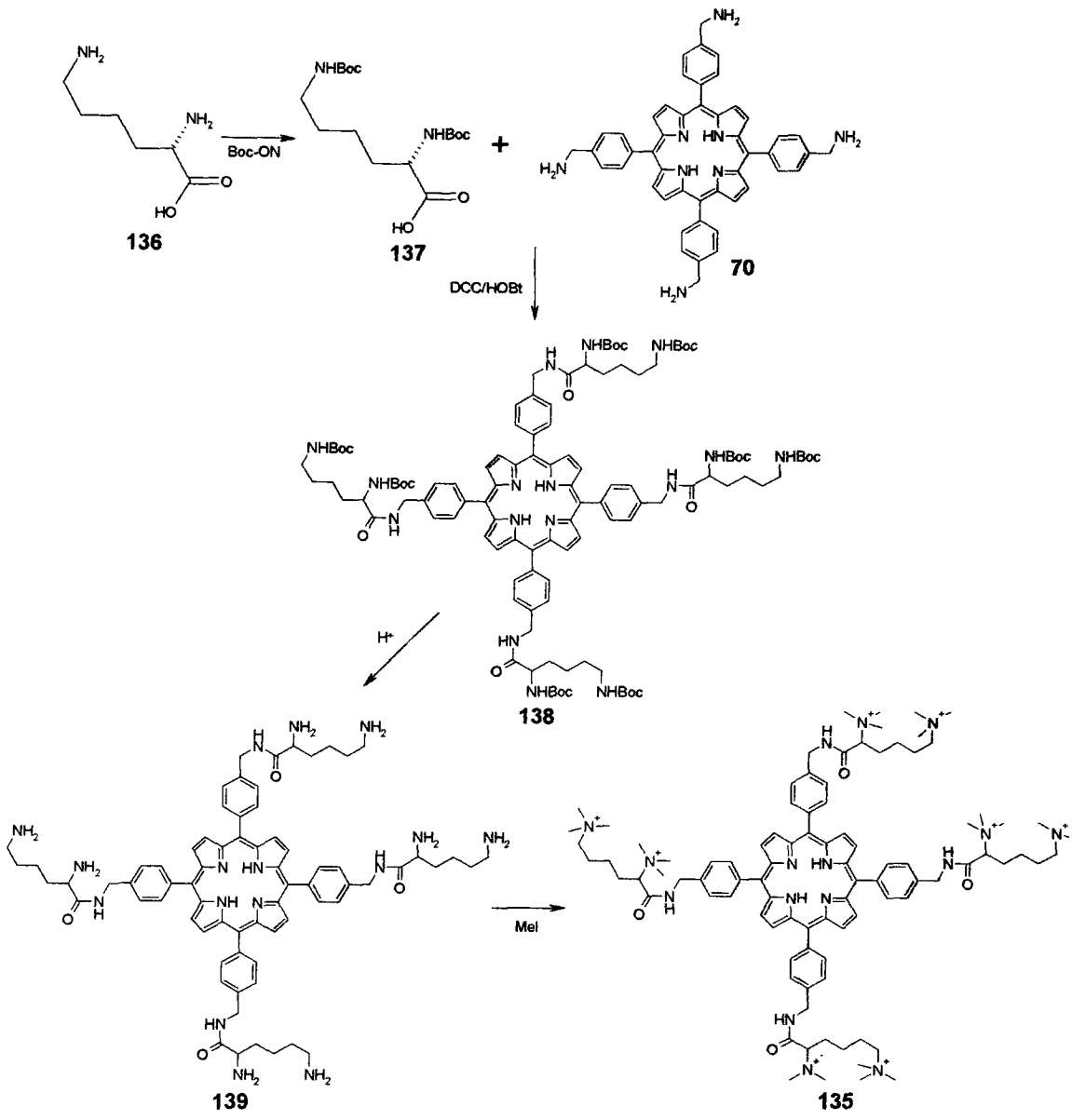

Scheme 20. Synthetic route to porphyrin dendrimer **135**.

The lysine **(136)** was Boc-protected via the methodology of Kohl *et al* [91]. Following aqueous work up, the doubly protected lysine **(137)** was produced with a free carboxylic acid group for attachment to the porphyrin core. A test reaction, shown in scheme 21, was carried out using benzylamine in place of the porphyrin core. DCC [92] was used to couple the Boc-protected lysine to benzylamine and the product was then deprotected and quaternized using methyl iodide.

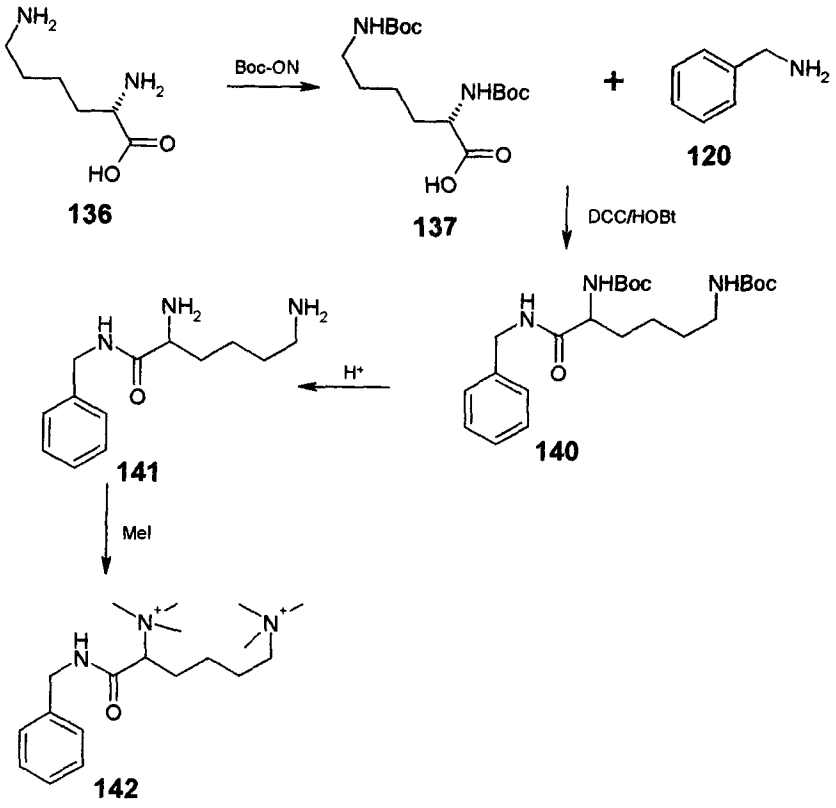

Scheme 21. Synthesis testing the methodology of porphyrin dendrimer **135**.

However, problems occurred producing the porphyrin core as previously stated in section 2.1, and hence it was not possible to make porphyrin dendrimer **135**.

3.2.2.4. Synthesis of porphyrin dendrimer 143.

Figure 59 shows the retrosynthesis of porphyrin dendrimer **143**.

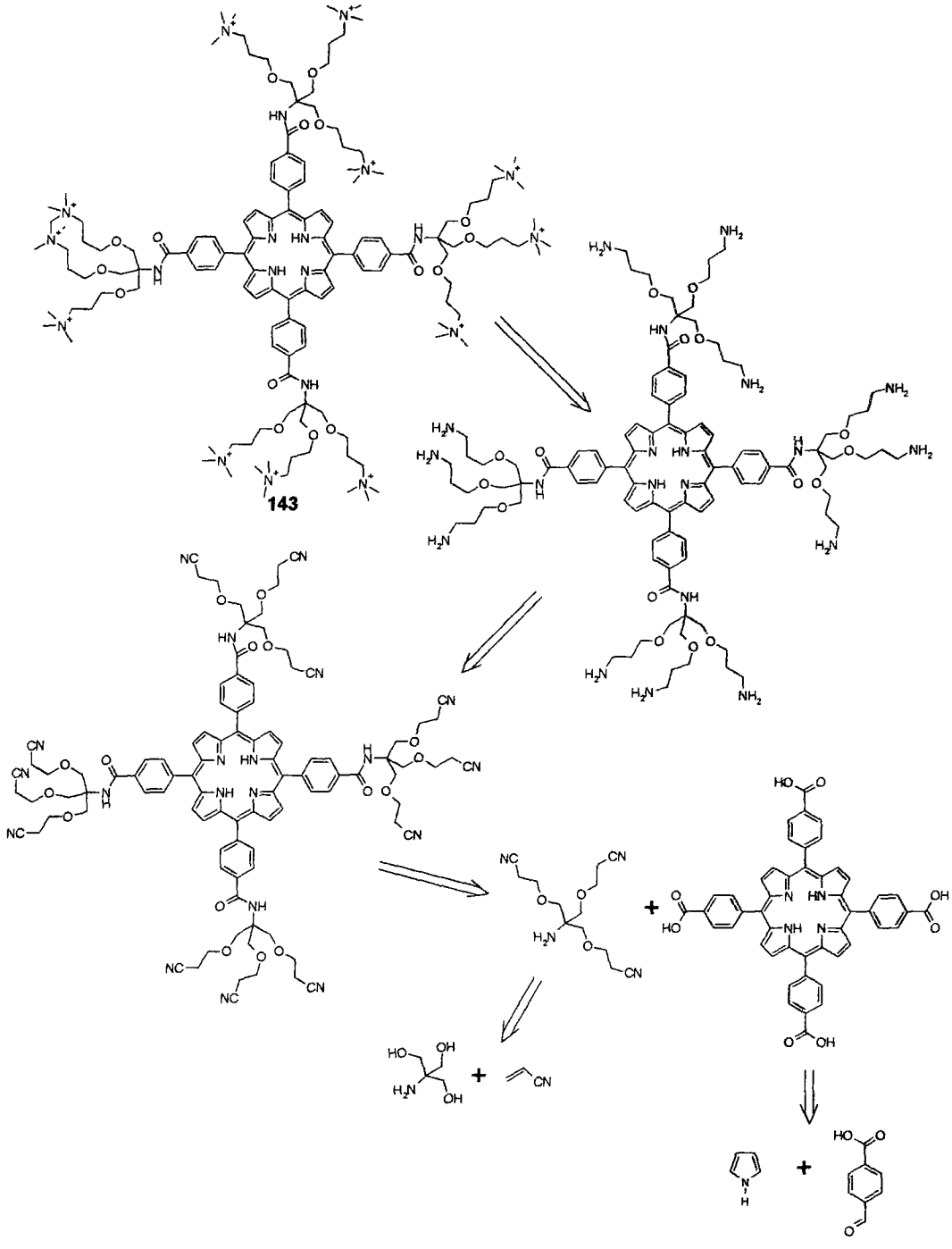

Figure 59. Retrosynthesis of porphyrin dendrimer **143**

The dendritic wedge **(145)** for porphyrin dendrimer **143** was prepared via a method described by Dupraz *et al* [93] and Dayan *et al* [94], and is shown in scheme 22.

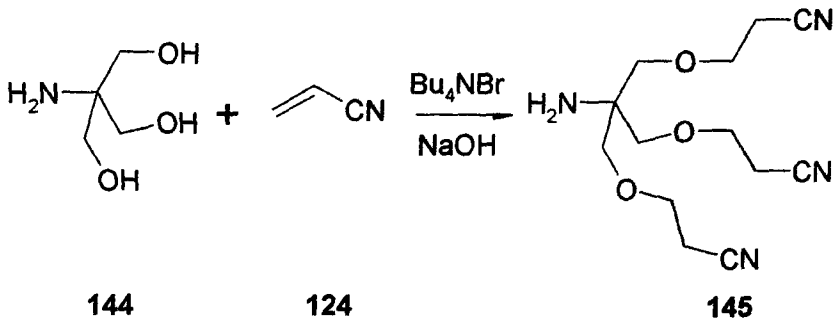

144 **124** **145**

Scheme 22. Synthetic route to the dendritic wedge.

To a vigorously stirred solution of tris **(144)**, acrylonitrile **(124)** and Bu_4NBr in DCM, 40% NaOH was added whilst controlling the temperature between 10°C and 20°C. This was stirred overnight and following aqueous work up the desired product was recovered.

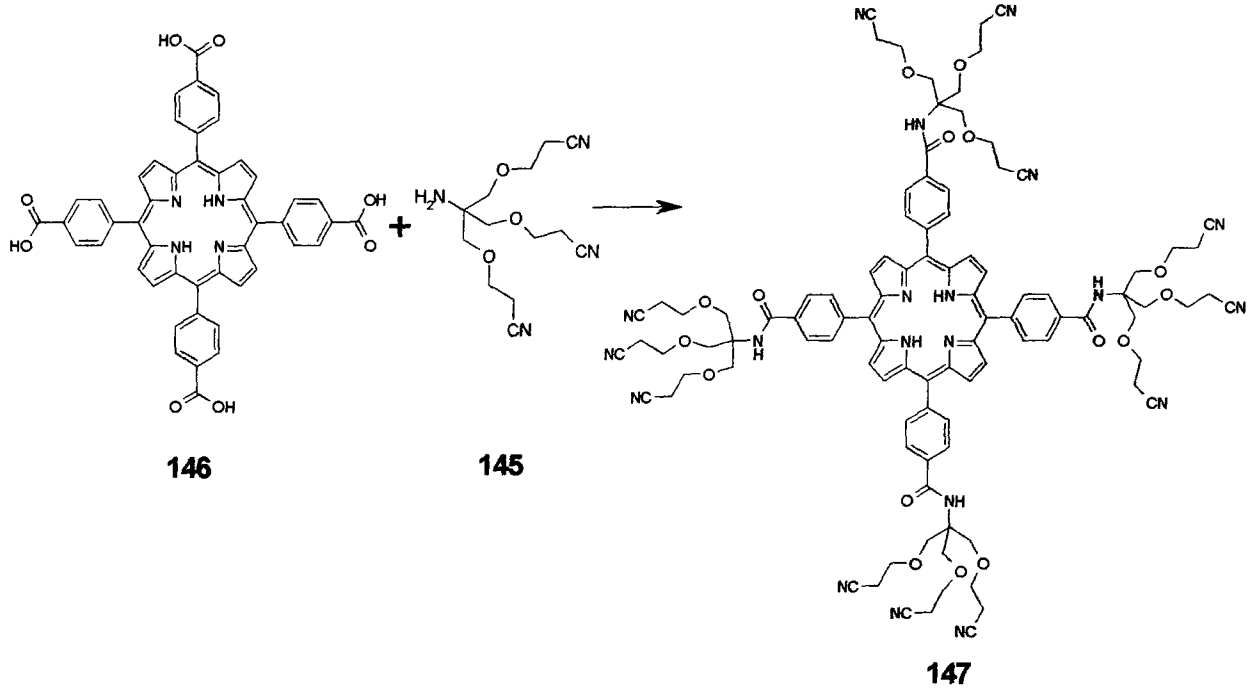

146 **145** **147**

Scheme 23. Coupling dendritic wedge to porphyrin core.

Attempts were then made to couple **145** to 5, 10, 15, 20-tetra-(4-(carboxy)phenyl) porphyrin **(146)** (scheme 23) via a variety of coupling conditions as reviewed by Han *et al* [94]. These included the methodologies of Dandliker *et al* [96] (DCC, HOBt, THF), Vinogradov *et al* [97] (DCC, pyridine, THF), Gradl *et al* [98] (oxalyl chloride, DMF in DCM) and Dourtoglou *et al* [99] (HBTU, HOBT, N-methyl morpholine). However all attempts to couple the dendritic wedge to 5, 10, 15, 20-tetra-(4-(carboxy)phenyl) porphyrin proved unsuccessful. In some attempts it was possible to see, by TLC, that one or two of the wedges had reacted with the carboxylic acid group of porphyrin **146**. These however were not isolated from the reaction mixture, due to the extensive chromatography that would be needed and low yields of either cis or trans isomers that would be produced. It is believed that the bulky size of amine wedge **145**, caused steric hindrance to occur, preventing the attachment of all four amines to the porphyrin core.

It was decided to investigate the use of photosensitizers with greater than four cationic charges to allow the comparison of bacterial PDI for both the tetra-cationic compounds and compounds with greater than four cationic charges, however various problems were encountered with the syntheses. The main problem encountered in the synthesis of the octa-cationic porphyrins was purification of the products. This was also the case for the dendritic porphyrins which did not go to completion. An additional problem was encountered in the synthesis of the starting porphyrin, 5, 10, 15, 20-tetra-(4-aminomethyl)phenyl) porphyrin **(70)**, Several synthetic routes to this porphyrin were attempted without success as discussed in chapter 2.1.3.

Chapter 4. Bacterial assay development.

4.1. Bacterial assay.

Several different assays exist in the literature for use in PACT, however many of these suffer from problems including the use of white light, not washing cells, inconsistent light doses and not using single, discrete molecules for assays against bacteria. For this reason it was decided to develop a new bacterial assay to avoid all of these problems and find the optimum conditions needed for assays used in PACT.

4.1.1 Compound used for assay development.

For this study it was decided to use 5, 10, 15, 20- tetra-(4-*N*, *N*, *N*-trimethyl-anilinium) porphyrin **(23)** for the development of the bacterial assay because it has been widely used in the literature (See chapter 2) and has been shown to cause an effective PDI of Gram positive and Gram negative bacteria. The compound is also commercially available, thus ensuring consistency between batches.

4.1.2 Bacterial strains used.

A Gram positive and a Gram negative bacterium were used for the development of the bacterial assay so that it would be possible to compare and contrast the differences between the two types of bacteria. All organisms were obtained from Hull Royal Infirmary Microbiological services. The Gram negative bacterium used was *E. coli NCTC* and the Gram positive bacterium used was *MRSA* (see 4.2.2 for sensitivities), as this is a major cause of hospital acquired infection, especially in the elderly or immunocompromised patients.

4.1.3. Drug concentrations.

The initial drug concentration range used was from 0 to 50 μM. This was in order to gain an understanding of the amount of compound needed for the PDI of bacteria and so accurate dose response curves could be plotted. Thus the optimum concentration of drug needed for the PDI of bacteria using this compound could be identified and used as a

eference point for future assays. All drug concentrations were performed in triplicate to llow a statistical estimate of accuracy.

1.1.4. Overnight Culture preparation.

Bacteria were grown over night in Luria-Bertani media [3]. 10µl of this was then diluted ither 1in 1000, 1 in 10,000 or 1 in 100,000. 100µl of this diluted culture was then spread ver agar plates and left to incubate over night. The colony forming units were then ounted and the number of cells per 10µl of the undiluted overnight culture was alculated. The number of cells used in each well was calculated to be $3.5*10^8$ per well.

1.1.5. Initial Protocol followed.

Assays were performed in 96-well conical bottomed plates. The initial protocol was as ollows: overnight culture (10µl), drug solution (10µl) and Luria-Bertani (LB) media 190µl) were placed in each well. The plates were left to incubate at 37°C for 4 hours. fter incubation the plates were washed twice (centrifuged for ten minutes (1500 g, 0°C), then re-suspended in fresh media). The contents of the wells were re-suspended in esh media and transferred to 96-well flat bottomed plates. Two plates were used in the ssay, one to be kept in the dark as a control and the other to be irradiated. The plate was radiated for 10 minutes using a panel of red light emitting diodes (Omnilux®), with a aximal output at 633 nm ± 3 nm. After irradiation the cells were incubated overnight id the absorbance read at 630nm from both the dark control and the irradiated plate.

1.6 Initial results.

he initial assay results for the commercially available 5, 10, 15, 20-tetra-(4-*N*, *N*, *N*-imethylanilinium) porphyrin (**23**) against MRSA and *E. coli* are shown in figures 60 and respectively.

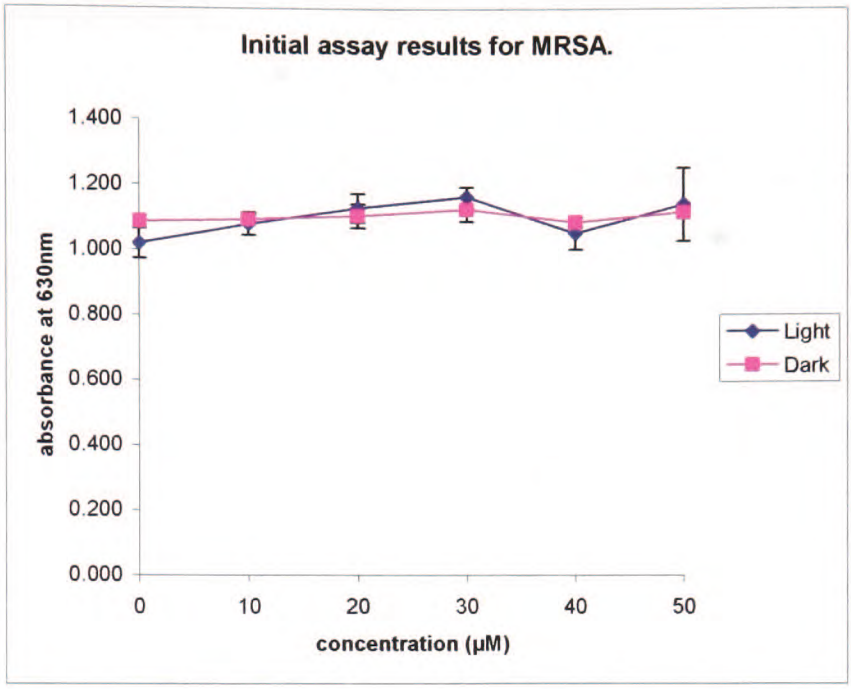

Figure 60. Initial assay results for MRSA using 5, 10, 15, 20- tetra-(4-*N*, *N*, *N*-trimethyl-anilinium) porphyrin (**23**).

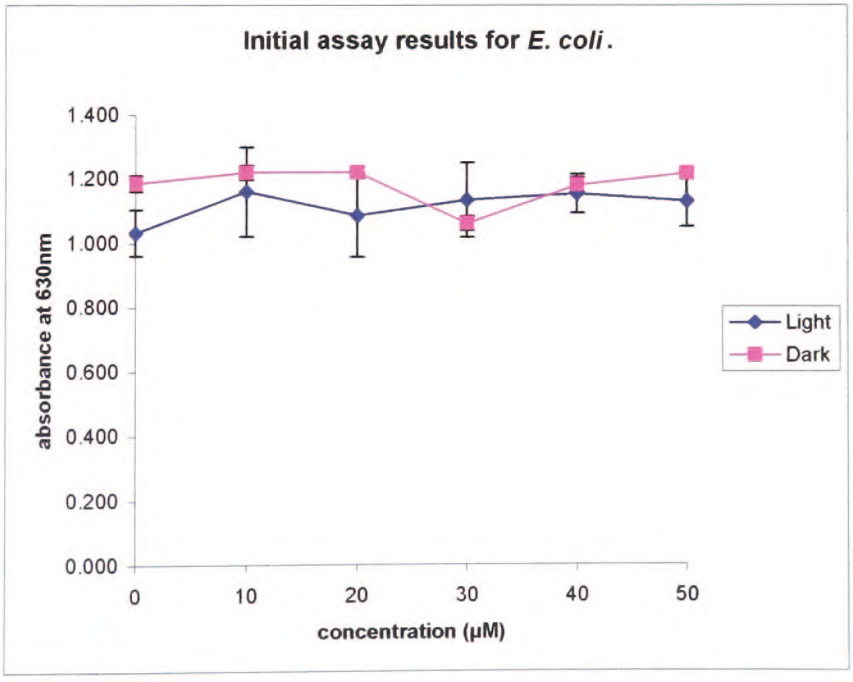

Figure 61. Initial assay results for *E. coli* using 5, 10, 15, 20- tetra-(4-*N*, *N*, *N*-trimethyl-anilinium) porphyrin (**23**).

ɔ cell kill was seen for either the Gram positive MRSA or the Gram negative *E. coli*.

4.2. Protocol optimisation.

4.2.1. Higher drug concentrations.

No cell kill was seen for drug concentrations between 0 - 50μM so it was decided to try higher drug concentrations of up to 200μM. The results of this showed no cell kill for either MRSA or *E. coli.*

4.2.2. Bacterial viability assay

No cell death had been observed for the assays using 5, 10, 15, 20-tetra-(4-*N*, *N*, *N*-trimethyl-anilinium) porphyrin despite literature sources reporting that it was effective in killing bacteria. Therefore it was decided to check that the cell lines were still viable by assaying them against gentamycin. Overnight culture (10μl) and LB media (190μl) were placed in each well and gentamycin was added, at concentrations from 0-20 μM. The cells were incubated for 5 hours and 24 hours respectively and the absorbance was read at 630nm. The results, shown in figures 62 and 63, show a significant decrease in absorbance after both 5 and 24 hours for both MRSA and *E. coli.* Therefore it was decided that both cell lines were still viable for use in the assay.

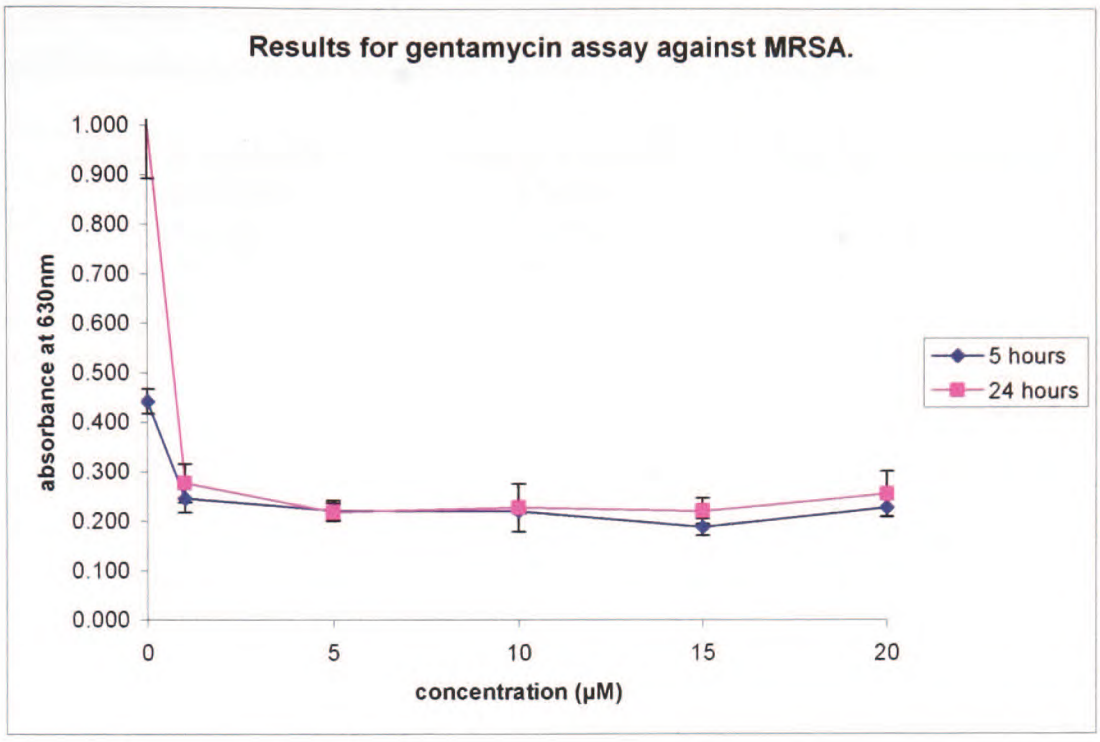

Figure 62. Dose response curve for gentamycin against MRSA

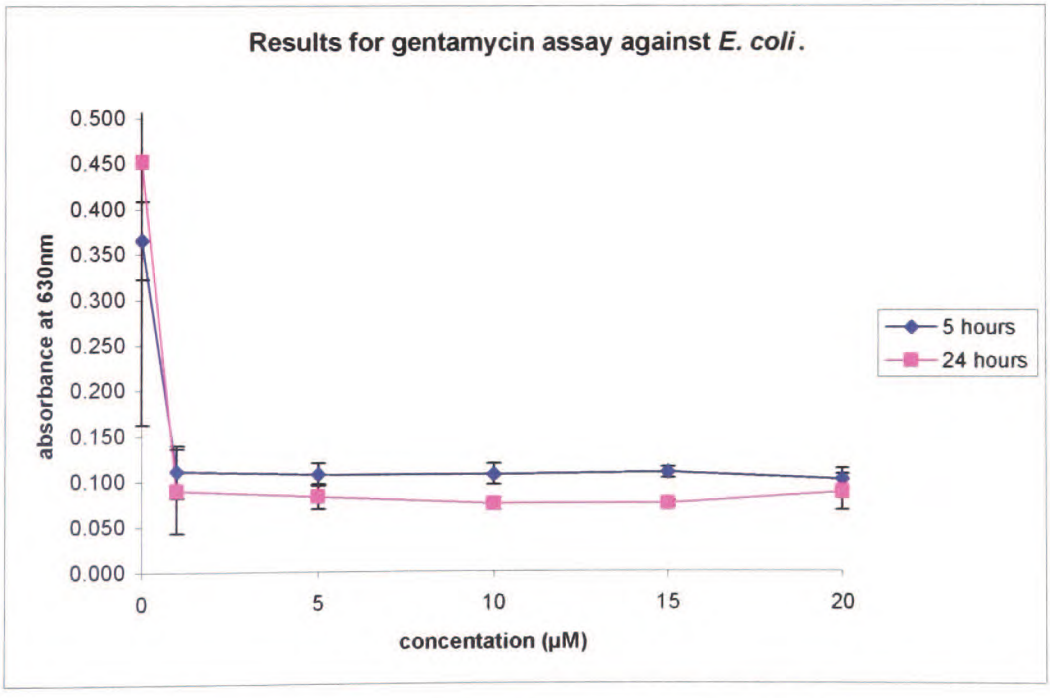

Figure 63. Dose response curve for gentamycin against *E. coli*.

It was decided to test the sensitivities of the MRSA used against a number of other antibiotics using a disc diffusion test, the results of which are shown in table 7.

Name of Anitbiotic	Type of Antibiotic	Resistant or sensitive
Flucloxacillin	β-lactam	R
Penicillin	β-lactam	R
Clarithromycin	Macrolide	R
Fusidic acid	Cholestadienes	S
Vancomycin	Glycopeptide	S
Gentamycin	Aminoglycoside	S
Linezolid	Oxazolidinone	S
Ciprofloxacin	Fluoroquinolone	R
Mupirocin	Polyketide	S
Trimox	β-lactam	S
Neomycin	Aminoglycoside	S
Rifampin	Semi-synthetic. Inhibits RNA synthesis	S
Tetracycline	Tetracycline	S

Table 7. Antibiotic sensitivities of MRSA.

1.2.3 Possible problems with reading absorbance.

t was thought that the colour of the porphyrins in the media may have been affecting the esults. The plates were read at 630nm with only porphyrin and media at drug oncentrations of 0-50 μM. It was found that there was no significant change in bsorbance with increasing drug concentration and hence the colour of the solution was ot adversely affecting the results.

.2.4. Varying fluence.

, light dose of 40 J/cm^2 had been used up to this point and it was decided to increase the ght dose in order to ascertain if this had any effect on the results. An increased light ose of 80 J/cm^2 was used and the results are shown in figure 64 and 65. Again no ecrease in absorbance was seen for either MRSA or *E. coli*.

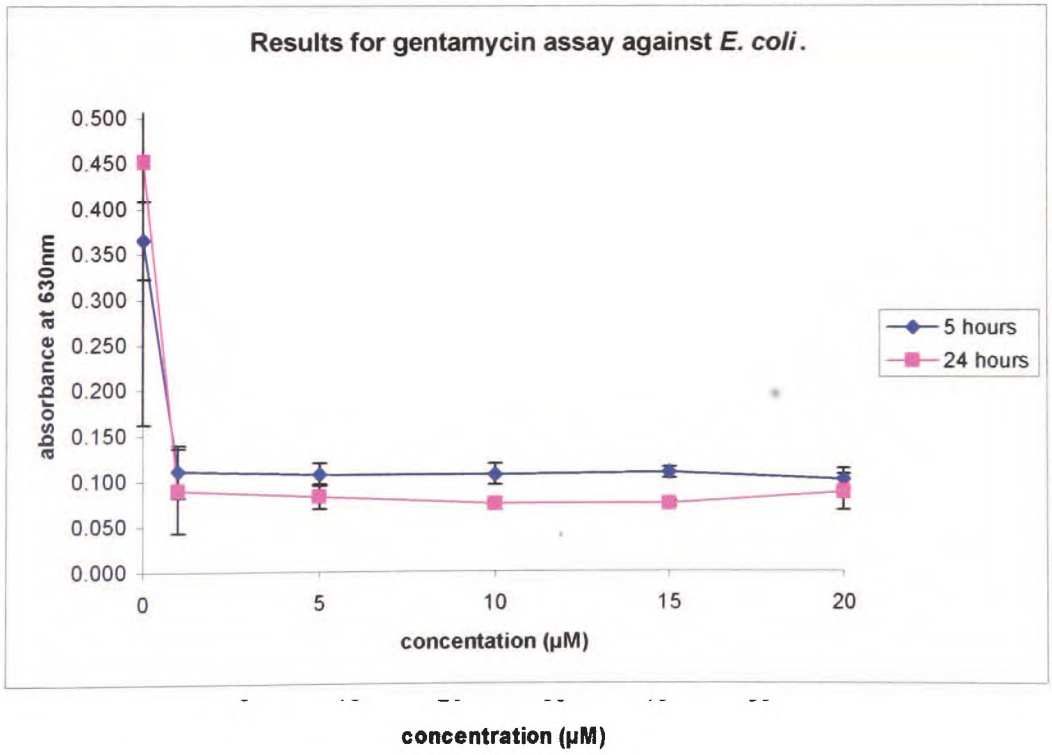

Figure 64. Results of increased light dose on MRSA, where series 1 is a light dose of 40 J/cm^2, series 2 is a light dose of 80 J/cm^2 and series 3 is the dark control.

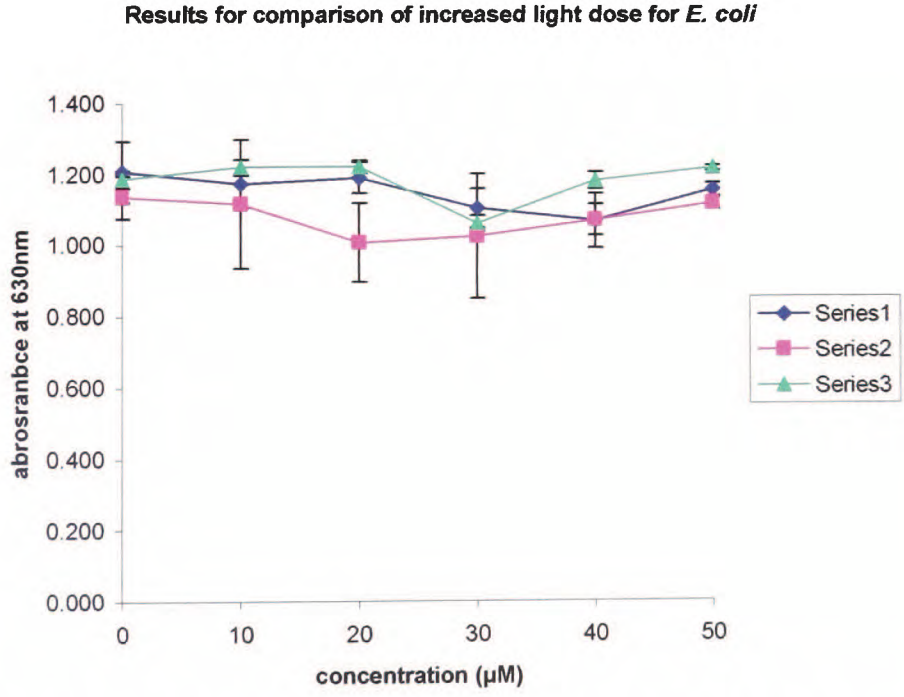

gure 65. Results of increased light dose for *E. coli* , where series 1 is a light dose of 40 J/cm^2, series 2 is a light dose of 80 J/cm^2 and series 3 is the dark control.

4.2.5. Alternative method for determining cell viability.

It was decided at this point that reading the absorbance of the wells on a plate reader may not be accurate enough for determining cell death. The MTS assay was therefore used in order to achieve a stronger absorbance per well. The MTS assay involves the use of the tetrazolium compound (3-(4,5-dimethylthiazol-2-yl)-5-(3-carboxymethoxyphenyl)-2-(4-sulfophenyl)-2H-tetrazolium, inner salt; MTS) and the electron-coupling reagent, phenazine methosulfate (PMS) [99]. MTS is chemically reduced by cells into formazan, which is soluble in tissue culture medium. The measurement of the absorbance of the formazan can be carried out using 96-well microplates. The assay measures dehydrogenase enzyme activity found in metabolically active cells. Since the production of formazan is proportional to the number of living cells, the intensity of the produced colour is a good indication of the viability of the cells. Unfortunately this assay was difficult to use due to the number of bacteria present per well making all wells very dark, and hence it was not possible to read the difference in absorbance per well. It was decided to plate out the bacteria from the wells and count the number of colony forming units (CFU's) per well in order to determine a more accurate picture of what was happening. The assay was performed as previously with the exception that after irradiation and incubation overnight the cells were serially diluted by a factor of 10^{-4} or 10^{-5} and spread onto agar plates. The plates were then incubated overnight and the CFU's were counted. It was found that diluting the wells 10^{-4} gave too many CFU's to count and diluting them 10^{-5} showed no cell kill for either MRSA or *E. coli*. This method was used for optimisation of assay conditions, however it was very time-consuming and hence not appropriate for screening the library of compounds.

4.2.6. Determining bacteriostatic vs. bacteriocidal activity.

It was hypothesised that the protocol may have been inducing bacteriostasis, as opposed to cell death, and the bacteria were re-growing after 18 hours. Therefore it was decided to plate out the bacteria 30 minutes after incubation, after 60 minutes and after 18 hours to enable us to determine if any re-growth had occurred. The results show no significant diminution in CFU's for any of the time points after incubation, so it was concluded that no initial cell knockdown and re-growth had occurred.

4.2.7. Effects of washing cells.

Cell washing steps were added to the initial protocol so that only porphyrin either taken up by or bound to the cell was irradiated. It was decided to remove the cell washing step in order to determine whether the porphyrin was indeed capable of killing the cells. The results of this showed that the porphyrin can kill bacteria although there is no difference between the light and dark toxicities so this cell kill was not due to a PDT effect.

4.2.8. Fractionating light dose.

The next hypothesis tested was that there is only a limited amount of oxygen in the wells and, upon irradiation, this is depleted. Therefore, it was decided to fractionate the light dose with 30 minutes in a shaking incubator between doses in order to allow oxygen levels to replenish. The light dose was split into two doses of 40 J/cm^2 with 30 minutes incubation between doses. The results, as shown in figures 66 and 67, show a significant cell kill after irradiation with a fractionated light dose although again there is no difference between light and dark controls.

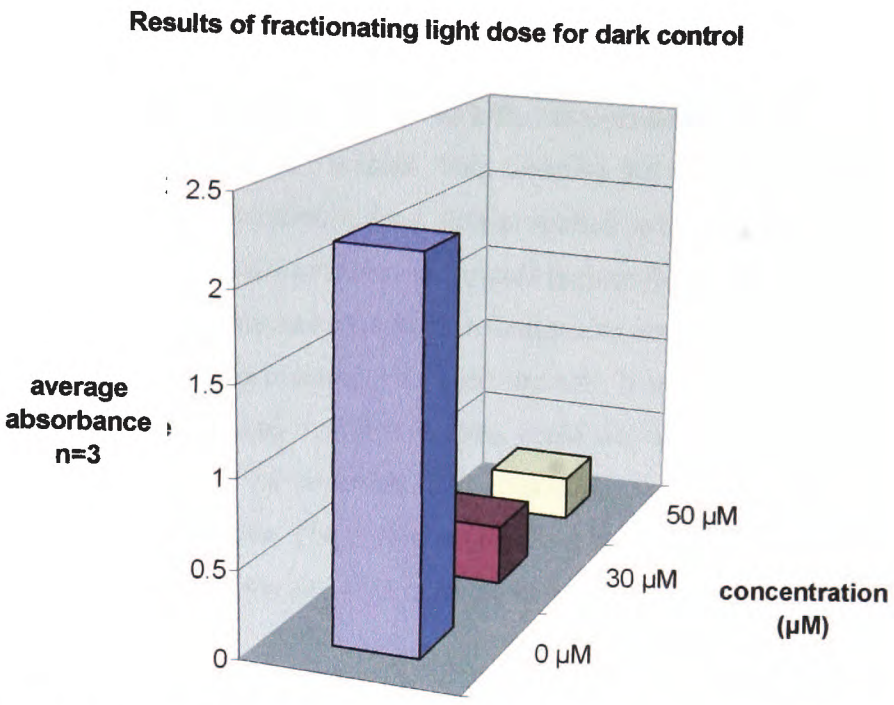

Figure 66. Results of fractionating light dose show a decrease in cell growth for dark controls using MRSA

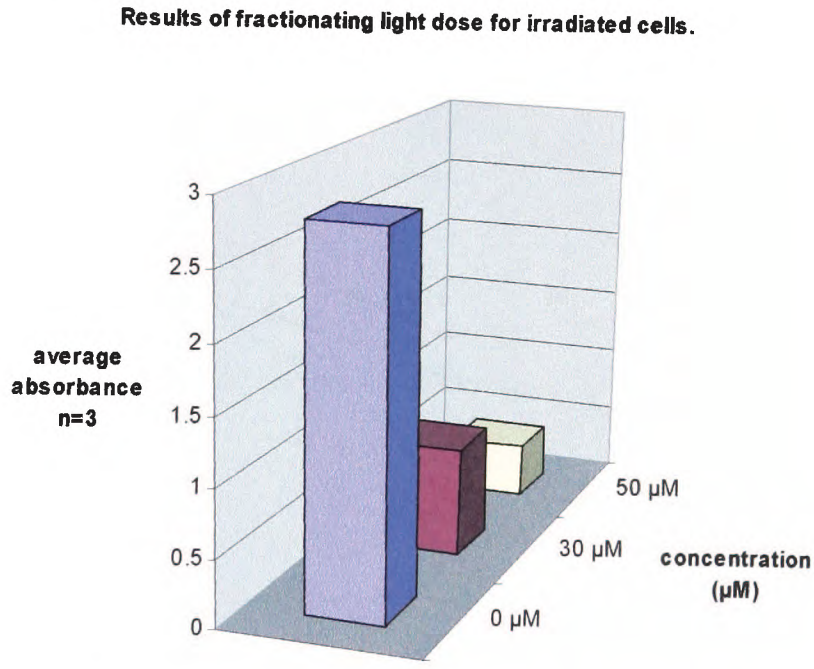

Figure 67. Results of fractionating light dose show a decrease in cell growth for irradiated cells using MRSA.

4.2.9. Importance of incubation time.

The cells have previously been shown to be killed independently of whether they were irradiated or kept in the dark as a control. This could be due to self-promoted uptake of the drug during the 4 hour incubation time. Self-promoted uptake, as described in chapter 1, is the process whereby poly-cationic compounds replace the divalent cations from the outside of the cell membrane and, due to their bulky size, create gaps in the membrane which allow additional drug molecules to enter the cell. It was hypothesised that if the incubation time was shortened then this process could not occur to such an extent and hence a PDT effect would be observed. This hypothesis was tested by shortening the incubation time to 20 minutes. The results after 20 minutes incubation, shown in figure 68, show some cell knockdown although no selectivity between light and dark. (μM)

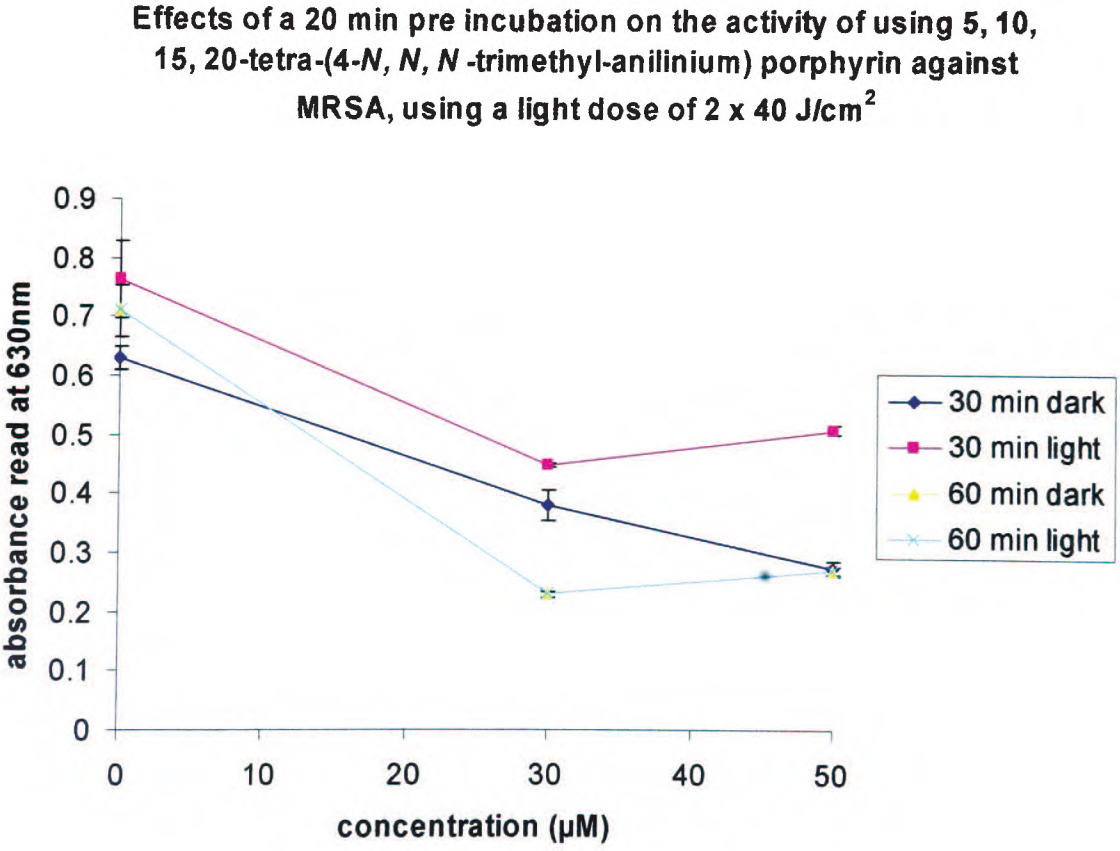

Figure 68. Results of 20 minute incubation time for MRSA.

It was then decided to reinstate the washing step and reduce the incubation time further to 5 minutes and this gave the graph showing the dose response curve for MRSA. The results, as shown in figure 69, show that there is significant light toxicity after 5 minutes incubation, but importantly no dark toxicity.

4.3. Dose response curves

4.3.1. MRSA.

Figures 69 and 70 show the dose response curve for MRSA using 5, 10, 15, 20-tetra-(4-*N*, *N*, *N*-trimethyl-anilinium) porphyrin.

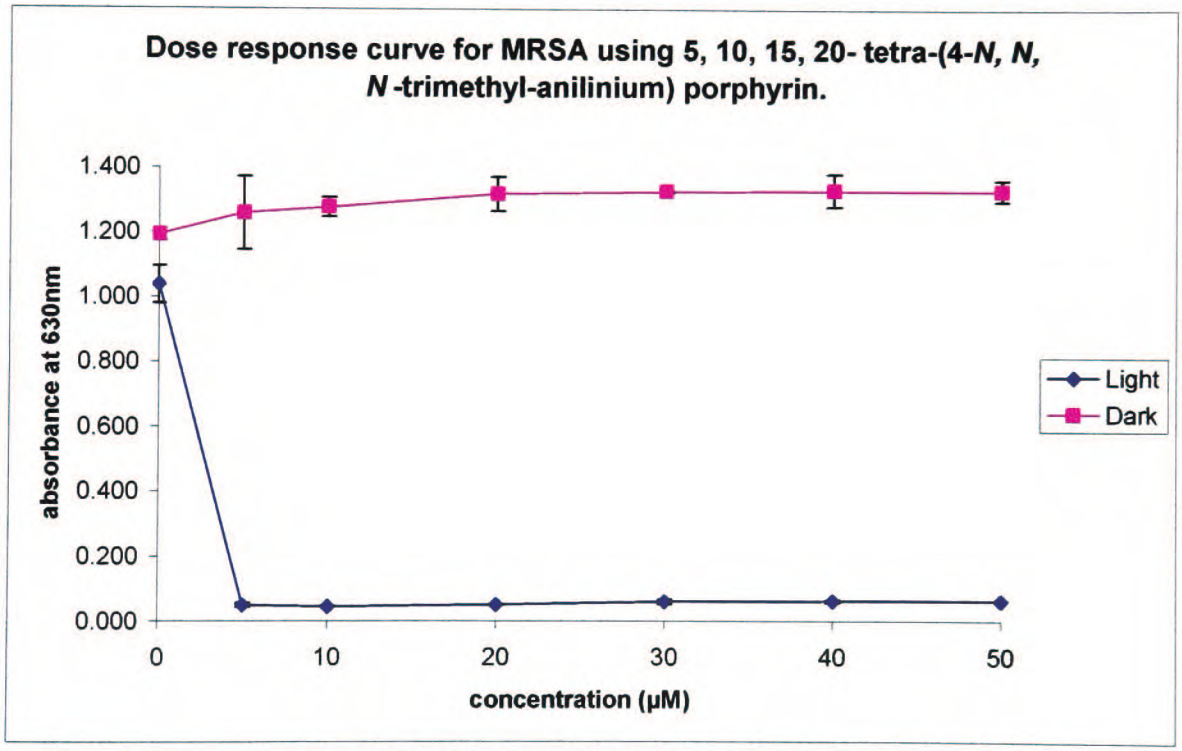

Figure 69. Dose response curve for MRSA using 5, 10, 15, 20-tetra-(4-*N*, *N*, *N*-trimethyl-anilinium) porphyrin.

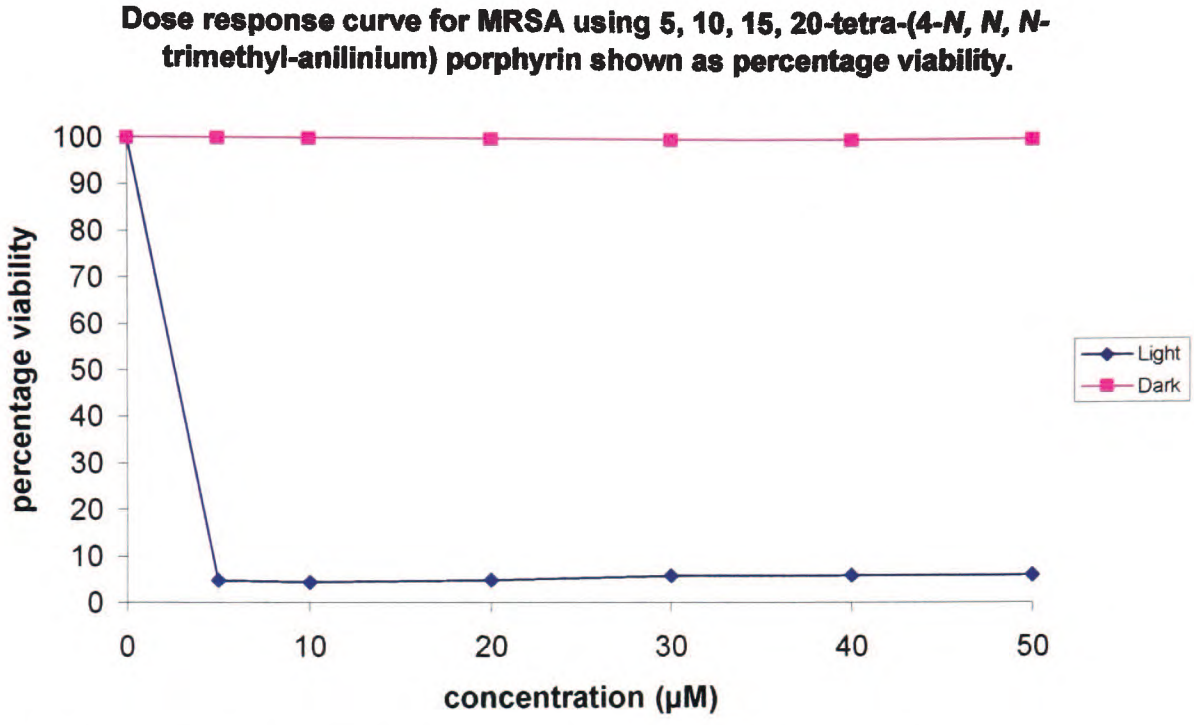

Figure 70. Dose response curve for MRSA using 5, 10, 15, 20-tetra-(4-*N*, *N*, *N*-trimethyl-anilinium) porphyrin shown as percentage viability.

4.3.2. *E. coli.*

Although the assay was now working for the Gram positive bacteria it was still not producing any PDT effect for Gram negative bacteria, as shown in figure 71, for which the same method was used as for the MRSA in figure 69. This could be due to the outer membrane on the Gram negative bacteria preventing the drug binding to the cell and/or the compound not having enough positive charge on the periphery in order to be taken up by the cell via self-promoted uptake. Therefore, it could be important to look at compounds with more than four cationic charges in order to determine whether they can be effective in the PDI of Gram-negative bacteria.

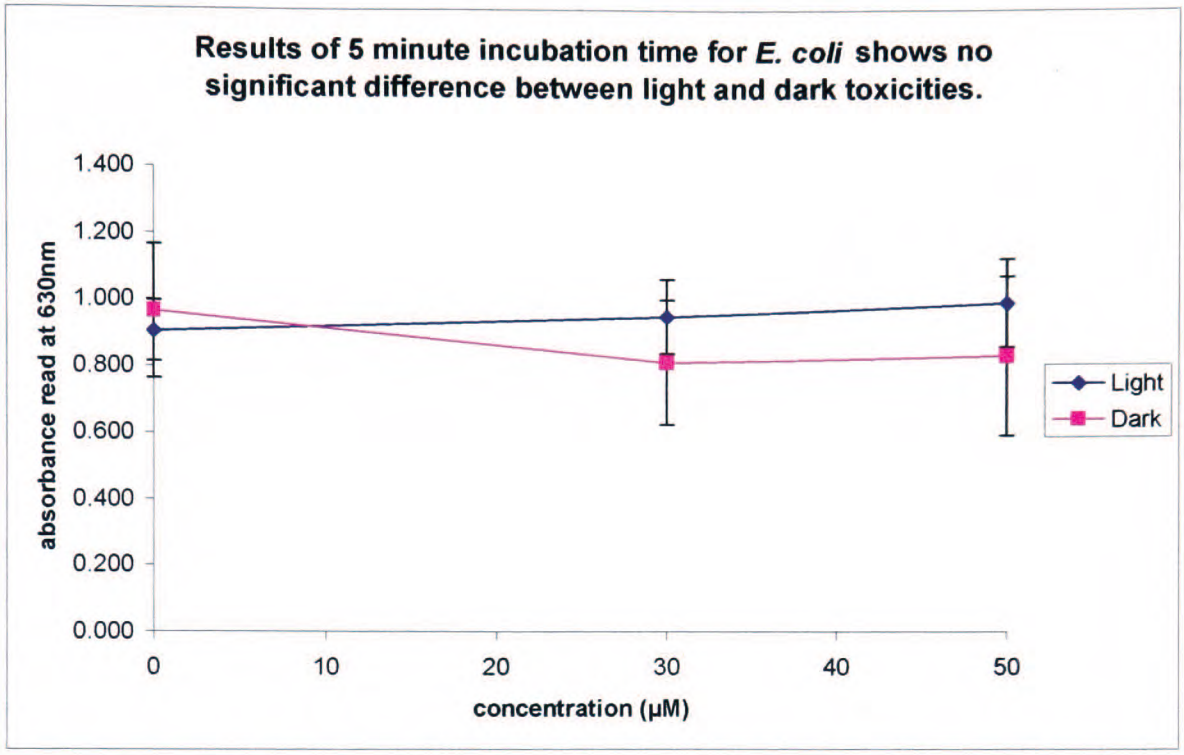

Figure 71. Results from *E. coli* with 5 minute incubation time.

Chapter 5. PACT Results and Discussion.

Using the methods developed in chapter 4 we were able to generate, and present in this chapter, data showing the activity of a number of synthetic porphyrins tested against *S. aureus*, MRSA and *E. coli*. In this chapter we also present data in relation to potential factors that impact on activity.

5.1 Biological methods.

5.1.1. General

5.1.1.1. Bacterial cells

The cells used were graciously obtained from Hull Royal Infirmary and the sensitivities of the MRSA isolate are shown in chapter 4.2.2. (table 7). They were grown under aseptic conditions (see chapter 4.1.4) and stored between 2 - 4°C when not in use. 3×10^8 cells were used per well

5.1.1.2. Assay conditions.

Assays were completed in 96 well, conical bottomed plates and the contents were transferred to 96 well flat-bottomed plates prior to irradiation. Luria-Bertani (LB) growth media was used in the assay.

5.1.1.3. Assay controls.

Two plates were used per assay, one of which was irradiated and the other kept in the dark as a control. The assay was conducted in a darkened room to ensure accurate control of the light dose and all drug concentrations were performed in triplicate.

5.1.1.4. Light Source.

The light source used was a panel of light emitting diodes (633 nm) (Omnilux EL1000A Phototherapeutics Ltd, Altrincham).

5.1.1.5. Reading Absorbances.

The plates were read at 630 nm using an MRX II microtitre plate reader (Dynex technologies).

5.1.2. Assay protocol.

The optimized method used for the *in-vitro* phototoxicity assay, was as follows:

To each well, 10µl of an overnight culture of bacteria was added with 180µl of LB media. 10µl of drug solution at the appropriate concentration range for each well (made up using DMSO) or DMSO (for controls) was then added to each well. The plates were incubated for 5 min at 37°C prior to being centrifuged (10 min, 1500g, 20°C). The media was removed and fresh media added. The contents of each well were then transferred to the 96 well, flat bottomed plate. The plates were irradiated with 40 J/cm^2 red light then incubated for 30 minutes in shaking incubator. The plates were removed from the incubator and were irradiated with a further 40 J/cm^2 red light. The plates were then returned to the shaking incubator and incubated overnight at 37°C. Absorbances were then measured at 630 nm using a microtitre plate reader.

5.2. Partition coefficients - method used.

The method used for calculating partition coefficients was that developed by Cunderlikova *et al* [101]. Namely, 15 ml phosphate buffered saline (PBS) (pH 7.43) and 15 ml 1-octanol were agitated for 2 minutes then centrifuged (1500G, 10 min, room temp). Porphyrin (3 mg) was added to 10 ml octanol and 0.3 ml of the resulting solution was added to 1.35 ml PBS and 1.35 ml octanol. This solution was agitated for 4 mins then centrifuged. 1 ml of each layer was analysed by UV/Vis absorption at 514 nm. Partition coefficients were calculated by equation 1 where [octanol] and [PBS] are the concentrations of drug in the octanol and PBS layer respectively.

$$P = \frac{[\text{octanol}]}{[\text{PBS}]} \qquad \text{equation 1}$$

To determine the concentration of drug in each layer, the extinction coefficients (ε) for octanol and PBS must be calculated using Beer's law. Serial dilutions of known

concentrations of drug solution were taken and the absorbance read at 514 nm. The wavelength was measured at 514 nm rather than at the Soret band due to the peak being less affected by aggregation at this wavelength (broader peaks would mean less accurate readings at the concentrations used). From this it was possible to calculate $^{Oct}\varepsilon$ and $^{PBS}\varepsilon$ for each compound using Beer's law, ε = A/Cb, where C is concentration A is absorbance read at 514 nm, and b is the cell path length in centimeters.

5.3. Statistics.

5.3.1. Data Analysis.

The LD_{50} and LD_{90} values were calculated by graphical analysis, using MS Excel, however this method does not easily allow for statistical differences between the results to be determined. . Standard deviations were calculated from the data and give some indication as to significance however we also used probit regression analysis (SPSS for windows, v14). This analysis gives median concentration values for the LD_{50}, with 95% confidence limits on those as an indication of the accuracy of the output. Probit analysis was initially carried out on results from irradiated cells only. In addition to deriving regression equations from which endpoints (LD_{50}, LD_{90}) can be calculated, probit analysis also gives a chi-square (χ^2) statistic as an indication of the goodness of fit of the regression model. Table 8 shows the results of the analysis using SPSS and the problems associated with this method for our data set. The majority of data is included to show how difficult the statistical analysis was using our data set. Note the negative values produced, using this method, for compounds **89** and **92**. These values are clearly impossible and highlight that special care must be taken when interpreting the statistics. Due to the small data set and the small values of some of the data it was not possible to perform meaningful statistical analysis on these data, however simple standard deviations were generated for all of the values and these are presented in table 9 for the same data set.

Compound number	LD_{50}	Lower bound	Upper bound	LD_{90}	Lower bound	Upper bound	χ^2	p
88	93.537	NG	NG	226.102	NG	NG	4.076	1.000
89	-9.118	NG	NG	15.029	NG	NG	13.384	0.818
90	14.074	8.042	29.240	27.979	18.751	67.885	26.265	0.240
91	17.744	10.173	33.286	30.712	21.266	67.210	15.629	0.407
92	-763.637	NG	NG	-1456.504	NG	NG	0.839	1.000
82	73.236	NG	NG	160.707	NG	NG	4.661	1.000
93	7.578	0.333	15.137	25.131	16.886	53.104	23.495	0.862
94	3.710	NG	NG	22.614	NG	NG	15.476	0.079

Table 8. Mean LD_{50} and LD_{90} for MRSA for irradiated cells. Calculated using SPSS. NG=not given. This table shows the limitations of this method of analysis, the highlighted values are clearly not accurate

Compound number	LD_{50}	Lower bound	Upper bound	LD_{90}	Lower bound	Upper bound
88	-	-	-	-	-	-
89	2.5	1.87	2.83	3.5	3.04	3.96
90	8	7.2	8.8	18	16.2	19.8
91	19	16.72	21.28	24	21.12	26.88
92	-	-	-	-	-	-
82	-	-	-	-	-	-
93	4	3.76	4.24	9	6.75	11.25
94	4.5	4.18	4.82	9.5	5.41	13.59

Table 9. Mean LD_{50} and LD_{90} for MRSA for irradiated cells. Calculated using Excel. This table shows the advantages of using this method compared to using SPSS. (- = no cell kill).

5.3.2. Statistical analysis.

Statistical testing between compounds was carried out by one way analysis of variance (ANOVA) followed by a *posteriori* comparison of means. All data were tested for homogeneity of variance and in cases where this assumption was seriously violated,

attempts were made to transform the data or the appropriate non-parametric test (Kruskal-Wallis) was carried out. Post-hoc testing of such data was carried out using the Gamess and Howell test.

The results from the one way ANOVA tests are shown in appendix 1.

However due to the limitations of this analysis (small sample size and values outside the limits of this test, the data generated was of little use, as shown in tables 8 and 9. With the data from the irradiated cells being of little use it was decided not to continue this analysis using the dark control values.

5.4. Structure activity relationships.

5.4.1. The effect of chain length.

Compounds **88** to **91** (shown in figure 72) vary in chain length. The chain lengths used are methyl, ethyl, propyl or butyl, and these surround a phosphorus cation. The dose response curves for MRSA are shown in figures 73 to 76. The LD_{50} and LD_{90} values of each compound were calculated, from assay results for both irradiated cells and dark control and the results for MRSA are compared in table 10.

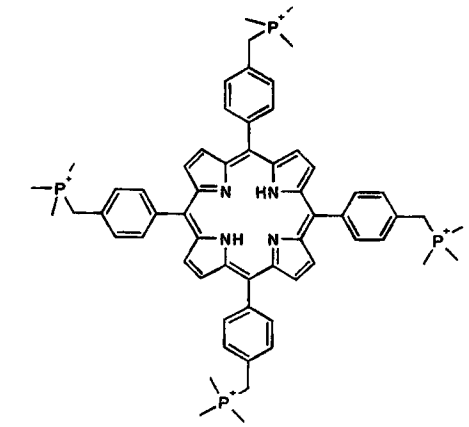

88

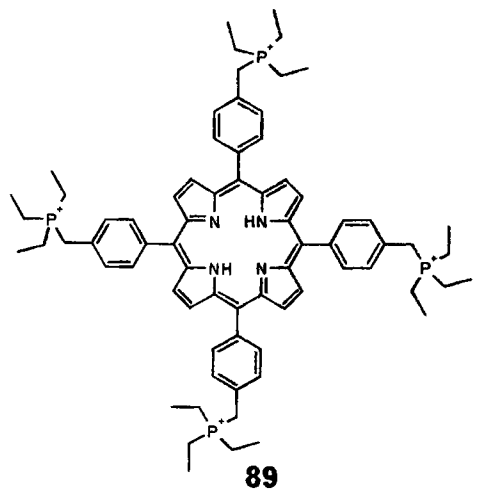

89

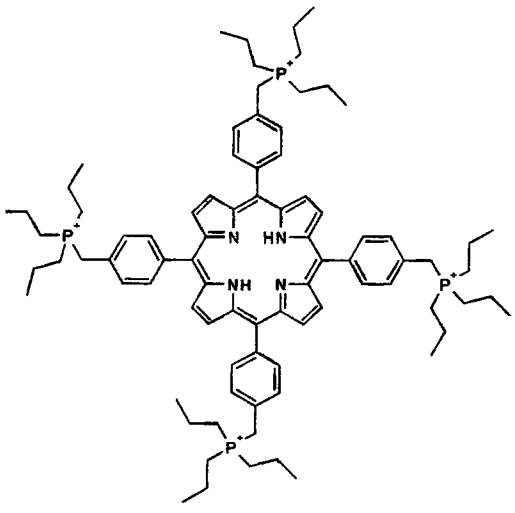

90

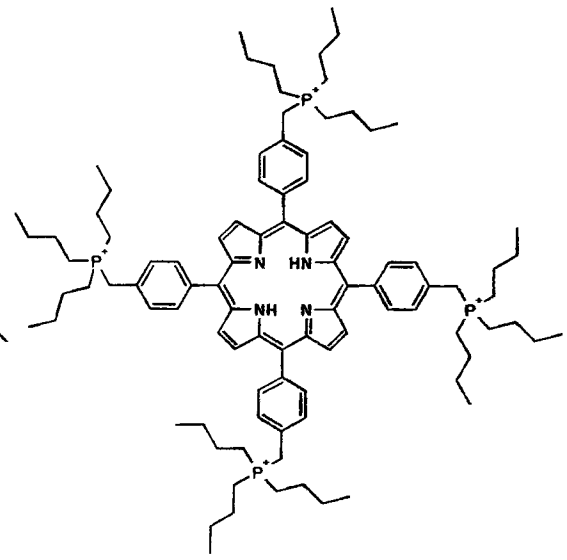

91

Figure 72. Compounds **88** to **91** vary in aliphatic chain length around the phosphorus cation.

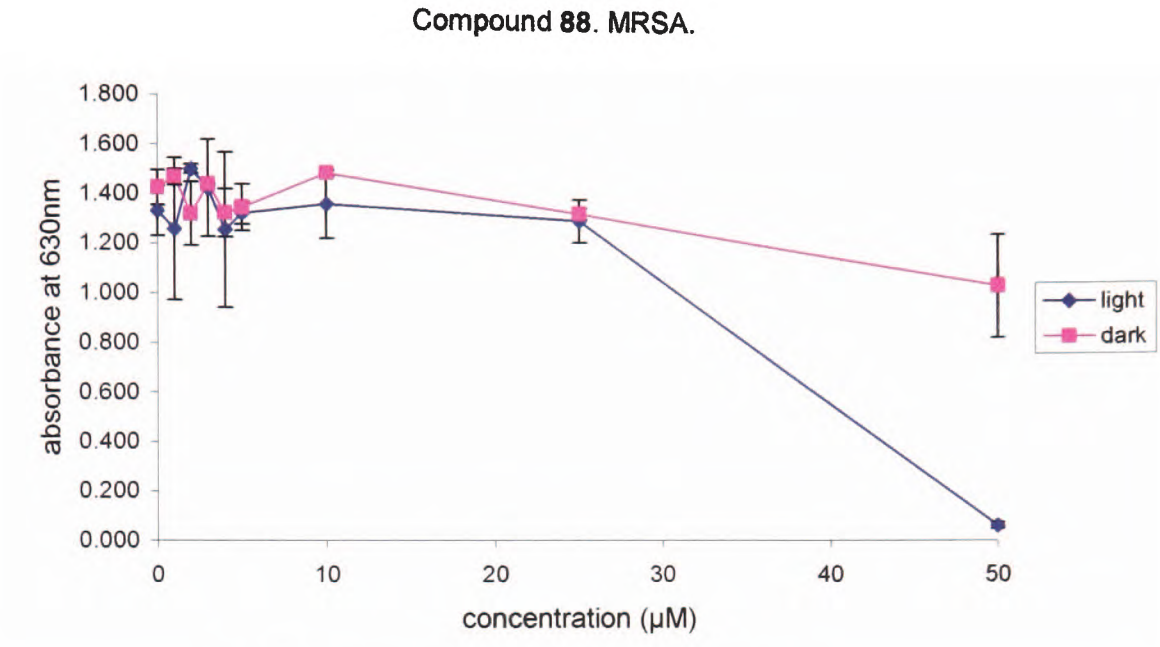

Figure 73. Dose response curve for compound **88**, for MRSA.

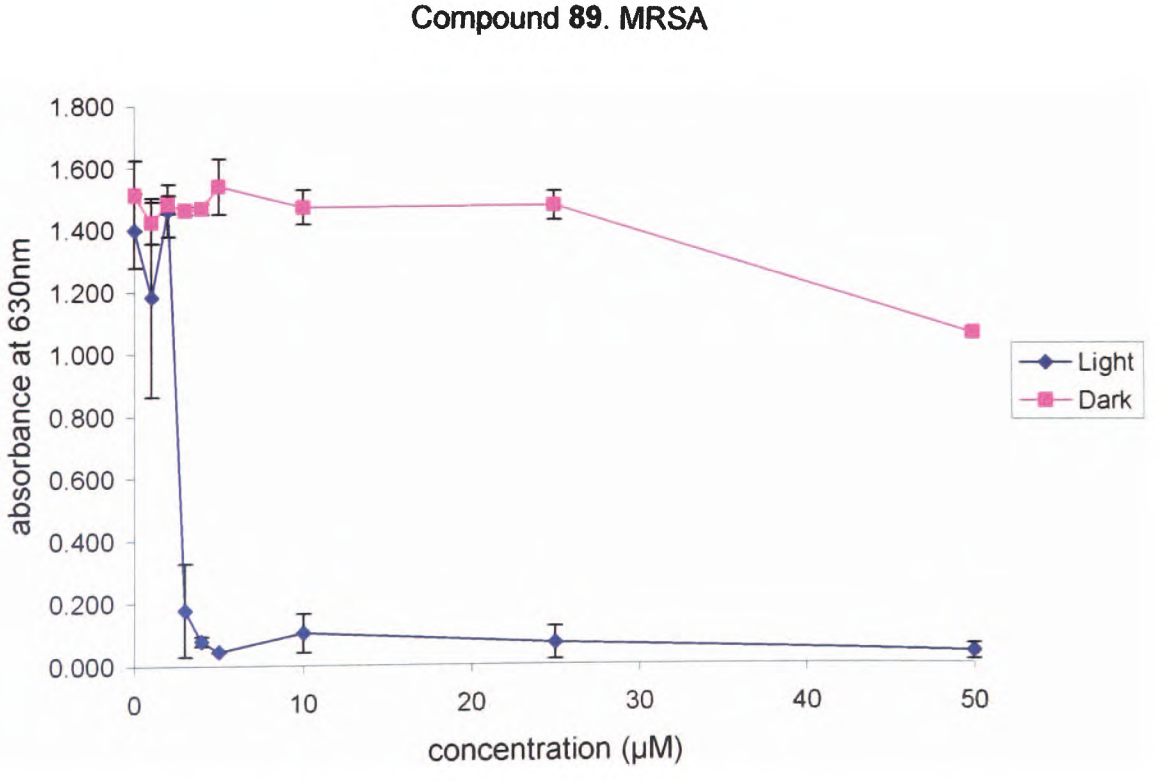

Figure 74. Dose response curve for compound **89**, for MRSA

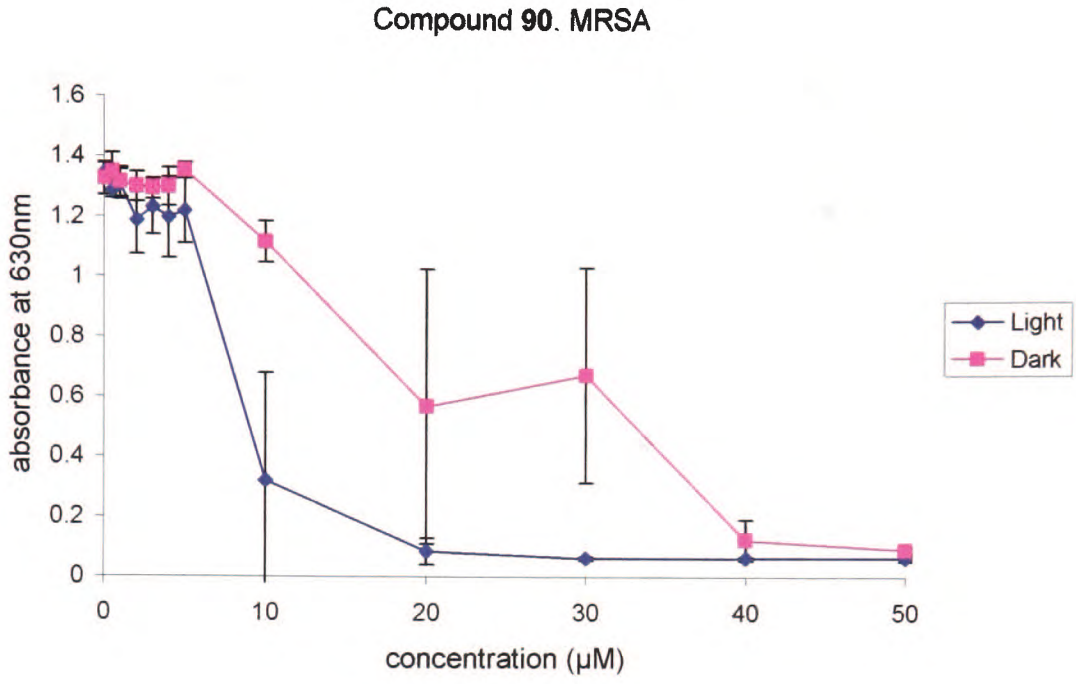

Figure 75. Dose response curve for compound **90**, for MRSA

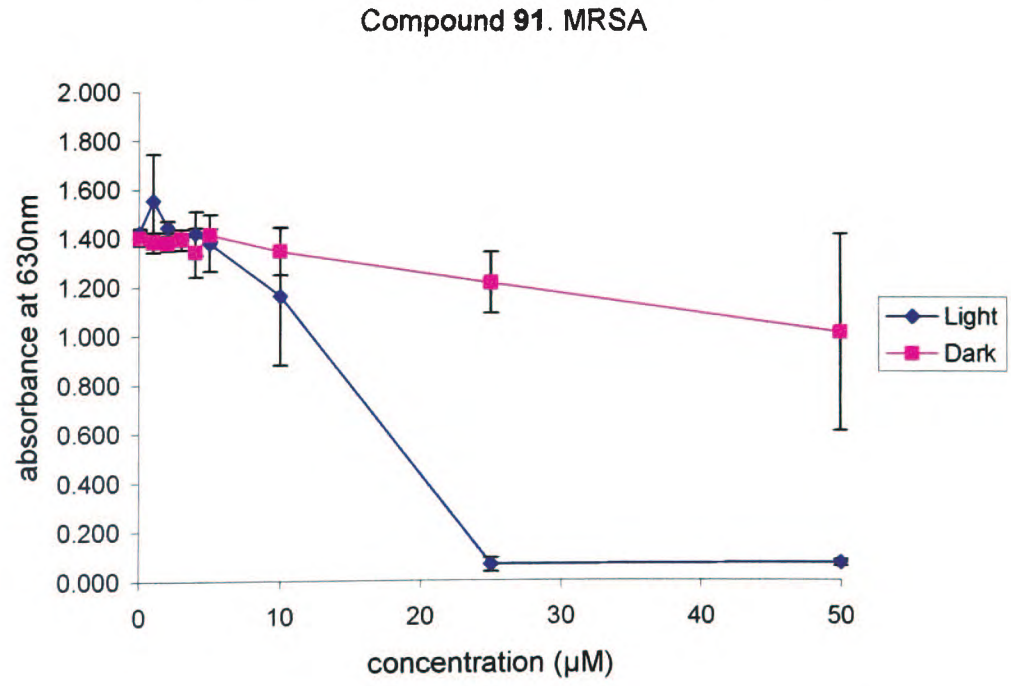

Figure 76. Dose response curve for compound **91**, for MRSA

Compound number	Partition coefficient	LD_{50} Light (± SD)	LD_{90} Light (± SD)	LD_{50} Dark (± SD)	LD_{90} Dark (± SD)
88	0.057	-	-	-	-
89	0.02	2.5 (0.33)	3.5 (0.46)	-	-
90	0.97	8 (0.8)	18 (1.8)	18 (7.0)	40 (15.6)
91	N/A	19 (2.28)	24 (2.88)	-	-

Table 10. Data observed from dose response curves for MRSA. Values shown are in μM (N/A = no absorption in PBS). N.B. Extinction coefficients were determined in homogeneous solution for each compound and were used to determine P.

It can be seen from these results that the optimum aliphatic chain length around a phosphorus cation is two carbon atoms. Increasing the carbon chain length decreases the activity of the compounds whilst decreasing the carbon chain length to methyl groups gives no activity. Interestingly, significant dark toxicity was detected as the chain length increased from two to three however this effect was not observed for the next compound in the series. Figure 77 shows the nitrogen analogues of these compounds, figures 78 to 81 show the dose response curves for MRSA and table 11 gives the tabulated assay results. It can be seen that, in moving from phosphorus to a nitrogen centred cation, there is a shift in optimum chain length from 2 to 3 carbons atoms. The data from the partition coefficients shows no correlation between P values and LD_{90} values. This is highlighted by looking at compounds **89** and **90**, where the LD_{90} values are 3.5 and 18 respectively, with P values being 0.02 and 0.97 respectively. Unfortunately there are not enough data within this set to be more precise. Interestingly neither compound **91** or **94** partitioned into the aqueous phase, but both still exhibited photodynamic activity against bacteria.

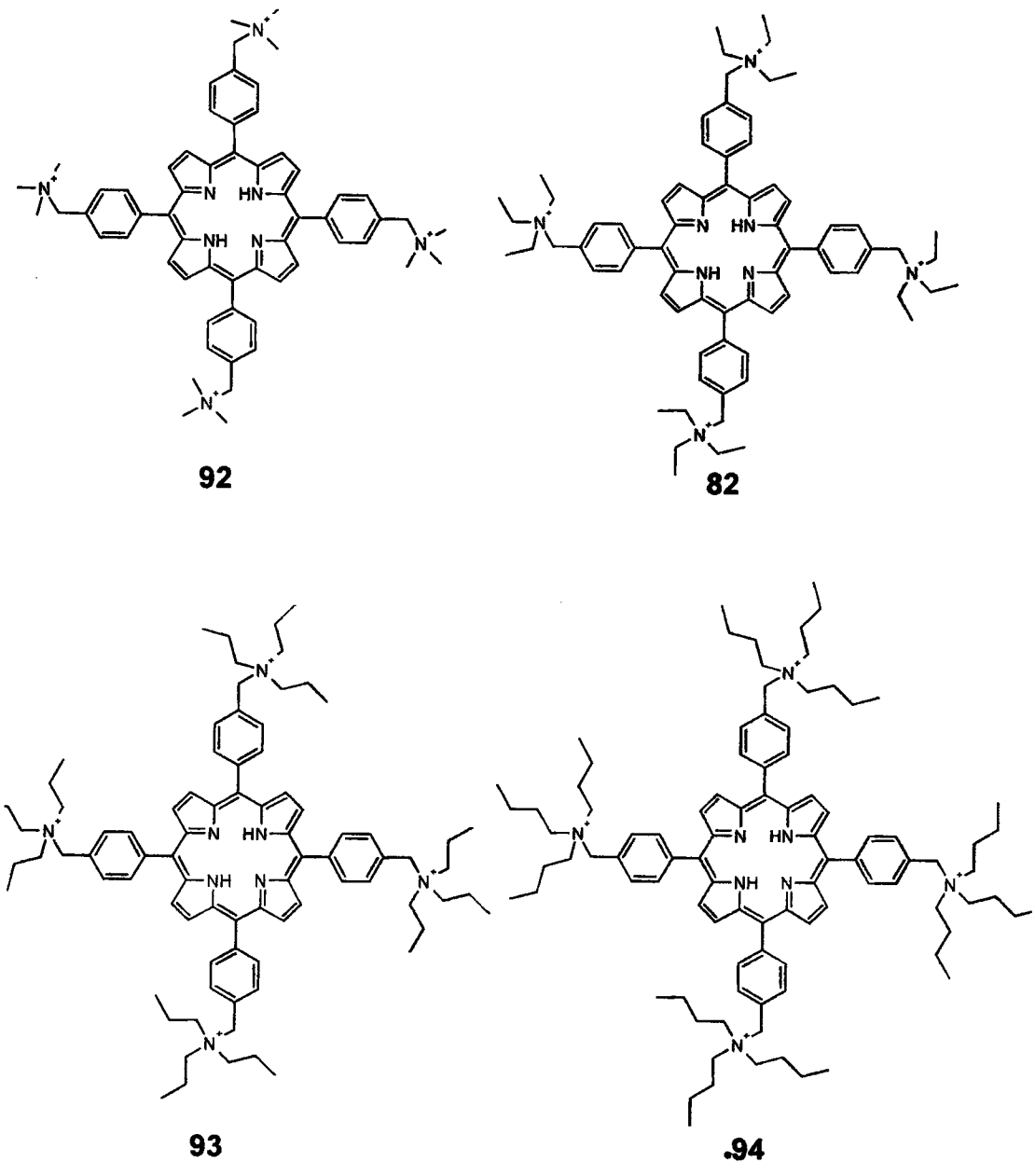

Figure 77. Compounds **92**, **82**, **93** and **94** vary in aliphatic chain length around the nitrogen cation.

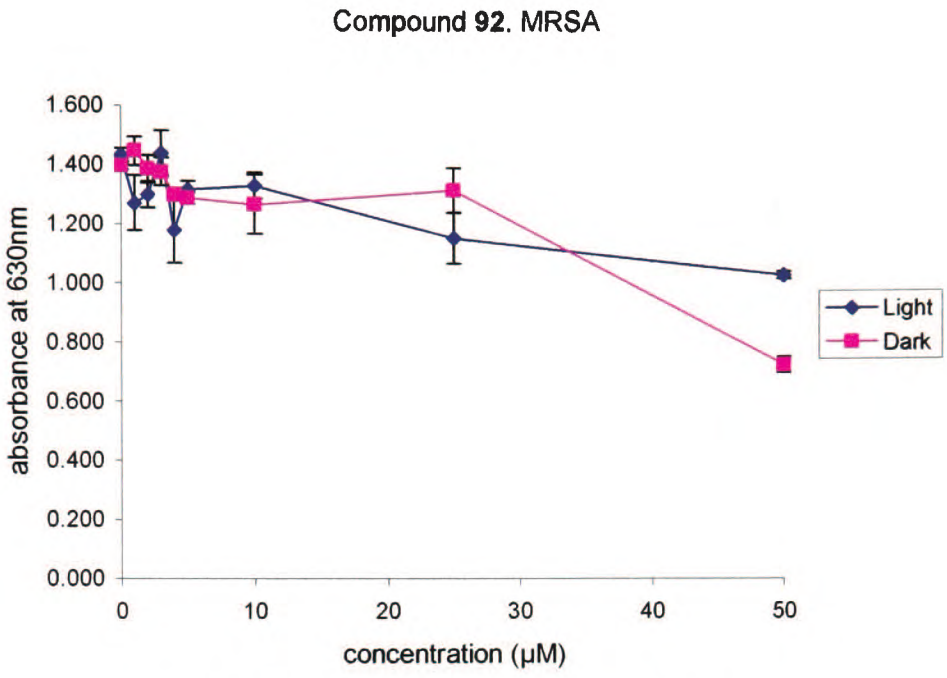

Figure 78. Dose response curve for compound **92**, for MRSA

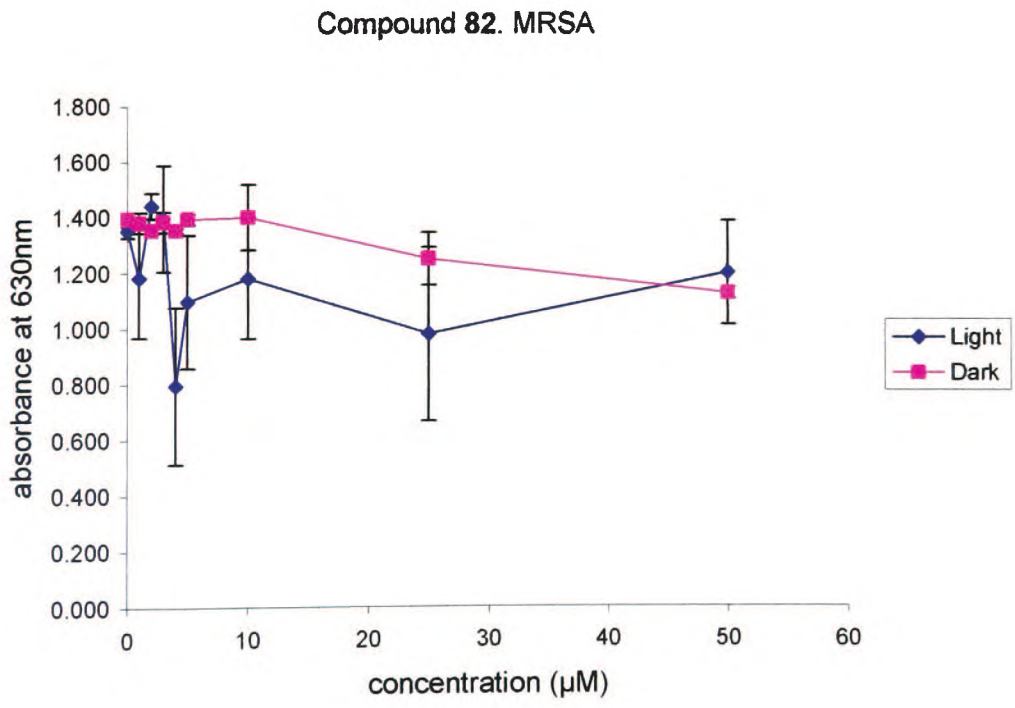

Figure 79. Dose response curve for compound **82**, for MRSA

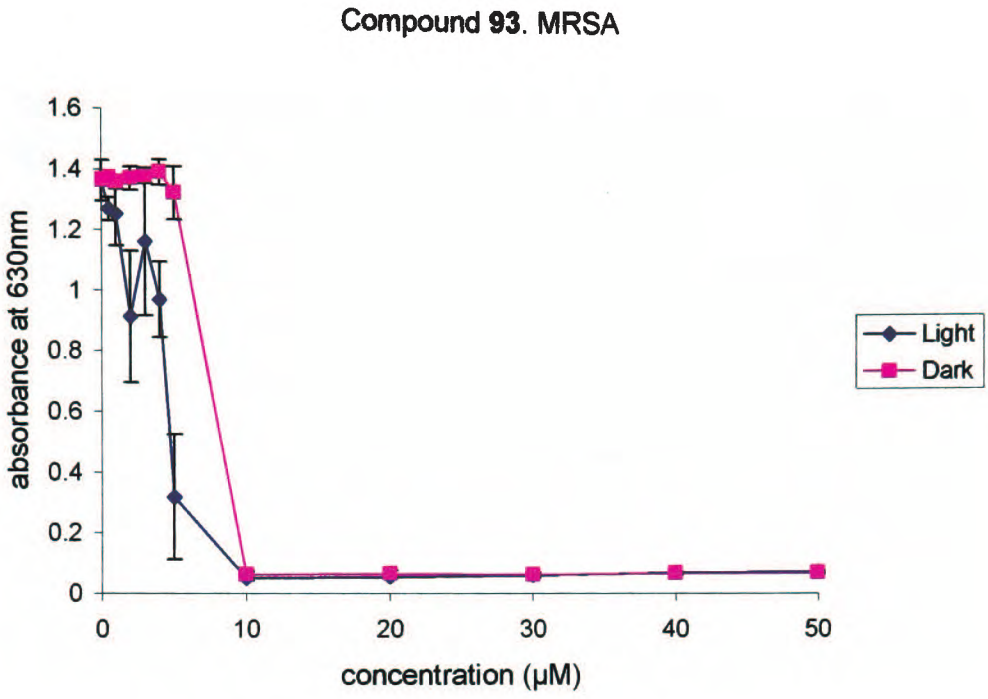

Figure 80. Dose response curve for compound **93**, for MRSA

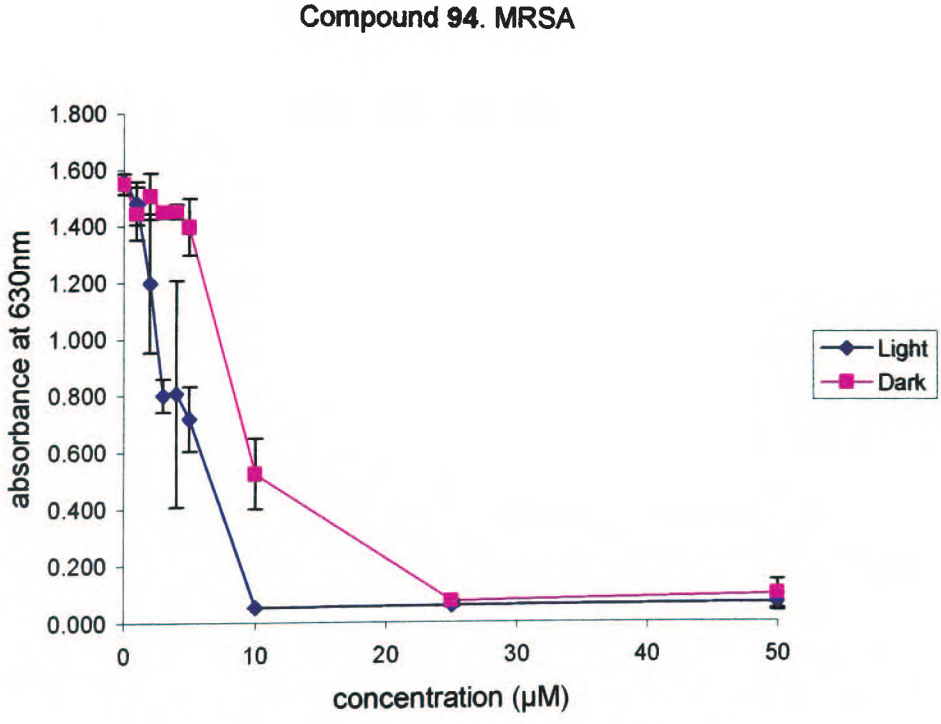

Figure 81. Dose response curve for compound **94**, for MRSA

Compound number	Partition coefficient	LD_{50} Light (±SD)	LD_{90} Light (± SD)	LD_{50} Dark (± SD)	LD_{90} Dark (± SD)
92	0.71	-	-	-	-
82	0.037	-	-	-	-
93	0.177	4 (0.24)	9 (2.25)	8.5 (0.60)	9.5 (0.95)
94	N/A	4.5 (0.32)	9.5 (4.09)	9.5 (0.57)	22 (5.5)

Table 11. Data observed from dose response curves for MRSA. Values shown are in μM (N/A = no absorption in PBS). N.B. Extinction coefficients were determined in homogeneous solution for each compound and were used to determine P.

5.4.2. Aliphatic vs. Aromatic

It was found that, in general, the compounds with aromatic groups surrounding the cation had less activity when compared with those having aliphatic groups surrounding the cation. Partition coefficients for compounds **98**, **95**, **81**, and **96** could not be calculated as we were unable to detect drug in the aqueous phase. However compounds **97**, **99** and **96** gave good biological results and the structures and activities of these are shown in figures 82-85 and table 12 respectively.

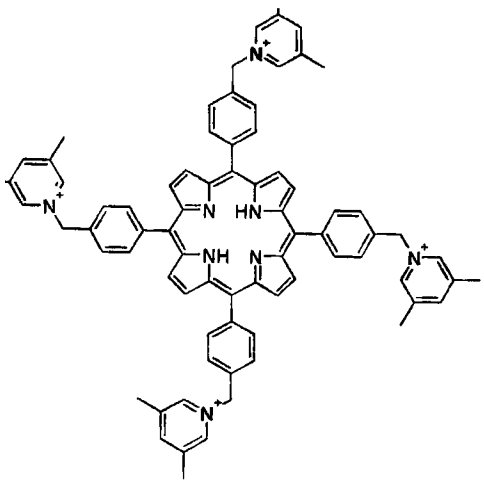

97

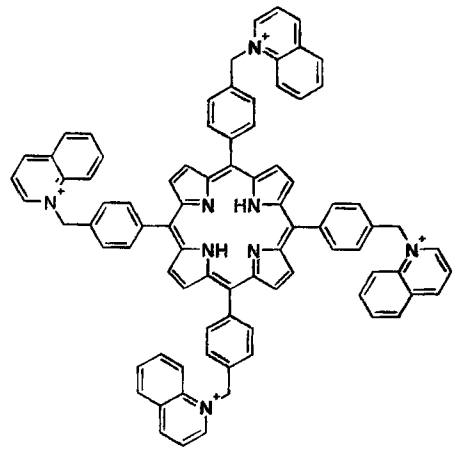

99

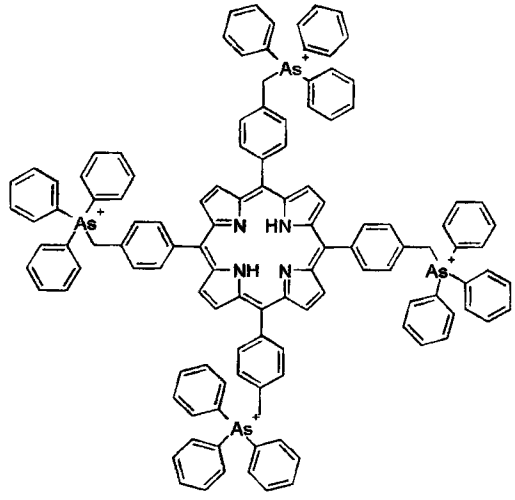

96

Figure 82. Aromatic R groups which gave good activity.

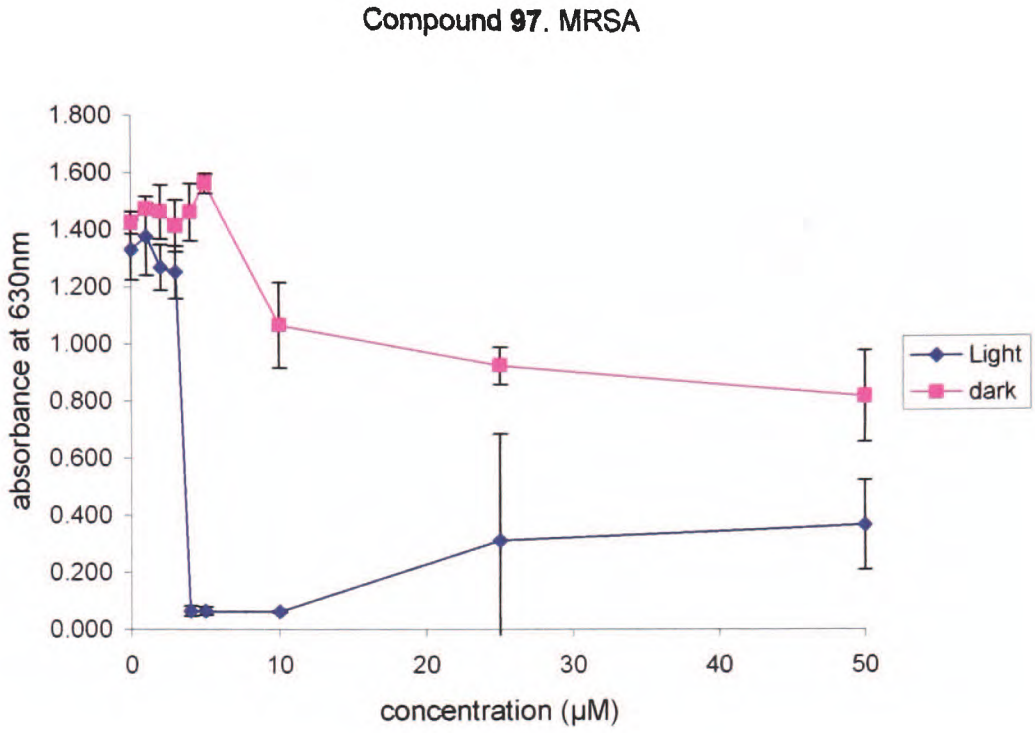

Figure 83. Dose response curve for compound 97, for MRSA

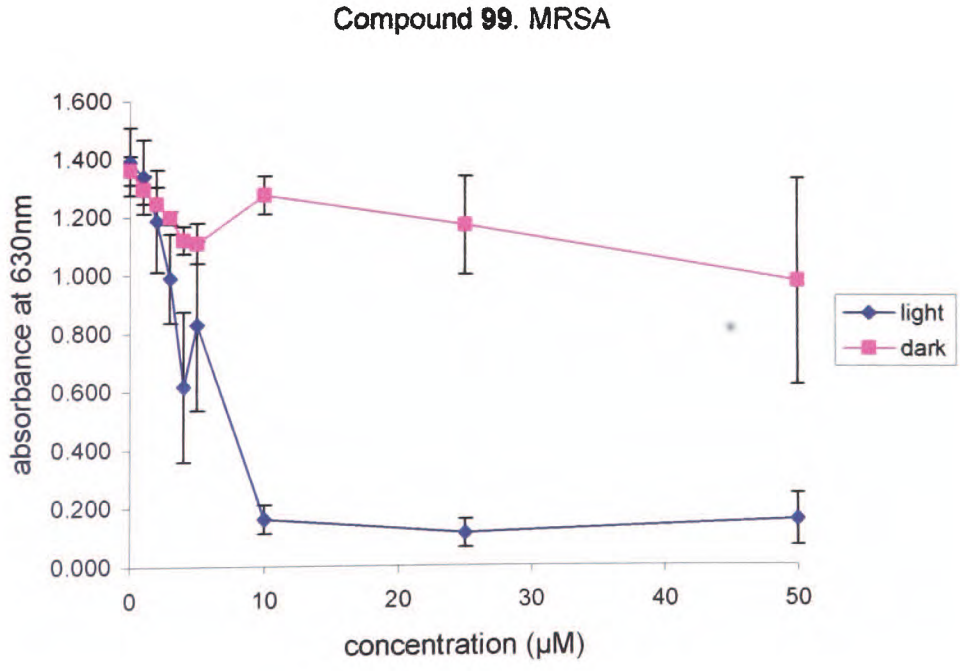

Figure 84. Dose response curve for compound 99, for MRSA

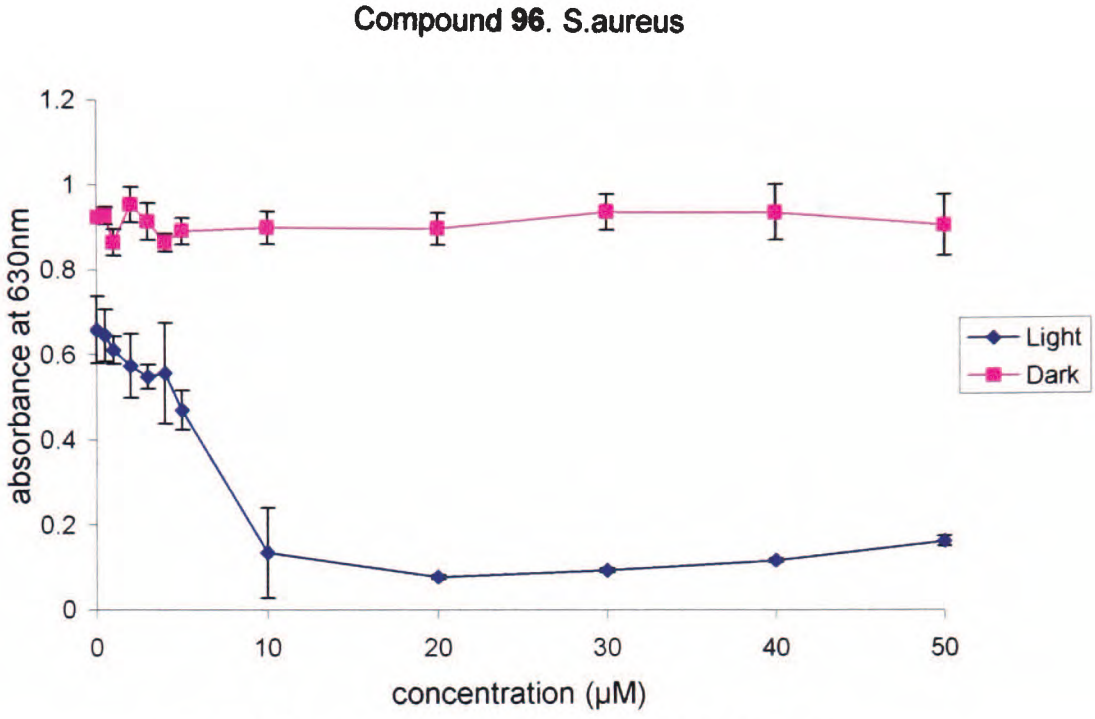

Figure 85. Dose response curve for compound **96**, for *S. aureus*.

Comp	Bacterial strain	LD_{50} Light (±SD)	LD_{90} Light (±SD)	LD_{50} Dark (±SD)	LD_{90} Dark (±SD)
97	MRSA	3.5 (0.24)	4 (0.4)	-	-
99	MRSA	4 (0.64)	15 (4.2)	-	-
96	MRSA	-	-	-	-
97	*S. aureus*	4.5 (0.27)	7.5 (0.23)	-	-
99	*S. aureus*	20 (1.8)	-	-	-
96	*S. aureus*	8 (1.12)	20 (1.2)	-	-

Table 12. Activities of compounds **97**, **99** and **96** expressed in μM for MRSA and *S. aureus*. Calculated using Excel.

Although compound **96** gave good activity with *S. aureus* there was no activity for the analogous triphenyl phosphoniumyl compound, **81**, and possible reasons for this are

discussed in section 5.4.6. For compound **96** there was no measurable distribution into the aqueous phase, making meaningful comparisons of Partition coefficients difficult. Tables 10 and 11 suggest that P is not a good predictor for activity. A graph of log P vs.1/C, which would normally be a good model for structure-activity relationships, is not possible in this case due to the small data set. The size of the available data set is primarily due to compounds not distributing to any significant degree into the aqueous phase, therefore rendering P values meaningless or, alternatively, lack of activity of compounds, hence negating the 1/C value. A similar conclusion was reached by Banfi *et al* [102] who investigated structure activity relationships of 7 different cationic porphyrins and were unable to find an unambiguous relationship between the PS's lipophilicity and activity. The reason why the compounds appear not to follow any observable trends in hydrophobicity vs. activity could be due to interaction of the cationic porphyrin with the bacterial cell wall. The porphyrins are flat, relatively rigid molecules and they are therefore limited in the number of orientations in which the cations can approach and bind to the membrane. It may therefore be possible that charge distribution around the cationic sites, rather than simple hydrophilic / hipophilic character, could be important in determining photosensitiser-bacteria interactions. It was decided therefore to investigate different representations of each compound to determine whether the molecular models and Mulliken charges [103] could be used to construct a hypothesis of how the charge on each cation would interact with the membrane. Mulliken charges provide model representation of charge distribution within a molecule and are a means of estimating partial atomic charges via computational chemistry methods [104]. The Mulliken charges were calculated using the GAMESS function of Chem3D. The porphyrin ring was excluded from this process due to programme limitations, and as it could essentially be assumed to remain constant for all compounds due to its rigid aromatic framework, hence only the charges on the various R groups were calculated. Initially each structure around the cationic centres were minimised using MM2 (molecular mechanics force field method) to give an overall steric energy. Other conformations were then attempted as starting points and the MM2 was minimised and compared to the energies with the lowest values being the most stable conformer. Once the minimised structure was obtained the GAMESS calculation of charges was carried

out and produced as a text file. The results of this are shown in table 13. It was unfortunately not possible to calculate the Mulliken charges for the tribenzylphosphoniumyl, triphenylphosphiumyl or triphenylarsiniumyl moieties due to the computer programme limitations.

Table 13 compares the different compounds with their activities against MRSA and Mulliken charges on either the phosphorus or nitrogen atoms. From this it can be seen that there is no correlation between the activity and Mulliken charge on the P or N atom.

R group	LD_{50} (Light) (±SD)	Mulliken charge
	-	2.16
	2.5 (0.33)	1.797
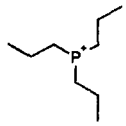	8 (0.8)	1.809
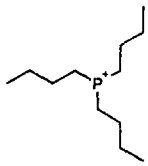	19 (2.28)	1.779
	-	-0.747
	-	-0.733
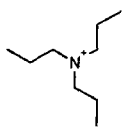	4 (0.24)	-0.752
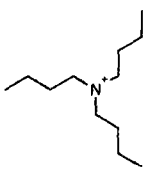	4.5 (0.32)	-0.753
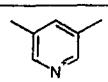	3.5 (0.24)	-0.889
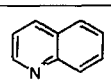	4 (0.64)	-0.955
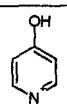	-	-0.893

ble 13. Comparison of R groups with analogous compounds activity in μM and Mulliken charge values oted for charges on either nitrogen or phosphorus atom, calculated using GAMESS function in Chem3D.

Two methods were used to determine the relationship between the variables of Mulliken charge and LD_{50}. The Pearson and Spearman's rank correlation coefficient were both used as we were unsure of the frequency distribution of the variables. However it can be seen from tables 14 and 15 that neither indicated any correlation between activity and Mulliken charge given for the cation.

Pearson Correlation		LD50	mulliken
LD50	Correlation co efficient	1	.096
	Sig. (2-tailed)		.734
	N	15	15
mulliken	Correlation coefficient	.096	1
	Sig. (2-tailed)	.734	
	N	15	15

Table 14. Shows correlations between LD_{50} values against MRSA and Mulliken charge on either the N or P atom.

Spearman's rank correlation coefficient			LD50	mulliken
	LD50	Correlation Coefficient	1.000	.364
		Sig. (2-tailed)	.	.182
		N	15	15
	mulliken	Correlation Coefficient	.364	1.000
		Sig. (2-tailed)	.182	.
		N	15	15

Table 15. Shows non-parametric correlations between LD_{50} values against MRSA and Mulliken charge on either the N or P atom.

5.4.3. MRSA vs *S. aureus*.

Although antibiotic-resistant bacteria are able to survive in the presence of the antibiotic, this resistance comes at a price. When there is no antibiotic present they take longer to grow and take up vital nutrients. MRSA and *S. aureus* have many similarities in their phenotype but do contain some subtle differences. Majcherczyk *et al* [105] showed that matrix-assisted laser desorption ionization-time of flight mass spectrometry (MADLI-

TOF-MS) can successfully differentiate between isogenic strains of bacteria. They tested isogenic strains of MRSA and methicillin-sensitive *S. aureus* (MSSA) isolates and determined that this technique may facilitate identification of surface components altered by expression of antibiotic resistance. It is possible that the differences in the surface components of MRSA and *S. aureus* are responsible for the differences in results between the two strains in this study and this may impact on their sensitivity to the different compounds. Tables 16 and 17 show the results for MRSA and *S. aureus* respectively.

Compound	LD_{50} Light (±SD)	LD_{90} Light (±SD)	LD_{50} Dark (±SD)	LD_{90} Dark (±SD)
88	-	-	-	-
89	2.5 (0.33)	3.5 (0.46)	-	-
90	8 (0.8)	18 (1.8)	18 (7.0)	40 (15.6)
91	19 (2.28)	24 (2.88)	-	-
92	-	-	-	-
82	-	-	-	-
93	4 (0.24)	9 (2.25)	8.5 (0.60)	9.5 (0.95)
94	4.5 (0.32)	9.5 (4.09)	9.5 (0.57)	22 (5.5)
97	3.5 (0.24)	4 (0.4)	-	-
98	-	-	-	-
99	4 (0.64)	15 (4.2)	-	-
95	-	-	-	-
81	-	-	-	-
96	-	-	-	-

Table 16. Results of assays for MRSA in μM

Compound	LD_{50} Light (±SD)	LD_{90} Light (±SD)	LD_{50} Dark (±SD)	LD_{90} Dark (±SD)
88	-	-	-	-
89	3.5 (0.42)	-	-	-
90	4.5 (0.67)	13 (3.7)	13 (0.52)	19 (4.37)
91	15.5 (1.08)	23.5 (8.9)	-	-
92	-	-	-	-
82	-	-	-	-
93	3.75 (0.3)	8 (1.12)	5.75 (0.3)	50 (27)
94	3 (0.3)	10 (1.5)	19 (4.0)	31 (5.58)
97	4.5 (0.27)	7.5 (0.22)	-	-
98	-	-	-	-
99	20 (1.8)	-	-	-
95	-	-	-	-
81	-	-	-	-
96	8 (1.12)	20 (1.2)	-	-

Table 17. Results of assays for *S. aureus* in μM

It can be seen from tables 16 and 17 that *S. aureus* was generally more susceptible to PDT than MRSA for most compounds although they produced similar trends in results when comparing groups of compounds, with the exception of compound **96**.

5.4.4. *E. coli.*

The assay produced no cell kill for *E. coli* with the exception of compounds **90**, **93** and **97**. The structures and activities of these compounds are shown in figure 86, figures 87-89 and table 18 respectively.

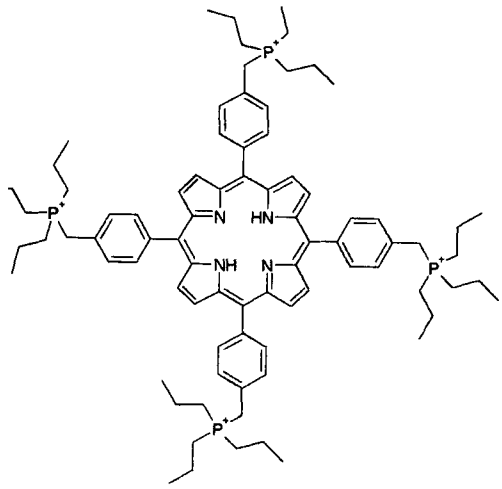

90

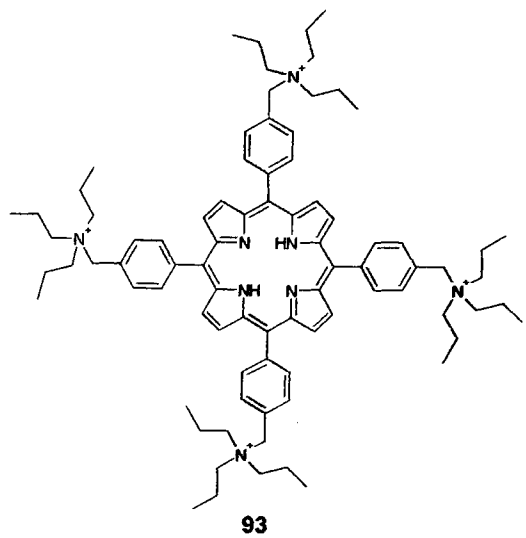

93

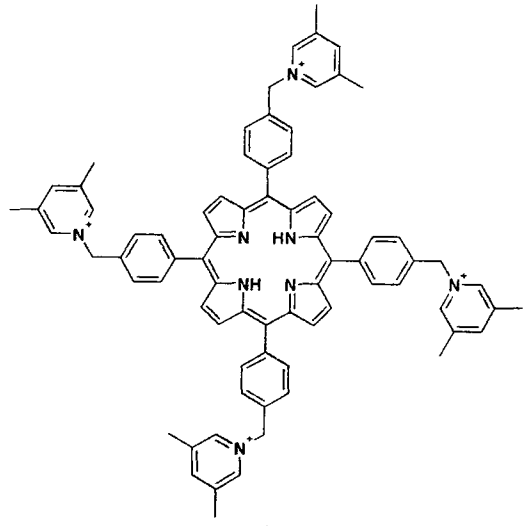

97

Figure 86. Structures of compounds showing activity against *E. coli*.

Compound 90. *E. coli*

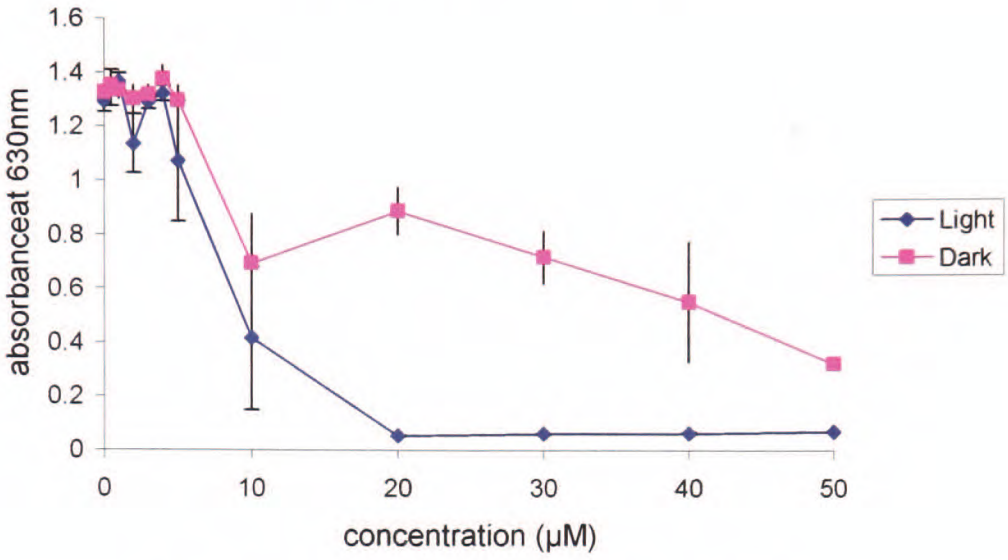

Figure 87. Dose response curve for compound **90** for *E. coli*

Compound 93. *E. coli*

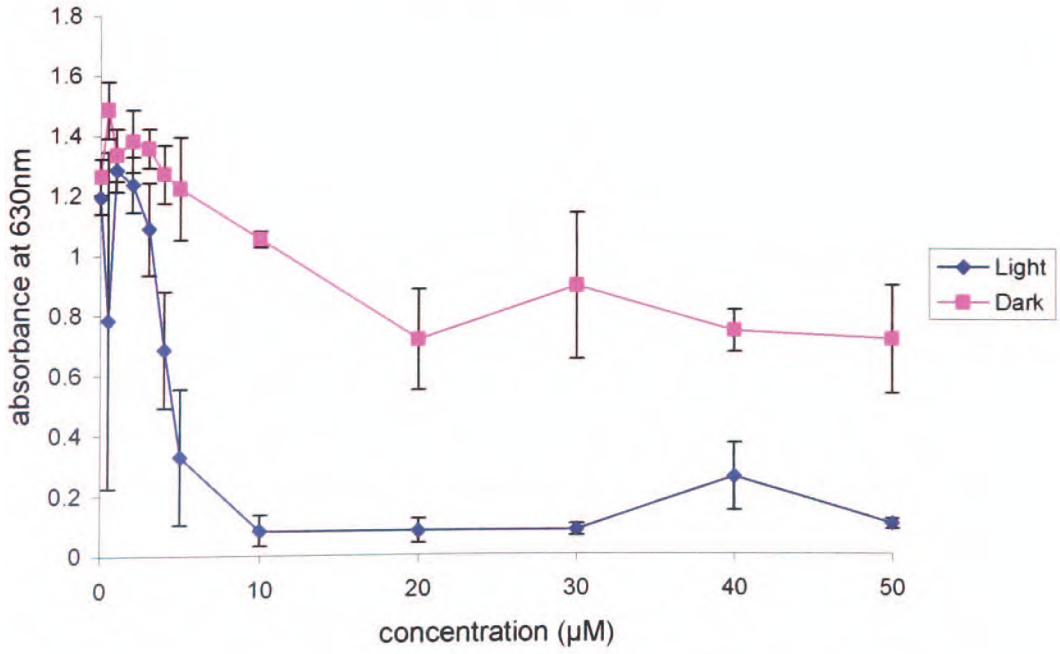

Figure 88. Dose response curve for compound **93** for *E. coli*

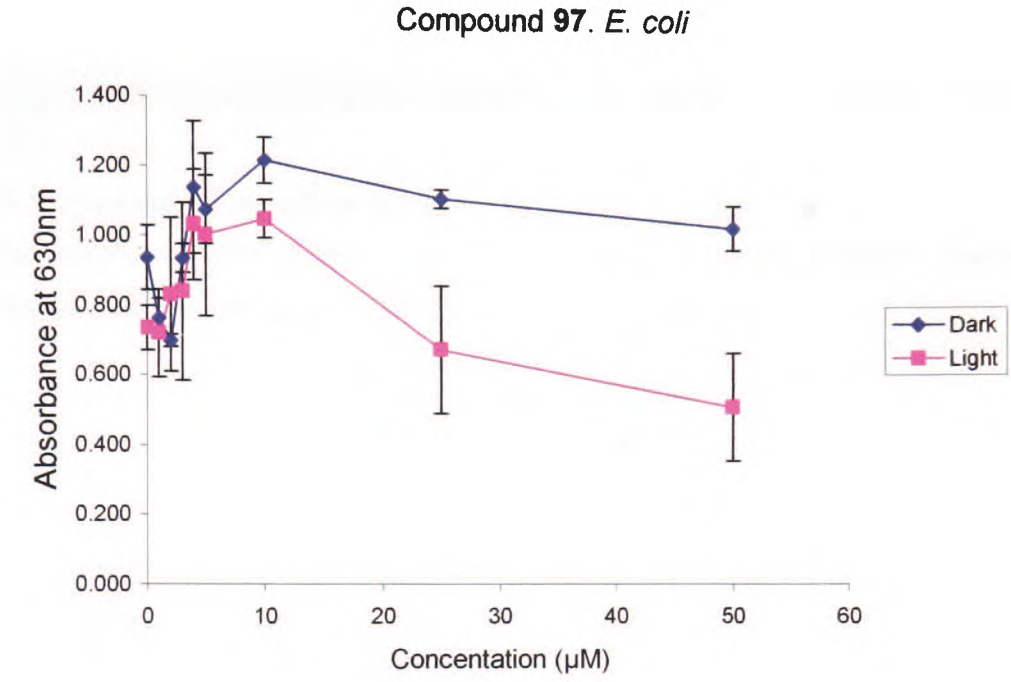

Figure 89. Dose response curve for compound **97** for *E. coli*

Comp	LD_{50} Light (±SD)	LD_{90} Light (±SD)	LD_{50} Dark (±SD)	LD_{90} Dark (±SD)
90	8 (1.68)	18 (4.14)	34 (3.74)	-
93	4 (0.48)	9 (3.9)	-	-
97	50 (5.0)	-	-	-

Table 18. Compounds with activity against *E. coli*. Concentration values given in μM.

It can be seen, from table 18, that although compound **97** has an LD_{50} of 50 μM, this is the MIC for this compound. Compounds **90** and **93**, the phosphorus and nitrogen cations respectively, contain R groups consisting of propyl chains and both have relatively low LD_{50} and LD_{90} values which differ by a factor of two. These are clearly interesting, having very similar structures and activities against both Gram positive (MRSA and *S. aureus*) and Gram negative (*E. coli*) bacteria. It is suggested that these compounds have a broader spectrum of activity compared with the other compounds tested. This makes

them extremely interesting candidates for use in PACT, as wounds generally consist of multiple bacterial strains and hence these compounds could be expected to perform significantly better in eradicating all of the bacteria in a wound.

5.4.5. Compound 96. Arsenium cation.

Compound **96** was active against *S. aureus* but not against *E. coli* or MRSA. The assay results for compound **96** against *S. aureus* are shown in figure 90.

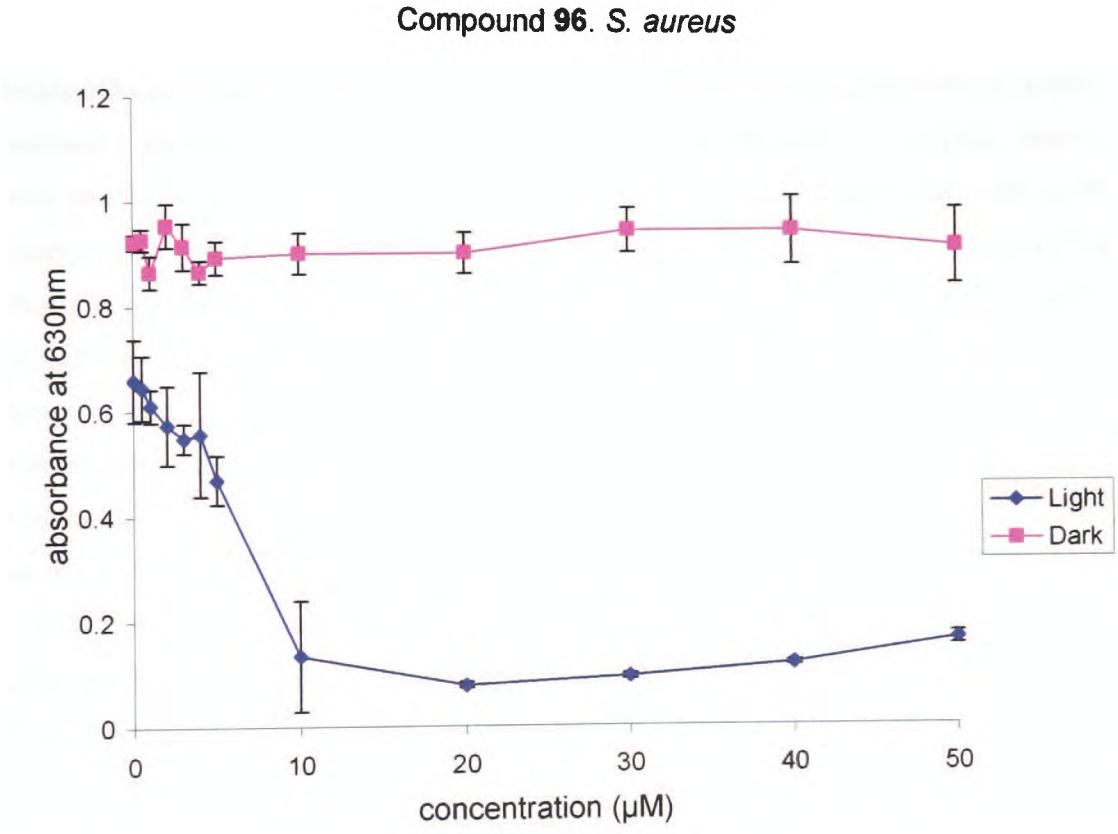

Figure 90. Results of assay for compound **96** for *S. aureus*.

There are two possible reasons why this difference in activity between compound **96** and compound **81** (the analogous phosphorus compound) occurs, and why there is a difference between the activities of *S. aureus* and MRSA.

Arsenic resistance is known to exist in both *E. coli* and *S. aureus*. Lowered net accumulation of arsenic is achieved via an active efflux pump [106, 107]. In *E. coli* this is encoded via plasmid R773 and in *S. aureus* it is encoded by plasmid pI258. This resistance is plasmid mediated so it is possible that the *E. coli* and MRSA in this study contain the plasmids for arsenate resistance, and hence pump out the drug, whilst the *S. aureus* does not contain the plasmid therefore a PDT effect is shown for *S. aureus* and not for the other two organisms. The presence of arsenic has increased the activity over the analogous phosphorus compound (compound **81**) which gave no cell kill in either the light or dark control. Compound **96** does show a PDT effect in that there is cell kill in the irradiated cells but not in the dark controls. It is possible that the differences in activity between compounds **81** and **96** are due to compound **96** showing a combined effect of both arsenic poisoning and PDT. If the membrane is damaged photolytically this could inactivate the efflux pump and allow the build-up of arsenic to toxic levels. However this theory is somewhat controversial in that the arsenic resistance mechanisms are usually associated with inorganic arsenic. A second theory as to the cause of these results is that lysis occurs on irradiation of the porphyrin to produce triphenylarsine which is a toxic compound. However if this was the reason for compound **96** having toxicity when compound **81** does not then this should have been seen in all bacteria, with no difference in activity expected between *S. aureus* and MRSA. Although these theories have some data to both support and contradict them, there is not enough data on this compound to give an accurate idea of what is happening and hence further tests on a broader range of bacteria would have to be carried out in order to be able to determine the mechanism by which the differences in cell killing occurs.

The data presented in this chapter highlights some interesting results. We were able to observe that both MRSA and *S. aureus* showed similar, but not identical, activities with the PDT agents tested. Also three compounds that showed good activity with Gram positive bacteria also showed activity with *E. coli* - this is an unusual finding as a number of PDT agents show no or little activity against Gram negative organisms due to the presence of the outer membrane which makes Gram negative bacteria less susceptible to attack [102].

lowever, we were unable to establish any clear SAR/QSAR with the compounds tested. Although only two physiochemical parameters were examined, it is likely that the ability to correlate this with photodynamic activity is in part due to the small sample et. From my data I feel that it is likely that compounds with greater specificity for articular groups can be synthesised but more importantly it would seem to be possible to roduce compounds with a broad spectrum of activity – which may be of greater benefit or the control of more complex infections such as those found in ulcers and wounds.

.5. Summary

n summary, from this range of compounds differential activity can be seen and some lea of an optimum structure derived, with compounds **90** and **93** being the most active ver a broad spectrum.

nterestingly, there is a difference between *S. aureus* and MRSA, possibly due to fferent surface structures, with some compounds even showing activity against *E. coli*.

he results in this thesis show that porphyrins can be synthesised and optimized for the lling of bacteria. It has also been shown that relatively subtle differences in structure n yield either strain-specific or broad spectrum drugs for use in Photodynamic ntimicrobial Chemotherapy.

Chapter 6. Experimental.

6.1. General.

- ^{1}H and ^{13}C NMR spectra were recorded on either a JEOL JNM-LA400 or JEOL JNM-GX270 NMR spectrometer. Chemical shifts (δ) are quoted in ppm relative to $SiMe_4$ signal as internal standard. Coupling constants are given in Hz.
- UV-Visible spectra were measured on an Agilent 8453 diode array spectrometer.
- TLC was performed with Merck aluminium plates coated with silica gel 60 F_{254} and visualised under UV light. Chromatography was performed using Fluorochem silica gel 35-70μ 60Å or ICU silica gel 32-63μ 60Å.
- THF was distilled from sodium and benzophenone.
- Low resolution mass spectra were recorded on either a SHIMADZU GCMS-QP5050 or a Bruker Reflex IV mass spectrometers. Electrospray mass spectra were obtained from EPSRC National Mass Spectrometry Service centre, University of Wales, Swansea.
- Compounds **81**, **82**, **88**, **89**, **90**, **91**, **92**, **93**, **94**, **95**, and **96**, due to the limitations of the resolution of the mass spectrometer, do not show the isotopomers clearly resolved as one would normally expect. The data does support the presence of isotopomers, showing them as a shoulder on the main peak, however these are not fully resolved. The theoretical data on peak shape received from Swansea matches that of the actual data in all cases.
- HPLC analysis was recorded on a high pressure liquid chromatography system with UV/visible multi-wavelength detector from JASCO (UK) LTD. (Jasco PU-1580 intelligent HPLC pump, HG-1580-32 dynamic mixer, MD-1515 multiwavelength detector, AS-1555 intelligent sampler).
- All reagents were purchased from commercial companies and used without further purification unless otherwise specified.
- Compounds **97**, **98** and **99** were synthesised by Dr.R.Hudson.

6.2. Synthesis.

5, 10, 15, 20-tetra-(4-pyridyl)porphyrin (53) [62]

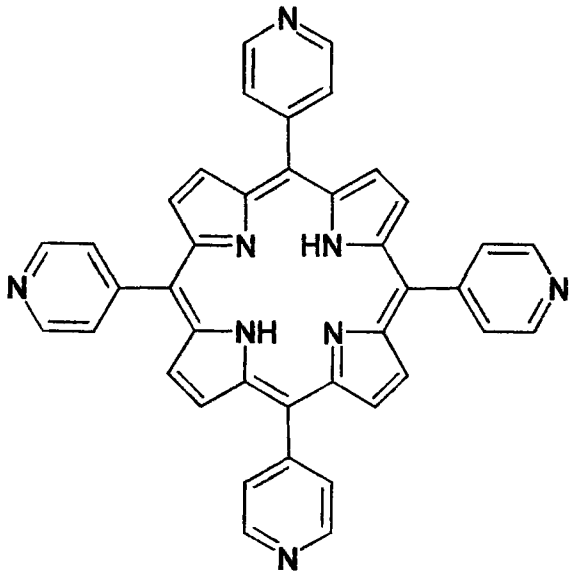

Pyridine-4-carboxaldehyde (15.4ml, 0.127mol) was dissolved in propionic acid (250ml) and heated to reflux. Pyrrole (8.82ml, 0.127mol) was added drop wise and the reaction refluxed for 30 mins. Upon cooling the fine purple precipitate was collected by filtration and washed with propionic acid then water. The crystals were dried under vacuum overnight to give compound **53.** (1.98g, 10%), ^{1}H NMR [400MHz, CD_3Cl_3] δ-2.92 (2H, br s, N-*H*) δ8.16 (8H, d, J = 4 Hz, Ar-3,5-*H*), δ8.87 (8H, s, β-*H*), δ9.06 (8H, d, J = 4 Hz, Ar-2,6-*H*); ^{13}C NMR [100MHz,$CDCl_3$] δ77.00, 77.32, 76.67, 129.30,148.44; UV/Vis (CH_2Cl_2, nm) λ_{max} 416, 512, 547, 586; MS (MALDI) *m/z* 619.5 (M + H).

5, 10, 15, 20-tetra-((4-dimethylamino)phenyl)porphyrin (23) [108]

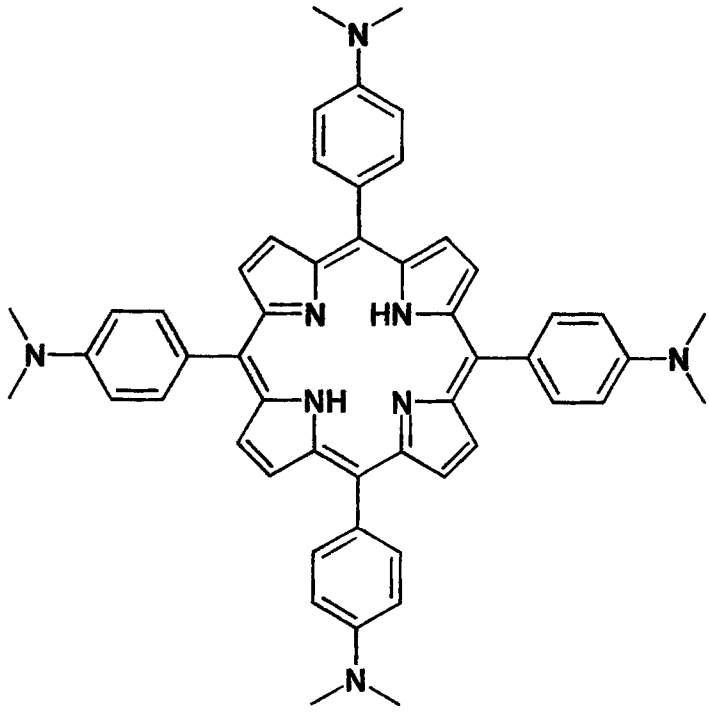

4-Dimethylaminobenzaldehyde (18.95g, 0.127mol) was dissolved in propionic acid (250ml) and heated to reflux. Pyrrole (8.82ml, 0.127mol) was added drop wise and the reaction refluxed for 30 mins. Upon cooling the fine purple precipitate was collected by filtration and washed with propionic acid then water. The crystals were dried under vacuum overnight to give compound **23**. (2.29g, 9%); ^{1}H NMR [400MHz, $(CD_3)_2SO$] δ-2.82 (2H, br s, N-*H*) δ3.36 (24H, s, NCH_3), δ7.52 (8H, d, ^{3}J = 8Hz, Ar-3,5-*H*), 8.35 (8H, s, β-H), 8.53 (8H, d, ^{3}J = 8Hz, Ar-2,6-*H*); UV/Vis (MeOH, nm) λ_{max} 419, 515, 547, 587, 646; MS (MALDI) *m/z* 787.8 (M + H).

5, 10, 15, 20-tetra-(4-cyanophenyl)porphyrin (71) [26]

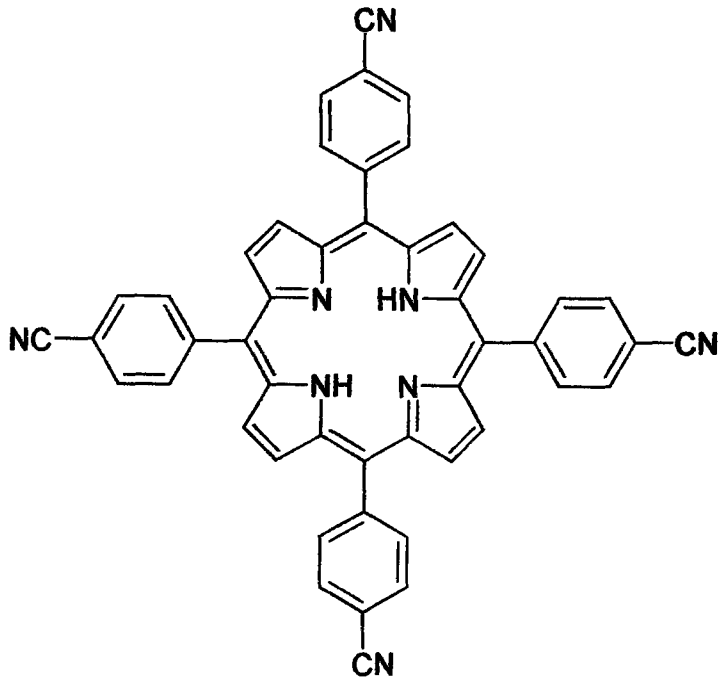

4-Cyanobenzaldehyde (6.22g, 0.0474mol) was dissolved in propionic acid (250ml) and heated to reflux. Pyrrole (3.29ml, 0.0474mol) was added drop wise and the reaction refluxed for 30mins. Upon cooling the fine purple precipitate was collected by filtration and washed with propionic acid then water. The crystals were dried under vacuum overnight to give compound **71** a fine purple solid. (1.31g, 15%); ^{1}H NMR [400MHz, CD_3OD] δ-3.00 (2H, br s, N*H*), δ8.18 (8H, d, ^{3}J = 8 Hz, Ar-3,5-*H*), δ8.35 (8H, d, ^{3}J= 8 Hz, Ar-2,6-*H*), δ8.79 (8H, s, β-*H*); UV/Vis (MeOH, nm) λ_{max} 420, 514, 549, 590, 644; MS (MALDI) *m/z* 715 (M +H).

5, 10, 15, 20-tetra-(4-carbomethoxyphenyl)porphyrin (87) [109]

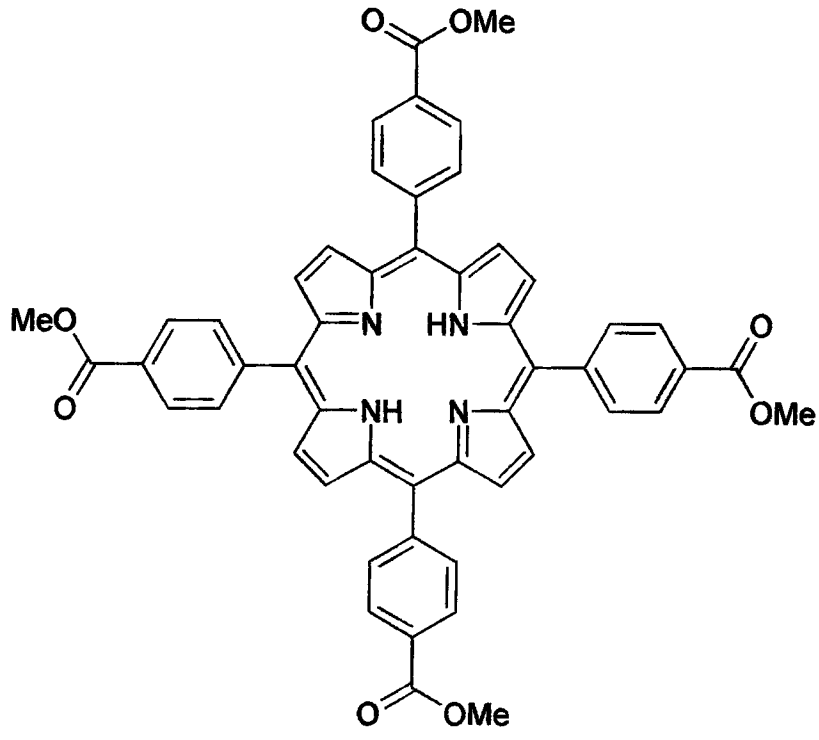

Methyl 4-formylbenzoate (10.00g, 0.061mol) was dissolved in propionic acid (250ml) and heated to reflux. Pyrrole (4.23ml, 0.061mol) was added drop wise and the reaction refluxed for 30mins. Upon cooling the fine purple precipitate was collected by filtration and washed with propionic acid then water. The crystals were dried under vacuum overnight to give **87** as lustrous purple needles. (2.39g, 18%), R*f* =0.14 (silica, 5%MeOH/CH_2Cl_2); ^{1}H NMR [400MHz, $CDCl_3$] δ-2.81 (2H, br s, N*H*), δ4.11(12H, s, OCH_3), δ8.30 (8H, d, ^{3}J = 8 Hz, Ar-3,5-*H*), δ8.45 (8H, d, ^{3}J = 8Hz, Ar-2,6-*H*), δ8.81 (8H, s, β-*H*); ^{13}C NMR [100MHz, $CDCl_3$] δ 52.46, 119.38, 127.98, 129.77, 134.51, 146.61, 167.24; UV/Vis (MeOH, nm) λ_{max} 427, 515, 550, 590, 645; MS (MALDI) *m/z* 846.7 (M + H)

5, 10, 15, 20-tetra-(4-(hydroxymethyl)phenyl)porphyrin (73) [109]

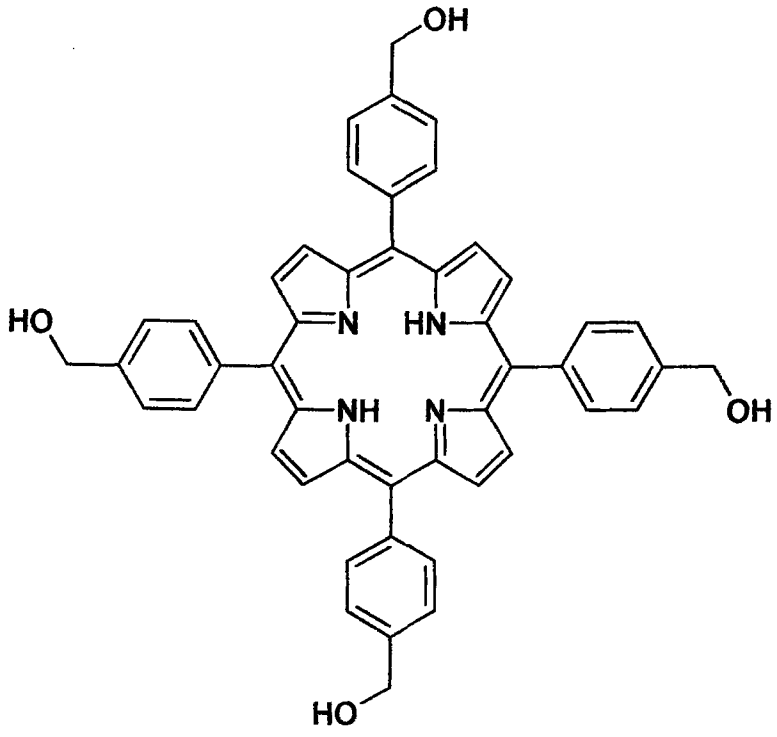

A solution of compound **87** (1.00g, 1.18mmol) in freshly distilled THF (250ml) was cooled to 0°C under a nitrogen atmosphere. Lithium aluminium hydride (4.47g, 0.18mol) was added and the reaction was stirred in the dark for 18 hours at room temperature. 5% H_2SO_4 (100ml) was added drop wise and the product was extracted into ethyl acetate (3*100ml). The combined organic layer was washed with saturated aqueous sodium hydrogen carbonate (200ml), water (200ml) and brine (200ml). The organic layer was dried over $MgSO_4$, filtered and the solvent removed *in vacuo* to give **73** as lustrous purple needles (0.77g, 88%); Rf= 0.65 (silica, 20%MeOH/CH_2Cl_2); ^{1}H NMR [400MHz, $(CD_3)_2SO$] δ-2.91 (2H, br s, N*H*), δ4.84 (8H, d, ^{3}J = 8 Hz, CH_2), δ5.50 (4H, t, ^{3}J =6Hz, O*H*), δ7.74 (8H, d, ^{3}J =8 Hz, Ar-3,5-*H*), δ8.14 (8H, d, ^{3}J =8Hz, Ar-2,6-*H*), δ8.80 (8H, s, β-*H*); UV/Vis (MeOH, nm) λ_{max} 423, 515, 557, 598, 626; MS (MALDI) *m/z* 735.8 (M + H).

5, 10, 15, 20-tetra-(4-(bromomethyl)phenyl)porphyrin (83) [109]

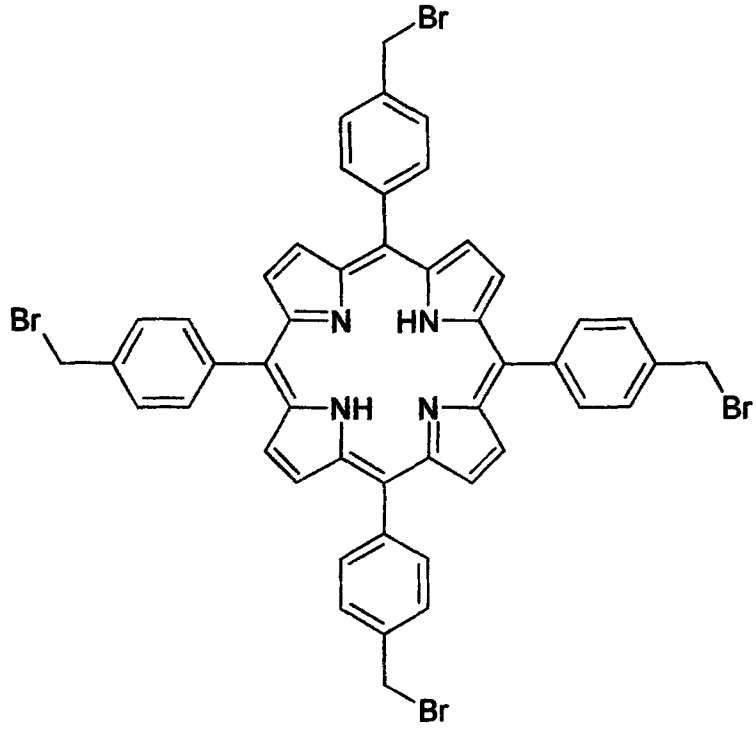

To a solution of **73** (0.150g, 0.2mmol) in freshly distilled dioxane (10ml), under a nitrogen atmosphere, was added phosphorous tribromide (1.00ml, 10.00mmol) and the reaction was stirred overnight at room temperature in the dark. MeOH (5ml) was added drop wise and the reaction stirred for a further 5 minutes. CH_2Cl_2 (50ml) was added and the organic layer was washed with saturated sodium hydrogen carbonate (3*50ml) and brine (3*50ml). The organic layer was dried over $MgSO_4$, filtered and the solvent was removed *in vacuo*. The purple solid was adsorbed onto silica and purified by gravity percolation chromatography (silica, eluent: CH_2Cl_2). Relevant fractions were combined and the solvent removed *in vacuo* to yield compound **83** as a fine purple solid (0.138g, 70%); R*f*= 0.86 (silica, CH_2Cl_2); ^{1}H NMR [400MHz, $CDCl_3$] δ-2.81 (2H, br s, N*H*), δ4.86 (8H, s, C*H*$_2$Br), δ7.84 (8H, d, ^{3}J =8Hz, Ar-3,5-*H*), δ8.24 (8H, d, ^{3}J = 8Hz, Ar-2,6-*H*), δ8.84 (8H, s, β-*H*); ^{13}C NMR [100MHz,$CDCl_3$] δ33.48, 119.54, 127.48, 134.92, 137.40, 142.21; UV/Vis (CH_2Cl_2, nm) λ_{max} 420, 516, 552, 592, 647; MS (MALDI) *m/z* 987 (M + H).

5, 10, 15, 20-tetra-(4-(phthalimidomethyl)phenyl)porphyrin (74)

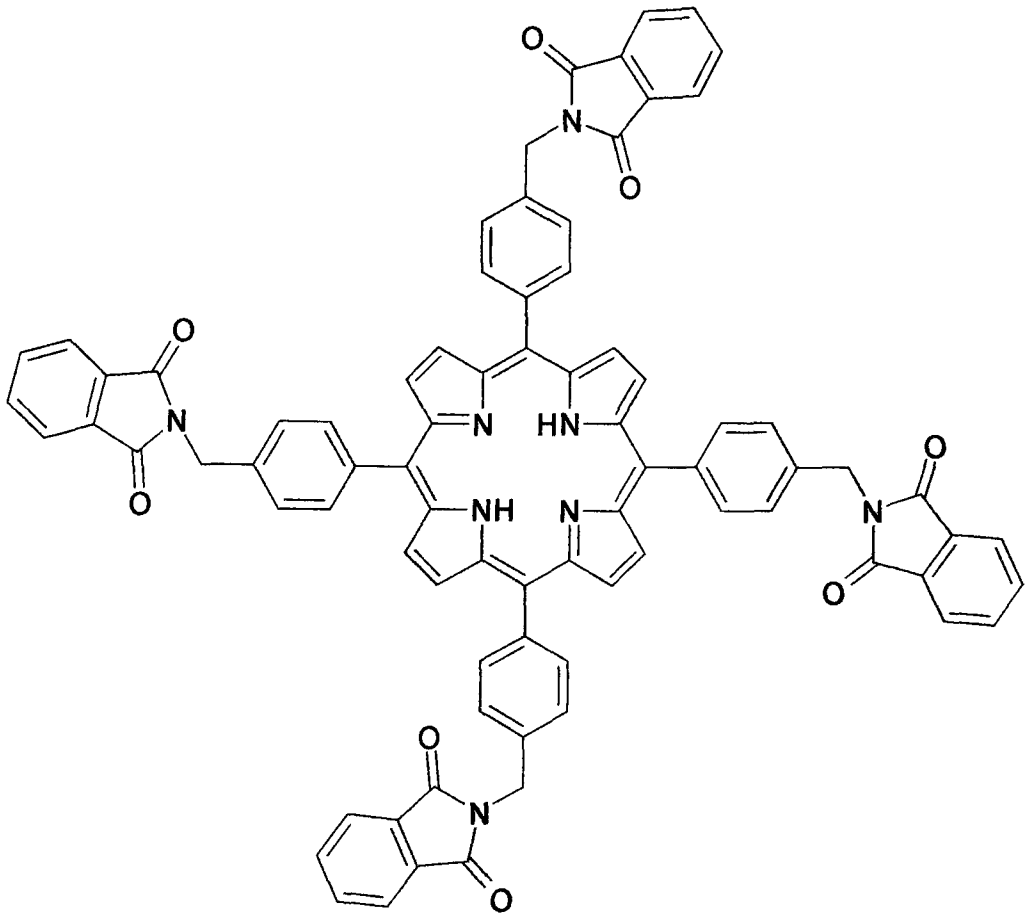

ɔ a solution of **73** in dry THF (100ml) was added triphenyl phosphine (0.098g, 37mmol) and potassium phthalimide (0.069g, 0.37mmol). The reaction was cooled to C and stirred for 15 minutes. Diethylazodicarboxylate (0.072ml, 0.37mmol) was added ıd the reaction was stirred at room temperature for 48 hours. Column chromatography ilica, eluent: 5% MeOH in CH_2Cl_2) afforded **74** as a purple solid. (0.067g, 79%), ^{1}H MR [400MHz, $(CD_3)_2SO$] δ-2.79 (2H, br s, N*H*), δ4.97 (8H, s, CH_2), δ 7.65 (8H, d, ^{3}J = Hz, Ar-3,5-*H*), δ 7.69 (8H, d, ^{3}J = 8Hz, Ar-2,6-*H*), δ 7.76 (8H, q, J = 8Hz) δ 7.87 (8H, q, = 8Hz), δ8.81 (8H, s, β-*H*); UV/Vis (MeOH, nm) λ_{max} 417, 515, 545, 594, 637; MS IALDI) *m/z* 1251.7 (M + H).

5, 10, 15, 20-tetra-(4-((triphenylphosphoniumyl)methyl)phenyl)porphyrin tetrabromide (81) [109]

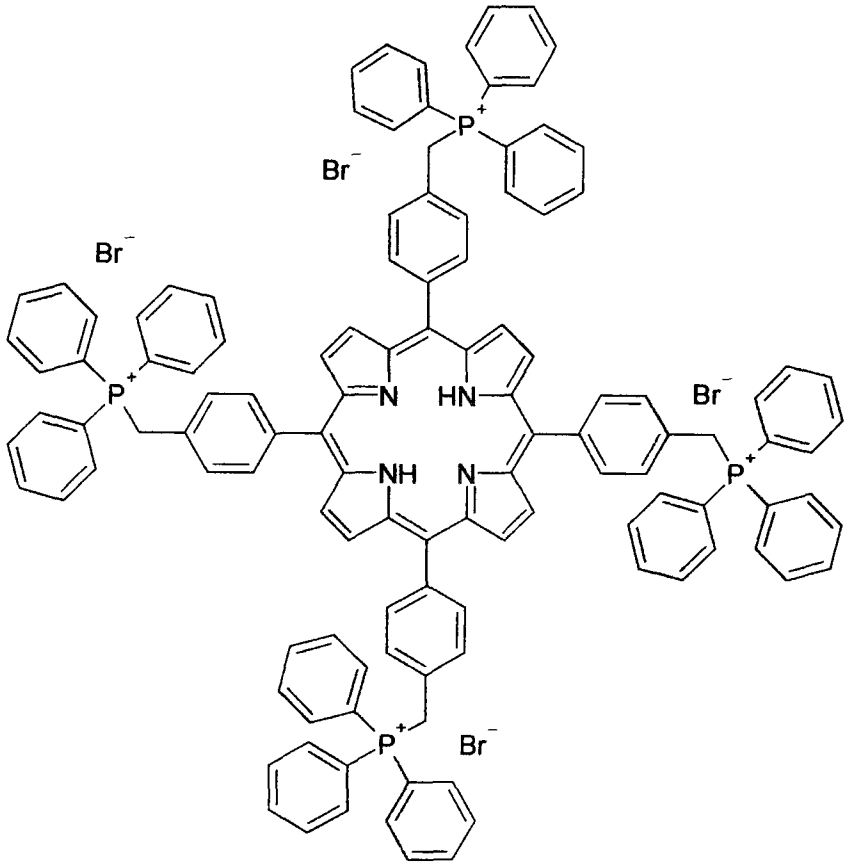

To a flame dried flask under a nitrogen atmosphere was added compound **83** (20mg, 0.02mmol) and triphenylphosphine (3g). The mixture was heated to 110°C and was stirred for 48 hours effecting reaction solvolysis. On cooling the solid was ground up and methanol added (5ml). The suspension was stirred for 5 minutes and the unreacted triphenylphosphine was collected by microfiltration (Millipore®) and washed with methanol. The recovered filtrate was added to 50ml diethyl ether. The resultant precipitate was collected by microfiltration (Millipore®) and this process was repeated wice. The purple solid was dried under vacuum to give compound **81.** (0.022g, 63%); H NMR [400MHz, $(CD_3)_2SO$] δ-3.12 (2H,br s, N*H*), 5.53 (8H, d, ^2J=15.2 Hz, CH_2P), 7.41(8H, dd, ^4J=2.24Hz, ^3J=8.44Hz, 5,10,15,20-Ar-3,5-H), 7.91-8.02 (64H, m overlapping, 5,10,15,20-Ar-2,6-H & *ortho, meta, para*-Ar-H), 8.75 (8H, s, β-H); UV/Vis H_2O, nm) λ_{max} 416, 520, 557, 587, 643; MS (ES) *m/z* 429 (M^{4+}), 599 $(M + Br)^{3+}$, 938 $M + 2\ Br)^{2+}$. HPLC t_r = 17.3 min (flow rate= 1ml/min;eluent A, H_2O and 0.1%TFA; eluent B, methanol; gradient 0min,0%B; 10min, 75% B; 15min, 75% B; 18min 0% B; 9min 0% B; column, Phenomenex Luna 5μ C18(2) 250*4.6mm

5, 10, 15, 20-tetra-(4-((triethylamino)methyl)phenyl)porphyrin tetrabromide (82) [109]

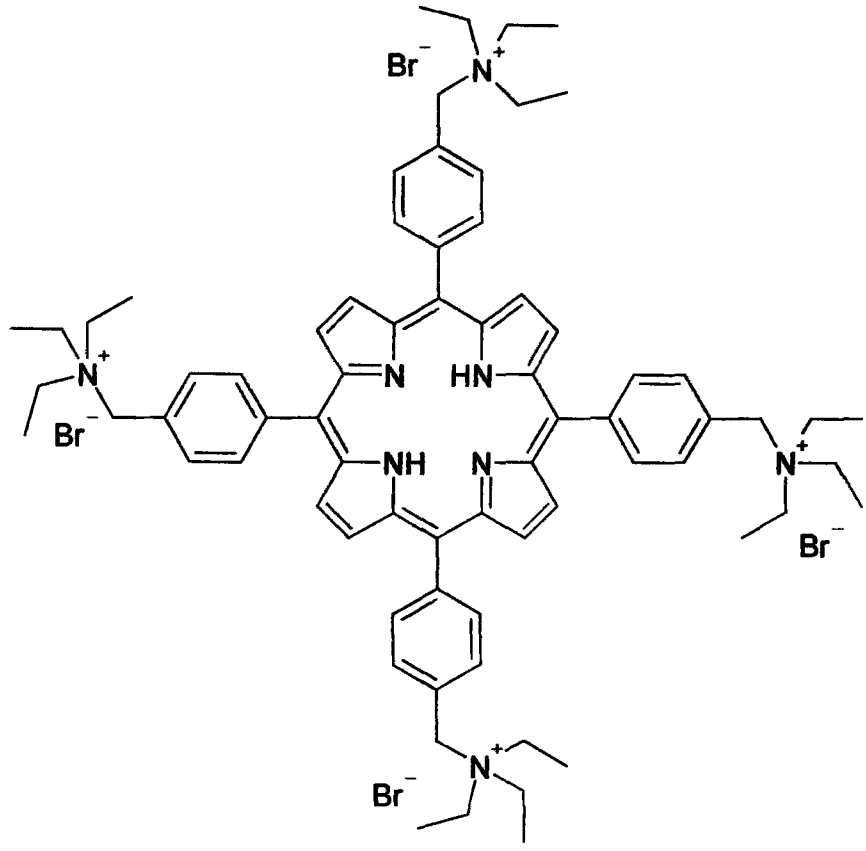

To a flame dried flask under a nitrogen atmosphere was added a solution of **83** (20mg, 0.02mmol) in DMF (10ml). To this solution was added triethylamine (0.11ml, 0.80mmol). The reaction was allowed to proceed for 24 hours at room temperature in the dark. Upon completion of the reaction the solvent was removed *in vacuo* to yield a crude purple solid. The solid was dissolved in 2ml MeOH and this was added to 50ml diethyl ether. The resultant precipitate was collected by microfiltration (Millipore®) and this process was repeated twice. The purple solid was dried under vacuum to give compound **82.** (0.0178g, 86%) ^{1}H NMR [400MHz, $(CD_3)_2SO$] δ-2.96 (2H, br s, N*H*), 1.47 (36H, t, ^{3}J = 8 Hz, CH_3), 2.47-2.49 (24H, m, NCH_2), 4.83 (8H, s, PhCH_2), 7.95 (8H, d, J = 8 Hz, Ar-3,5-*H*), 8.34 (8H, d, J = 8 Hz, Ar-2,6-*H*), 8.90 (8H, s, β-*H*); UV/Vis (octanol, nm) λ_{max} 420, 515, 549, 592, 649; MS (ES) *m/z* 268 (M^{4+}), 383 $(M + Br)^{3+}$, 615 $(M + 2\ Br)^{2+}$; HPLC t_r = 4.00 min (flow rate= 1ml/min;eluent A, H_2O and 0.1%TFA; eluent B, methanol; gradient 0min,0%B; 10min, 75% B; 15min, 75% B; 18min 0% B; 19min 0% B; column, Phenomenex Luna 5μ C18(2) 250*4.6mm

5, 10, 15, 20-tetra-(4-((trimethylphosphoniumyl)methyl)phenyl)porphyrin tetrabromide (88)

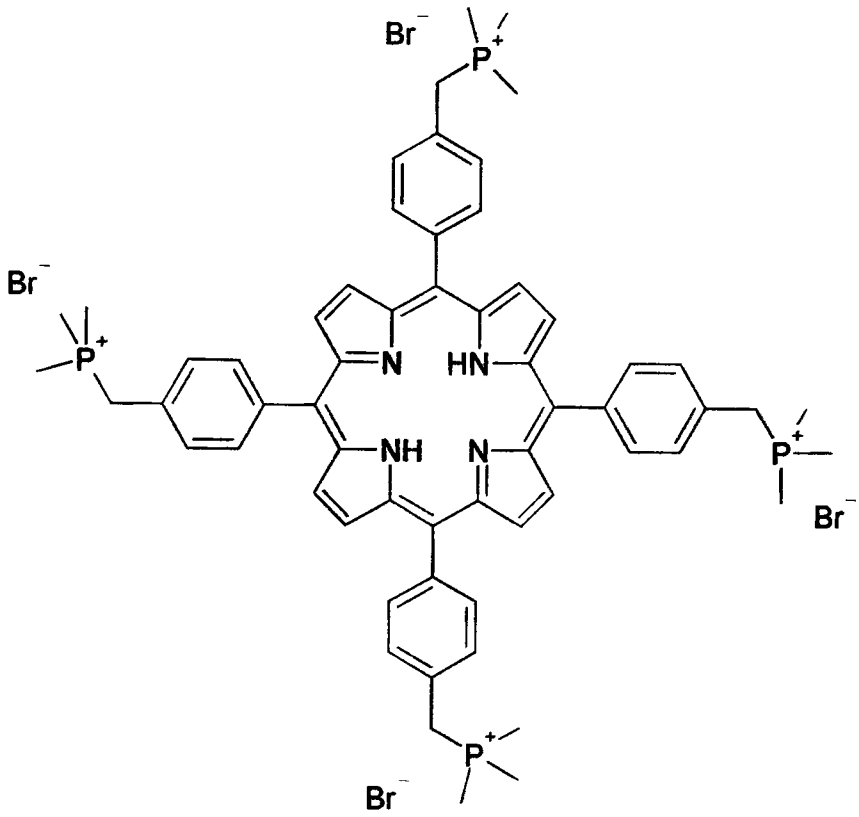

To a flame dried flask under a nitrogen atmosphere was added a solution of **83** (20mg, 0.02mmol) in DMF (10ml). To this solution was added trimethyl phosphine (0.08ml, 0.80mmol). The reaction was allowed to proceed for 24 hours at room temperature in the dark. Upon completion of the reaction the solvent was removed *in vacuo* to yield a crude purple solid. The solid was dissolved in 2ml MeOH and this was added to 50ml diethyl ether. The resultant precipitate was collected by microfiltration (Millipore®) and this process was repeated twice. The purple solid was dried under vacuum to give compound **88.** (0.0048g, 27%), ^{1}H NMR [400MHz,$(CD_3)_2SO$] δ-2.96 (2H, br s, N*H*), δ2.03 (36H, d,^{3}J = 16 Hz C*H*$_3$), δ4.12 (8H, d, J=16 Hz, PhC*H*$_2$), δ7.74 (8H, d, J= 8 Hz, Ar-3,5-*H*), δ8.25 (8H, d, J=8 Hz, Ar-2,6-*H*), δ8.90 (8H, s, β-*H*); UV/Vis (Octanol, nm) λ_{max} 414, 517, 549, 585, 620; MS (ES) *m/z* 243 (M^{4+}), 351 $(M + Br)^{3+}$, 565 $(M + 2\ Br)^{2+}$; HPLC t_r = 8.40 min (flow rate= 1ml/min;eluent A, H_2O and 0.1%TFA; eluent B, methanol; gradient 0min,0%B; 10min, 75% B; 15min, 75% B; 18min 0% B; 19min 0% B; column, Phenomenex Luna 5μ C18(2) 250*4.6mm.

5, 10, 15, 20-tetra-(4-((triethylphosphoniumyl)methyl)phenyl)porphyrin tetrabromide (89)

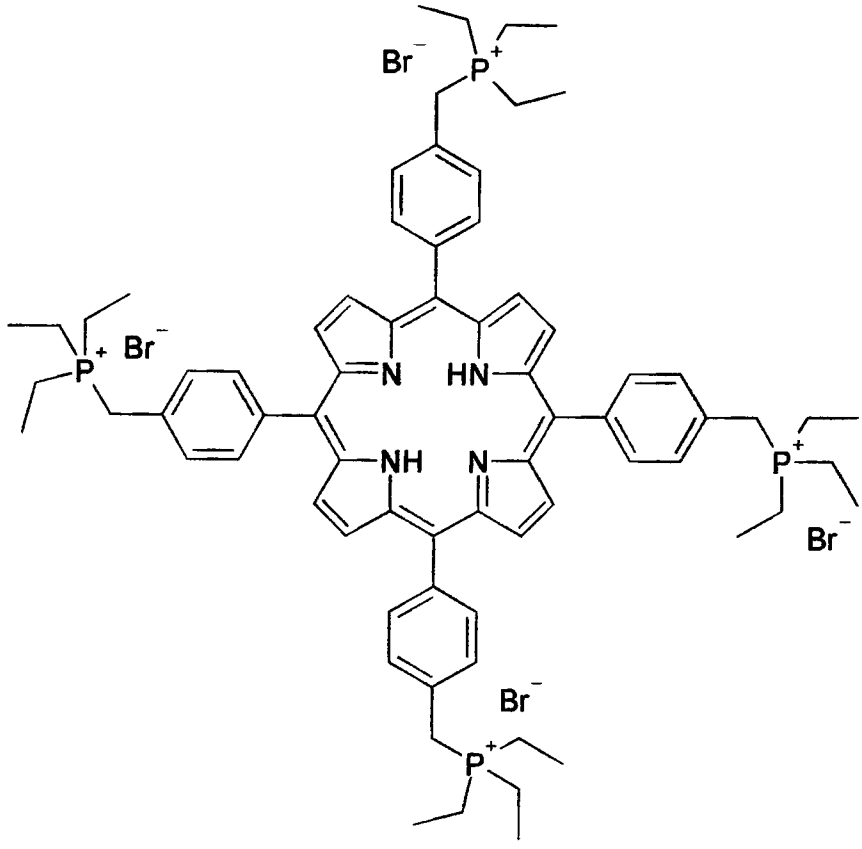

To a flame dried flask under a nitrogen atmosphere was added a solution of **83** (20mg, 0.02mmol) in DMF (10ml). To this solution was added triethyl phosphine (0.12ml, 0.80mmol). The reaction was allowed to proceed for 24 hours at room temperature in the dark. Upon completion of the reaction the solvent was removed *in vacuo* to yield a crude purple solid. The solid was dissolved in 2ml MeOH and this was added to 50ml diethyl ether. The resultant precipitate was collected by microfiltration (Millipore®) and this process was repeated twice. The purple solid was dried under vacuum to give compound **89.** (0.0056g, 38%) ^{1}H NMR [400MHz, $(CD_3)_2SO$] δ-2.95 (2H, br s, N*H*), δ1.27 (t, ^{3}J = 8Hz, overlapping with δ1.32 (t, ^{3}J =8 Hz, 60H CH_2CH_3 + CH_2CH_3), δ4.19 (8H, d, J = 16 Hz, PhCH_2), δ7.81 (8H, d, J= 4 Hz, Ar-3,5-*H*), δ8.25 (8H, d, J = 4 Hz, Ar-2,6-*H*), δ8.87 (8H, s, β-*H*); UV/Vis (octanol, nm) λ_{max} 424, 517, 558, 590, 624; MS (ES) *m/z* 285 (M^{4+}), 407 (M + Br)$^{3+}$, 649 (M + 2 Br)$^{2+}$; HPLC t_r = 4.38 min (flow rate= 1ml/min;eluent A, H_2O and 0.1%TFA; eluent B, methanol; gradient 0min,0%B; 10min, 75% B; 15min, 75% B; 18min 0% B; 19min 0% B; column, Phenomenex Luna 5μ C18(2) 250*4.6mm

5, 10, 15, 20-tetra-(4-((tripropylphosphoniumyl)methyl)phenyl)porphyrin tetrabromide (90) [109]

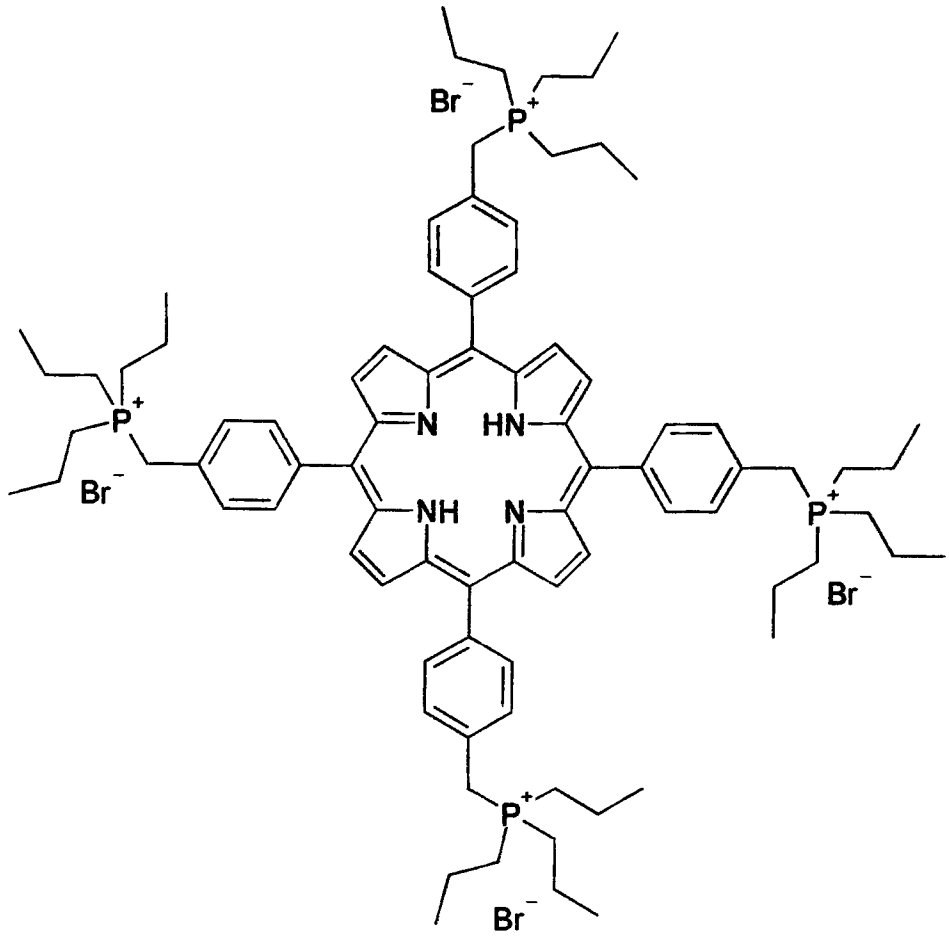

To a flame dried flask under a nitrogen atmosphere was added a solution of **83** (20mg, 0.02mmol) in DMF (10ml). To this solution was added tripropyl phosphine (0.16 ml, 0.80mmol). The reaction was allowed to proceed for 24 hours at room temperature in the dark. Upon completion of the reaction the solvent was removed *in vacuo* to yield a crude purple solid. The solid was dissolved in 2ml MeOH and this was added to 50ml diethyl ether. The resultant precipitate was collected by microfiltration (Millipore®) and this process was repeated twice. The purple solid was dried under vacuum to give compound **90.** (0.019g, 72%) ^{1}H NMR [400MHz, $(CD_3)_2SO$] δ-2.98 (2H, br s, N*H*), δ1.08 (36H, t, ^{3}J= 6 Hz, CH_3), δ1.64-1.60 (24H, m, CH_2CH$_3$), δ2.38-2.30 (24H, m, PCH_2), δ4.13 (8H, d, J = 16 Hz, PhCH_2), δ7.76 (8H, d, J = 8 Hz, Ar-3,5-*H*), δ8.22 (8H, d, J = 8 Hz, Ar-2,6-*H*), δ8.79 (8H, s, β-*H*); UV/Vis (octanol, nm) λ_{max} 426, 515, 549, 591, 648 ; MS (ES) *m/z* 327 (M^{4+}), 463 $(M + Br)^{3+}$, 734 $(M + 2\ Br)^{2+}$; HPLC t_r = 9.52 min (flow rate= 1ml/min;eluent A, H_2O and 0.1%TFA; eluent B, methanol; gradient 0min,0%B; 10min, 75% B; 15min, 75% B; 18min 0% B; 19min 0% B; column, Phenomenex Luna 5μ C18(2) 250*4.6mm

5, 10, 15, 20-tetra-(4-((tributylphosphoniumyl)methyl)phenyl)porphyrin tetrabromide (91) [109]

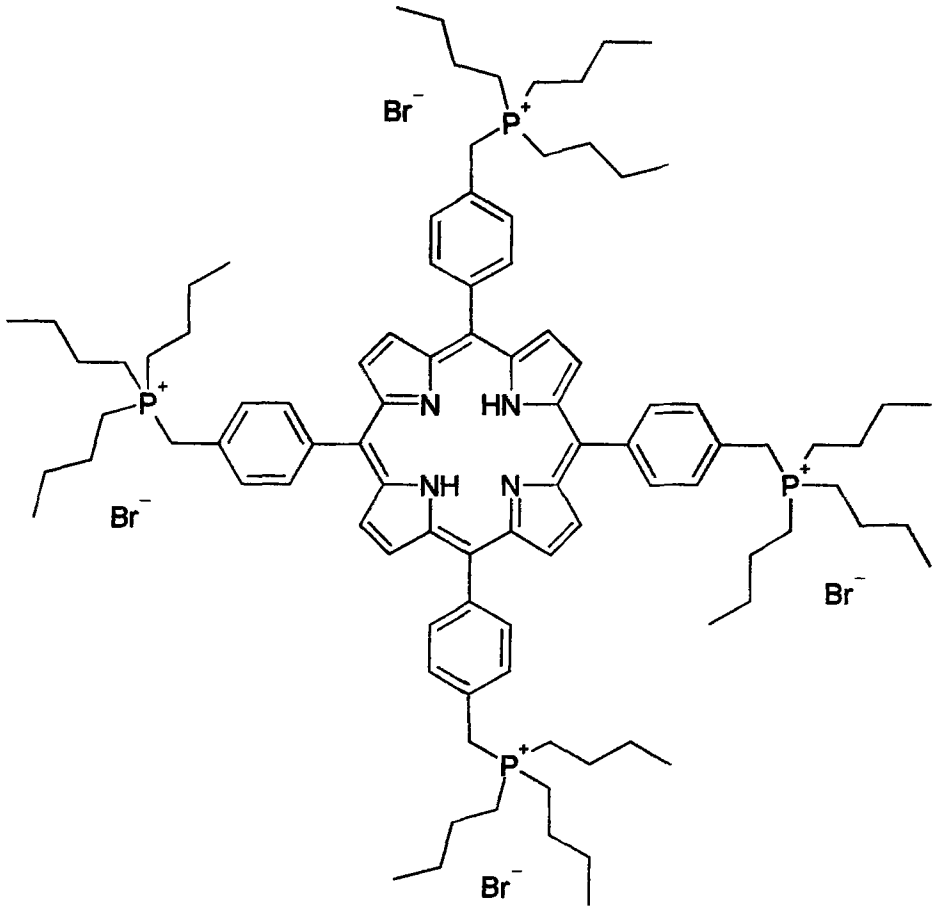

To a flame dried flask under a nitrogen atmosphere was added a solution of **83** (20mg, 0.02mmol) in DMF (10ml) and the solution was stirred at 80°C for five minutes. To this solution was added tributyl phosphine (0.197ml, 0.80mmol). The reaction was allowed to proceed for three days at 80°C in the dark. Upon completion of the reaction the solvent was removed *in vacuo* to yield a crude purple solid. The solid was dissolved in 2ml MeOH and this was added to 50ml diethyl ether. The resultant precipitate was collected by microfiltration (Millipore®) and this process was repeated twice. The purple solid was dried under vacuum to give compound **91.** (0.0219g, 74%); ^{1}H NMR [400MHz,$(CD_3)_2SO$] δ-2.95 (2H, br s, N*H*), δ0.99 (36H, t, ^{3}J= 8 Hz, CH_3), δ1.53-1.48 (m, CH_2CH$_3$ overlapping with δ1.62-1.58 (m, CH_2CH$_2$CH$_3$, 48H), δ2.49-2.48 (24H, m, PCH_2), δ4.18 (8H, d, J= 16Hz, PhCH_2), δ7.81 (8H, d, J= 8 Hz, Ar-3,5-*H*), 8.26 (8H, d, J= 8 Hz, Ar-2,6-*H*), δ8.82 (8H, s, β-*H*); UV/Vis (Octanol, nm) λ_{max} 424, 517, 548, 593, 650; MS (ES) *m/z* 369 (M^{4+}), 519 $(M + Br)^{3+}$, 818 $(M + 2\ Br)^{2+}$; HPLC t_r = 13.7 min flow rate= 1ml/min;eluent A, H_2O and 0.1%TFA; eluent B, methanol; gradient 0min,0%B; 10min, 75% B; 15min, 75% B; 18min 0% B; 19min 0% B; column, Phenomenex Luna 5μ C18(2) 250*4.6mm

5, 10, 15, 20-tetra-(4-((trimethylamino)methyl)phenyl)porphyrin tetrabromide (92)

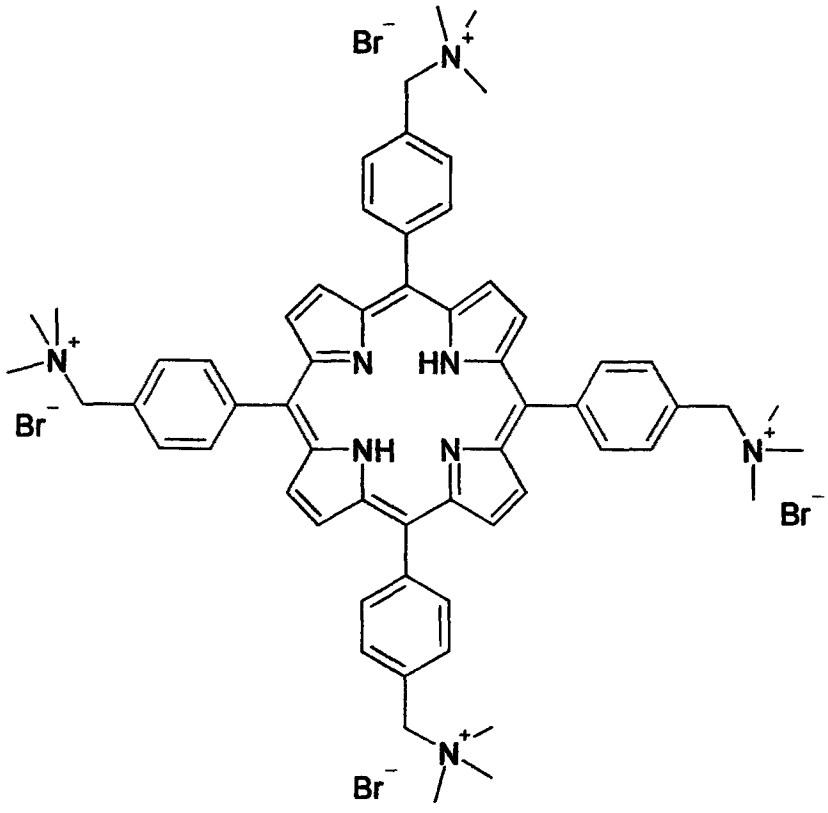

To a flame dried flask under a nitrogen atmosphere was added a solution of **83** (20mg, 0.02mmol) in DMF (10ml). To this solution was added trimethylamine hydrochloride (0.076g, 0.80mmol) and DBU (0.119ml, 0.8mmol). The reaction was allowed to proceed for 24 hours at room temperature in the dark. Upon completion of the reaction the solvent was removed *in vacuo* to yield a crude purple solid. The solid was dissolved in 2ml MeOH and this was added to 50ml diethyl ether. The resultant precipitate was collected by microfiltration (Millipore®) and this process was repeated twice. The purple solid was dried under vacuum to give compound **92.** (0.007g, 39%) ^{1}H NMR [400MHz, $(CD_3)_2SO$] δ-2.94 (2H, br s, N*H*), δ2.17 (36H, s, CH_3), δ4.94 (8H, s, PhCH_2), δ8.00 (8H, d, J= 8 Hz, Ar-3,5-*H*), δ8.35 (8H, d, J = 8 Hz, Ar-2,6-*H*), δ8.93 (8H, s, β-*H*); MS (ES) *m/z* 226 (M^{4+}), 327 $(M + Br)^{3+}$, 531 $(M + 2\ Br)^{2+}$; UV/Vis (octanol, nm) λ_{max} 421, 516, 549, 593, 650; HPLC t_r = 7.72 min (flow rate= 1ml/min;eluent A, H_2O and 0.1%TFA; eluent B, methanol; gradient 0min,0%B; 10min, 75% B; 15min, 75% B; 18min 0% B; 19min 0% B; column, Phenomenex Luna 5μ C18(2) 250*4.6mm

5, 10, 15, 20-tetra-(4-((tripropylamino)methyl)phenyl)porphyrin tetrabromide (93)

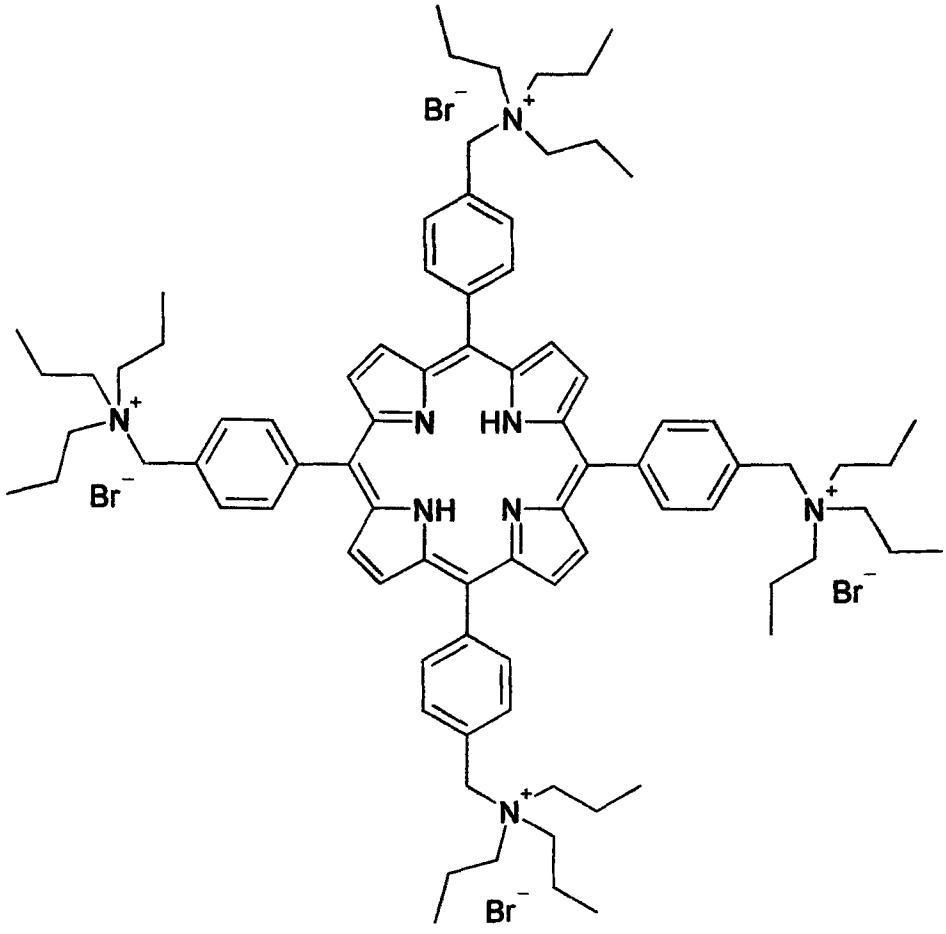

To a flame dried flask under a nitrogen atmosphere was added a solution of **83** (20mg, 0.02mmol) in DMF (10ml). To this solution was added tripropylamine (0.15ml, 0.80mmol). The reaction was allowed to proceed for 24 hours at room temperature in the dark. Upon completion of the reaction the solvent was removed *in vacuo* to yield a crude purple solid. The solid was dissolved in 2ml MeOH and this was added to 50ml diethyl ether. The resultant precipitate was collected by microfiltration (Millipore®) and this process was repeated twice. The purple solid was dried under vacuum to give compound **93.** (0.0106g, 44%), ^{1}H NMR [400MHz, $(CD_3)_2SO$] δ-3.01 (2H, br s, N*H*), δ0.99 (36H, t, ^3J = 8Hz, C*H*$_3$), δ1.97-1.85 (24H, m, C*H*$_2$CH$_3$), δ2.63-2.60 (24H,m, NC*H*$_2$), δ4.84 (8H, s, PhC*H*$_2$), δ7.87 (8H, d, ^3J = 8 Hz, Ar-3,5-*H*), δ8.32 (8H, d, ^3J = 8 Hz, Ar-2,6-*H*), δ8.87 (8H, s, β-*H*); UV/Vis (octanol, nm) λ_{max} 415, 515, 549, 591, 648 ; MS (ES) *m/z* 310 (M^{4+}), 440 $(M + Br)^{3+}$, 670 $(M + 2\ Br)^{2+}$; HPLC t_r = 10.7 min (flow rate= 1ml/min;eluent A, H_2O and 0.1%TFA; eluent B, methanol; gradient 0min,0%B; 10min, 75% B; 15min, 75% B; 18min 0% B; 19min 0% B; column, Phenomenex Luna 5μ C18(2) 250*4.6mm

5, 10, 15, 20-tetra-(4-((tributylamino)methyl)phenyl)porphyrin tetrabromide (94) [109]

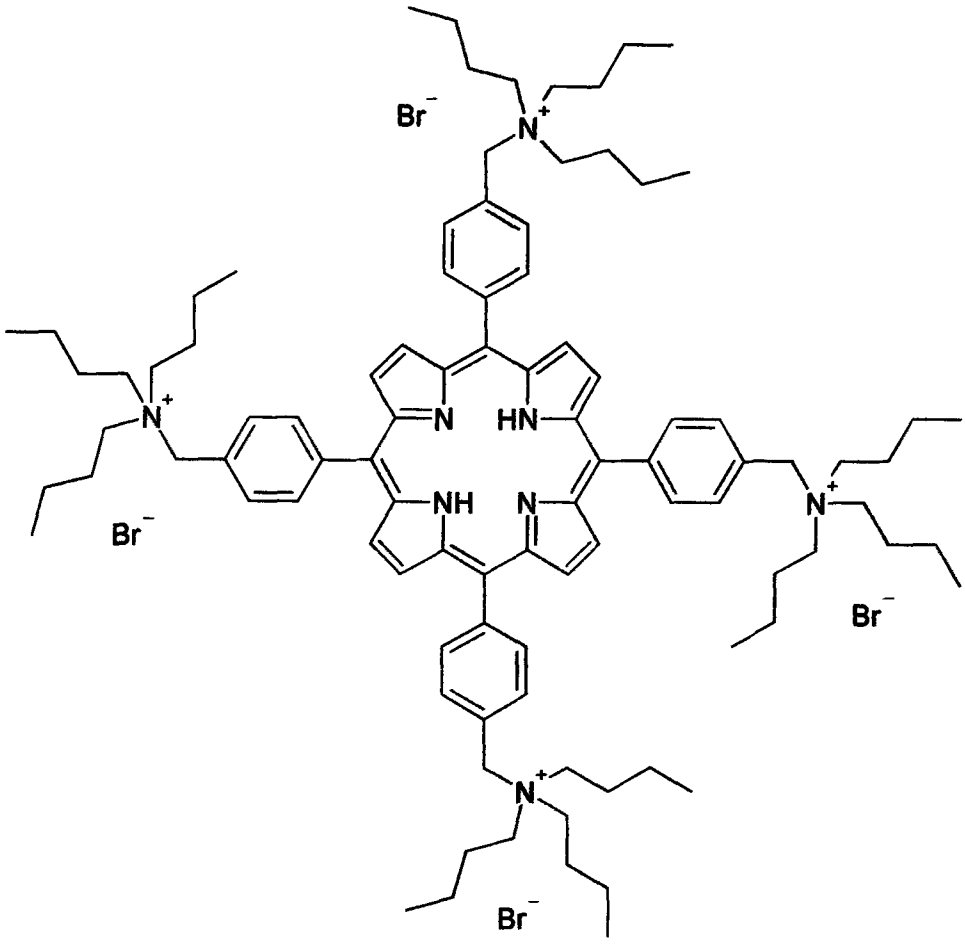

To a flame dried flask under a nitrogen atmosphere was added a solution of **83** (20mg, 0.02mmol) in DMF (10ml) and the solution was stirred at 80°C for five minutes. To this solution was added tributyl amine (0.191ml, 0.80mmol). The reaction was allowed to proceed for three days at 80°C in the dark. Upon completion of the reaction the solvent was removed *in vacuo* to yield a crude purple solid. The solid was dissolved in 2ml MeOH and this was added to 50ml diethyl ether. The resultant precipitate was collected by microfiltration (Millipore®) and this process was repeated twice. The purple solid was dried under vacuum to give compound **94.** (0.0208g, 74%); ^{1}H NMR [400MHz, $(CD_3)_2SO$] δ-2.96 (2H, br s, N*H*), δ1.03 (36H, t, ^3J = 8Hz, CH_3), δ1.48-1.40 (24H, m, CH_2CH_3), δ1.96-1.83 (24H, m, $CH_2CH_2CH_3$), δ2.51-2.48 (24H, m, NCH_2), δ4.88 (8H, s, $PhCH_2$), δ7.92 (8H, d, J= 8Hz, Ar-3,5-*H*), δ8.35 (8H, d, J= 8Hz, Ar-2,6-*H*), δ8.89 (8H, s, β-*H*); UV/Vis (octanol, nm) λ_{max} 429, 515, 550, 592, 648; MS (ES) *m/z* 352 (M^{4+}), 496 $(M + Br)^{3+}$; HPLC t_r = 14.8 min (flow rate= 1ml/min;eluent A, H_2O and 0.1%TFA; eluent B, methanol; gradient 0min,0%B; 10min, 75% B; 15min, 75% B; 18min 0% B; 19min 0% B; column, Phenomenex Luna 5μ C18(2) 250*4.6mm

5, 10, 15, 20-tetra-(4-((tribenzylphosphoniumyl)methyl)phenyl)porphyrin tetrabromide (95)

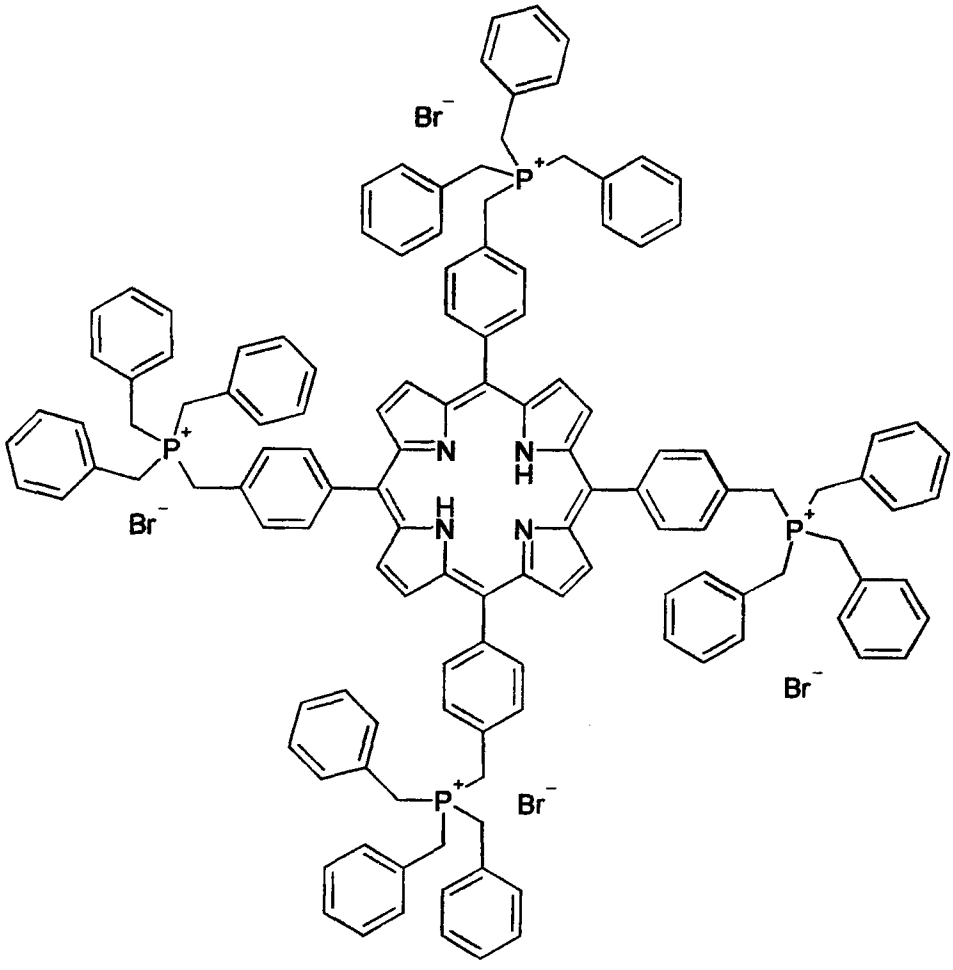

To a flame dried flask under a nitrogen atmosphere was added a solution of **83** (20mg, 0.02mmol) in DMF (10ml). To this solution was added tribenzyl phosphine (0.24g, 0.80mmol). The reaction was allowed to proceed for 72 hours at room temperature in the dark. Upon completion of the reaction the solvent was removed *in vacuo* to yield a crude purple solid. The solid was dissolved in 2ml MeOH and this was added to 50ml diethyl ether. The resultant precipitate was collected by microfiltration (Millipore®) and this process was repeated twice. The purple solid was dried under vacuum to give compound **95.** (0.0242g, 56%); ^{1}H NMR [400MHz, $(CD_3)_2SO$] δ-2.99 (2H, br s, N*H*), δ2.32 (24H, d, ^{3}J = 16Hz, PC*H*$_2$Ph), δ4.01 (8H, d, ^{3}J=12, C*H*$_2$P), δ7.41 (8H, d, ^{3}J = 8Hz, 5,10,15,20-Ar-3,5-H), δ8.12-8.28 (68H, m overlapping, 5,10,15,20-Ar-2,6-H & *ortho, meta, para*-Ar-H), δ8.98 (8H, s, β-H); UV/Vis (octanol, nm) λ_{max} 415, 516 550, 593, 649; MS (ES) *m/z* 471 (M^{4+}), 655 $(M + Br)^{3+}$; HPLC t_r = 17.1 min (flow rate= 1ml/min;eluent A, H_2O and 0.1%TFA; eluent B, methanol; gradient 0min,0%B; 10min, 75% B; 15min, 75% B; 18min 0% B; 19min 0% B; column, Phenomenex Luna 5μ C18(2) 250*4.6mm

5, 10, 15, 20-tetra-(4-((triphenylarsonium)methyl)phenyl)porphyrin tetrabromide (96)

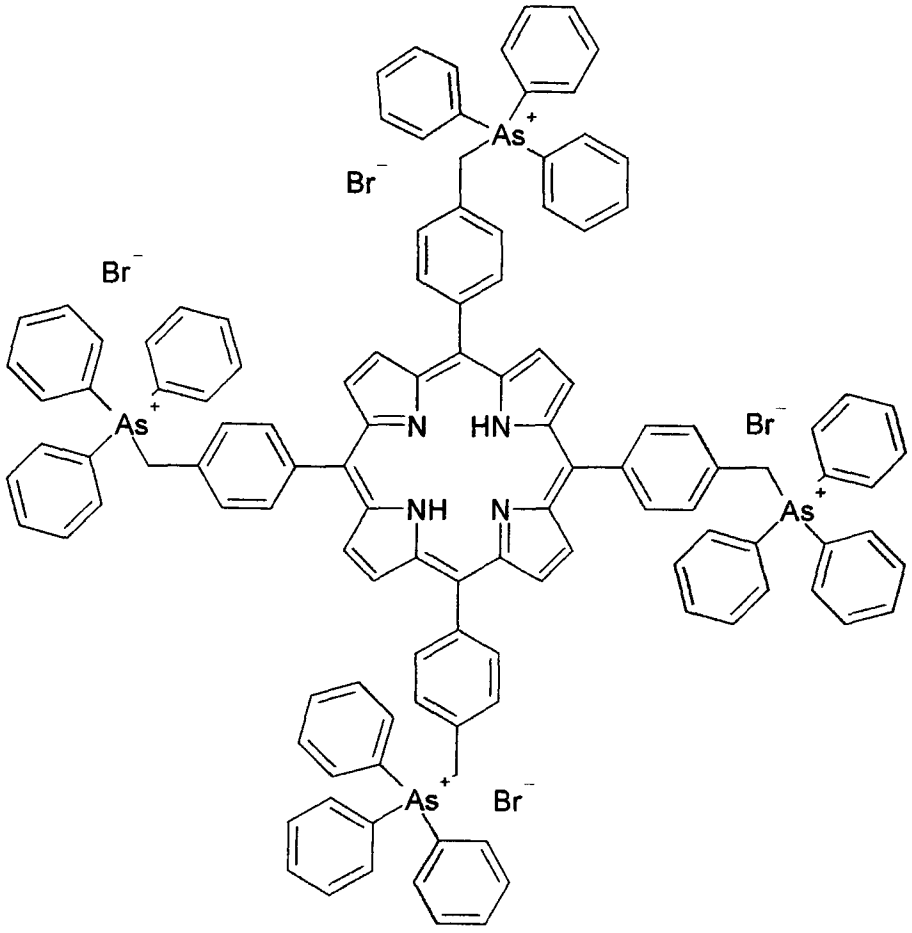

To a flame dried flask under a nitrogen atmosphere was added compound **83** (20mg, 0.02mmol) and triphenylarsine (3g). The mixture was heated to 110°C and was stirred for 48 hours effecting reaction solvolysis. On cooling the solid was ground up and methanol added (5ml). The suspension was stirred for 5 minutes and the unreacted triphenylarsine was collected by microfiltration (Millipore®) and washed with methanol. The recovered filtrate was added to 50ml diethyl ether. The resultant precipitate was collected by microfiltration (Millipore®) and this process was repeated twice. The purple solid was dried under vacuum to give compound **96.** (0.0089g, 60%) ^{1}H NMR [400MHz, $(CD_3)_2SO$] δ-2.94 (2H,br s, N*H*), δ4.86 (8H, s, CH_2As), δ7.41 (8H, d, ^{3}J= 8Hz, 5,10,15,20-Ar-3,5-H), 7.87-7.96 (64H, m overlapping, 5,10,15,20-Ar-2,6-H & *ortho, meta, para*-Ar-H), δ8.71 (8H, s, β-H); UV/Vis (octanol, nm) λ_{max} 423, 515, 550, 592,648; MS (ES) *m/z* 472 (M^{4+}), 657 $(M + Br)^{3+}$, 1025 $(M + 2\ Br)^{2+}$; HPLC t_r = 18.4 min (flow rate= 1ml/min;eluent A, H_2O and 0.1%TFA; eluent B, methanol; gradient 0min,0%B; 10min, 75% B; 15min, 75% B; 18min 0% B; 19min 0% B; column, Phenomenex Luna 5μ C18(2) 250*4.6mm

5, 10, 15, 20-tetra-(4-hydroxyphenyl)porphyrin (106)

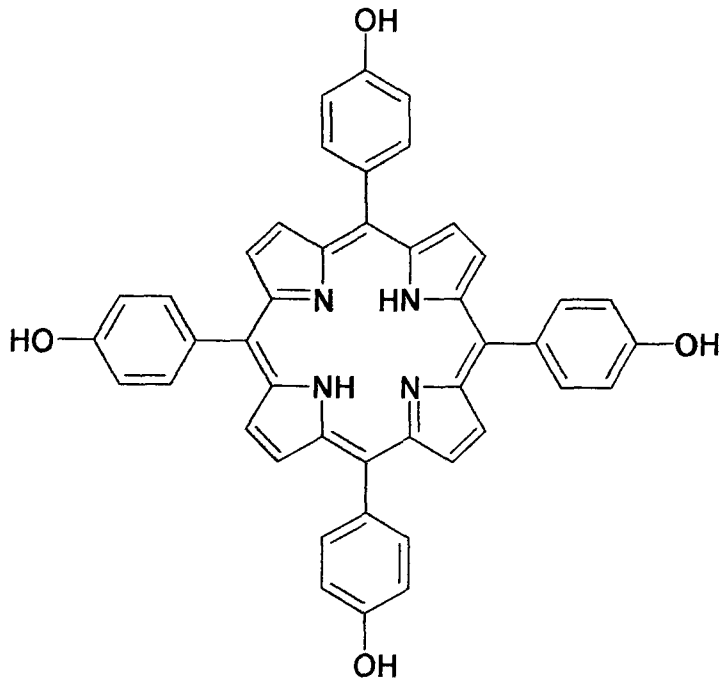

4-Hydroxybenzaldehyde (15.51g, 0.127mol) was dissolved in propionic acid (250ml) and heated to reflux. Pyrrole (8.82ml, 0.127mol) was added drop wise and the reaction refluxed for 30mins. Upon cooling the fine purple precipitate was collected by filtration and washed with propionic acid then water. The crystals were dried under vacuum overnight to give compound **106**. (2.51g, 11%) *Rf*=0.54 (silica, 10% EtOH/$CHCl_3$); ^1H NMR [400MHz, CD_3OD] δ7.22 (8H, d, J= 8 Hz, Ar-3,5-*H*), δ8.02 (8H, d, J= 8 Hz, Ar-2,6-*H*), δ8.90 (8H, br s, β-*H*); UV/Vis (MeOH, nm) λ_{max} 413, 517, 554, 593, 650. MS (MALDI) *m/z* (M^+) 680.

5, 10, 15, 20-tetra-(4-(3-bromopropoxy)phenyl)porphyrin (101) [83]

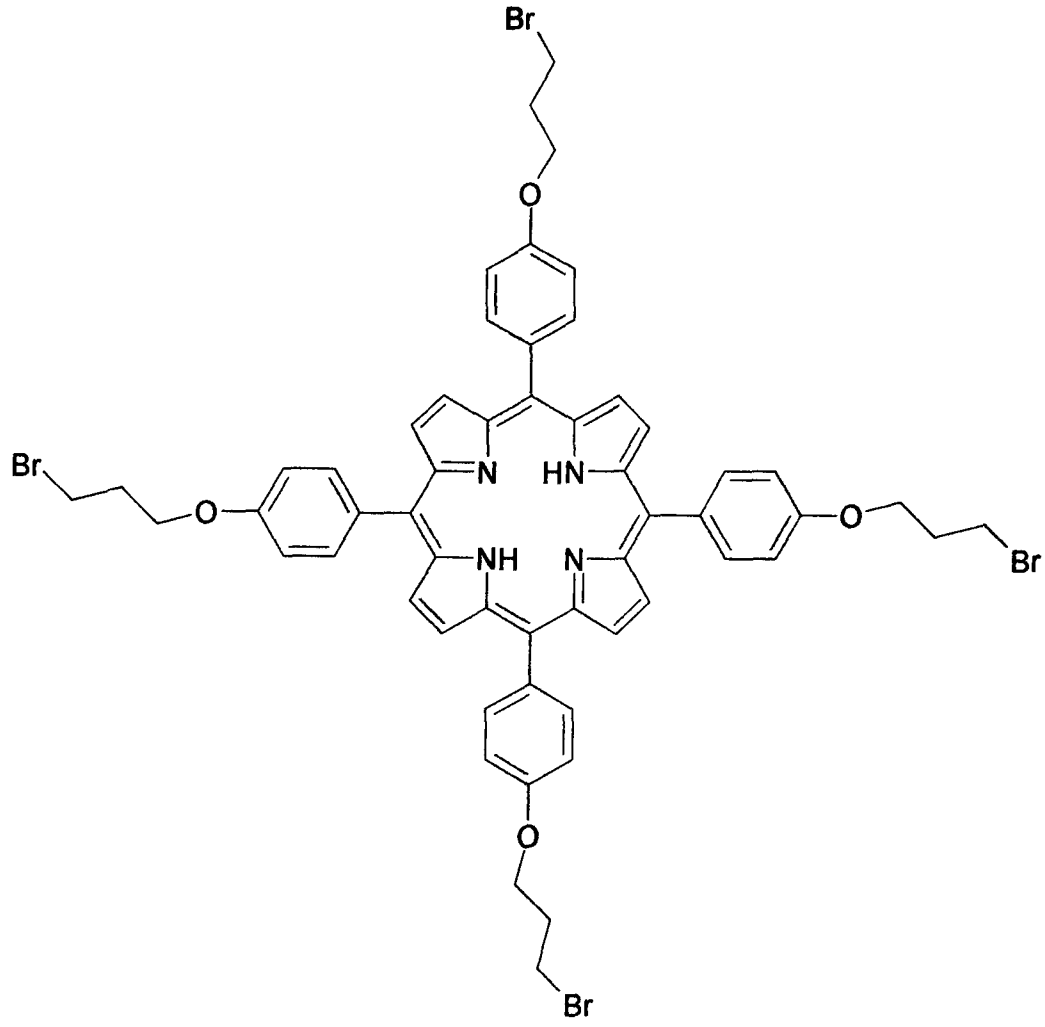

Compound **106** (0.5g, 0.737mmol) was dissolved in dry dioxane (100ml). K_2CO_3 (1.02g, 0.737mmol) was added and the reaction was heated to 100°C. 1,3 Dibromopropane (0.0368mol, 14.74ml) was dissolved in 35ml dry dioxane and this was added drop wise to the reaction mixture. The reaction was stirred at 100°C for 4 days in the dark then it was cooled to room temperature and filtered to remove the potassium carbonate. The filtrate was concentrated *in vacuo* and the crude product was adsorbed onto silica and purified by gravity percolation chromatography (silica, eluent: 1% MeOH in DCM), the relevant fractions were combined and the solvent removed *in vacuo* to give **101** as fine purple crystals. (0.89g, 18%) ^{1}H NMR [400MHz, $CDCl_3$] δ-2.76 (2H, br s, N-H), δ 2.60-2.48 (8H, m, $CH_2CH_2CH_2$), δ3.80 (8H, t, ^{3}J = 8Hz, Br-CH_2), δ4.41 (8H, t, ^{3}J = 8Hz, OCH_3), δ7.29 (8H, d, ^{3}J= 8Hz, Ar-3,5-*H*) δ8.12 (8H, d, ^{3}J = 8 Hz, Ar-2,6-*H*), δ8.86 (8H, s, β-H). UV/Vis (MeOH, nm) λ_{max} 423, 519, 555, 594, 651; MS (MALDI) *m/z* (M + /H) 1165.

5, 10, 15, 20-tetra-(4-carboxyphenyl)porphyrin (146) [110]

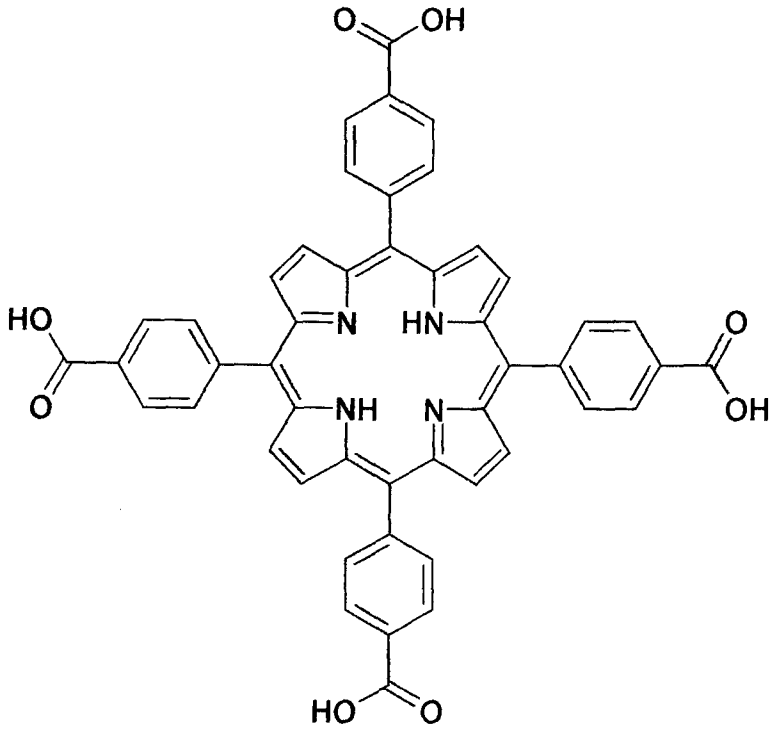

4-Carboxybenzaldehyde (19.06g, 0.127mol) was dissolved in propionic acid (250ml) and heated to reflux. Pyrrole (8.82ml, 0.127mol) was added drop wise and the reaction refluxed for 30 mins. Upon cooling the fine purple precipitate was collected by filtration and washed with propionic acid then water. The crystals were dried under vacuum overnight to give compound **21**. (9.46g, 38%) ^{1}H NMR [400MHz, CD_3OD] δ-3.00 (2H, br s, N*H*), δ8.36 (8H, d, ^{3}J = 8 Hz, Ar-3,5-*H*), δ8.40 (8H, d, ^{3}J = 8 Hz, Ar-2,6-*H*), δ8.86 (8H, s, β-*H*), δ12.00 (4H, bs, O*H*); UV/Vis (CH_2Cl_2, nm) λ_{max} 420, 517, 551, 595, 650; MS (MALDI) *m/z* 791.61(M + H).

121 4-Benzylaminobutanenitrile

127 4-(N-Benzyl-N-(3-cyanopropyl)amino)butanenitrile

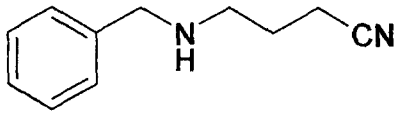

121

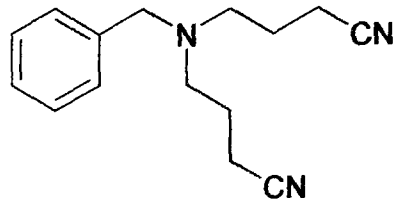

127

Benzylamine (0.01mol, 1.09ml), chlorobutanenitrile (0.022mol, 2.10ml) and Na_2CO_3 (0.01mol, 1.0599g) were dissolved in butanol (50ml) and stirred for 48 hours. No product was seen so the reaction was refluxed for 24 hours. The Na_2CO_3 was removed by filtration and the solvent removed *in vacuo*. TLC in 2%MeOH in DCM showed 2 spots (rf = 0.177 and 0.84). Column chromatography (2% MeOH in DCM) afforded both compound **121** and compound **127**.

Compound **121**. (0.62g, 36%) ^{1}H NMR [400MHz, $CDCl_3$] δ1.34 (1H, bs, N-*H*), δ1.73 (2H, quint, J = 3Hz, CH_2-C*H*$_2$-CH_2), δ2.36 (2H, t, ^{3}J = 5Hz, C*H*$_2$-CN), δ2.69 (2H, t, ^{3}J = 6Hz, N-C*H*$_2$-CH_2), δ3.71 (2H, s, Ar-C*H*$_2$), δ7.25 (5H, m, Ar-*H*); MS (ES) *m/z* 174.

Compound **127**. (0.54g, 22%) ^{1}H NMR [400MHz, $CDCl_3$] δ1.72 (4H, quint, J = 3Hz, CH_2-C*H*$_2$-CH_2), δ2.28 (4H, t, ^{3}J = 5Hz, C*H*$_2$-CN), δ2.49 (4H, t, ^{3}J = 6Hz, N-C*H*$_2$-CH_2), δ3.47 (2H, s, Ar-C*H*$_2$), δ7.25 (5H, m, Ar-*H*); MS (ES) *m/z* 241.

t-Butyl N-(3-chloropropyl)carbamate (129) [92]

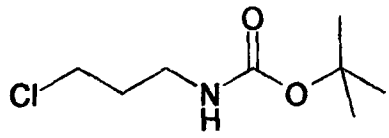

3- Chloropropylamine hydrochloride (2.31g,22.91mmol) and di-tert-butyl di-carbonate (5g, 22.91mmol) were dissolved in 1:1 THF/H_2O and the pH was adjusted to 8.5 using 4% aqueous NaOH. The reaction was stirred overnight and the pH was adjusted 2 using 0.1M HCl. The product was extracted into chloroform and dried over $MgSO_4$. The solvent was removed *in vacuo* to give **129** (3.26g, 73%); ^{1}H NMR [400MHz,$CDCl_3$] δ1.41 (9H, s, CH_3), δ1.93 (2H, quint, ^{3}J = 5Hz, $ClCH_2CH_2$), δ3.25 (2H, t, ^{3}J = 8Hz, $NHCH_2$), δ3.56 (2H, t, ^{3}J = 4Hz, CH_2Cl); MS (ES) *m/z* 194,196 (3:1) (M + H).

N^{α},N^{ε}-Di(*t*-butoxycarbonyl) lysine (137) [91]

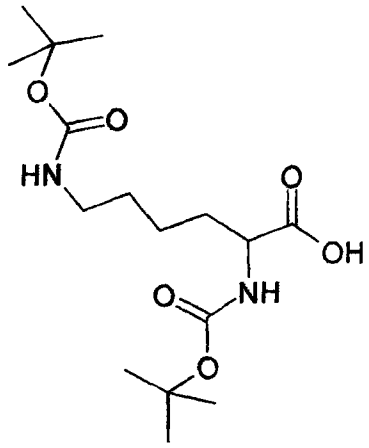

To a solution of lysine (10mmol, 1.826g), triethylamine (15mmol, 2.09ml) in 50% aq dioxane (14ml) was added BOC-ON (22mmol, 5.41g). The reaction was stirred for 2 days. Water was added to the reaction mixture and 2-hydroxyimino-2-phenylacetone was extracted into diethyl ether (50ml). The ether layers were washed with water to ensure the product remained in the aqueous layer. The aqueous layer was acidified using 5% aq citric acid and the product extracted into EtOAc. The organic layer was dried over $MgSO_4$, filtered and the solvent removed *in vacuo* to produce **137** as a foam. (2.64g; 76%). ^{1}H NMR [400MHz, $CDCl_3$] δ1.37 (9H, s, CH_3), δ1.40 (9H, s, CH_3), δ1.66-1.64 (2H, m, $NHCH_2CH_2$), δ1.73-1.70 (2H, m, $CHCH_2CH_2$), δ1.87-1.83 (2H, m, $CHCH_2$), 3.01 (2H, t, ^{3}J= 8Hz, $NHCH_2$), δ4.30-4.28 (2H, m, CH); MS (ES) *m/z* 347 (M + H).

140 N^{α},N^{ε}-Di(*t*-butoxycarbonyl) lysine N-benzylamine

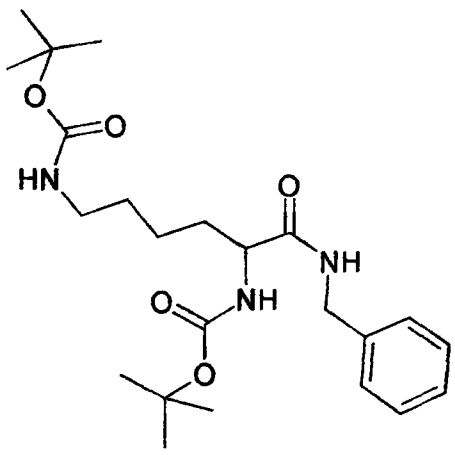

N'-*N'*-diboc-lysine (**137**) (4.6mmol, 1.607g) and benzylamine (4.6mmol, 0.5ml) were dissolved in DCM (30ml). HOBt (9.2mmol, 1.24g) was added and the reaction was cooled to 0°C. DCC (4.6mmol, 0.95g) in DCM (10ml) was added and the reaction was stirred under nitrogen for 24 hours. The reaction mixture was filtered to remove the precipitate and the solvent was removed *in vacuo*. The product was adsorbed onto silica and purified by gravity percolation chromatography (silica, eluent: 2% MeOH in DCM) to afford **140**. (1.93g, 97%) MS (ES) *m/z* 436 (M + H).

141 Lysine N-benzylamide

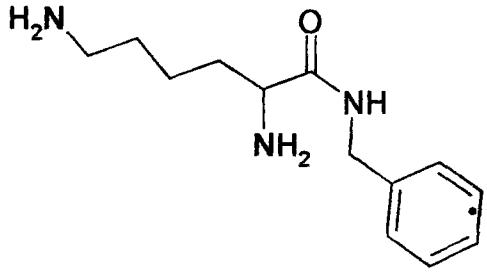

140 (1.00g, 2.29mmol) was dissolved in 1:1 DCM:TFA (20ml) and stirred for 2 hours. The solvent was removed *in vacuo*. The product was washed with DCM and filtered to give **141** as white crystals. (0.47g, 88%) ^{1}H NMR [400MHz, D_2O] δ1.51-1.32 (2H, m, $CHCH_2CH_2$), δ1.72-1.62 (2H, m, $CHCH_2$), δ1.88-1.80 (2H, m, $NH_2CH_2CH_2$), δ3.00-2.92 (2H, t, ^3J = 8Hz, NH_2CH_2), δ3.33-3.30 (2H, m, CH_2Ph) ,δ3.83-3.72 (1H, m, CH), δ7.34-7.27 (5H, m, Ph); MS (ES) *m/z* 235(M+).

142 2,6- Bis-trimethylamino-hexanoic acid benzylamide

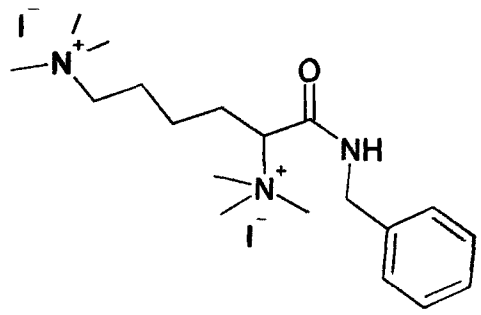

141 (0.4g, 1.7mmol) was dissolved in dry dioxane (20ml) and MeI (15ml) was added. The reaction was refluxed overnight and the solvent and excess MeI were removed *in vacuo* to give **142** (0.23g, 42%) ^{1}H NMR [400MHz, D_2O] δ1.51-1.33 (2H, m, $CHCH_2CH_2$), δ1.73-1.62 (2H, m, $CHCH_2$), δ1.88-1.80 (2H, m, $N^+CH_2CH_2$), δ3.33-3.30 (4H, m, N^+CH_2 and CH_2Ph overlapping), δ3.35 (9H, s, CH_3), δ3.37 (9H, s, CH_3), δ3.99-3.87 (1H, m, CH), δ7.34-7.27 (5H, m, Ph); MS (ES) *m/z* 160.7 (M^{2+}).

3-(3-Amino-2,2-bis-(2-cyano-ethoxymethyl)-propoxy)-propionitrile (145) [94]

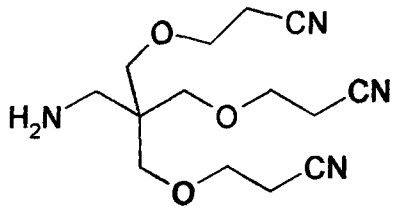

To a vigorously stirred solution of tris (hydroxymethyl) methylamine (9.99g, 0.0825mol), acrylonitrile (18.43ml, 0.28mol) and NBu_4Br (5.32g, 0.0165mol) in 100ml DCM was added NaOH (25g) in H_2O(100ml). The reaction was stirred between 5 and 10°C for 3 days. The organic layer was separated and dried over $MgSO_4$. This was filtered and the filtrate evaporated *in vacuo*. The crude sample was purified by chromatography (silica, 5%MeOH in DCM) and relevant fractions were combined and evaporated *in vacuo* to give **145** as a white solid. (14.62g; 60%). ^{1}H NMR [400MHz, $CDCl_3$] δ1.67 (2H, s, NH_2), δ2.56 (6H, t, ^{3}J= 6Hz, CH_2CN), δ3.38 (6H, s, CCH_2O), δ3.63 (6H, t, ^{3}J = 6Hz, OCH_2CH_2). MS (ES) *m/z* 294(M+).

Phenylcarboxy(3-(3-amino-2,2-bis-(2-cyano-ethoxymethyl)-propoxy)-propionitrile (148)

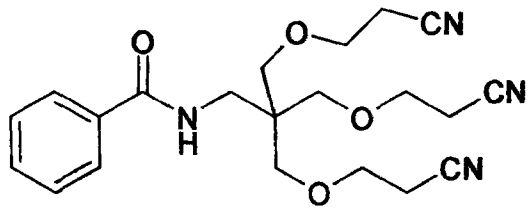

145 (0.25g, 0.8mmol), benzoic acid (0.1089g, 0.8mmol) and HOBt (0.241g, 1.78mmol) were dissolved in DCM (10ml). The solution was cooled to 0°C and *N-N'*-diisopropylcarbodiimide (DIC) (0.139ml, 0.8mmol) was added. The reaction was stirred under nitrogen for 24 hours and the solvent removed *in vacuo*. Column chromatography (silica, EtOAc) afforded the product. (0.12g, 37%) ^{1}H NMR [400MHz, $CDCl_3$] δ2.61 (6H, t, ^{3}J= 6Hz ,CH_2CN), δ3.72 (6H, t, ^{3}J = 6Hz, OCH_2CH_2), δ4.01 (6H, s, CCH_2O), δ6.52 (1H, s, N*H*), δ7.49-7.42 (3H, m, Ar-3,4,5-*H*), δ7.77-7.76 (2H, m, Ar-2,6-*H*); MS (ES) *m/z* 399 (M + H).

References:

[1] Lambrechts, S., Schwartz, K., Aalders, M., Dankert, J. (2005) Photodynamic inactivation of fibroplasts by cationic porphyrin. Laser. Med. Sci. 20, 62-67.

[2] Orenstein, A., Klein, D., Kopolovic, J., Winkler, E., Malik, Z., Keller, N., Nitzan, Y. (1998) The use of porphyrins for eradication of *Staphylococcus aureus* in burn wound infections. FEMS Immunol. Med. Microbiol.19, 307-314.

[3] Singleton, P. Bacteria in biology, biotechnology and medicine. John Wiley and sons Ltd. 5th edition, 1999.

[4] Sleigh, J, D., Timbury, M, C., Medical Bacteriology. Churchill Livingstone. 3rd edition, 1990.

[5]http://en.wikipedia.org/wiki/Image:Average_prokaryote_cell_-_en.svg#filelinks (08/04/08)

[6] http:lecturer.ukdw.ac.id/dhira/BacterialStructure/CellWall.html (14/02/07)

[7] Brock, T, D., Madigan, M, T. Biology of microorganisms. Prentice-Hall international editions. 6th edition, 1991.

[8] Uttley, A, H., Collins, C, H., Naidoo, J., George, R, C. (1988) Vancomycin-resistant *Enterococci.* Lancet 331, 57-58.

[9] Hiramatsu, K., Hanaki, H., Ino, T., Yabuta, K., Oguri, T., Tenover, F, C. (1997) Methicillin-resistant *Staphylococcus aureus* clinical strain with reduced vancomycin susceptibility. J. Antimicrob. Chemother 40:135-136.

[10] http://www.harcourt-international.com/e-books/pdf/360.pdf. (14/02/07)

[11] Hemstreet, B, A., Page, R, L. (2006) Sulfonamide allergies and outcomes related to use of potentially cross-reactive drugs in hospitalized patients. Pharmacotherapy. 26, 551-557.

[12] Antimicrobial resistance: World health organisation fact sheet number 194. Jan 2002

[13] File, T, M. (1999) Overview of resistance in the 1990s. Chest 115, 3-8

[14] Bush, K. (2004) Antibacterial drug discovery in the 21st century. Clin. Microbiol. Infect. 10, (s4), 10-17.

[15] Poole, K. (2002) Mechanisms of bacterial biocide and antibiotic resistance. J. Appl. Microbiol. 92, (s1), 55S-64S.

[16] Lewis, K. (2001) Riddle of biofilm resistance. Antimicrob. Agents. Chemother. 45, 999-1007.

[17] Livermore, D, M., (2002) Multiple mechanisms of Antimicrobial resistance in *Pseudomonas aeruginosa*: Our worst nightmare? Clin. Infect. Dis. 34, 634-640.

[18] Dé E, Baslé A, Jaquinod M, Saint N, Malléa M, Molle G, Pagès J M. (2001) A new mechanism of antibiotic resistance in *Enterobacteriaceae* induced by structural modification of the major porin. Mol. Microbiol. 41, 189-198.

[19] Nikaido, H. (1996) Mini review: Multidrug efflux pumps of Gram-negative bacteria. J. Bacteriol. 178, 5853-5859.

[20] Kumar, A., Schweizer, H,P., (2005) Bacterial resistance to antibiotics: Active efflux and reduced uptake. Adv. Drug. Deliv.Rev. 57, 1486-1513.

[21] Lambert, P, A., (2005) Bacterial resistance to antibiotics: Modified target sites. Adv. Drug. Deliv. Rev. 57, 1471-1485.

[22] Franklin, T, J., Snow, G, A. Biochemistry of antimicrobial action. Chapman and Hall. 4th edition, 1989.

[23] Rice, K, C., Bayles, K, W. (2003) Death's toolbox: examining the molecular components of bacterial programmed cell death. Mol. Microbiol. 50, 3, 729-738.

[24] Lewis, K. (2000) Programmed cell death. Microbiol. Mol. Biol. Rev. 64, 3, 503-514.

[25] Sat, B., Hazan, R., Fisher, T., Khaner, I., Glaser, G., Engelberg-Kulka, H. (2001) Programmed Cell Death in *Escherichia coli*: Some antibiotics can Trigger *mazEF* Lethality. J. Bacteriol. 183, 6, 2041-2045.

[26] Lindsey, J, S., Schreiman, I, C., Hsu, H, C., Kearney, P, C., Marguerettaz, A, M., (1987) Rothmund and Adler-Longo reactions revisited: Synthesis of tetraphenylporphyrins under equilibrium conditions. J. Org. Chem. 52, 827-836.

[27] Shanmugathasan, S., Edwards, C., Boyle, R, W., (2000) Advances in modern synthetic porphyrin chemistry. Tetrahedron 56, 1025-1046.

[28] Nyman, E, S., Hynninen, P, H. (2004) Research advances in the use of tetrapyrrolic photosensitizers for photodynamic therapy. J. Photochem. Photobiol. B 73,1-28.

[29] http://www.bmb.leeds.ac.uk/pdt/PDToverview.htm (16/02/07)

[30] Bonnett, R. (1995) Photosensitizers of the porphyrin and phthalocyanine series for photodynamic therapy. Chem. Soc. Rev. 24, 19-33.

[31] Macdonald, I, J., Dougherty, T, J. (2001) Basic principles of photodynamic therapy. J. Porphyrin Phthalocyanines 5, 105-129.

[32] QLT inc, 887 Great Northern Way, Vancouver,BC, Canada, V5T 4T5.

[33] Mang, T, S. (2004) Lasers and light sources for PDT: past, present and future. Photodiagnosis. Photodynamic Therapy. 1, 43-48.

[34] Allison, R, R., Downie, G, H., Cuenca, R., Hu, X, H., Childs, C, J, H., Sibata, C. (2004) Photosensitizers in clinical PDT. Photodiagnosis. Photodynamic Therapy. 1, 27-42.

[35] Barr, H., Kendal, C., Reyes-Goddard, J., Stone, N. (2002) Clinical aspects of photodynamic therapy. Sci. prog. 85, 2, 131-150.

[36] Monfrecola, G., Procaccini, E, M., Bevilacqua, M., Manco, A., Calabro, G., Santoianni, P. (2004) *In-vitro* effect of 5-aminolaevulinic acid plus visible light on *Candida albicans*. Photochem. Photobiol. Sci. 3, 419-422.

[37] Wainwright, M. (2004) Photoinactivation of viruses. Photochem. Photobiol. Sci. 3, 406-411.

[38] Wainwright, M. (2002) The emerging chemistry of blood product disinfection. Chem. Soc. Rev. 31, 128-136.

[39] Cook, N. (1998) Methicillin-resistant *Staphylococcus aureus* versus the burn patient. Burns. 24, 91-98.

[40]http://www.bu.edu/woundbiotech/bioengineered/VenousUlcersPresentation/images/Picture%2017.jpg (17/02/07)

[41] Wainwright, M. (2001) Acridine-a neglected chromophore. J. Antimicrob. Chemother. 47, 1-13.

[42] Detty, M, R., Gibson, S, L., Wagner, S, J. (2004) Current and preclinical photosensitizers for use in photodynamic therapy. J. Med. Chem. 47, 3897-3915.

[43] Orenstein, A., Klein, D., Kopolovic, J., Winkler, E., Malik, Z., Keller, N., Nitzan, Y. (1997) The use of porphyrins for eradication of *Staphylococcus aureus* in burn wound infections. FEMS Immun. Med. Microbiol.19, 307-314.

[44] Malik, Z., Ladan, H., Nitzan, Y. (1992) Photodynamic inactivation of Gram-negative bacteria: problems and possible solutions. J. Photochem. Photobiol. B: Biology. 14, 262-266.

[45] Scalise, I., Durantini, E, N. (2003) Synthesis and photodynamic activity of tetracatioinc and non-charged zinc phthalocyanine derivatives in homogeneous and biological media. 7th international electronic conference on synthetic organic chemistry (ECSOC-7) 2003: http://www.mdpi.net/ec/papers/ecsoc-7/c002/c002.htm (14/02/07)

[46] Minnock, A., Vernon, D, I., Schofield, J., Griffiths, J., Parish, H., Brown, S, B. (1996) Photoinacitvation of bacteria. Use of a cationic water-soluble zinc phthalocyanine to photoinactivate both Gram negative and Gram positive bacteria. J. Photochem. Photobiol. B: Biology. 32,159-164.

[47] Nitzan, Y., Ashkenazi, H. (2001) Photoinactivation of *Acinetobacter baumannii* and *Escherichia coli B* by a cationic hydrophilic porphyrin at various light wavelengths. Curr. Microbiol. 42, 408-414.

[48] Merchat, M., Bertolini, G., Giacomini, P., Villanueva, A., Jori, G. (1996) Meso-substituted cationic porphyrins as efficient photosensitizers of Gram-positive and Gram-negative bacteria. J. Photochem. Photobiology B: Biology. 32, 153-157.

[49] Salmon-Divon, M., Nitzan, Y., Malik, Z. (2004) Mechanistic aspects of *Escherichia coli* photodynamic inactivation by cationic tetra-*meso*(N-methylpyridyl)porphine. Photochem. Photobiol. Sci. 3, 423-429.

[50] Hamblin, M, R., Hasan, T. (2004) Photodynamic therapy: a new antimicrobial approach to infectious disease? Photochem. Photobiol. Sci. 3, 436-450.

[51] Lazzeri, D., Rovera, M., Pascual, L., Durantini, E, N. (2004) Photodynamic studies and photoinactivation of *Escherichia coli* using *meso*-substituted cationic porphyrin derivatives with asymmetric charge distribution. Photochem. Photobiol. 80, 286-293.

[52] Spesia, M, B., Lazzeri, D., Pascual, L., Rovera, M., Durantini, E, N. (2005) Photoinactivation of *Escherichia coli* using porphyrin derivatives with different number of cationic charges. FEMS Immuno. Med. Microbiol. 44, 289-295.

[53] Merchat, M., Spikes, J, D., Bertoloni, G., Jori, G. (1996) Studies on the mechanism of bacteria photosensitization by meso-substituted cationic porphyrins. J. Photochem. Photobiol. B: Biology. 35, 149-157.

[54] Reddi, E., Ceccon, M., Valduga, G., Jori, G., Bommer, J, C., Elisei, F., Latterini, L., Mazzucato, U. (2002) Photophysical and antibacterial activity of meso-substituted cationic porphyrins. Photochem. Photobiology 75, 462-470.

[55] Trannoy, L, L., Lagerberg, J, W, M., Dubbelman, T, M, A, R., Schuitmaker, H, J., Brand, A. (2004) Positively charged porphyrins: a new series of photosensitizers for sterilization of RBCs. Transfusion 44,1186-1196.

[56] Tomé, J, P., Neves, M, G, P, M, S., Tomé, A, C., Cavaleiro, J, A, S., Soncin, M., Magaraggia, M., Ferro, S., Jori, G. (2004) Synthesis and antibacterial activity of new poly-S-lysine-porphyrin conjugates. J. Med. Chem. 47, 6649-6652.

[57] Polo, L., Segalla, A., Bertoloni, G., Jori, G., Schaffner, K., Reddi, E. (2000) Polylysine-porphycene conjugates as efficient photosensitizers for the inactivation of microbial pathogens. J. Photochem. Photobiol. B: Biology 59,152-158.

[58] Soukos, N, S., Ximenez-Fyvie, L, A., Hamblin, M, R., Socransky, S, S., Hasan, T. (1998) Targeted antimicrobial chemotherapy. Antimicrob. Agents. Chemother. 42, 2595-2601.

[59] Hamblin, M, R., O'Donnell, D, A., Murthy, N., Rajagopalan, K., Michaud, N., Sherwood, M, E., Hasan, T.(2002) Polycationic photosenstizer conjugates: effects of chain length and Gram classification on the photodynamic inactivation of bacteria. J. Antimicrob. Chemother. 49, 941-951.

[60] Hamblin, M, R., Zarha, T., Contag, C, H., McManus, A, T., Hasan, T. (2003) Optical monitoring and treatment of potentially lethal wound infections *in-vivo*. J. Infect. Dis.187, 1717-1725.

[61] Gad, F., Zahra, T., Francis, K, P., Hasan, T., Hamblin, M, R. (2004) Targeted photodynamic therapy of established soft-tissue infections in mice. Photochem. Photobiol. Sci. 3, 451-458.

[62] Dancil, K, P, S., Hilario, L, F., Khoury, R, G., Mai, K, U., Nguyen, C, K., Weddle, K, S., Shachter, A, M. (1997) Synthesis and aggregation of cationic porphyrins. J. Heterocyclic. Chem. 34, 749-755.

[63] Dias, A, M, A., Caço, A, I., Coutinho, J, A, P., Santos, L, M, N, B, F., Piñeiro, M, M., Vega, L, F., Costa Gomes, M, F., Marrucho, I, M. (2004) Thermodynamic properties of perfluoro-*n*-octane. Fluid Phase Equilib. 225, 39-47.

[64] Freire, M, G., Dias, A, M, A., Coutinho, J, A, P., Coelho, M, A, Z., Marrucho, I, M. (2005) Enzymatic method for determining oxygen solubility in perfluorocarbon emulsions. Fluid Phase Equilib. 231, 109-113.

[65] Costa Gomes, M, F., Deschamps, J., Menz, D, H. (2004) Solubility of dioxygen in seven fluorinated liquids. J. Fluorine. Chem. 125, 1325-1329.

[66] Dias, A, M, A., Freire, M, G., Coutinho, J, A, P., Marrucho, I, M. (2004) Solubility of oxygen in liquid perfluorocarbons. Fluid Phase Equilib. 222-223, 325-330.

[67] Lowe, K, C. (2002) Perfluorochemical respiratory gas carriers: benefits to cell culture systems. J. Fluorine. Chem.118, 19-26.

[68] Tjahjono DH, Akutsu T, Yoshioka N, Inoue H. (1999) Cationic porphyrins bearing diazolium rings: synthesis and their interaction with calf thymus DNA. Biochimica et Biophysica Acta. 1472, 333-343.

[69] Tjahjono DH, Mima S, Akutsu T, Yoshioka N, Inoue H.(2001) Interaction of metallopyrazoliumylporpyrins with calf thymus DNA. J.Inorg. Biochem 85, 219-228.

[70] Nystrom, R, F., Brown, W, G. (1948) Reduction of organic compounds by lithium aluminium hydride. III. Halides, Quinones, Miscellaneous Nitrogen compounds. J. Am. Chem. Soc. 70, 3738-3740.

[71] Nystrom, R, F. (1955) Reduction of organic compounds by mixed hydrides. I. Nitriles. J. Am. Chem. Soc 77, 2544-2545.

[72] Koenig, T, M., Mitchell, D. (1994). A convenient method for preparing enantiomerically pure norfluoxetine, fluoxetine and tomoxetine. Tetrahedron Lett.35, 1339-1342.

[73] Brown, H, C., Choi, Y, M., Narasimhan, S. (1982) Selective reductions 29. A simple technique to achieve an enhanced rate of reduction of representative organic compounds by borane-dimethyl sulphide. J. Org. Chem. 47, 3153

[74] White, J, D., Yager, K, M., Yakura, T. (1994) Synthetic studies of the pyrroloquinoline nucleus of the makaluvamine alkaloids. Synthesis of the topoisomerase II inhibitor makaluvamine. J. Am. Chem. Soc. 116, 1831-1838.

[75] Zhang, X, X., Lippard, S, J. (2000) Synthesis of PDK, a novel porphyrin-linked dicarboxylate ligand. J. Org. Chem. 65, 5298-5305.

[76] Brunner, H., Schellerer, K, M. (2002) Double porphyrin platinum conjugates. Z. Naturforsch. B57, 751-756.

[77] Mitsunobu, O., Wada, M., Sano, T. (1972) Stereospecific and stereoselective reactions. I. Preparation of amines from alcohols. J. Am. Chem. Soc. 94, 679-680.

[78] Lavallee, D, K., Xu, Z., Pina, R. (1993) Synthesis and properties of new cationic-periphery porphyrins, tetrakis(p-(aminomethyl)phenyl)porphyrin and N-methyltetrakis(p-(aminomethyl)phenyl)porphyrin. J. Org. Chem. 58, 6000-6008.

[79] Jin, R, H., Aoki, S., Shima, K. (1996) A new route to water soluble porphyrins: phosphonium and ammonium type cationic porphyrins and self assembly. Chem. Commun. 1939-1940.

[80] Jin, R, H., Aoki, S., Shima, K. (1997) Phosphoniumyl cationic porphyrins- self aggregation origin from π-π and cation-π interactions. J. Chem. Soc, Faraday Trans. 93, 22, 3945-3953.

[81] Marzilli, L, G., Pethö, G., Lin, M., Kim, M, S., Dixon, D, W.(1992) Tentacle porphyrins: DNA-interactions. J. Am. Chem. Soc. 114, 7575-7577.

[82] Schneider, H, J., Wang, M. (1994) DNA interactions with porphyrins bearing ammonium side chains. J. Org. Chem. 59, 7473-7478.

[83] Momenteau, M., Mispelter, J., Loock, B., Bisagni, E. (1983) Both-faces hindered porphyrins. Part 1. Synthesis and characterization of basket-handle porphyrins and their iron complexes. J. Chem. Soc, Perkin Trans. 1. 189-196.

[84] Buhleir, E., Wehner, W., Vögtle, F. (1978) "Cascade"- and "non-skid-chain-like" synthesis of molecular cavity topologies. Synthesis 155-158.

[85] Moors, R., Vögtle, F. (1993) Dendrimere Polyamine. Chem. Ber. 126, 2133-2135.

[86] Wörner, C., Mülhaupt, R. (1993) Polynitrile- and polyamine-functional poly(trimethylene imine) dendrimers. Angew. Chem. Int. Ed. Engl. 32, 1306-1311.

[87] Newkome, G, R., Moorefield, C, N., Vögtle, F. (1996) Dendritic molecules concepts, syntheses, perspectives.1996.VCH Verlaggesellschaft mbH, Weinhein and VCH publishers inc. New York{USA).

[88] Boas, U., Heegaard, P, M, H. (2004) Dendrimers in drug research. Chem. Soc. Rev. 33, 43-63.

[89] Bosman, A, W., Janssen, H, M., Meijer, E, W. (1999) About dendrimers: structure, physical properties, and applications. Chem. Rev. 99, 1665-1688.

[90] Zhang, G, D., Harada, A., Nishiyama, N., Jiang, D, L., Koyama, H., Aida, T., Kataoka, K. (2003) Polyion complex micelles entrapping cationic dendrimer porphyrin-

effective photosensitizer for photodynamic therapy of cancer. J. Controlled Release 93, 141-150.

[91] Kohl, M, J., Lejeune, R, G. (2002) Coupling of biologically active steroids to conjugating arms through ether linkages for use in immunochemistry. Steroids 67, 71-75.

[92] König, W., Geiger, R. (1973) *N*-Hydroxyverbindungen als Katalysatoren für die aminolyse aktivierter Ester. Chem. Ber 106, 3626-3635.

[93] Dupraz, A., Guy, P., Dupuy, C. (1996) Polyalkylation of primary polyols by 1,4-addition to tert-butyl acrylate and acrylonitrile. Tetrahedron Lett. 37, 1237-1240.

[94] Dayan, I., Libman, J., Shanzer, A., Felder, C., Lifson, S. (1991) Regulation of molecular conformation of chiral tripodal structures by Ca^{2+} binding. J. Am. Chem. Soc. 113, 3431-3439.

[95] Han, S, Y., Kim, Y, A. (2004) Recent development of peptide coupling reagents in organic synthesis. Tetrahedron 60, 2447-2467.

[96] Dandliker, P, J., Diederich, F., Zingg, A. (1997) Dendrimers with porphyrin cores: synthetic models for globular heme proteins. Helv. Chim. Acta 80, 1773-1801.

[97] Vinogradov, S, A., Lo, L, W., Wilson, D, F. (1999) Dendritic polyglutamic porphyrins: probing porphyrin protection by oxygen-dependent quenching of phosphorescence. Chem. Eur. J. 5, 1338-1347.

[98] Gradl, S, N., Felix, J, P., Isacoff, E, Y., Garcia, M, L., Trauner, D. (2003) Protein recognition by rational design: nanomolar ligands for potassium channels. J. Am. Chem. Soc 125, 42, 12668-12669.

[99] Dourtoglou, V., Ziegler, J, C., Gross, B. (1978) L'hexafluorophosphate de O-benzotriazolyl-*N, N*-tetramethyluromium: Un reactif de couplage peptidique nouveau et efficace. Tetrahedron Lett.19, 1269-1272.

[100] http://www.promega.com/enotes/applications/0004/ap0017.htm (14/02/07)

[101] Cunderlikova, B., Kaalhus, O., Cunderlik, R., Mateasik, A., Moan, J., Kongshaug, M. (2004). pH dependent modification of lipophilicity of porphyrin-type photosensitizers: Photochem. Photobiol. 79, 242-247.

[102] Banfi, S., Caruso, E., Buccafurni, L., Battini, V., Zazzaron, S., Barbieri, P., Orlandi, V. (2006) Antibacterial activity of tetraaryl-porphyrin photosensitizers: An *in-*

vitro study on Gram negative and Gram positive bacteria: J. Photochem. Photobiol. B:Biology 85, 28-38.

[103] Mulliken, R, S. (1955) Electronic population analysis on LCAO-MO molecular wave functions. I. J. Chem. Phys 23, 1833-1840.

[104] I.G.CSizmadia. (1976) Theory and practice of MO Calculations on Organic Molecules: Progress in Theoretical Organic Chemistry, vol. 1, Elsevier, 1976.

[105] Majcherczyk, P, A., McKenna, T., Moreillon, P., Vaudaux, P. (2006) The discriminatory power of MALDI-TOF mass spectrometry to differentiate between isogenic teicoplanin-susceptible and teicoplanin-resistant strains of methicillin-resistant *Staphylococcus aureus*: FEMS Microbiol. Lett. 255, 233-239.

[106] Bröer, S., Guangyong, J, I., Bröer, A., Silver, S. (1993) Arsenic efflux governed by the arsenic resistance determinant of *Staphylococcus aureus* plasmid pI258: J. Bacteriol. 175, 11, 3480-3485.

[107] Guangyong, J, I., Silver, S. (1992) Regulation and expression of the arsenic resistance operon from staphylococcus aureus plasmid pI258: J. Bacteriol.174, 3684-3694.

[108] Ojadi, E,C,A., Linschitz, H., Gouterman, M., Walter, R,I., Lindsey, J. (1993) Sequential protonation of meso-[p-(dimethylamino)phenyl] porpyrins: Charge transfer excited states producing hyperporphyrins: J.Phys.Chem.97, 50, 13192-13197

[109] Hudson, R., Savoie, H., Boyle, R,W. (2005) Lipophilic cationic porphyrins as photodynamic sensitizers – Synthesis and structure – activity relationships: Photodiagnosis. Photodynamic Therapy: 2, 193-196.

[110] Garcia, G., Sol, V., Lamarche, F., Granet, R., Guilloton, M., Champavier, Y., Krausz, P. Synthesis and photocytotoxic activity of new chlorin–polyamine conjugates (2006) Bioorg. Med. Chem. Lett.16,12, 3188 - 3192.

Appendix 1. Statistics.

1.1 Probit Analysis

1.1.1. MRSA

1.1.1.1. Compound 88. MRSA

Parameter Estimates

	Parameter	Estimate	Std. Error	Z	Sig.	95% Confidence Interval	
						Lower Bound	Upper Bound
PROBIT[a]	Conc	-.010	.015	-.635	.526	-.040	.020
	Intercept	.904	.353	2.561	.010	.551	1.257

a. PROBIT model: PROBIT(p) = Intercept + BX

Chi-Square Tests

		Chi-Square	df[a]	Sig.
PROBIT	Pearson Goodness-of-Fit Test	4.076	19	1.000[b]

a. Statistics based on individual cases differ from statistics based on aggregated cases.

b. Since the significance level is greater than .150, no heterogeneity factor is used in the calculation of confidence limits.

Cell Counts and Residuals

	Number	Conc	Number of Subjects	Observed Responses	Expected Responses	Residual	Probability
PROBIT	1	2.000	1	1	1.088	-.033	.812
	2	3.000	1	1	1.084	.255	.809
	3	4.000	1	1	1.081	-.157	.807
	4	5.000	1	1	1.077	.175	.804
	5	10.000	1	1	1.059	.119	.790
	6	25.000	1	1	1.000	.040	.746
	7	50.000	1	1	.889	-.038	.663
	8	1.000	1	1	1.100	.118	.814
	9	2.000	1	1	1.096	-.515	.812
	10	4.000	1	1	1.089	-.469	.807
	11	5.000	1	1	1.085	.142	.804
	12	10.000	1	1	1.067	.088	.790
	13	25.000	1	1	1.007	.062	.746
	14	50.000	1	1	.895	-.037	.663
	15	2.000	1	1	1.072	-.290	.812
	16	3.000	1	1	1.068	.191	.809
	17	4.000	1	1	1.065	.155	.807
	18	5.000	1	1	1.061	.078	.804
	19	10.000	1	1	1.043	.157	.790
	20	25.000	1	1	.985	.029	.746
	21	50.000	1	1	.875	-.067	.663

Confidence Limits

	Probability	95% Confidence Limits for Conc		
		Estimate	Lower Bound	Upper Bound
PROBIT	.010	334.176	.	.
	.020	305.979	.	.
	.030	288.088	.	.
	.040	274.630	.	.
	.050	263.682	.	.
	.060	254.364	.	.
	.070	246.194	.	.
	.080	238.879	.	.
	.090	232.226	.	.
	.100	226.102	.	.
	.150	200.747	.	.
	.200	180.595	.	.
	.250	163.307	.	.
	.300	147.782	.	.
	.350	133.395	.	.
	.400	119.744	.	.
	.450	106.536	.	.
	.500	93.537	.	.
	.550	80.539	.	.
	.600	67.331	.	.
	.650	53.680	.	.
	.700	39.293	.	.
	.750	23.768	.	.
	.800	6.479	.	.
	.850	-13.672	.	.
	.900	-39.027	.	.
	.910	-45.151	.	.
	.920	-51.804	.	.
	.930	-59.120	.	.
	.940	-67.290	.	.
	.950	-76.608	.	.
	.960	-87.555	.	.
	.970	-101.013	.	.
	.980	-118.904	.	.
	.990	-147.102	.	.

Probit Transformed Responses

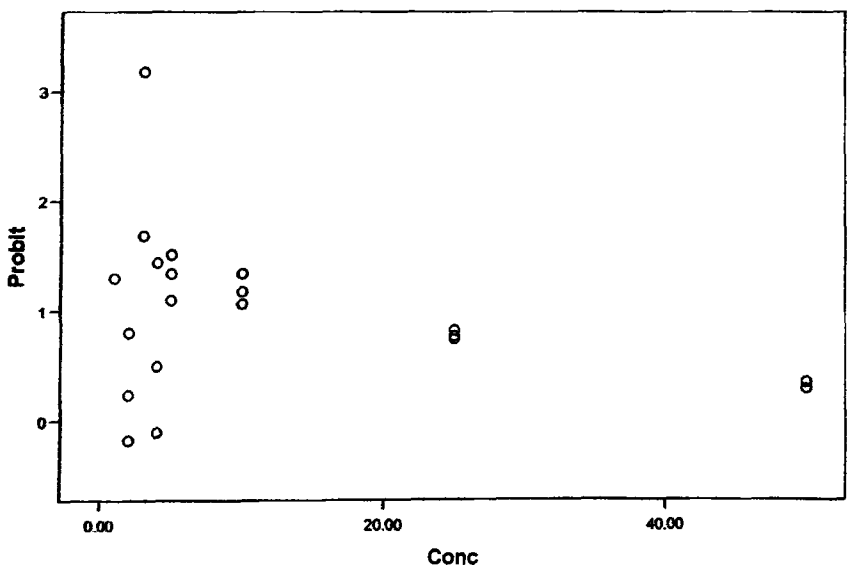

1.1.1.2. Compound 89. MRSA

Parameter Estimates

	Parameter	Estimate	Std. Error	Z	Sig.	95% Confidence Interval	
						Lower Bound	Upper Bound
PROBIT[a]	Conc	-.053	.038	-1.409	.159	-.127	.021
	Intercept	-.484	.365	-1.324	.185	-.849	-.119

a. PROBIT model: PROBIT(p) = Intercept + BX

Chi-Square Tests

		Chi-Square	df[a]	Sig.
PROBIT	Pearson Goodness-of-Fit Test	13.384	19	.818[b]

a. Statistics based on individual cases differ from statistics based on aggregated cases.

b. Since the significance level is greater than .150, no heterogeneity factor is used in the calculation of confidence limits.

Cell Counts and Residuals

	Number	Conc	Number of Subjects	Observed Responses	Expected Responses	Residual	Probability
PROBIT	1	.000	2	2	.484	1.053	.314
	2	1.000	2	1	.455	.359	.296
	3	3.000	2	0	.401	-.052	.260
	4	4.000	2	0	.374	-.313	.243
	5	5.000	2	0	.349	-.306	.227
	6	10.000	2	0	.239	-.176	.155
	7	25.000	2	0	.054	.066	.035
	8	50.000	2	0	.001	.049	.001
	9	3.000	1	0	.343	-.250	.260
	10	4.000	1	0	.321	-.229	.243
	11	5.000	1	0	.299	-.254	.227
	12	10.000	1	0	.205	-.135	.155
	13	25.000	1	0	.046	-.032	.035
	14	50.000	1	0	.001	.051	.001
	15	.000	1	1	.421	.915	.314
	16	3.000	1	0	.348	-.258	.260
	17	4.000	1	0	.326	-.245	.243
	18	5.000	1	0	.304	-.258	.227
	19	10.000	1	0	.208	-.034	.155
	20	25.000	1	0	.047	.022	.035
	21	50.000	1	0	.001	.004	.001

Confidence Limits

	Probability	95% Confidence Limits for Conc		
		Estimate	Lower Bound	Upper Bound
PROBIT	.010	34.715	.	.
	.020	29.579	.	.
	.030	26.320	.	.
	.040	23.869	.	.
	.050	21.875	.	.
	.060	20.177	.	.
	.070	18.689	.	.
	.080	17.357	.	.
	.090	16.145	.	.
	.100	15.029	.	.
	.150	10.411	.	.
	.200	6.740	.	.
	.250	3.591	.	.
	.300	.763	.	.
	.350	-1.857	.	.
	.400	-4.344	.	.
	.450	-6.750	.	.
	.500	-9.118	.	.
	.550	-11.485	.	.
	.600	-13.891	.	.
	.650	-16.378	.	.
	.700	-18.998	.	.
	.750	-21.826	.	.
	.800	-24.975	.	.
	.850	-28.646	.	.
	.900	-33.265	.	.
	.910	-34.380	.	.
	.920	-35.592	.	.
	.930	-36.924	.	.
	.940	-38.413	.	.
	.950	-40.110	.	.
	.960	-42.104	.	.
	.970	-44.556	.	.
	.980	-47.814	.	.
	.990	-52.951	.	.

Probit Transformed Responses

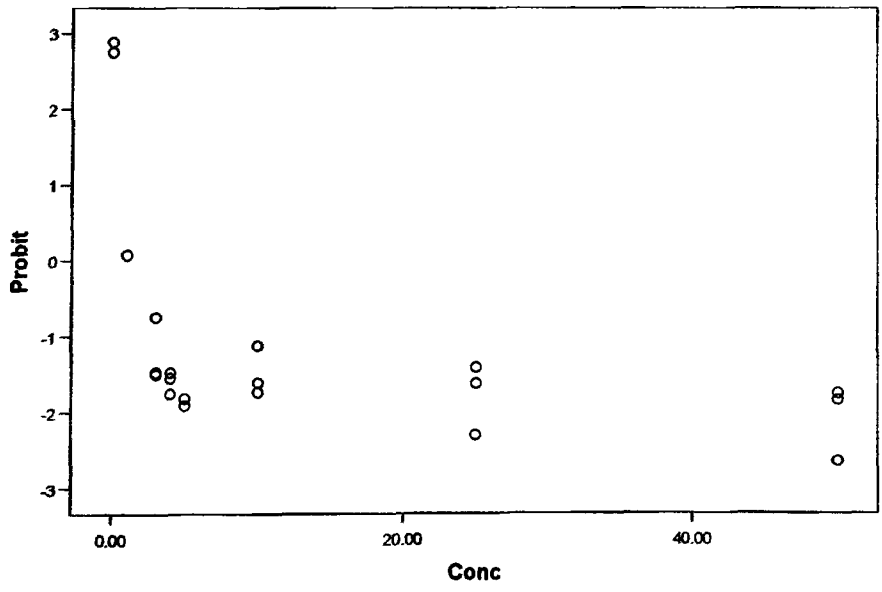

1.1.1.3. Compound 90. MRSA

Parameter Estimates

	Parameter	Estimate	Std. Error	Z	Sig.	95% Confidence Interval	
						Lower Bound	Upper Bound
PROBIT[a]	Conc	-.092	.031	-2.967	.003	-.153	-.031
	Intercept	1.297	.381	3.406	.001	.916	1.678

a. PROBIT model: PROBIT(p) = Intercept + BX

Chi-Square Tests

		Chi-Square	df[a]	Sig.
PROBIT	Pearson Goodness-of-Fit Test	26.265	22	.240[b]

a. Statistics based on individual cases differ from statistics based on aggregated cases.

b. Since the significance level is greater than .150, no heterogeneity factor is used in the calculation of confidence limits.

Cell Counts and Residuals

	Number	Conc	Number of Subjects	Observed Responses	Expected Responses	Residual	Probability
PROBIT	1	1.000	1	1	1.215	.031	.886
	2	2.000	1	1	1.188	.064	.867
	3	3.000	1	1	1.159	-.062	.846
	4	4.000	1	1	1.128	-.117	.823
	5	5.000	1	1	1.094	.047	.799
	6	10.000	1	0	.886	-.824	.646
	7	25.000	1	0	.215	-.152	.157
	8	50.000	1	0	.001	.071	.000
	9	.000	1	1	1.180	.127	.903
	10	2.000	1	1	1.133	.139	.867
	11	3.000	1	1	1.106	.151	.846
	12	4.000	1	1	1.076	.109	.823
	13	5.000	1	1	1.044	.068	.799
	14	10.000	1	0	.845	-.757	.646
	15	25.000	1	0	.205	-.143	.157
	16	50.000	1	0	.001	.069	.000
	17	1.000	1	1	1.169	.146	.886
	18	2.000	1	1	1.145	.056	.867
	19	3.000	1	1	1.117	.164	.846
	20	4.000	1	1	1.087	.207	.823
	21	5.000	1	1	1.054	.263	.799
	22	10.000	1	1	.853	-.017	.646
	23	25.000	1	0	.207	-.056	.157
	24	50.000	1	0	.001	.052	.000

Confidence Limits

		95% Confidence Limits for Conc		
	Probability	Estimate	Lower Bound	Upper Bound
PROBIT	.010	39.316	26.054	100.818
	.020	36.358	24.184	92.190
	.030	34.481	22.987	86.726
	.040	33.069	22.081	82.622
	.050	31.921	21.339	79.288
	.060	30.944	20.704	76.454
	.070	30.087	20.143	73.973
	.080	29.319	19.639	71.754
	.090	28.622	19.178	69.738
	.100	27.979	18.751	67.885
	.150	25.320	16.954	60.243
	.200	23.206	15.482	54.212
	.250	21.393	14.176	49.062
	.300	19.764	12.956	44.521
	.350	18.255	11.773	40.349
	.400	16.823	10.585	36.454
	.450	15.438	9.356	32.766
	.500	14.074	8.042	29.240
	.550	12.711	6.588	25.855
	.600	11.325	4.921	22.604
	.650	9.893	2.939	19.504
	.700	8.384	.505	16.582
	.750	6.756	-2.553	13.860
	.800	4.942	-6.450	11.321
	.850	2.829	-11.509	8.678
	.900	.169	-18.395	6.324
	.910	-.473	-20.116	5.765
	.920	-1.171	-22.006	5.178
	.930	-1.939	-24.103	4.551
	.940	-2.796	-26.466	3.873
	.950	-3.773	-29.184	3.122
	.960	-4.921	-32.403	2.265
	.970	-6.333	-36.390	1.242
	.980	-8.210	-41.731	-.077
	.990	-11.167	-50.217	-2.090

Probit Transformed Responses

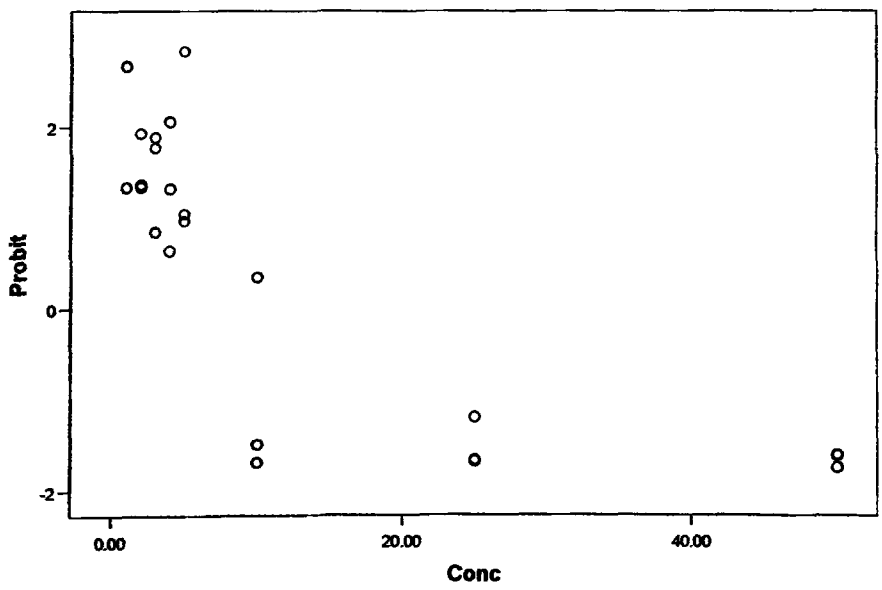

1.1.1.4. Compound 91. MRSA

Parameter Estimates

	Parameter	Estimate	Std. Error	Z	Sig.	95% Confidence Interval	
						Lower Bound	Upper Bound
PROBIT[a]	Conc	-.099	.033	-3.010	.003	-.163	-.034
	Intercept	1.754	.552	3.178	.001	1.202	2.305

a. PROBIT model: PROBIT(p) = Intercept + BX

Chi-Square Tests

		Chi-Square	df[a]	Sig.
PROBIT	Pearson Goodness-of-Fit Test	15.629	15	.407[b]

a. Statistics based on individual cases differ from statistics based on aggregated cases.

b. Since the significance level is greater than .150, no heterogeneity factor is used in the calculation of confidence limits.

Cell Counts and Residuals

	Number	Conc	Number of Subjects	Observed Responses	Expected Responses	Residual	Probability
PROBIT	1	1.000	1	1	1.369	.055	.951
	2	2.000	1	1	1.354	.079	.940
	3	3.000	1	1	1.336	.027	.927
	4	4.000	1	1	1.314	.016	.913
	5	5.000	1	1	1.290	.013	.896
	6	10.000	1	1	1.120	.034	.778
	7	25.000	1	0	.341	-.296	.237
	8	50.000	1	0	.001	.070	.001
	9	3.000	1	1	1.298	.078	.927
	10	25.000	1	0	.331	-.236	.237
	11	50.000	1	0	.001	.081	.001
	12	.000	1	1	1.364	.052	.960
	13	4.000	1	1	1.296	.120	.913
	14	5.000	1	1	1.272	.052	.896
	15	10.000	1	1	1.105	-.220	.778
	16	25.000	1	0	.336	-.289	.237
	17	50.000	1	0	.001	.054	.001

Confidence Limits

		95% Confidence Limits for Conc		
	Probability	Estimate	Lower Bound	Upper Bound
PROBIT	.010	41.284	28.429	96.748
	.020	38.525	26.614	88.987
	.030	36.775	25.447	84.078
	.040	35.459	24.560	80.396
	.050	34.388	23.831	77.407
	.060	33.476	23.205	74.869
	.070	32.677	22.651	72.649
	.080	31.962	22.150	70.665
	.090	31.311	21.692	68.864
	.100	30.712	21.266	67.210
	.150	28.232	19.461	60.405
	.200	26.260	17.964	55.059
	.250	24.569	16.621	50.531
	.300	23.050	15.354	46.526
	.350	21.643	14.113	42.882
	.400	20.308	12.859	39.499
	.450	19.016	11.559	36.315
	.500	17.744	10.173	33.286
	.550	16.473	8.658	30.387
	.600	15.181	6.961	27.599
	.650	13.845	5.010	24.913
	.700	12.438	2.716	22.322
	.750	10.919	-.048	19.814
	.800	9.228	-3.462	17.357
	.850	7.257	-7.829	14.881
	.900	4.776	-13.775	12.217
	.910	4.177	-15.270	11.632
	.920	3.527	-16.913	11.016
	.930	2.811	-18.742	10.361
	.940	2.012	-20.809	9.653
	.950	1.100	-23.193	8.873
	.960	.029	-26.026	7.988
	.970	-1.287	-29.547	6.939
	.980	-3.037	-34.281	5.597
	.990	-5.796	-41.835	3.576

Probit Transformed Responses

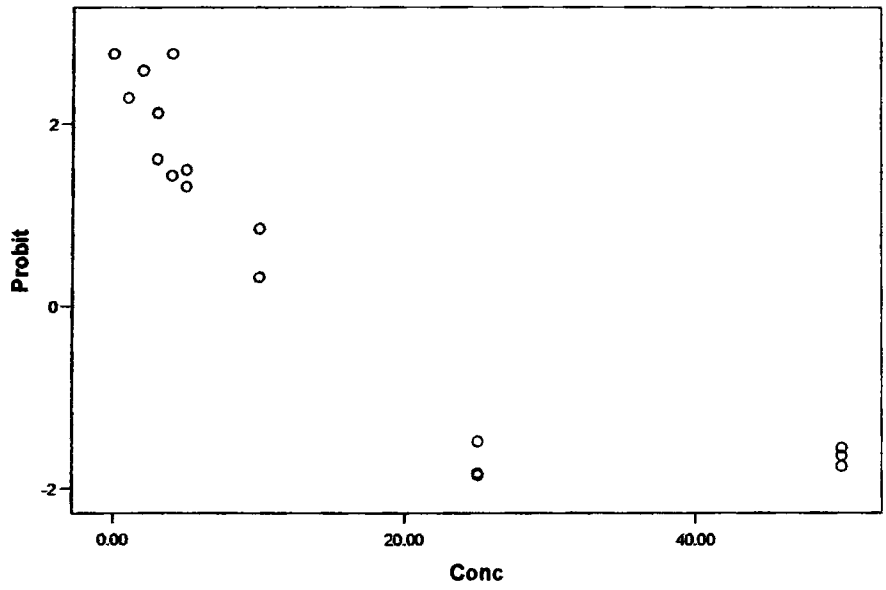

1.1.1.5. Compound 92. MRSA

Parameter Estimates

	Parameter	Estimate	Std. Error	Z	Sig.	95% Confidence Interval	
						Lower Bound	Upper Bound
PROBIT[a]	Conc	.002	.029	.064	.949	-.055	.058
	Intercept	1.412	.640	2.205	.027	.772	2.052

a. PROBIT model: PROBIT(p) = Intercept + BX

Chi-Square Tests

		Chi-Square	df[a]	Sig.
PROBIT	Pearson Goodness-of-Fit Test	.839	14	1.000[b]

a. Statistics based on individual cases differ from statistics based on aggregated cases.

b. Since the significance level is greater than .150, no heterogeneity factor is used in the calculation of confidence limits.

Cell Counts and Residuals

	Number	Conc	Number of Subjects	Observed Responses	Expected Responses	Residual	Probability
PROBIT	1	.000	1	1	.881	.076	.921
	2	.500	1	1	.882	-.036	.921
	3	2.000	1	1	.882	.016	.922
	4	3.000	1	1	.882	-.017	.922
	5	10.000	1	1	.884	-.136	.924
	6	20.000	1	1	.886	-.067	.926
	7	30.000	1	1	.889	-.027	.929
	8	40.000	1	1	.891	-.010	.931
	9	.000	1	1	.828	.071	.921
	10	20.000	1	1	.833	-.023	.926
	11	50.000	1	1	.839	.050	.934
	12	.000	1	1	.879	.075	.921
	13	1.000	1	1	.879	.065	.921
	14	2.000	1	1	.879	-.060	.922
	15	20.000	1	1	.884	-.025	.926
	16	50.000	1	1	.891	.048	.934

Confidence Limits

		95% Confidence Limits for Conc		
	Probability	Estimate	Lower Bound	Upper Bound
PROBIT	.010	-2021.915	.	.
	.020	-1874.471	.	.
	.030	-1780.923	.	.
	.040	-1710.550	.	.
	.050	-1653.307	.	.
	.060	-1604.585	.	.
	.070	-1561.864	.	.
	.080	-1523.614	.	.
	.090	-1488.826	.	.
	.100	-1456.804	.	.
	.150	-1324.224	.	.
	.200	-1218.854	.	.
	.250	-1128.456	.	.
	.300	-1047.275	.	.
	.350	-972.050	.	.
	.400	-900.668	.	.
	.450	-831.605	.	.
	.500	-763.637	.	.
	.550	-695.669	.	.
	.600	-626.606	.	.
	.650	-555.224	.	.
	.700	-479.999	.	.
	.750	-398.818	.	.
	.800	-308.420	.	.
	.850	-203.050	.	.
	.900	-70.470	.	.
	.910	-38.448	.	.
	.920	-3.660	.	.
	.930	34.590	.	.
	.940	77.311	.	.
	.950	126.033	.	.
	.960	183.276	.	.
	.970	253.649	.	.
	.980	347.197	.	.
	.990	494.640	.	.

Probit Transformed Responses

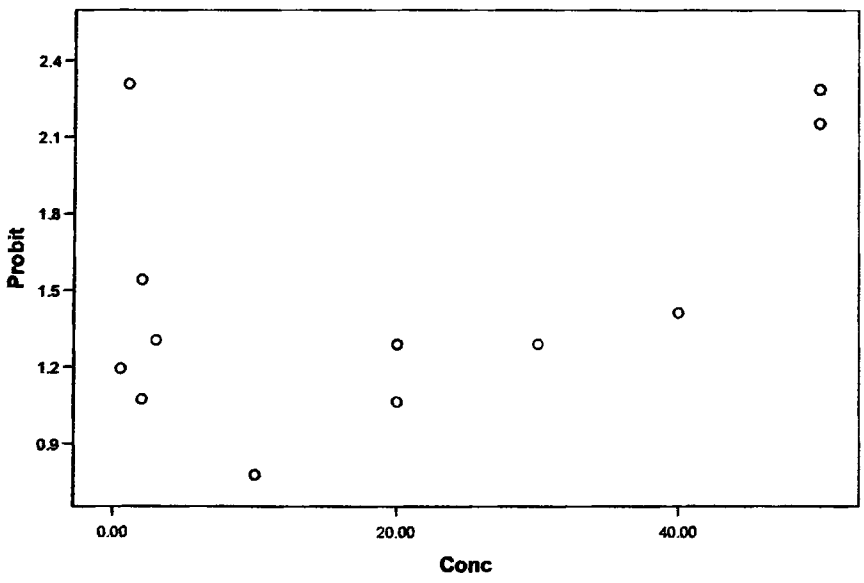

1.1.1.6. Compound 82. MRSA.

Parameter Estimates

	Parameter	Estimate	Std. Error	Z	Sig.	95% Confidence Interval	
						Lower Bound	Upper Bound
PROBIT[a]	Conc	-.015	.012	-1.185	.236	-.039	.010
	Intercept	1.073	.318	3.375	.001	.755	1.391

a. PROBIT model: PROBIT(p) = Intercept + BX

Chi-Square Tests

		Chi-Square	df[a]	Sig.
PROBIT	Pearson Goodness-of-Fit Test	4.661	28	1.000[b]

a. Statistics based on individual cases differ from statistics based on aggregated cases.

b. Since the significance level is greater than .150, no heterogeneity factor is used in the calculation of confidence limits.

Cell Counts and Residuals

	Number	Conc	Number of Subjects	Observed Responses	Expected Responses	Residual	Probability
PROBIT	1	.000	2	2	1.297	.214	.858
	2	.500	2	2	1.294	.212	.857
	3	1.000	2	2	1.292	.208	.855
	4	2.000	2	1	1.287	.204	.852
	5	3.000	2	1	1.282	.059	.848
	6	4.000	2	1	1.276	-.346	.845
	7	5.000	2	1	1.271	-.247	.841
	8	10.000	2	1	1.243	.008	.823
	9	20.000	2	1	1.182	-.236	.782
	10	30.000	2	1	1.113	-.193	.737
	11	40.000	2	1	1.038	-.065	.687
	12	50.000	2	1	.957	.116	.633
	13	.000	1	1	1.239	.205	.858
	14	3.000	1	1	1.225	.110	.848
	15	4.000	1	1	1.220	-.235	.845
	16	5.000	1	1	1.215	.127	.841
	17	10.000	1	1	1.188	.049	.823
	18	20.000	1	1	1.130	-.178	.782
	19	30.000	1	1	1.064	-.127	.737
	20	40.000	1	1	.992	.353	.687
	21	50.000	1	1	.914	.063	.633
	22	.000	1	1	1.233	.204	.858
	23	3.000	1	1	1.219	.112	.848
	24	4.000	1	1	1.214	-.264	.845
	25	5.000	1	1	1.209	-.184	.841
	26	10.000	1	1	1.183	-.111	.823
	27	20.000	1	1	1.124	-.170	.782
	28	30.000	1	1	1.059	-.080	.737
	29	40.000	1	1	.987	.052	.687
	30	50.000	1	1	.910	.129	.633

Confidence Limits

		95% Confidence Limits for Conc		
	Probability	Estimate	Lower Bound	Upper Bound
PROBIT	.010	232.019	.	.
	.020	213.413	.	.
	.030	201.608	.	.
	.040	192.728	.	.
	.050	185.504	.	.
	.060	179.356	.	.
	.070	173.965	.	.
	.080	169.138	.	.
	.090	164.748	.	.
	.100	160.707	.	.
	.150	143.977	.	.
	.200	130.680	.	.
	.250	119.273	.	.
	.300	109.029	.	.
	.350	99.536	.	.
	.400	90.528	.	.
	.450	81.813	.	.
	.500	73.236	.	.
	.550	64.659	.	.
	.600	55.944	.	.
	.650	46.936	.	.
	.700	37.443	.	.
	.750	27.199	.	.
	.800	15.792	.	.
	.850	2.495	.	.
	.900	-14.235	.	.
	.910	-18.276	.	.
	.920	-22.666	.	.
	.930	-27.493	.	.
	.940	-32.884	.	.
	.950	-39.032	.	.
	.960	-46.256	.	.
	.970	-55.136	.	.
	.980	-66.941	.	.
	.990	-85.547	.	.

Probit Transformed Responses

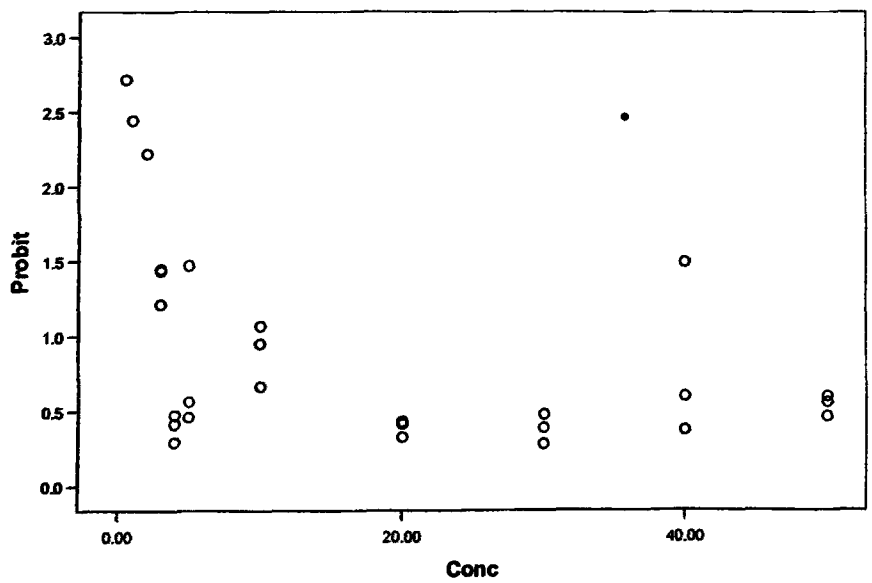

1.1.1.7. Compound 93. MRSA

Parameter Estimates

	Parameter	Estimate	Std. Error	Z	Sig.	95% Confidence Interval	
						Lower Bound	Upper Bound
PROBIT[a]	Conc	-.073	.022	-3.284	.001	-.117	-.029
	Intercept	.553	.274	2.018	.044	.279	.828

a. PROBIT model: PROBIT(p) = Intercept + BX

Chi-Square Tests

		Chi-Square	df[a]	Sig.
PROBIT	Pearson Goodness-of-Fit Test	23.495	32	.862[b]

a. Statistics based on individual cases differ from statistics based on aggregated cases.

b. Since the significance level is greater than .150, no heterogeneity factor is used in the calculation of confidence limits.

Cell Counts and Residuals

	Number	Conc	Number of Subjects	Observed Responses	Expected Responses	Residual	Probability
PROBIT	1	.000	1	1	.902	.366	.710
	2	.500	1	1	.886	.326	.697
	3	1.000	1	1	.869	.228	.684
	4	2.000	1	1	.836	-.112	.658
	5	4.000	1	1	.766	.064	.603
	6	5.000	1	0	.730	-.482	.575
	7	10.000	1	0	.546	-.493	.430
	8	20.000	1	0	.231	-.180	.182
	9	30.000	1	0	.065	-.007	.051
	10	40.000	1	0	.011	.058	.009
	11	50.000	1	0	.001	.073	.001
	12	.500	1	1	.976	.312	.697
	13	1.000	1	1	.958	.348	.684
	14	2.000	1	1	.921	-.192	.658
	15	3.000	1	1	.883	-.086	.631
	16	4.000	1	0	.844	-.689	.603
	17	5.000	1	0	.805	-.652	.575
	18	10.000	1	0	.602	-.552	.430
	19	20.000	1	0	.255	-.199	.182
	20	30.000	1	0	.071	-.006	.051
	21	40.000	1	0	.013	.059	.009
	22	50.000	1	0	.001	.073	.001
	23	.000	1	1	.966	.394	.710
	24	.500	1	1	.948	.346	.697
	25	1.000	1	1	.931	.366	.684
	26	2.000	1	1	.895	.188	.658
	27	3.000	1	1	.858	.430	.631
	28	4.000	1	1	.820	.249	.603
	29	5.000	1	1	.782	.007	.575
	30	10.000	1	0	.585	-.526	.430
	31	20.000	1	0	.248	-.196	.182
	32	30.000	1	0	.069	-.009	.051
	33	40.000	1	0	.012	.051	.009
	34	50.000	1	0	.001	.071	.001

Confidence Limits

	Probability	95% Confidence Limits for Conc		
		Estimate	Lower Bound	Upper Bound
PROBIT	.010	39.440	26.522	87.916
	.020	35.707	24.069	78.772
	.030	33.338	22.497	72.986
	.040	31.556	21.304	68.644
	.050	30.107	20.325	65.121
	.060	28.873	19.484	62.129
	.070	27.791	18.742	59.512
	.080	26.822	18.071	57.174
	.090	25.942	17.456	55.052
	.100	25.131	16.886	53.104
	.150	21.774	14.459	45.103
	.200	19.105	12.426	38.848
	.250	16.816	10.568	33.596
	.300	14.761	8.761	29.018
	.350	12.856	6.916	24.946
	.400	11.048	4.950	21.298
	.450	9.300	2.781	18.035
	.500	7.578	.333	15.137
	.550	5.857	-2.454	12.578
	.600	4.109	-5.619	10.311
	.650	2.301	-9.187	8.265
	.700	.396	-13.198	6.358
	.750	-1.659	-17.730	4.505
	.800	-3.949	-22.947	2.612
	.850	-6.617	-29.176	.554
	.900	-9.974	-37.157	-1.893
	.910	-10.785	-39.101	-2.468
	.920	-11.666	-41.219	-3.086
	.930	-12.634	-43.554	-3.760
	.940	-13.716	-46.168	-4.506
	.950	-14.950	-49.157	-5.349
	.960	-16.399	-52.677	-6.331
	.970	-18.181	-57.015	-7.528
	.980	-20.550	-62.797	-9.104
	.990	-24.284	-71.937	-11.561

Probit Transformed Responses

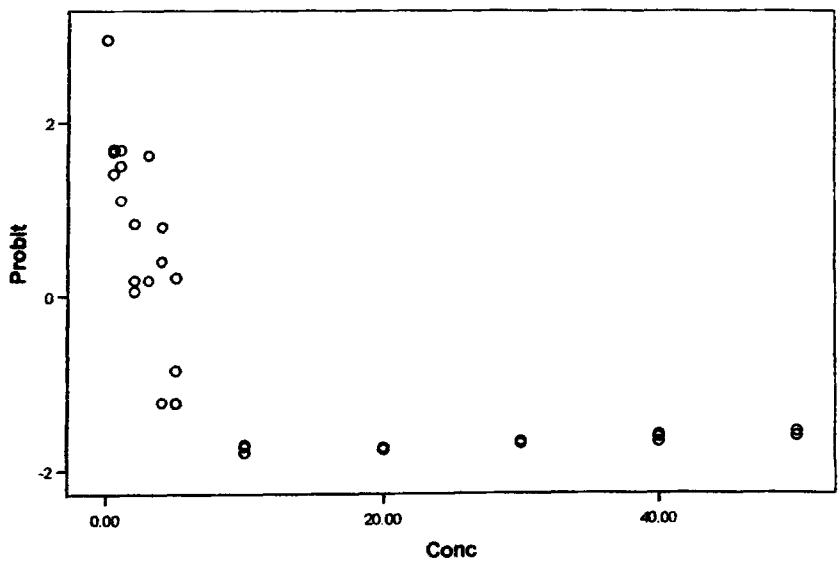

1.1.1.8. Compound 94. MRSA

Parameter Estimates

	Parameter	Estimate	Std. Error	Z	Sig.	95% Confidence Interval	
						Lower Bound	Upper Bound
PROBIT[a]	Conc	-.068	.038	-1.779	.075	-.142	.007
	Intercept	.251	.594	.424	.672	-.342	.845

a. PROBIT model: PROBIT(p) = Intercept + BX

Chi-Square Tests

		Chi-Square	df[a]	Sig.
PROBIT	Pearson Goodness-of-Fit Test	15.476	9	.079[b]

a. Statistics based on individual cases differ from statistics based on aggregated cases.

b. Since the significance level is less than .150, a heterogeneity factor is used in the calculation of confidence limits.

Cell Counts and Residuals

	Number	Conc	Number of Subjects	Observed Responses	Expected Responses	Residual	Probability
PROBIT	1	.000	2	2	.899	.601	.599
	2	10.000	2	0	.502	-.457	.335
	3	20.000	2	0	.202	-.142	.135
	4	50.000	2	0	.001	.058	.001
	5	.000	1	1	.875	.583	.599
	6	10.000	1	0	.489	-.433	.335
	7	20.000	1	0	.197	-.133	.135
	8	50.000	1	0	.001	.099	.001
	9	10.000	2	0	.529	-.193	.335
	10	20.000	2	0	.213	-.163	.135
	11	50.000	2	0	.001	.043	.001

Confidence Limits

	Probability	95% Confidence Limits for Conc		
		Estimate	Lower Bound	Upper Bound
PROBIT[a]	.010	38.027	.	.
	.020	34.005	.	.
	.030	31.454	.	.
	.040	29.535	.	.
	.050	27.974	.	.
	.060	26.645	.	.
	.070	25.480	.	.
	.080	24.437	.	.
	.090	23.488	.	.
	.100	22.614	.	.
	.150	18.999	.	.
	.200	16.125	.	.
	.250	13.659	.	.
	.300	11.445	.	.
	.350	9.394	.	.
	.400	7.447	.	.
	.450	5.564	.	.
	.500	3.710	.	.
	.550	1.856	.	.
	.600	-.027	.	.
	.650	-1.974	.	.
	.700	-4.026	.	.
	.750	-6.240	.	.
	.800	-8.705	.	.
	.850	-11.579	.	.
	.900	-15.195	.	.
	.910	-16.068	.	.
	.920	-17.017	.	.
	.930	-18.060	.	.
	.940	-19.225	.	.
	.950	-20.554	.	.
	.960	-22.115	.	.
	.970	-24.034	.	.
	.980	-26.586	.	.
	.990	-30.607	.	.

a. A heterogeneity factor is used.

Probit Transformed Responses

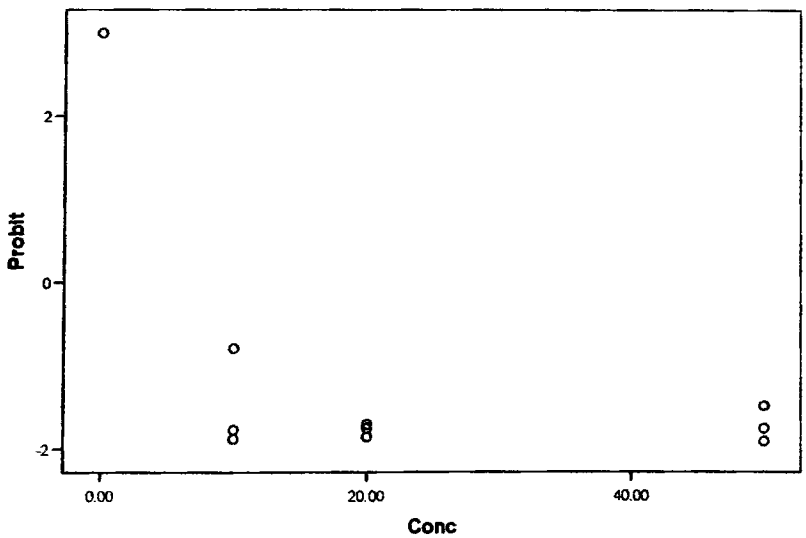

1.1.1.9. Compound 97. MRSA.

Parameter Estimates

	Parameter	Estimate	Std. Error	Z	Sig.	95% Confidence Interval	
						Lower Bound	Upper Bound
PROBIT[a]	Conc	-.010	.016	-.633	.526	-.042	.021
	Intercept	-.347	.359	-.967	.333	-.705	.012

a. PROBIT model: PROBIT(p) = Intercept + BX

Chi-Square Tests

		Chi-Square	df[a]	Sig.
PROBIT	Pearson Goodness-of-Fit Test	12.296	16	.723[b]

a. Statistics based on individual cases differ from statistics based on aggregated cases.

b. Since the significance level is greater than .150, no heterogeneity factor is used in the calculation of confidence limits.

Cell Counts and Residuals

	Number	Conc	Number of Subjects	Observed Responses	Expected Responses	Residual	Probability
PROBIT	1	1.000	1	1	.516	.706	.361
	2	2.000	1	1	.510	.698	.357
	3	3.000	1	1	.505	.829	.353
	4	4.000	1	0	.499	-.423	.349
	5	5.000	1	0	.494	-.445	.345
	6	10.000	1	0	.467	-.410	.327
	7	25.000	1	0	.391	-.306	.273
	8	50.000	1	0	.279	-.053	.195
	9	4.000	1	0	.426	-.375	.349
	10	5.000	1	0	.421	-.345	.345
	11	10.000	1	0	.398	-.334	.327
	12	25.000	1	0	.333	-.228	.273
	13	50.000	1	1	.238	.301	.195
	14	3.000	1	1	.469	.682	.353
	15	5.000	1	0	.459	-.393	.345
	16	10.000	1	0	.434	-.373	.327
	17	25.000	1	1	.363	.384	.273
	18	50.000	1	0	.259	.078	.195

Confidence Limits

	Probability	95% Confidence Limits for Conc		
		Estimate	Lower Bound	Upper Bound
PROBIT	.010	192.842	.	.
	.020	166.286	.	.
	.030	149.438	.	.
	.040	136.763	.	.
	.050	126.453	.	.
	.060	117.678	.	.
	.070	109.984	.	.
	.080	103.095	.	.
	.090	96.829	.	.
	.100	91.062	.	.
	.150	67.184	.	.
	.200	48.206	.	.
	.250	31.925	.	.
	.300	17.304	.	.
	.350	3.755	.	.
	.400	-9.101	.	.
	.450	-21.540	.	.
	.500	-33.781	.	.
	.550	-46.023	.	.
	.600	-58.461	.	.
	.650	-71.318	.	.
	.700	-84.866	.	.
	.750	-99.487	.	.
	.800	-115.768	.	.
	.850	-134.746	.	.
	.900	-158.625	.	.
	.910	-164.392	.	.
	.920	-170.657	.	.
	.930	-177.547	.	.
	.940	-185.241	.	.
	.950	-194.016	.	.
	.960	-204.326	.	.
	.970	-217.000	.	.
	.980	-233.849	.	.
	.990	-260.404	.	.

Probit Transformed Responses

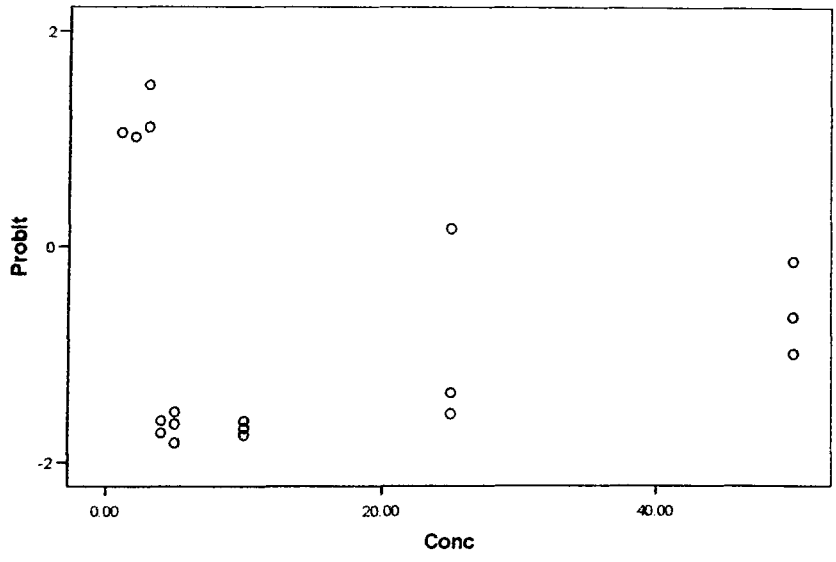

1.1.1.10. Compound 98. MRSA.

Parameter Estimates

	Parameter	Estimate	Std. Error	Z	Sig.	95% Confidence Interval	
						Lower Bound	Upper Bound
PROBIT[a]	Conc	-.017	.017	-1.009	.313	-.051	.016
	Intercept	1.631	.447	3.649	.000	1.184	2.078

a. PROBIT model: PROBIT(p) = Intercept + BX

Chi-Square Tests

		Chi-Square	df[a]	Sig.
PROBIT	Pearson Goodness-of-Fit Test	1.875	20	1.000[b]

a. Statistics based on individual cases differ from statistics based on aggregated cases.

b. Since the significance level is greater than .150, no heterogeneity factor is used in the calculation of confidence limits.

Cell Counts and Residuals

	Number	Conc	Number of Subjects	Observed Responses	Expected Responses	Residual	Probability
PROBIT	1	4.000	1	1	1.336	.032	.941
	2	5.000	1	1	1.333	.050	.939
	3	10.000	1	1	1.317	-.081	.928
	4	25.000	1	1	1.257	-.055	.885
	5	50.000	1	1	1.107	.099	.779
	6	.000	2	1	1.423	.073	.949
	7	1.000	2	1	1.420	.001	.947
	8	2.000	2	1	1.417	-.006	.945
	9	3.000	2	1	1.414	.004	.943
	10	4.000	2	1	1.411	-.025	.941
	11	5.000	2	1	1.408	.030	.939
	12	10.000	2	1	1.391	.045	.928
	13	25.000	2	1	1.328	-.334	.885
	14	50.000	2	1	1.169	-.064	.779
	15	.000	2	2	1.442	.078	.949
	16	2.000	2	1	1.436	.037	.945
	17	3.000	2	1	1.433	.028	.943
	18	4.000	2	1	1.430	.054	.941
	19	5.000	2	1	1.427	.036	.939
	20	10.000	2	1	1.410	-.229	.928
	21	25.000	2	1	1.345	.014	.885
	22	50.000	2	1	1.185	.211	.779

Confidence Limits

	Probability	95% Confidence Limits for Conc		
		Estimate	Lower Bound	Upper Bound
PROBIT	.010	229.951	.	.
	.020	214.110	.	.
	.030	204.059	.	.
	.040	196.498	.	.
	.050	190.348	.	.
	.060	185.114	.	.
	.070	180.524	.	.
	.080	176.414	.	.
	.090	172.677	.	.
	.100	169.236	.	.
	.150	154.992	.	.
	.200	143.671	.	.
	.250	133.958	.	.
	.300	125.236	.	.
	.350	117.154	.	.
	.400	109.485	.	.
	.450	102.065	.	.
	.500	94.762	.	.
	.550	87.460	.	.
	.600	80.040	.	.
	.650	72.371	.	.
	.700	64.288	.	.
	.750	55.566	.	.
	.800	45.854	.	.
	.850	34.533	.	.
	.900	20.289	.	.
	.910	16.848	.	.
	.920	13.111	.	.
	.930	9.001	.	.
	.940	4.411	.	.
	.950	-.823	.	.
	.960	-6.974	.	.
	.970	-14.534	.	.
	.980	-24.585	.	.
	.990	-40.426	.	.

Probit Transformed Responses

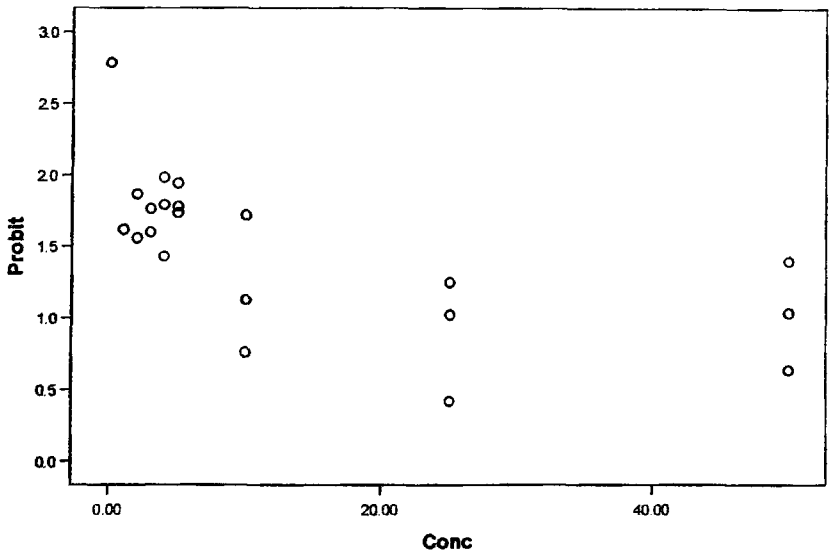

1.1.1.11. Compound 99. MRSA.

Parameter Estimates

	Parameter	Estimate	Std. Error	Z	Sig.	95% Confidence Interval	
						Lower Bound	Upper Bound
PROBIT[a]	Conc	-.052	.021	-2.471	.013	-.094	-.011
	Intercept	.507	.298	1.701	.089	.209	.805

a. PROBIT model: PROBIT(p) = Intercept + BX

Chi-Square Tests

		Chi-Square	df[a]	Sig.
PROBIT	Pearson Goodness-of-Fit Test	10.296	22	.983[b]

a. Statistics based on individual cases differ from statistics based on aggregated cases.

b. Since the significance level is greater than .150, no heterogeneity factor is used in the calculation of confidence limits.

Cell Counts and Residuals

	Number	Conc	Number of Subjects	Observed Responses	Expected Responses	Residual	Probability
PROBIT	1	1.000	2	1	1.027	.405	.675
	2	2.000	2	1	.998	.334	.656
	3	3.000	2	1	.968	-.157	.637
	4	4.000	2	0	.938	-.608	.617
	5	5.000	2	1	.908	-.373	.597
	6	10.000	2	0	.751	-.640	.494
	7	25.000	2	0	.323	-.260	.213
	8	50.000	2	0	.027	.046	.018
	9	1.000	1	1	.878	.315	.675
	10	2.000	1	1	.853	.137	.656
	11	3.000	1	1	.828	.254	.637
	12	4.000	1	1	.802	-.121	.617
	13	5.000	1	1	.776	.344	.597
	14	10.000	1	0	.642	-.431	.494
	15	25.000	1	0	.276	-.167	.213
	16	50.000	1	0	.023	.227	.018
	17	.000	1	1	.937	.410	.694
	18	2.000	1	1	.886	.351	.656
	19	3.000	1	1	.860	.213	.637
	20	4.000	1	1	.833	.002	.617
	21	5.000	1	1	.806	.020	.597
	22	10.000	1	0	.667	-.510	.494
	23	25.000	1	0	.287	-.129	.213
	24	50.000	1	0	.024	.116	.018

Confidence Limits

		95% Confidence Limits for Conc		
	Probability	Estimate	Lower Bound	Upper Bound
PROBIT	.010	54.304	32.947	231.002
	.020	49.079	29.894	205.888
	.030	45.764	27.938	189.974
	.040	43.271	26.452	178.015
	.050	41.242	25.234	168.298
	.060	39.516	24.188	160.036
	.070	38.002	23.264	152.800
	.080	36.646	22.429	146.328
	.090	35.414	21.663	140.448
	.100	34.279	20.952	135.042
	.150	29.581	17.923	112.744
	.200	25.847	15.371	95.166
	.250	22.643	13.009	80.258
	.300	19.767	10.660	67.100
	.350	17.101	8.153	55.235
	.400	14.571	5.269	44.463
	.450	12.124	1.671	34.888
	.500	9.715	-3.127	26.701
	.550	7.307	-9.605	20.196
	.600	4.859	-17.913	15.310
	.650	2.330	-27.848	11.608
	.700	-.336	-39.218	8.608
	.750	-3.213	-52.073	5.955
	.800	-6.416	-66.786	3.398
	.850	-10.150	-84.232	.715
	.900	-14.848	-106.436	-2.409
	.910	-15.983	-111.826	-3.136
	.920	-17.216	-117.690	-3.917
	.930	-18.571	-124.148	-4.766
	.940	-20.085	-131.371	-5.705
	.950	-21.812	-139.619	-6.764
	.960	-23.840	-149.322	-7.996
	.970	-26.334	-161.267	-9.495
	.980	-29.649	-177.166	-11.467
	.990	-34.874	-202.263	-14.537

Probit Transformed Responses

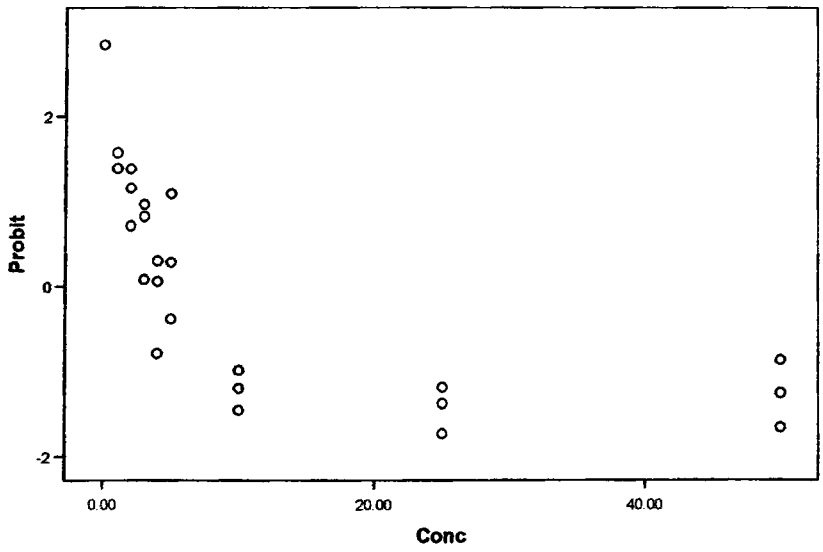

1.1.2. *S. aureus*

1.1.2.1. Compound 88. *S.aureus*

Parameter Estimates

	Parameter	Estimate	Std. Error	Z	Sig.	95% Confidence Interval	
						Lower Bound	Upper Bound
PROBIT[a]	Conc	-.016	.015	-1.071	.284	-.046	.014
	Intercept	1.374	.368	3.729	.000	1.005	1.742

a. PROBIT model: PROBIT(p) = Intercept + BX

Chi-Square Tests

		Chi-Square	df[a]	Sig.
PROBIT	Pearson Goodness-of-Fit Test	1.181	22	1.000[b]

a. Statistics based on individual cases differ from statistics based on aggregated cases.

b. Since the significance level is greater than .150, no heterogeneity factor is used in the calculation of confidence limits.

Cell Counts and Residuals

	Number	Conc	Number of Subjects	Observed Responses	Expected Responses	Residual	Probability
PROBIT	1	1.000	1	1	1.314	-.006	.913
	2	2.000	1	1	1.311	-.018	.910
	3	4.000	1	1	1.303	-.058	.905
	4	5.000	1	1	1.299	.011	.902
	5	10.000	1	1	1.277	.028	.887
	6	25.000	1	1	1.199	-.132	.833
	7	50.000	1	1	1.024	.020	.711
	8	.000	1	1	1.287	.119	.915
	9	1.000	1	1	1.283	-.119	.913
	10	2.000	1	1	1.280	.067	.910
	11	4.000	1	1	1.272	-.221	.905
	12	5.000	1	1	1.268	.021	.902
	13	10.000	1	1	1.247	.063	.887
	14	25.000	1	1	1.171	.066	.833
	15	50.000	1	1	1.000	.020	.711
	16	.000	1	1	1.327	.121	.915
	17	1.000	1	1	1.323	.016	.913
	18	2.000	1	1	1.320	-.063	.910
	19	3.000	1	1	1.316	.038	.907
	20	4.000	1	1	1.312	-.070	.905
	21	5.000	1	1	1.308	.041	.902
	22	10.000	1	1	1.286	.096	.887
	23	25.000	1	1	1.207	-.043	.833
	24	50.000	1	1	1.031	.000	.711

Confidence Limits

	Probability	95% Confidence Limits for Conc		
		Estimate	Lower Bound	Upper Bound
PROBIT	.010	226.208	.	.
	.020	209.544	.	.
	.030	198.970	.	.
	.040	191.017	.	.
	.050	184.547	.	.
	.060	179.040	.	.
	.070	174.211	.	.
	.080	169.888	.	.
	.090	165.956	.	.
	.100	162.337	.	.
	.150	147.352	.	.
	.200	135.443	.	.
	.250	125.226	.	.
	.300	116.050	.	.
	.350	107.548	.	.
	.400	99.480	.	.
	.450	91.674	.	.
	.500	83.992	.	.
	.550	76.310	.	.
	.600	68.504	.	.
	.650	60.436	.	.
	.700	51.934	.	.
	.750	42.759	.	.
	.800	32.541	.	.
	.850	20.632	.	.
	.900	5.647	.	.
	.910	2.028	.	.
	.920	-1.904	.	.
	.930	-6.227	.	.
	.940	-11.056	.	.
	.950	-16.563	.	.
	.960	-23.033	.	.
	.970	-30.986	.	.
	.980	-41.560	.	.
	.990	-58.224	.	.

Probit Transformed Responses

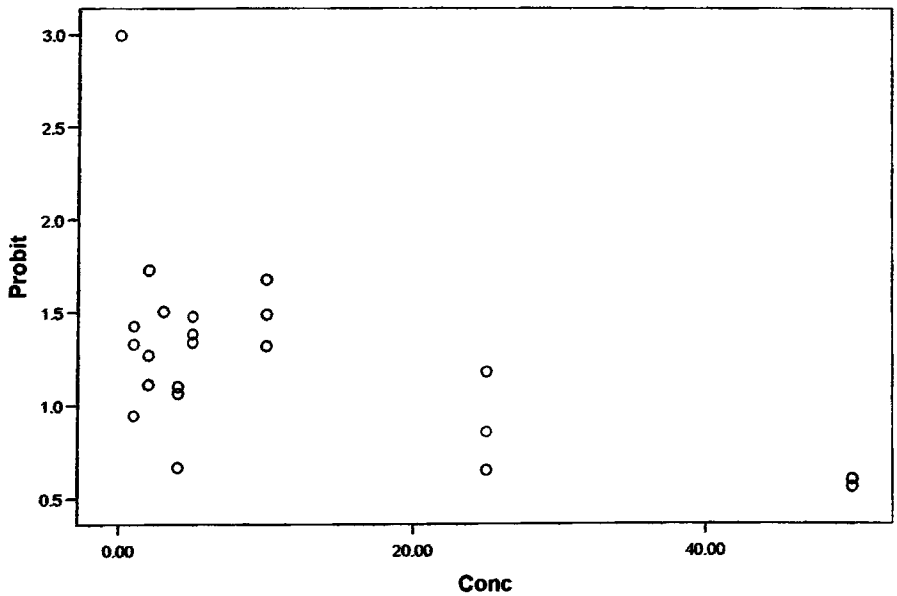

1.1.2.2. Compound 89. *S.aureus*

Parameter Estimates

	Parameter	Estimate	Std. Error	Z	Sig.	95% Confidence Interval	
						Lower Bound	Upper Bound
PROBIT[a]	Conc	-.018	.013	-1.374	.170	-.045	.008
	Intercept	.610	.282	2.162	.031	.328	.893

a. PROBIT model: PROBIT(p) = Intercept + BX

Chi-Square Tests

		Chi-Square	df[a]	Sig.
PROBIT	Pearson Goodness-of-Fit Test	7.325	22	.999[b]

a. Statistics based on individual cases differ from statistics based on aggregated cases.

b. Since the significance level is greater than .150, no heterogeneity factor is used in the calculation of confidence limits.

Cell Counts and Residuals

	Number	Conc	Number of Subjects	Observed Responses	Expected Responses	Residual	Probability
PROBIT	1	.000	2	1	1.094	.404	.729
	2	1.000	2	1	1.085	.302	.723
	3	3.000	2	1	1.066	-.056	.711
	4	4.000	2	0	1.056	-.612	.704
	5	5.000	2	1	1.047	.005	.698
	6	10.000	2	0	.998	-.526	.665
	7	25.000	2	1	.839	-.083	.560
	8	50.000	2	1	.567	.366	.378
	9	.000	1	1	1.072	.393	.729
	10	1.000	1	1	1.063	.339	.723
	11	2.000	1	1	1.054	.316	.717
	12	3.000	1	1	1.045	.034	.711
	13	4.000	1	1	1.035	-.392	.704
	14	5.000	1	1	1.026	.068	.698
	15	10.000	1	1	.978	-.194	.665
	16	25.000	1	0	.823	-.679	.560
	17	50.000	1	1	.556	.091	.378
	18	.000	1	1	1.050	.385	.729
	19	3.000	1	1	1.023	.000	.711
	20	4.000	1	1	1.014	-.256	.704
	21	5.000	1	1	1.005	-.029	.698
	22	10.000	1	1	.958	-.112	.665
	23	25.000	1	1	.806	.062	.560
	24	50.000	1	1	.544	.132	.378

Confidence Limits

	Probability	95% Confidence Limits for Conc		
		Estimate	Lower Bound	Upper Bound
PROBIT	.010	159.449	.	.
	.020	144.648	.	.
	.030	135.258	.	.
	.040	128.194	.	.
	.050	122.448	.	.
	.060	117.558	.	.
	.070	113.269	.	.
	.080	109.430	.	.
	.090	105.938	.	.
	.100	102.724	.	.
	.150	89.415	.	.
	.200	78.838	.	.
	.250	69.764	.	.
	.300	61.616	.	.
	.350	54.064	.	.
	.400	46.899	.	.
	.450	39.967	.	.
	.500	33.144	.	.
	.550	26.322	.	.
	.600	19.389	.	.
	.650	12.224	.	.
	.700	4.673	.	.
	.750	-3.476	.	.
	.800	-12.550	.	.
	.850	-23.127	.	.
	.900	-36.435	.	.
	.910	-39.649	.	.
	.920	-43.141	.	.
	.930	-46.981	.	.
	.940	-51.269	.	.
	.950	-56.160	.	.
	.960	-61.906	.	.
	.970	-68.970	.	.
	.980	-78.360	.	.
	.990	-93.160	.	.

Probit Transformed Responses

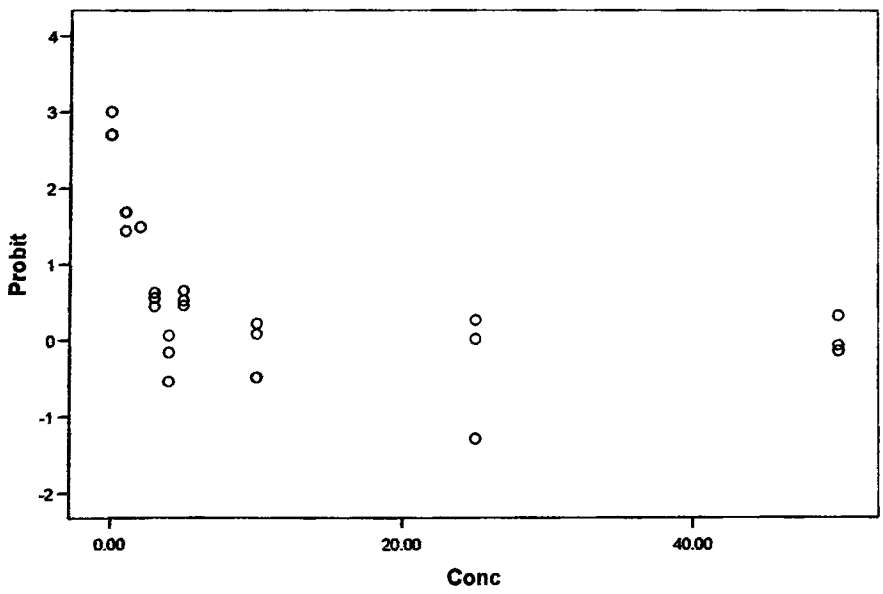

1.1.2.3. Compound 90. *S.aureus*

Parameter Estimates

	Parameter	Estimate	Std. Error	Z	Sig.	95% Confidence Interval	
						Lower Bound	Upper Bound
PROBIT[a]	Conc	-.083	.034	-2.419	.016	-.150	-.016
	Intercept	.750	.370	2.027	.043	.380	1.120

a. PROBIT model: PROBIT(p) = Intercept + BX

Chi-Square Tests

		Chi-Square	df[a]	Sig.
PROBIT	Pearson Goodness-of-Fit Test	28.000	20	.109[b]

a. Statistics based on individual cases differ from statistics based on aggregated cases.

b. Since the significance level is less than .150, a heterogeneity factor is used in the calculation of confidence limits.

Cell Counts and Residuals

	Number	Conc	Number of Subjects	Observed Responses	Expected Responses	Residual	Probability
PROBIT	1	2.000	1	1	.864	.309	.720
	2	3.000	1	1	.830	.214	.692
	3	5.000	1	1	.757	.238	.631
	4	10.000	1	0	.562	-.368	.468
	5	25.000	1	0	.111	-.059	.093
	6	50.000	1	0	.000	.054	.000
	7	.000	1	1	.951	.275	.773
	8	1.000	1	1	.920	.298	.748
	9	2.000	1	1	.886	.291	.720
	10	3.000	1	1	.851	.338	.692
	11	4.000	1	1	.814	.036	.662
	12	5.000	1	1	.776	-.123	.631
	13	10.000	1	0	.576	-.283	.468
	14	25.000	1	0	.114	-.064	.093
	15	50.000	1	0	.000	.055	.000
	16	2.000	1	1	.944	.313	.720
	17	3.000	1	1	.906	-.104	.692
	18	4.000	1	1	.867	-.362	.662
	19	5.000	1	0	.827	-.739	.631
	20	10.000	1	0	.613	-.553	.468
	21	25.000	1	0	.121	-.065	.093
	22	50.000	1	0	.000	.056	.000

Confidence Limits

	Probability	95% Confidence Limits for Conc		
		Estimate	Lower Bound	Upper Bound
PROBIT[a]	.010	37.070	.	.
	.020	33.785	.	.
	.030	31.701	.	.
	.040	30.133	.	.
	.050	28.858	.	.
	.060	27.772	.	.
	.070	26.820	.	.
	.080	25.968	.	.
	.090	25.193	.	.
	.100	24.480	.	.
	.150	21.526	.	.
	.200	19.178	.	.
	.250	17.164	.	.
	.300	15.355	.	.
	.350	13.679	.	.
	.400	12.089	.	.
	.450	10.550	.	.
	.500	9.036	.	.
	.550	7.522	.	.
	.600	5.983	.	.
	.650	4.393	.	.
	.700	2.717	.	.
	.750	.908	.	.
	.800	-1.106	.	.
	.850	-3.454	.	.
	.900	-6.407	.	.
	.910	-7.121	.	.
	.920	-7.896	.	.
	.930	-8.748	.	.
	.940	-9.700	.	.
	.950	-10.785	.	.
	.960	-12.061	.	.
	.970	-13.629	.	.
	.980	-15.713	.	.
	.990	-18.998	.	.

a. A heterogeneity factor is used.

Probit Transformed Responses

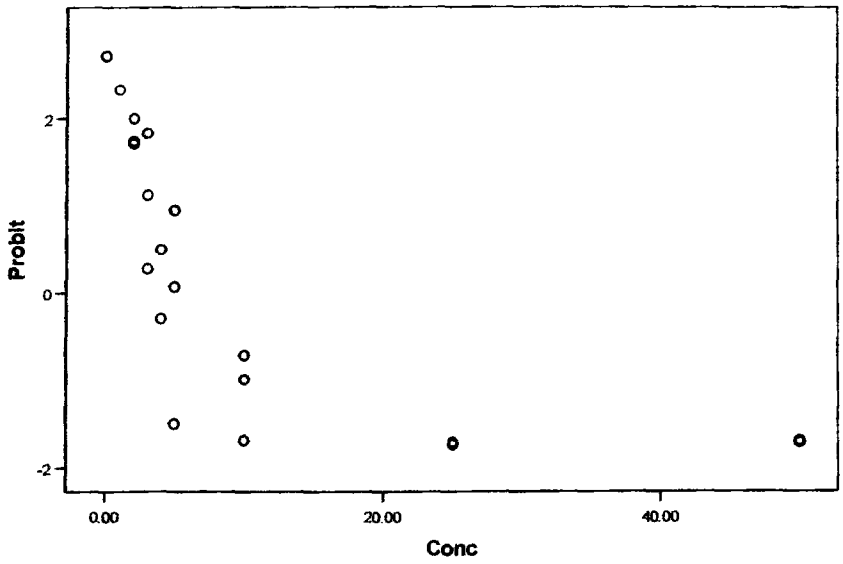

1.1.2.4. Compound 91. *S.aureus*

Parameter Estimates

	Parameter	Estimate	Std. Error	Z	Sig.	95% Confidence Interval	
						Lower Bound	Upper Bound
PROBIT[a]	Conc	-.095	.027	-3.445	.001	-.149	-.041
	Intercept	1.613	.365	4.416	.000	1.248	1.978

a. PROBIT model: PROBIT(p) = Intercept + BX

Chi-Square Tests

		Chi-Square	df[a]	Sig.
PROBIT	Pearson Goodness-of-Fit Test	14.732	24	.928[b]

a. Statistics based on individual cases differ from statistics based on aggregated cases.

b. Since the significance level is greater than .150, no heterogeneity factor is used in the calculation of confidence limits.

Cell Counts and Residuals

	Number	Conc	Number of Subjects	Observed Responses	Expected Responses	Residual	Probability
PROBIT	1	.000	2	2	1.524	.084	.947
	2	1.000	2	2	1.506	.081	.936
	3	2.000	2	1	1.486	-.020	.923
	4	3.000	2	1	1.462	.002	.908
	5	4.000	2	1	1.435	-.006	.891
	6	5.000	2	1	1.405	.047	.873
	7	10.000	2	1	1.203	.017	.747
	8	25.000	2	0	.362	-.313	.225
	9	50.000	2	0	.001	.055	.001
	10	.000	2	2	1.552	.084	.947
	11	1.000	2	2	1.534	.086	.936
	12	2.000	2	2	1.513	-.004	.923
	13	3.000	2	1	1.489	.000	.908
	14	4.000	2	1	1.462	-.059	.891
	15	5.000	2	1	1.431	.021	.873
	16	10.000	2	1	1.226	.101	.747
	17	25.000	2	0	.369	-.321	.225
	18	50.000	2	0	.001	.107	.001
	19	1.000	2	2	1.459	.068	.936
	20	2.000	2	1	1.439	.054	.923
	21	3.000	2	1	1.417	-.042	.908
	22	4.000	2	1	1.391	-.017	.891
	23	5.000	2	1	1.362	-.064	.873
	24	10.000	2	1	1.166	-.028	.747
	25	25.000	2	0	.351	-.304	.225
	26	50.000	2	0	.001	.069	.001

Confidence Limits

	Probability	95% Confidence Limits for Conc		
		Estimate	Lower Bound	Upper Bound
PROBIT	.010	41.590	28.866	85.665
	.020	38.712	26.953	79.069
	.030	36.886	25.731	74.891
	.040	35.512	24.808	71.753
	.050	34.395	24.053	69.205
	.060	33.444	23.407	67.038
	.070	32.610	22.839	65.141
	.080	31.864	22.328	63.445
	.090	31.185	21.861	61.903
	.100	30.560	21.430	60.486
	.150	27.972	19.625	54.640
	.200	25.915	18.161	50.023
	.250	24.151	16.877	46.090
	.300	22.566	15.696	42.586
	.350	21.098	14.571	39.369
	.400	19.705	13.468	36.353
	.450	18.357	12.360	33.475
	.500	17.030	11.218	30.694
	.550	15.704	10.013	27.976
	.600	14.356	8.705	25.298
	.650	12.962	7.241	22.643
	.700	11.494	5.544	19.999
	.750	9.910	3.498	17.359
	.800	8.145	.926	14.714
	.850	6.088	-2.466	12.024
	.900	3.501	-7.246	9.154
	.910	2.876	-8.469	8.528
	.920	2.197	-9.821	7.873
	.930	1.450	-11.333	7.177
	.940	.616	-13.050	6.428
	.950	-.335	-15.038	5.605
	.960	-1.452	-17.409	4.672
	.970	-2.826	-20.366	3.567
	.980	-4.651	-24.352	2.154
	.990	-7.529	-30.728	.021

Probit Transformed Responses

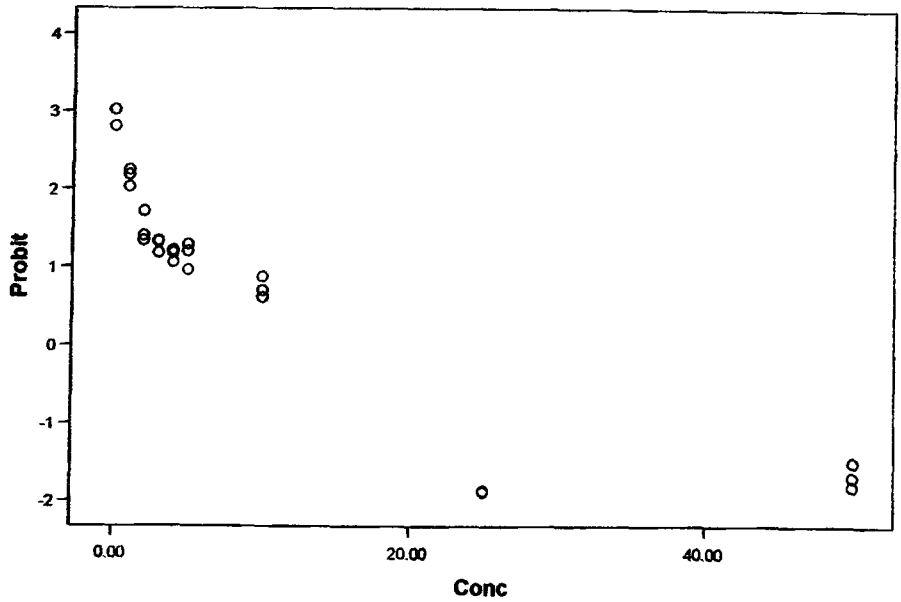

1.1.2.5. Compound 92. *S.aureus*

Parameter Estimates

	Parameter	Estimate	Std. Error	Z	Sig.	95% Confidence Interval	
						Lower Bound	Upper Bound
PROBIT[a]	Conc	-.008	.027	-.288	.773	-.061	.045
	Intercept	1.778	.652	2.726	.006	1.126	2.431

a. PROBIT model: PROBIT(p) = Intercept + BX

Chi-Square Tests

		Chi-Square	df[a]	Sig.
PROBIT	Pearson Goodness-of-Fit Test	.825	18	1.000[b]

a. Statistics based on individual cases differ from statistics based on aggregated cases.

b. Since the significance level is greater than .150, no heterogeneity factor is used in the calculation of confidence limits.

Cell Counts and Residuals

	Number	Conc	Number of Subjects	Observed Responses	Expected Responses	Residual	Probability
PROBIT	1	.000	1	1	.885	.030	.962
	2	5.000	1	1	.882	.016	.959
	3	40.000	1	1	.854	.000	.929
	4	.000	1	1	.991	.038	.962
	5	.500	1	1	.991	.013	.962
	6	3.000	1	1	.989	.015	.960
	7	4.000	1	1	.988	-.007	.960
	8	5.000	1	1	.988	.017	.959
	9	20.000	1	1	.976	.030	.948
	10	40.000	1	1	.957	-.055	.929
	11	50.000	1	1	.945	.070	.917
	12	.000	1	1	.991	.036	.962
	13	.500	1	1	.991	.005	.962
	14	1.000	1	1	.991	-.013	.962
	15	2.000	1	1	.990	.008	.961
	16	3.000	1	1	.989	-.127	.960
	17	5.000	1	1	.988	-.026	.959
	18	20.000	1	1	.976	-.051	.948
	19	30.000	1	1	.967	.054	.939
	20	40.000	1	1	.957	-.053	.929

Confidence Limits

	Probability	95% Confidence Limits for Conc		
		Estimate	Lower Bound	Upper Bound
PROBIT	.010	525.270	.	.
	.020	490.388	.	.
	.030	468.256	.	.
	.040	451.607	.	.
	.050	438.064	.	.
	.060	426.537	.	.
	.070	416.430	.	.
	.080	407.380	.	.
	.090	399.150	.	.
	.100	391.574	.	.
	.150	360.208	.	.
	.200	335.279	.	.
	.250	313.892	.	.
	.300	294.686	.	.
	.350	276.889	.	.
	.400	260.001	.	.
	.450	243.662	.	.
	.500	227.582	.	.
	.550	211.502	.	.
	.600	195.163	.	.
	.650	178.275	.	.
	.700	160.478	.	.
	.750	141.272	.	.
	.800	119.885	.	.
	.850	94.956	.	.
	.900	63.590	.	.
	.910	56.014	.	.
	.920	47.784	.	.
	.930	38.734	.	.
	.940	28.627	.	.
	.950	17.100	.	.
	.960	3.557	.	.
	.970	-13.092	.	.
	.980	-35.224	.	.
	.990	-70.106	.	.

Probit Transformed Responses

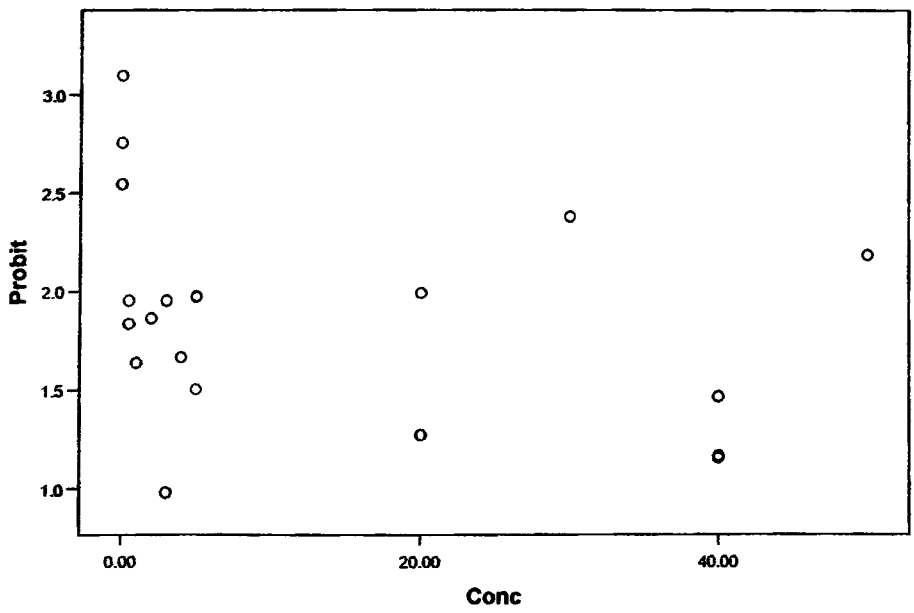

1.1.2.6. Compound 82. *S.aureus*

Parameter Estimates

	Parameter	Estimate	Std. Error	Z	Sig.	95% Confidence Interval	
						Lower Bound	Upper Bound
PROBIT[a]	Conc	-.014	.012	-1.153	.249	-.038	.010
	Intercept	1.090	.317	3.443	.001	.773	1.406

a. PROBIT model: PROBIT(p) = Intercept + BX

Chi-Square Tests

		Chi-Square	df[a]	Sig.
PROBIT	Pearson Goodness-of-Fit Test	5.161	28	1.000[b]

a. Statistics based on individual cases differ from statistics based on aggregated cases.

b. Since the significance level is greater than .150, no heterogeneity factor is used in the calculation of confidence limits.

Cell Counts and Residuals

	Number	Conc	Number of Subjects	Observed Responses	Expected Responses	Residual	Probability
PROBIT	1	.000	1	1	1.224	.193	.862
	2	.500	1	1	1.222	.155	.861
	3	2.000	1	1	1.215	.130	.856
	4	3.000	1	1	1.211	.177	.853
	5	4.000	1	1	1.206	-.165	.849
	6	5.000	1	1	1.201	-.210	.846
	7	10.000	1	1	1.177	.128	.829
	8	20.000	1	1	1.122	-.114	.790
	9	30.000	1	1	1.061	-.057	.747
	10	40.000	1	1	.994	-.036	.700
	11	50.000	1	1	.922	.281	.649
	12	.000	2	2	1.319	.211	.862
	13	.500	2	1	1.317	.037	.861
	14	4.000	2	1	1.299	-.331	.849
	15	5.000	2	1	1.294	-.473	.846
	16	10.000	2	1	1.268	.097	.829
	17	20.000	2	1	1.209	.125	.790
	18	30.000	2	1	1.143	.245	.747
	19	40.000	2	1	1.071	-.097	.700
	20	50.000	2	1	.993	.331	.649
	21	.500	2	1	1.299	.066	.861
	22	2.000	2	1	1.292	.065	.856
	23	3.000	2	1	1.287	-.012	.853
	24	4.000	2	1	1.282	-.230	.849
	25	5.000	2	1	1.277	.096	.846
	26	10.000	2	1	1.251	.073	.829
	27	20.000	2	1	1.193	.058	.790
	28	30.000	2	1	1.128	-.152	.747
	29	40.000	2	1	1.057	-.431	.700
	30	50.000	2	1	.980	-.161	.649

Confidence Limits

		95% Confidence Limits for Conc		
	Probability	Estimate	Lower Bound	Upper Bound
PROBIT	.010	241.757	.	.
	.020	222.466	.	.
	.030	210.226	.	.
	.040	201.018	.	.
	.050	193.529	.	.
	.060	187.154	.	.
	.070	181.564	.	.
	.080	176.560	.	.
	.090	172.008	.	.
	.100	167.818	.	.
	.150	150.472	.	.
	.200	136.685	.	.
	.250	124.857	.	.
	.300	114.236	.	.
	.350	104.393	.	.
	.400	95.054	.	.
	.450	86.017	.	.
	.500	77.125	.	.
	.550	68.232	.	.
	.600	59.196	.	.
	.650	49.856	.	.
	.700	40.013	.	.
	.750	29.392	.	.
	.800	17.564	.	.
	.850	3.778	.	.
	.900	-13.569	.	.
	.910	-17.759	.	.
	.920	-22.310	.	.
	.930	-27.315	.	.
	.940	-32.905	.	.
	.950	-39.280	.	.
	.960	-46.769	.	.
	.970	-55.977	.	.
	.980	-68.217	.	.
	.990	-87.508	.	.

Probit Transformed Responses

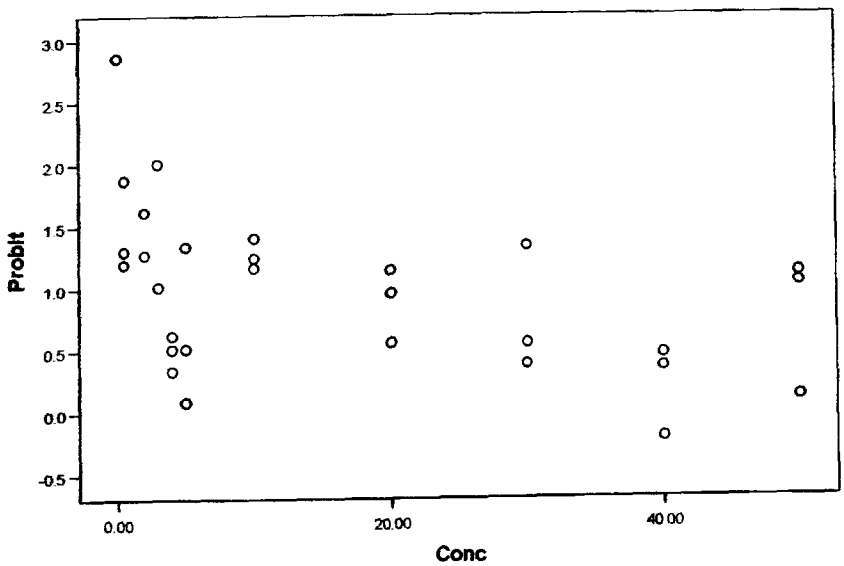

1.1.2.7. Compound 93. *S.aureus*

Parameter Estimates

	Parameter	Estimate	Std. Error	Z	Sig.	95% Confidence Interval	
						Lower Bound	Upper Bound
PROBIT[a]	Conc	-.077	.024	-3.168	.002	-.124	-.029
	Intercept	.463	.272	1.702	.089	.191	.736

a. PROBIT model: PROBIT(p) = Intercept + BX

Chi-Square Tests

		Chi-Square	df[a]	Sig.
PROBIT	Pearson Goodness-of-Fit Test	27.908	31	.626[b]

a. Statistics based on individual cases differ from statistics based on aggregated cases.

b. Since the significance level is greater than .150, no heterogeneity factor is used in the calculation of confidence limits.

Cell Counts and Residuals

	Number	Conc	Number of Subjects	Observed Responses	Expected Responses	Residual	Probability
PROBIT	1	.000	1	1	1.011	.477	.678
	2	.500	1	1	.990	.474	.665
	3	1.000	1	1	.969	.327	.651
	4	2.000	1	1	.926	-.195	.622
	5	3.000	1	1	.883	.152	.592
	6	4.000	1	1	.838	.117	.562
	7	5.000	1	1	.793	-.165	.532
	8	10.000	1	0	.568	-.519	.381
	9	20.000	1	0	.212	-.162	.143
	10	30.000	1	0	.050	.003	.033
	11	40.000	1	0	.007	.050	.005
	12	50.000	1	0	.001	.060	.000
	13	.000	1	1	.984	.466	.678
	14	1.000	1	1	.943	.423	.651
	15	2.000	1	1	.902	-.019	.622
	16	3.000	1	1	.859	.018	.592
	17	4.000	1	1	.815	-.172	.562
	18	5.000	1	0	.771	-.572	.532
	19	10.000	1	0	.552	-.503	.381
	20	20.000	1	0	.207	-.156	.143
	21	30.000	1	0	.048	.006	.033
	22	40.000	1	0	.007	.051	.005
	23	50.000	1	0	.001	.056	.000
	24	1.000	1	1	.930	.467	.651
	25	2.000	1	1	.889	.186	.622
	26	3.000	1	1	.847	.118	.592
	27	4.000	1	1	.804	-.272	.562
	28	5.000	1	0	.761	-.507	.532
	29	10.000	1	0	.545	-.495	.381
	30	20.000	1	0	.204	-.153	.143
	31	30.000	1	0	.048	.003	.033
	32	40.000	1	0	.007	.051	.005
	33	50.000	1	0	.001	.056	.000

Confidence Limits

	Probability	95% Confidence Limits for Conc		
		Estimate	Lower Bound	Upper Bound
PROBIT	.010	36.408	24.241	85.362
	.020	32.850	21.933	76.140
	.030	30.593	20.453	70.306
	.040	28.895	19.329	65.927
	.050	27.514	18.406	62.374
	.060	26.338	17.613	59.357
	.070	25.308	16.912	56.718
	.080	24.385	16.278	54.360
	.090	23.545	15.696	52.222
	.100	22.772	15.155	50.258
	.150	19.573	12.849	42.198
	.200	17.031	10.900	35.907
	.250	14.850	9.095	30.643
	.300	12.891	7.311	26.080
	.350	11.076	5.447	22.061
	.400	9.353	3.411	18.516
	.450	7.687	1.112	15.414
	.500	6.047	-1.520	12.731
	.550	4.407	-4.523	10.420
	.600	2.740	-7.906	8.402
	.650	1.018	-11.674	6.589
	.700	-.797	-15.859	4.891
	.750	-2.756	-20.543	3.227
	.800	-4.937	-25.895	1.510
	.850	-7.480	-32.250	-.374
	.900	-10.679	-40.360	-2.631
	.910	-11.451	-42.332	-3.163
	.920	-12.291	-44.479	-3.736
	.930	-13.214	-46.845	-4.362
	.940	-14.245	-49.492	-5.055
	.950	-15.420	-52.517	-5.840
	.960	-16.801	-56.078	-6.755
	.970	-18.499	-60.464	-7.871
	.980	-20.757	-66.308	-9.343
	.990	-24.314	-75.539	-11.641

Probit Transformed Responses

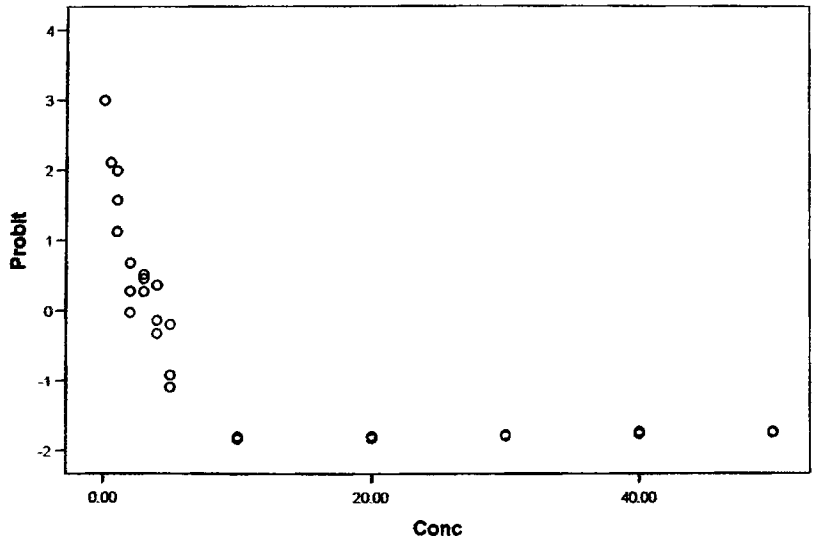

1.1.2.8. Compound 94. *S.aureus*

Parameter Estimates

	Parameter	Estimate	Std. Error	Z	Sig.	95% Confidence Interval	
						Lower Bound	Upper Bound
PROBIT[a]	Conc2	-.069	.037	-1.899	.058	-.141	.002
	Intercept	.290	.563	.515	.606	-.273	.853

a. PROBIT model: PROBIT(p) = Intercept + BX

Chi-Square Tests

		Chi-Square	df[a]	Sig.
PROBIT	Pearson Goodness-of-Fit Test	16.878	9	.051[b]

a. Statistics based on individual cases differ from statistics based on aggregated cases.

b. Since the significance level is less than .150, a heterogeneity factor is used in the calculation of confidence limits.

Cell Counts and Residuals

	Number	Conc2	Number of Subjects	Observed Responses	Expected Responses	Residual	Probability
PROBIT	1	.000	2	2	1.019	.640	.614
	2	10.000	2	0	.570	-.171	.343
	3	20.000	2	0	.226	-.159	.136
	4	50.000	2	0	.001	.084	.001
	5	.000	2	2	1.056	.659	.614
	6	10.000	2	0	.591	-.531	.343
	7	20.000	2	0	.235	-.164	.136
	8	50.000	2	0	.001	.042	.001
	9	10.000	2	0	.577	-.528	.343
	10	20.000	2	0	.229	-.118	.136
	11	50.000	2	0	.001	.086	.001

Confidence Limits

	Probability	95% Confidence Limits for Conc2		
		Estimate	Lower Bound	Upper Bound
PROBIT[a]	.010	37.740	.	.
	.020	33.807	.	.
	.030	31.313	.	.
	.040	29.436	.	.
	.050	27.909	.	.
	.060	26.610	.	.
	.070	25.470	.	.
	.080	24.450	.	.
	.090	23.523	.	.
	.100	22.669	.	.
	.150	19.133	.	.
	.200	16.323	.	.
	.250	13.912	.	.
	.300	11.747	.	.
	.350	9.741	.	.
	.400	7.837	.	.
	.450	5.995	.	.
	.500	4.182	.	.
	.550	2.370	.	.
	.600	.528	.	.
	.650	-1.376	.	.
	.700	-3.382	.	.
	.750	-5.547	.	.
	.800	-7.958	.	.
	.850	-10.768	.	.
	.900	-14.304	.	.
	.910	-15.158	.	.
	.920	-16.086	.	.
	.930	-17.106	.	.
	.940	-18.245	.	.
	.950	-19.544	.	.
	.960	-21.071	.	.
	.970	-22.948	.	.
	.980	-25.443	.	.
	.990	-29.375	.	.

a. A heterogeneity factor is used.

Probit Transformed Responses

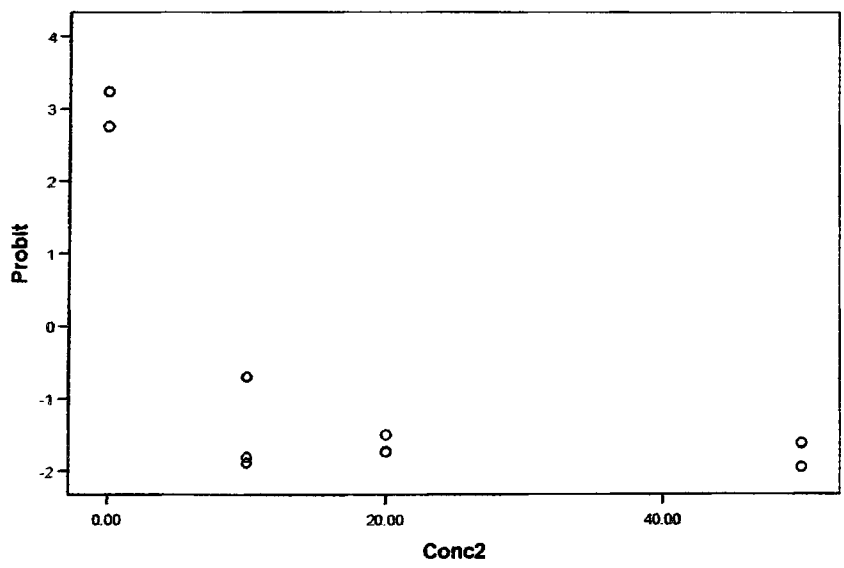

1.1.3 *E. coli.*
1.1.3.1. Compound 93 *E. Coli*

Parameter Estimates

	Parameter	Estimate	Std. Error	Z	Sig.	95% Confidence Interval	
						Lower Bound	Upper Bound
PROBIT(a)	Conc	-.043	.014	-3.021	.003	-.072	-.015
	Intercept	.288	.267	1.078	.281	.021	.556

a PROBIT model: PROBIT(p) = Intercept + BX

Chi-Square Tests

		Chi-Square	df(a)	Sig.
PROBIT	Pearson Goodness-of-Fit Test	16.388	37	.999(b)

a Statistics based on individual cases differ from statistics based on aggregated cases.
b Since the significance level is greater than .150, no heterogeneity factor is used in the calculation of confidence limits.

Cell Counts and Residuals

	Number	Conc	Number of Subjects	Observed Responses	Expected Responses	Residual	Probability
PROBIT	1	.000	1	1	.748	.472	.613
	2	.500	1	0	.738	-.528	.605
	3	3.000	1	1	.687	.515	.563
	4	4.000	1	1	.666	.067	.546
	5	5.000	1	0	.645	-.253	.528
	6	10.000	1	0	.539	-.479	.442
	7	20.000	1	0	.342	-.278	.281
	8	30.000	1	0	.189	-.123	.155
	9	40.000	1	0	.090	.126	.074
	10	50.000	1	0	.036	.047	.030
	11	.500	1	0	.696	-.300	.605
	12	3.000	1	1	.647	.474	.563
	13	4.000	1	1	.627	.267	.546
	14	5.000	1	0	.608	-.498	.528
	15	10.000	1	0	.508	-.350	.442
	16	20.000	1	0	.323	-.182	.281
	17	30.000	1	0	.178	-.078	.155
	18	40.000	1	0	.085	.248	.074
	19	50.000	1	0	.034	.085	.030
	20	.000	1	1	.705	.440	.613
	21	4.000	1	1	.627	.062	.546
	22	5.000	1	1	.608	.009	.528
	23	10.000	1	0	.508	-.446	.442
	24	20.000	1	0	.323	-.262	.281
	25	30.000	1	0	.178	-.079	.155
	26	40.000	1	0	.085	.280	.074
	27	50.000	1	0	.034	.059	.030
	28	.000	1	1	.773	.486	.613
	29	.500	1	1	.762	.471	.605

30	1.000	1	1	.752	.470	.597
31	2.000	1	1	.731	.468	.580
32	3.000	1	1	.709	.154	.563
33	4.000	1	0	.687	-.260	.546
34	5.000	1	0	.666	-.471	.528
35	10.000	1	0	.557	-.506	.442
36	20.000	1	0	.354	-.301	.281
37	30.000	1	0	.195	-.131	.155
38	40.000	1	0	.093	.025	.074
39	50.000	1	0	.037	.073	.030

Confidence Limits

		95% Confidence Limits for Conc		
	Probability	Estimate	Lower Bound	Upper Bound
PROBIT	.010	60.169	39.901	150.359
	.020	53.896	35.902	132.696
	.030	49.916	33.333	121.521
	.040	46.921	31.379	113.137
	.050	44.486	29.771	106.334
	.060	42.413	28.388	100.559
	.070	40.596	27.162	95.509
	.080	38.968	26.051	91.001
	.090	37.488	25.028	86.913
	.100	36.126	24.075	83.161
	.150	30.485	19.963	67.796
	.200	26.002	16.394	55.884
	.250	22.156	12.952	46.045
	.300	18.702	9.351	37.719
	.350	15.502	5.335	30.683
	.400	12.465	.686	24.845
	.450	9.527	-4.705	20.090
	.500	6.635	-10.809	16.209
	.550	3.743	-17.534	12.948
	.600	.805	-24.812	10.079
	.650	-2.232	-32.650	7.431
	.700	-5.433	-41.139	4.868
	.750	-8.886	-50.474	2.276
	.800	-12.732	-61.008	-.470
	.850	-17.215	-73.411	-3.549
	.900	-22.856	-89.136	-7.301
	.910	-24.218	-92.949	-8.193
	.920	-25.699	-97.096	-9.156
	.930	-27.326	-101.661	-10.211
	.940	-29.143	-106.766	-11.382
	.950	-31.216	-112.595	-12.712
	.960	-33.652	-119.451	-14.266
	.970	-36.646	-127.889	-16.166
	.980	-40.626	-139.121	-18.677
	.990	-46.899	-156.850	-22.610

Probit Transformed Responses

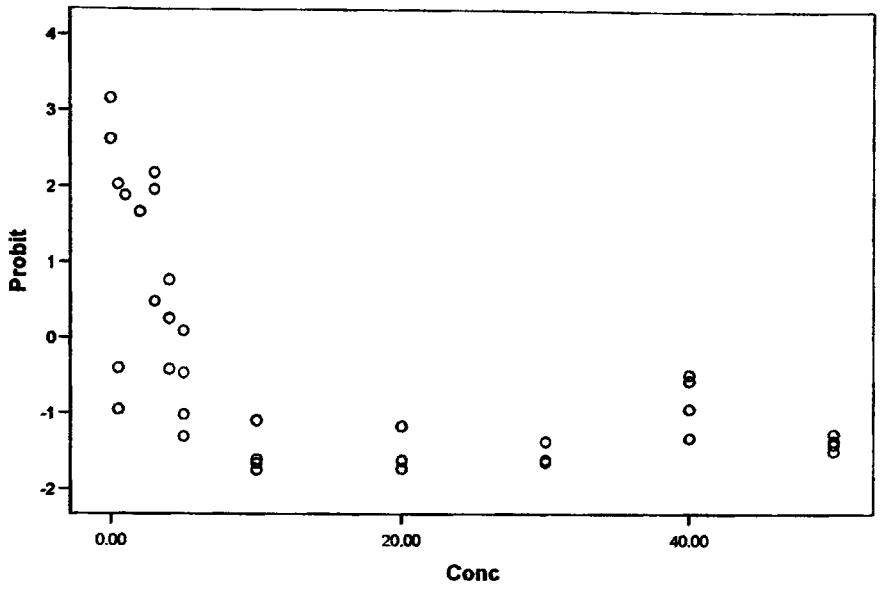

1.1.3.2. Compound 90. *E. coli*

Parameter Estimates

	Parameter	Estimate	Std. Error	Z	Sig.	95% Confidence Interval	
						Lower Bound	Upper Bound
PROBIT(a)	Conc	-.084	.021	-3.953	.000	-.125	-.042
	Intercept	1.102	.352	3.133	.002	.750	1.454

a PROBIT model: PROBIT(p) = Intercept + BX

Chi-Square Tests

		Chi-Square	df(a)	Sig.
PROBIT	Pearson Goodness-of-Fit Test	21.424	32	.922(b)

a Statistics based on individual cases differ from statistics based on aggregated cases.
b Since the significance level is greater than .150, no heterogeneity factor is used in the calculation of confidence limits.

Cell Counts and Residuals

	Number	Conc	Number of Subjects	Observed Responses	Expected Responses	Residual	Probability
PROBIT	1	.000	1	1	1.098	.172	.865
	2	2.000	1	1	1.048	.014	.825
	3	3.000	1	1	1.019	.240	.803
	4	10.000	1	0	.768	-.472	.604
	5	20.000	1	0	.360	-.308	.284
	6	30.000	1	0	.101	-.040	.079
	7	40.000	1	0	.016	.050	.012
	8	50.000	1	0	.001	.073	.001
	9	2.000	1	1	1.106	.161	.825
	10	3.000	1	1	1.075	.241	.803
	11	4.000	1	1	1.043	.253	.779
	12	5.000	1	1	1.009	.109	.753
	13	10.000	1	1	.810	.001	.604
	14	20.000	1	0	.380	-.329	.284
	15	30.000	1	0	.106	-.047	.079
	16	40.000	1	0	.017	.049	.012
	17	50.000	1	0	.001	.068	.001
	18	2.000	1	1	1.073	.112	.825
	19	3.000	1	1	1.043	.245	.803
	20	4.000	1	1	1.012	.288	.779
	21	5.000	1	1	.979	-.170	.753
	22	10.000	1	0	.786	-.452	.604
	23	20.000	1	0	.369	-.314	.284
	24	30.000	1	0	.103	-.042	.079
	25	40.000	1	0	.016	.044	.012
	26	50.000	1	0	.001	.070	.001
	27	.000	1	1	1.090	.165	.865
	28	2.000	1	1	1.040	-.009	.825
	29	5.000	1	1	.949	.067	.753
	30	10.000	1	0	.762	-.538	.604
	31	20.000	1	0	.357	-.302	.284
	32	30.000	1	0	.100	-.036	.079
	33	40.000	1	0	.016	.046	.012
	34	50.000	1	0	.001	.068	.001

Confidence Limits

	Probability	95% Confidence Limits for Conc		
		Estimate	Lower Bound	Upper Bound
PROBIT	.010	40.949	30.164	70.735
	.020	37.693	27.855	64.409
	.030	35.627	26.374	60.412
	.040	34.073	25.248	57.416
	.050	32.809	24.325	54.987
	.060	31.733	23.532	52.927
	.070	30.790	22.831	51.125
	.080	29.945	22.199	49.518
	.090	29.177	21.619	48.061
	.100	28.470	21.080	46.723
	.150	25.542	18.798	41.241
	.200	23.216	16.902	36.966
	.250	21.219	15.195	33.379
	.300	19.427	13.574	30.245
	.350	17.766	11.978	27.435
	.400	16.189	10.358	24.875
	.450	14.664	8.672	22.517
	.500	13.163	6.881	20.327
	.550	11.663	4.949	18.278
	.600	10.137	2.837	16.345
	.650	8.561	.503	14.499
	.700	6.900	-2.107	12.704
	.750	5.107	-5.069	10.911
	.800	3.111	-8.509	9.057
	.850	.784	-12.660	7.037
	.900	-2.143	-18.035	4.647
	.910	-2.850	-19.352	4.089
	.920	-3.618	-20.790	3.489
	.930	-4.463	-22.378	2.837
	.940	-5.407	-24.160	2.117
	.950	-6.482	-26.201	1.305
	.960	-7.746	-28.610	.361
	.970	-9.300	-31.585	-.785
	.980	-11.366	-35.560	-2.289
	.990	-14.622	-41.859	-4.626

Probit Transformed Responses

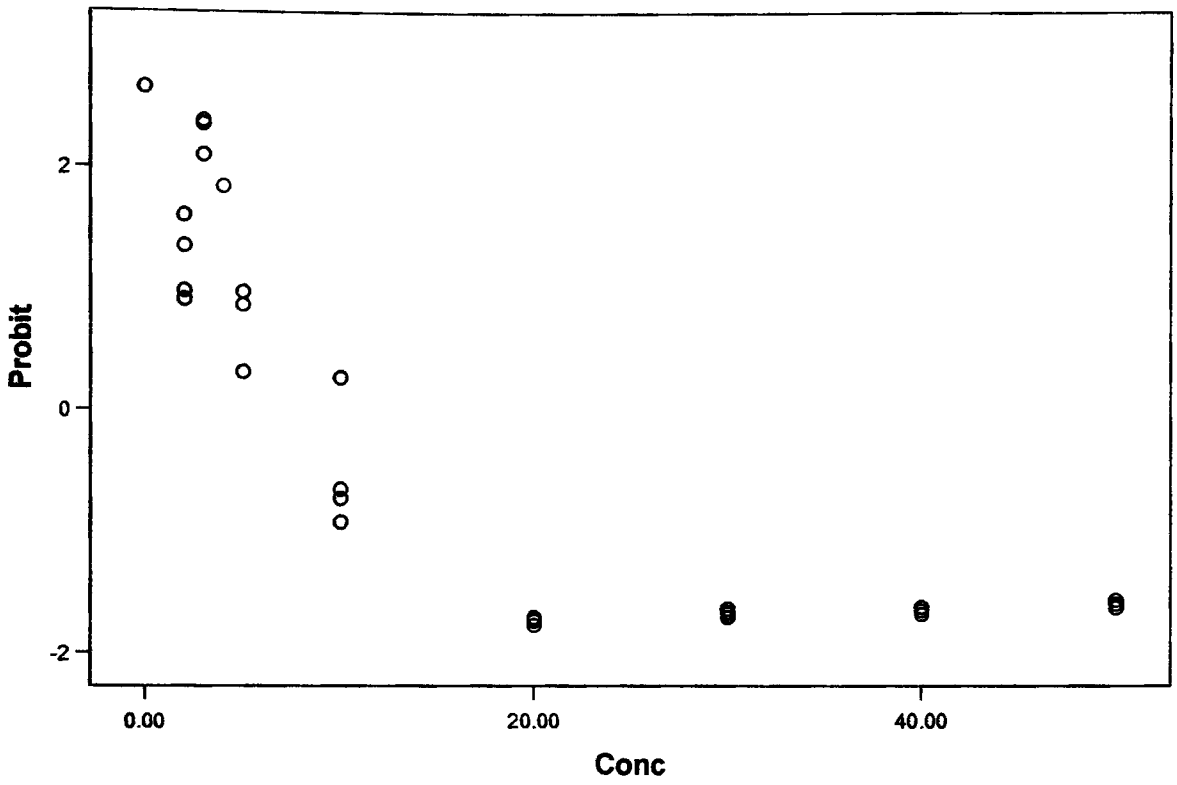

1.1.3.3. Compound 97. *E. coli*

Parameter Estimates

	Parameter	Estimate	Std. Error	Z	Sig.	95% Confidence Interval	
						Lower Bound	Upper Bound
PROBIT(a)	conc	.130	.821	.158	.874	-1.479	1.739
	Intercept	.648	1.495	.433	.665	-.847	2.143

a PROBIT model: PROBIT(p) = Intercept + BX

Chi-Square Tests

		Chi-Square	df(a)	Sig.
PROBIT	Pearson Goodness-of-Fit Test	.264	5	.998(b)

a Statistics based on individual cases differ from statistics based on aggregated cases.
b Since the significance level is greater than .150, no heterogeneity factor is used in the calculation of confidence limits.

Cell Counts and Residuals

	Number	conc	Number of Subjects	Observed Responses	Expected Responses	Residual	Probability
PROBIT	1	1.000	1	1	.696	.005	.782
	2	2.000	1	1	.728	-.032	.818
	3	1.000	1	1	.813	-.003	.782
	4	2.000	1	1	.851	-.135	.818
	5	3.000	1	1	.884	.095	.850
	6	1.000	1	1	.680	.098	.782
	7	2.000	1	1	.712	-.029	.818

Confidence Limits

	Probability	95% Confidence Limits for conc		
		Estimate	Lower Bound	Upper Bound
PROBIT	.010	-22.913	.	.
	.020	-20.813	.	.
	.030	-19.481	.	.
	.040	-18.479	.	.
	.050	-17.663	.	.
	.060	-16.969	.	.
	.070	-16.361	.	.
	.080	-15.816	.	.
	.090	-15.321	.	.
	.100	-14.865	.	.
	.150	-12.976	.	.
	.200	-11.476	.	.
	.250	-10.188	.	.
	.300	-9.032	.	.
	.350	-7.960	.	.
	.400	-6.944	.	.
	.450	-5.960	.	.
	.500	-4.992	.	.
	.550	-4.024	.	.
	.600	-3.040	.	.
	.650	-2.024	.	.
	.700	-.952	.	.
	.750	.204	.	.
	.800	1.491	.	.
	.850	2.992	.	.
	.900	4.880	.	.
	.910	5.336	.	.
	.920	5.832	.	.
	.930	6.377	.	.
	.940	6.985	.	.
	.950	7.679	.	.
	.960	8.494	.	.
	.970	9.497	.	.
	.980	10.829	.	.
	.990	12.929	.	.

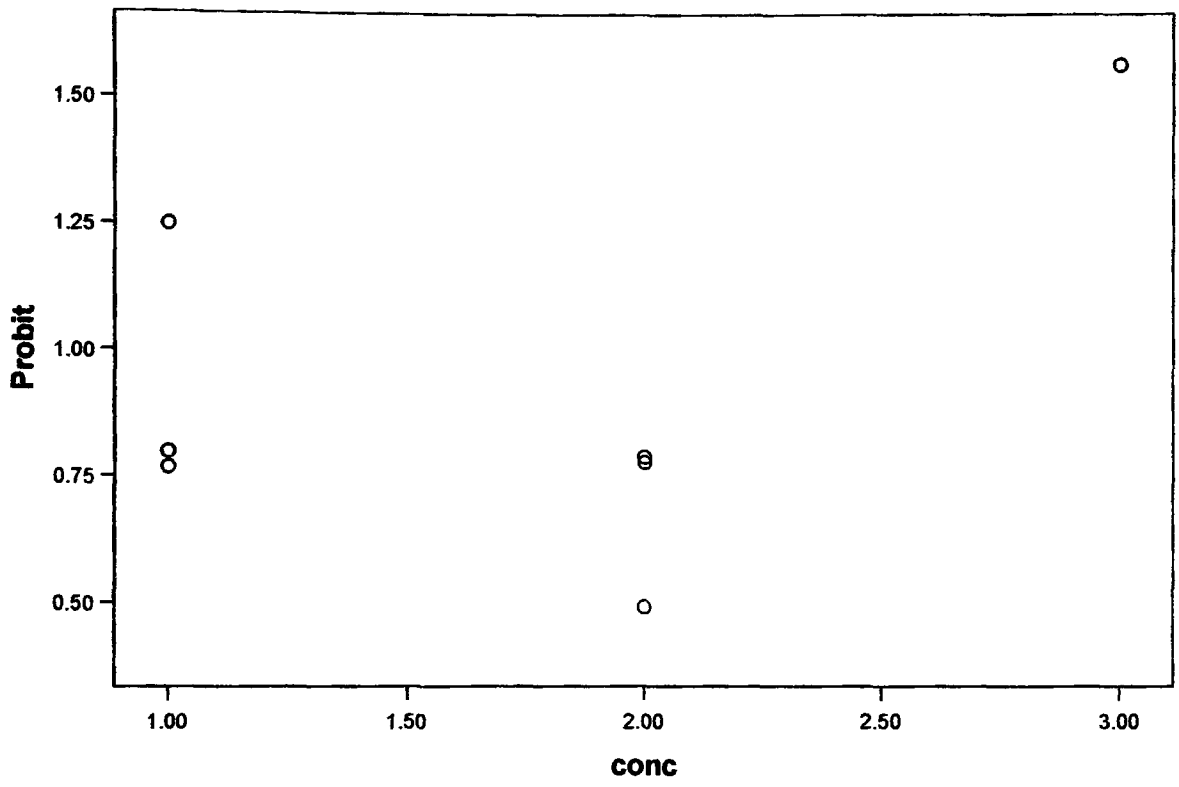
Probit Transformed Responses
Probit
1.50
1.25
1.00
0.75
0.50
1.00
1.50
2.00
2.50
3.00
conc

1.2. Comparison.

	N	Mean	Std. Deviation	Std. Error	95% Confidence Interval for Mean		Minimum	Maximum
					Lower Bound	Upper Bound		
compound 88. S.aureus.	3	86.0833	11.82083	6.82476	56.7188	115.4479	76.72	99.37
compound 89. S.aureus	3	37.8190	12.20855	7.04861	7.4913	68.1467	24.70	48.85
compound 90. S.aureus	3	8.3387	5.95364	3.43733	-6.4510	23.1283	1.46	11.78
compound 91. S.aureus	3	16.9720	1.12332	.64855	14.1815	19.7625	16.31	18.27
compound 82. S.aureus	2	64.8850	26.84460	18.98200	-176.3042	306.0742	45.90	83.87
compound 93. S.aureus	3	5.7180	1.91459	1.10539	.9619	10.4741	4.16	7.86
compound 94. S.aureus	2	7.3065	1.72605	1.22050	-8.2014	22.8144	6.09	8.53
compound 90. MRSA	3	14.1717	3.61418	2.08665	5.1935	23.1498	11.10	18.16
compound 91. MRSA	3	17.4003	.89802	.51847	15.1695	19.6311	16.39	18.10
compound 82. MRSA	3	79.9297	19.80112	11.43218	30.7410	129.1184	57.14	92.96
compound 93. MRSA	3	6.9573	4.79502	2.76841	-4.9542	18.8688	1.93	11.48
compound 94. MRSA	2	5.6135	.29204	.20650	2.9897	8.2373	5.41	5.82
compound 99. MRSA	3	10.3050	5.19126	2.99717	-2.5908	23.2008	4.41	14.18
Total	36	27.9638	30.03156	5.00526	17.8025	38.1250	1.46	99.37

Table 13.

1.3. Test of Homogeneity of Variances

LD50

Levene Statistic	df1	df2	Sig.
8.291	12	23	.000

1.4. ANOVA

	Sum of Squares	df	Mean Square	F	Sig.
Between Groups	29272.507	12	2439.376	24.460	.000
Within Groups	2293.794	23	99.730		
Total	31566.301	35			

1.5. Comparison of compounds.

(I) Compound	(J) Compound	Mean Difference (I-J)	Std. Error	Sig.	95% Confidence Interval	
					Lower Bound	Upper Bound
compound 88. S.aureus.	compound 89. S.aureus	48.26433(*)	8.15394	.000	18.2781	78.2506
	compound 90. S.aureus	77.74467(*)	8.15394	.000	47.7584	107.7309
	compound 91. S.aureus	69.11133(*)	8.15394	.000	39.1251	99.0976
	compound 82. S.aureus	21.19833	9.11639	.522	-12.3273	54.7240
	compound 93. S.aureus	80.36533(*)	8.15394	.000	50.3791	110.3516
	compound 94. S.aureus	78.77683(*)	9.11639	.000	45.2512	112.3025
	compound 90. MRSA	71.91167(*)	8.15394	.000	41.9254	101.8979
	compound 91. MRSA	68.68300(*)	8.15394	.000	38.6968	98.6692
	compound 82. MRSA	6.15367	8.15394	1.000	-23.8326	36.1399
	compound 93. MRSA	79.12600(*)	8.15394	.000	49.1398	109.1122
	compound 94. MRSA	80.46983(*)	9.11639	.000	46.9442	113.9955
	compound 99. MRSA	75.77833(*)	8.15394	.000	45.7921	105.7646
compound 89. S.aureus	compound 88. S.aureus.	-48.26433(*)	8.15394	.000	-78.2506	-18.2781
	compound 90. S.aureus	29.48033	8.15394	.057	-.5059	59.4666
	compound 91. S.aureus	20.84700	8.15394	.386	-9.1392	50.8332
	compound 82. S.aureus	-27.06600	9.11639	.200	-60.5916	6.4596
	compound 93. S.aureus	32.10100(*)	8.15394	.029	2.1148	62.0872
	compound 94. S.aureus	30.51250	9.11639	.099	-3.0131	64.0381
	compound 90. MRSA	23.64733	8.15394	.225	-6.3389	53.6336
	compound 91.	20.418	8.1539	.416	-9.5676	50.404

	MRSA	67	4			9
	compound 82. MRSA	-42.11067(*)	8.15394	.002	-72.0969	-12.1244
	compound 93. MRSA	30.86167(*)	8.15394	.040	.8754	60.8479
	compound 94. MRSA	32.20550	9.11639	.068	-1.3201	65.7311
	compound 99. MRSA	27.51400	8.15394	.093	-2.4722	57.5002
compound 90. S.aureus	compound 88. S.aureus.	-77.74467(*)	8.15394	.000	-107.7309	-47.7584
	compound 89. S.aureus	-29.48033	8.15394	.057	-59.4666	.5059
	compound 91. S.aureus	-8.63333	8.15394	.996	-38.6196	21.3529
	compound 82. S.aureus	-56.54633(*)	9.11639	.000	-90.0720	-23.0207
	compound 93. S.aureus	2.62067	8.15394	1.000	-27.3656	32.6069
	compound 94. S.aureus	1.03217	9.11639	1.000	-32.4935	34.5578
	compound 90. MRSA	-5.83300	8.15394	1.000	-35.8192	24.1532
	compound 91. MRSA	-9.06167	8.15394	.994	-39.0479	20.9246
	compound 82. MRSA	-71.59100(*)	8.15394	.000	-101.5772	-41.6048
	compound 93. MRSA	1.38133	8.15394	1.000	-28.6049	31.3676
	compound 94. MRSA	2.72517	9.11639	1.000	-30.8005	36.2508
	compound 99. MRSA	-1.96633	8.15394	1.000	-31.9526	28.0199
compound 91. S.aureus	compound 88. S.aureus.	-69.11133(*)	8.15394	.000	-99.0976	-39.1251
	compound 89. S.aureus	-20.84700	8.15394	.386	-50.8332	9.1392
	compound 90. S.aureus	8.63333	8.15394	.996	-21.3529	38.6196
	compound 82. S.aureus	-47.91300(*)	9.11639	.001	-81.4386	-14.3874
	compound 93. S.aureus	11.25400	8.15394	.967	-18.7322	41.2402
	compound 94. S.aureus	9.66550	9.11639	.996	-23.8601	43.1911
	compound 90. MRSA	2.80033	8.15394	1.000	-27.1859	32.7866
	compound 91. MRSA	-.42833	8.15394	1.000	-30.4146	29.5579
	compound 82. MRSA	-62.95767(*)	8.15394	.000	-92.9439	-32.9714
	compound 93. MRSA	10.01467	8.15394	.986	-19.9716	40.0009

	compound 94. MRSA	11.35850	9.11639	.985	-22.1671	44.8841
	compound 99. MRSA	6.66700	8.15394	1.000	-23.3192	36.6532
compound 82. S.aureus	compound 88. S.aureus.	-21.19833	9.11639	.522	-54.7240	12.3273
	compound 89. S.aureus	27.06600	9.11639	.200	-6.4596	60.5916
	compound 90. S.aureus	56.54633(*)	9.11639	.000	23.0207	90.0720
	compound 81. S.aureus	47.91300(*)	9.11639	.001	14.3874	81.4386
	compound 93. S.aureus	59.16700(*)	9.11639	.000	25.6414	92.6926
	compound 94. S.aureus	57.57850(*)	9.98650	.000	20.8530	94.3040
	compound 90. MRSA	50.71333(*)	9.11639	.001	17.1877	84.2390
	compound 91. MRSA	47.48467(*)	9.11639	.002	13.9590	81.0103
	compound 82. MRSA	-15.04467	9.11639	.895	-48.5703	18.4810
	compound 93. MRSA	57.92767(*)	9.11639	.000	24.4020	91.4533
	compound 94. MRSA	59.27150(*)	9.98650	.000	22.5460	95.9970
	compound 99. MRSA	54.58000(*)	9.11639	.000	21.0544	88.1056
compound 93. S.aureus	compound 88. S.aureus.	-80.36533(*)	8.15394	.000	-110.3516	-50.3791
	compound 89. S.aureus	-32.10100(*)	8.15394	.029	-62.0872	-2.1148
	compound 90. S.aureus	-2.62067	8.15394	1.000	-32.6069	27.3656
	compound 91. S.aureus	-11.25400	8.15394	.967	-41.2402	18.7322
	compound 82. S.aureus	-59.16700(*)	9.11639	.000	-92.6926	-25.6414
	compound 94. S.aureus	-1.58850	9.11639	1.000	-35.1141	31.9371
	compound 90. MRSA	-8.45367	8.15394	.997	-38.4399	21.5326
	compound 91. MRSA	-11.68233	8.15394	.957	-41.6686	18.3039
	compound 82. MRSA	-74.21167(*)	8.15394	.000	-104.1979	-44.2254
	compound 93. MRSA	-1.23933	8.15394	1.000	-31.2256	28.7469
	compound 94. MRSA	.10450	9.11639	1.000	-33.4211	33.6301
	compound 99. MRSA	-4.58700	8.15394	1.000	-34.5732	25.3992
compound 94. S.aureus	compound 88. S.aureus.	-78.776	9.11639	.000	-112.302	-45.251

		83(*)			5	2
	compound 89. S.aureus	-30.51250	9.11639	.099	-64.0381	3.0131
	compound 90. S.aureus	-1.03217	9.11639	1.000	-34.5578	32.4935
	compound 91. S.aureus	-9.66550	9.11639	.996	-43.1911	23.8601
	compound 82. S.aureus	-57.57850(*)	9.98650	.000	-94.3040	-20.8530
	compound 93. S.aureus	1.58850	9.11639	1.000	-31.9371	35.1141
	compound 90. MRSA	-6.86517	9.11639	1.000	-40.3908	26.6605
	compound 91. MRSA	-10.09383	9.11639	.994	-43.6195	23.4318
	compound 82. MRSA	-72.62317(*)	9.11639	.000	-106.1488	-39.0975
	compound 93. MRSA	.34917	9.11639	1.000	-33.1765	33.8748
	compound 94. MRSA	1.69300	9.98650	1.000	-35.0325	38.4185
	compound 99. MRSA	-2.99850	9.11639	1.000	-36.5241	30.5271
compound 90. MRSA	compound 88. S.aureus.	-71.91167(*)	8.15394	.000	-101.8979	-41.9254
	compound 89. S.aureus	-23.64733	8.15394	.225	-53.6336	6.3389
	compound 90. S.aureus	5.83300	8.15394	1.000	-24.1532	35.8192
	compound 91. S.aureus	-2.80033	8.15394	1.000	-32.7866	27.1859
	compound 82. S.aureus	-50.71333(*)	9.11639	.001	-84.2390	-17.1877
	compound 93. S.aureus	8.45367	8.15394	.997	-21.5326	38.4399
	compound 94. S.aureus	6.86517	9.11639	1.000	-26.6605	40.3908
	compound 91. MRSA	-3.22867	8.15394	1.000	-33.2149	26.7576
	compound 82. MRSA	-65.75800(*)	8.15394	.000	-95.7442	-35.7718
	compound 93. MRSA	7.21433	8.15394	.999	-22.7719	37.2006
	compound 94. MRSA	8.55817	9.11639	.999	-24.9675	42.0838
	compound 99. MRSA	3.86667	8.15394	1.000	-26.1196	33.8529
compound 91. MRSA	compound 88. S.aureus.	-68.68300(*)	8.15394	.000	-98.6692	-38.6968
	compound 89. S.aureus	-20.41867	8.15394	.416	-50.4049	9.5676

	compound 90. S.aureus	9.06167	8.15394	.994	-20.9246	39.0479
	compound 91. S.aureus	.42833	8.15394	1.000	-29.5579	30.4146
	compound 82. S.aureus	-47.48467(*)	9.11639	.002	-81.0103	-13.9590
	compound 93. S.aureus	11.68233	8.15394	.957	-18.3039	41.6686
	compound 94. S.aureus	10.09383	9.11639	.994	-23.4318	43.6195
	compound 90. MRSA	3.22867	8.15394	1.000	-26.7576	33.2149
	compound 82. MRSA	-62.52933(*)	8.15394	.000	-92.5156	-32.5431
	compound 93. MRSA	10.44300	8.15394	.981	-19.5432	40.4292
	compound 94. MRSA	11.78683	9.11639	.980	-21.7388	45.3125
	compound 99. MRSA	7.09533	8.15394	.999	-22.8909	37.0816
compound 82. MRSA	compound 88. S.aureus.	-6.15367	8.15394	1.000	-36.1399	23.8326
	compound 89. S.aureus	42.11067(*)	8.15394	.002	12.1244	72.0969
	compound 90. S.aureus	71.59100(*)	8.15394	.000	41.6048	101.5772
	compound 91. S.aureus	62.95767(*)	8.15394	.000	32.9714	92.9439
	compound 82. S.aureus	15.04467	9.11639	.895	-18.4810	48.5703
	compound 93. S.aureus	74.21167(*)	8.15394	.000	44.2254	104.1979
	compound 94. S.aureus	72.62317(*)	9.11639	.000	39.0975	106.1488
	compound 90. MRSA	65.75800(*)	8.15394	.000	35.7718	95.7442
	compound 91. MRSA	62.52933(*)	8.15394	.000	32.5431	92.5156
	compound 93. MRSA	72.97233(*)	8.15394	.000	42.9861	102.9586
	compound 94. MRSA	74.31617(*)	9.11639	.000	40.7905	107.8418
	compound 99. MRSA	69.62467(*)	8.15394	.000	39.6384	99.6109
compound 93. MRSA	compound 88. S.aureus.	-79.12600(*)	8.15394	.000	-109.1122	-49.1398
	compound 89. S.aureus	-30.86167(*)	8.15394	.040	-60.8479	-.8754
	compound 90. S.aureus	-1.38133	8.15394	1.000	-31.3676	28.6049
	compound 91. S.aureus	-10.01467	8.15394	.986	-40.0009	19.9716
	compound 82. S.aureus	-57.92767(*)	9.11639	.000	-91.4533	-24.4020
	compound 93. S.aureus	1.23933	8.15394	1.000	-28.7469	31.2256
	compound 94. S.aureus	-.34917	9.11639	1.000	-33.8748	33.1765
	compound 90.	-	8.15394	.999	-	22.771

	MRSA	7.21433	4		37.2006	9
	compound 91. MRSA	-10.44300	8.15394	.981	-40.4292	19.5432
	compound 82. MRSA	-72.97233(*)	8.15394	.000	-102.9586	-42.9861
	compound 94. MRSA	1.34383	9.11639	1.000	-32.1818	34.8695
	compound 99. MRSA	-3.34767	8.15394	1.000	-33.3339	26.6386
compound 94. MRSA	compound 88. S.aureus.	-80.46983(*)	9.11639	.000	-113.9955	-46.9442
	compound 89. S.aureus	-32.20550	9.11639	.068	-65.7311	1.3201
	compound 90. S.aureus	-2.72517	9.11639	1.000	-36.2508	30.8005
	compound 91. S.aureus	-11.35850	9.11639	.985	-44.8841	22.1671
	compound 82. S.aureus	-59.27150(*)	9.98650	.000	-95.9970	-22.5460
	compound 93. S.aureus	-.10450	9.11639	1.000	-33.6301	33.4211
	compound 94. S.aureus	-1.69300	9.98650	1.000	-38.4185	35.0325
	compound 90. MRSA	-8.55817	9.11639	.999	-42.0838	24.9675
	compound 91. MRSA	-11.78683	9.11639	.980	-45.3125	21.7388
	compound 82. MRSA	-74.31617(*)	9.11639	.000	-107.8418	-40.7905
	compound 93. MRSA	-1.34383	9.11639	1.000	-34.8695	32.1818
	compound 99. MRSA	-4.69150	9.11639	1.000	-38.2171	28.8341
compound 99. MRSA	compound 88. S.aureus.	-75.77833(*)	8.15394	.000	-105.7646	-45.7921
	compound 89. S.aureus	-27.51400	8.15394	.093	-57.5002	2.4722
	compound 90. S.aureus	1.96633	8.15394	1.000	-28.0199	31.9526
	compound 91. S.aureus	-6.66700	8.15394	1.000	-36.6532	23.3192
	compound 82. S.aureus	-54.58000(*)	9.11639	.000	-88.1056	-21.0544
	compound 93. S.aureus	4.58700	8.15394	1.000	-25.3992	34.5732
	compound 94. S.aureus	2.99850	9.11639	1.000	-30.5271	36.5241
	compound 90.	-	8.1539	1.00	-	26.119

	MRSA	3.86667	4	0	33.8529	6
	compound 91. MRSA	-7.09533	8.15394	.999	-37.0816	22.8909
	compound 82. MRSA	-69.62467(*)	8.15394	.000	-99.6109	-39.6384
	compound 93. MRSA	3.34767	8.15394	1.000	-26.6386	33.3339
	compound 94. MRSA	4.69150	9.11639	1.000	-28.8341	38.2171

* The mean difference is significant at the .05 level.

Appendix 2. Mulliken Charges.

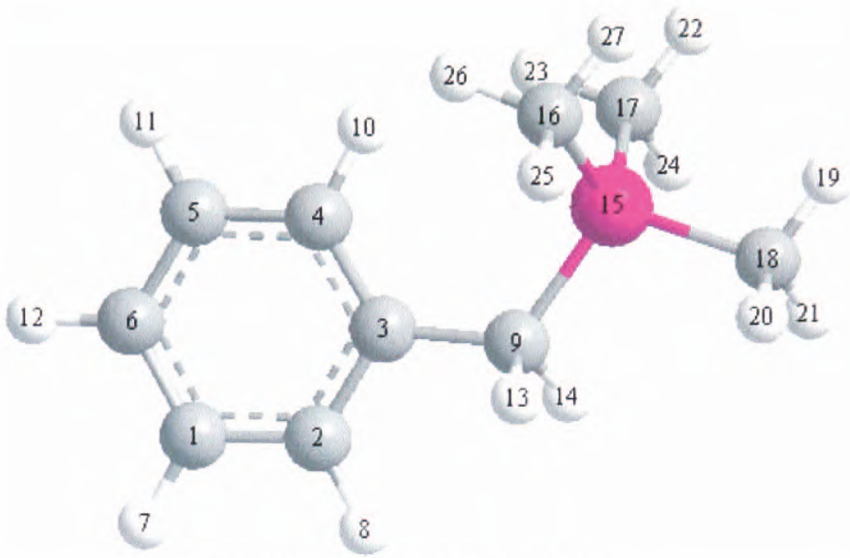

Figure 1. trimethylphosphoniumyl group.

Trimethylphosphoniumyl group	
C(1) -0.222177	**P(15) 2.162966**
C(2) -0.213277	C(16) -1.143236
C(3) 0.014848	C(17) -1.161136
C(4) -0.276021	C(18) -1.163300
C(5) -0.216624	H(19) 0.297914
C(6) -0.228538	H(20) 0.304726
H(7) 0.277859	H(21) 0.289493
H(8) 0.248322	H(22) 0.288541
C(9) -1.137709	H(23) 0.306278
H(10) 0.213902	H(24) 0.297168
H(11) 0.273105	H(25) 0.290679
H(12) 0.279131	H(26) 0.287863
H(13) 0.321121	H(27) 0.287248
H(14) 0.320852	

Table 1. Mulliken charges for atoms of trimethylphosphoniumyl group.

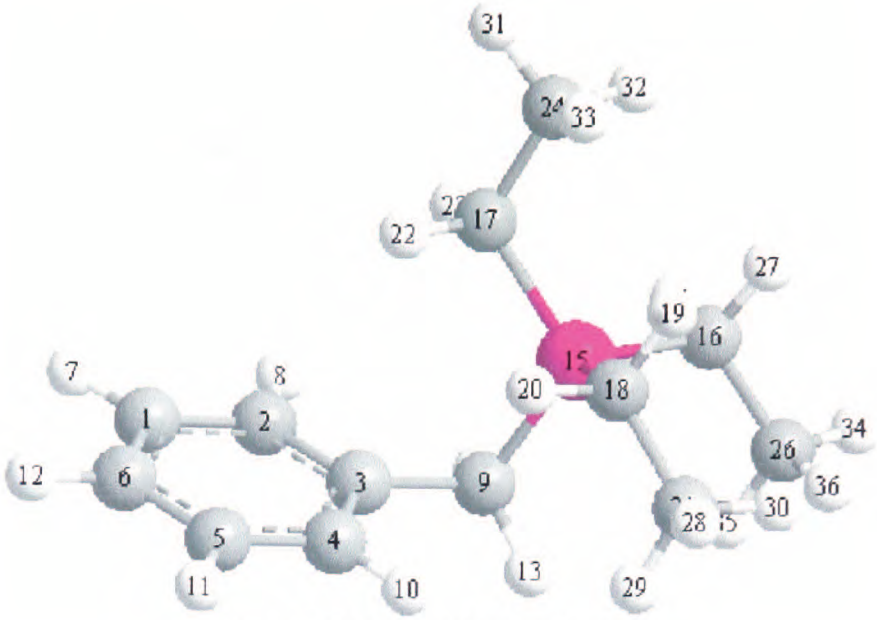

Figure 2. Triethyl phosphoniumyl group

Triethylphosphoniumyl group	
C(1) -0.226492	H(19) 0.282752
C(2) -0.219851	H(20) 0.290687
C(3) -0.080802	C(21) -0.599891
C(4) -0.228649	H(22) 0.299530
C(5) -0.225642	H(23) 0.269272
C(6) -0.228908	C(24) -0.601909
H(7) 0.272433	H(25) 0.276154
H(8) 0.242755	C(26) -0.600010
C(9) -0.890940	H(27) 0.282371
H(10) 0.245140	H(28) 0.265784
H(11) 0.271163	H(29) 0.217542
H(12) 0.275542	H(30) 0.234254
H(13) 0.299127	H(31) 0.266904
H(14) 0.290662	H(32) 0.221820
P(15) 1.797111	H(33) 0.222712
C(16) -0.885802	H(34) 0.266260
C(17) -0.870733	H(35) 0.222676
C(18) -0.887062	H(36) 0.234038

Table 2. Mulliken charges for triethyl phosphoniumyl group.

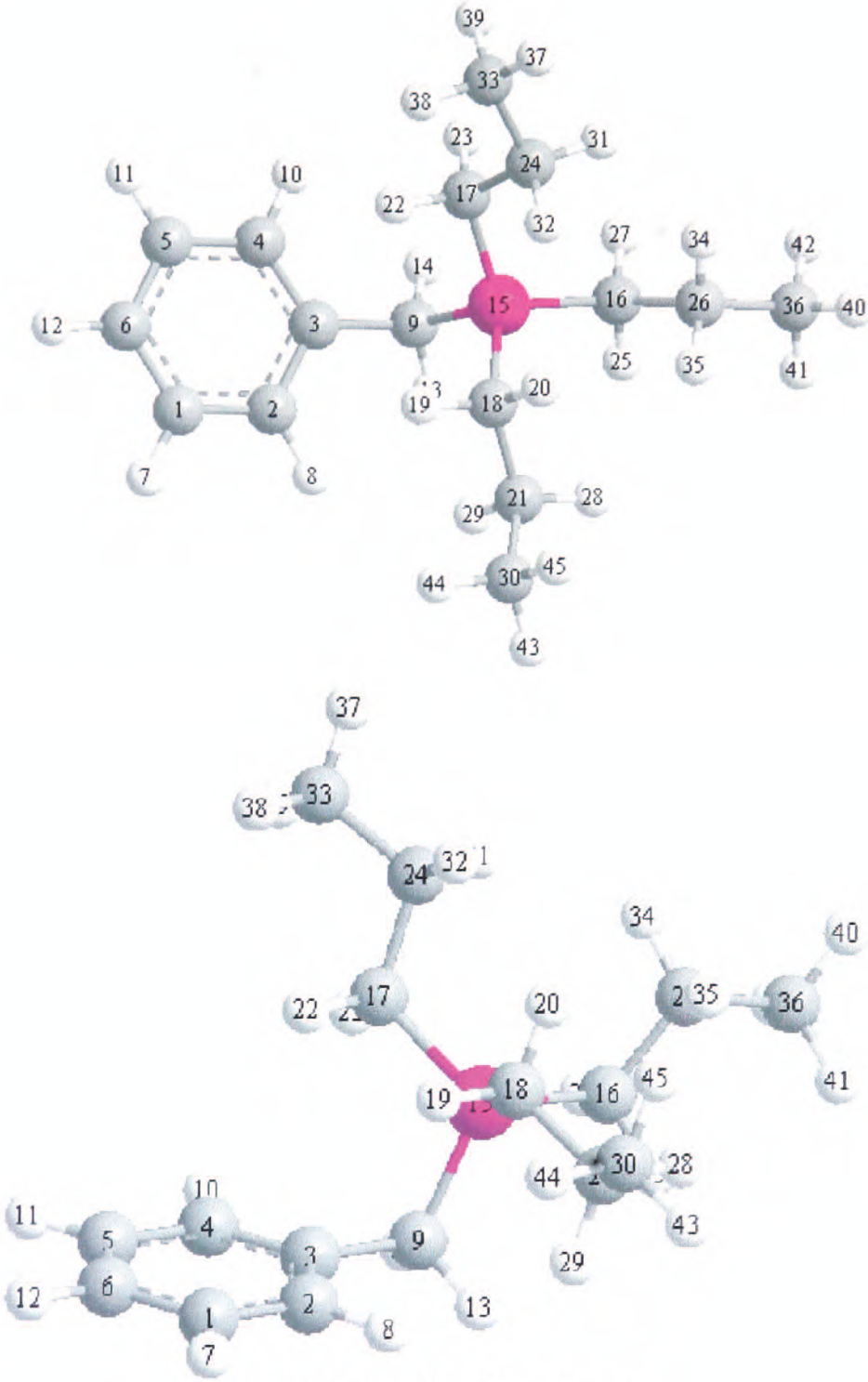

Figure 3. Tripropyl phosphoniumyl group.

tripropyl phosphoniumyl group	
C(1) -0.227416	C(24) -0.446750
C(2) -0.227352	H(25) 0.272380
C(3) -0.087249	C(26) -0.451595
C(4) -0.221251	H(27) 0.273642
C(5) -0.227134	H(28) 0.230099
C(6) -0.228636	H(29) 0.221952
H(7) 0.269811	C(30) -0.563331
H(8) 0.248610	H(31) 0.235033
C(9) -0.879826	H(32) 0.221499
H(10) 0.242708	C(33) -0.561668
H(11) 0.270468	H(34) 0.241486
H(12) 0.274048	H(35) 0.226282
H(13) 0.291789	C(36) -0.562804
H(14) 0.289009	H(37) 0.234347
P(15) 1.809179	H(38) 0.213653
C(16) -0.867403	H(39) 0.214628
C(17) -0.863923	H(40) 0.234654
C(18) -0.867555	H(41) 0.212074
H(19) 0.290794	H(42) 0.215587
H(20) 0.277454	H(43) 0.234438
C(21) -0.449273	H(44) 0.214615
H(22) 0.292609	H(45) 0.215704
H(23) 0.264614	

Table 3. Mulliken charges for tripropyl phosphoniumyl group

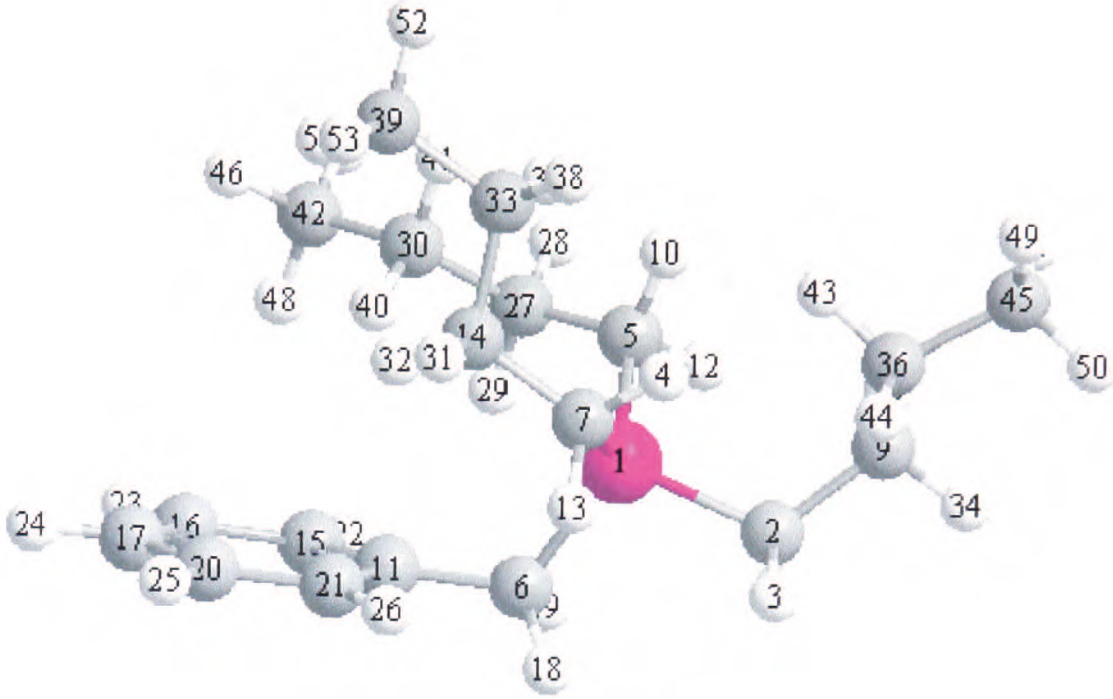

Figure 4. Tributyl phosphoniumyl group.

Tributylphosphoniumyl group	
P(1) 1.779372	H(28) 0.253248
C(2) -0.853854	H(29) 0.215937
H(3) 0.267912	C(30) -0.451282
H(4) 0.302154	H(31) 0.247123
C(5) -0.892660	H(32) 0.255885
C(6) -0.874856	C(33) -0.426841
C(7) -0.885380	H(34) 0.258352
H(8) 0.265516	H(35) 0.223820
C(9) -0.398465	C(36) -0.446327
H(10) 0.286303	H(37) 0.196221
C(11) -0.076338	H(38) 0.217326
H(12) 0.275583	C(39) -0.572980
H(13) 0.264422	H(40) 0.228692
C(14) -0.421117	H(41) 0.221784
C(15) -0.211756	C(42) -0.564689
C(16) -0.228546	H(43) 0.191861
C(17) -0.229595	H(44) 0.213558
H(18) 0.293920	C(45) -0.563345
H(19) 0.286240	H(46) 0.219111
C(20) -0.227716	H(47) 0.209647
C(21) -0.228228	H(48) 0.197162
H(22) 0.246568	H(49) 0.222645
H(23) 0.269571	H(50) 0.215558
H(24) 0.273408	H(51) 0.206734
H(25) 0.268667	H(52) 0.219002
H(26) 0.238864	H(53) 0.212613
C(27) -0.395381	H(54) 0.204579

Table 4. Mulliken charges for tributyl phosphoniumyl

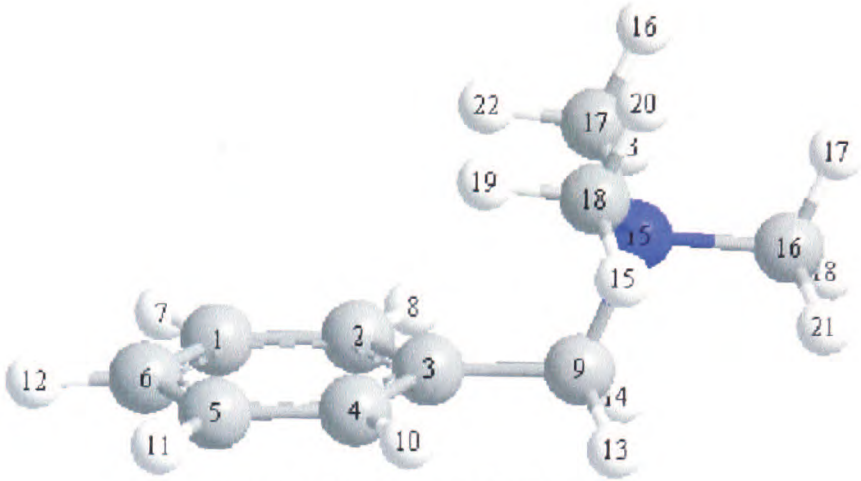

Figure 5. Trimethyl ammoniumyl group

Trimethylammoniumyl group	
C(1) -0.229409	**N(15) -0.747381**
C(2) -0.219067	H(16) 0.264724
C(3) -0.105802	H(17) 0.270278
C(4) -0.218911	C(18) -0.398747
C(5) -0.229400	C(19) -0.398136
C(6) -0.221250	H(20) 0.272719
H(7) 0.275998	C(21) -0.398131
H(8) 0.246496	H(22) 0.272937
C(9) -0.212746	H(23) 0.295684
H(10) 0.246663	H(24) 0.270293
H(11) 0.276030	H(25) 0.272941
H(12) 0.281493	H(26) 0.295891
H(13) 0.286071	H(27) 0.264652
H(14) 0.286108	

Table 5. Mulliken charges for trimethyl ammoniumyl.

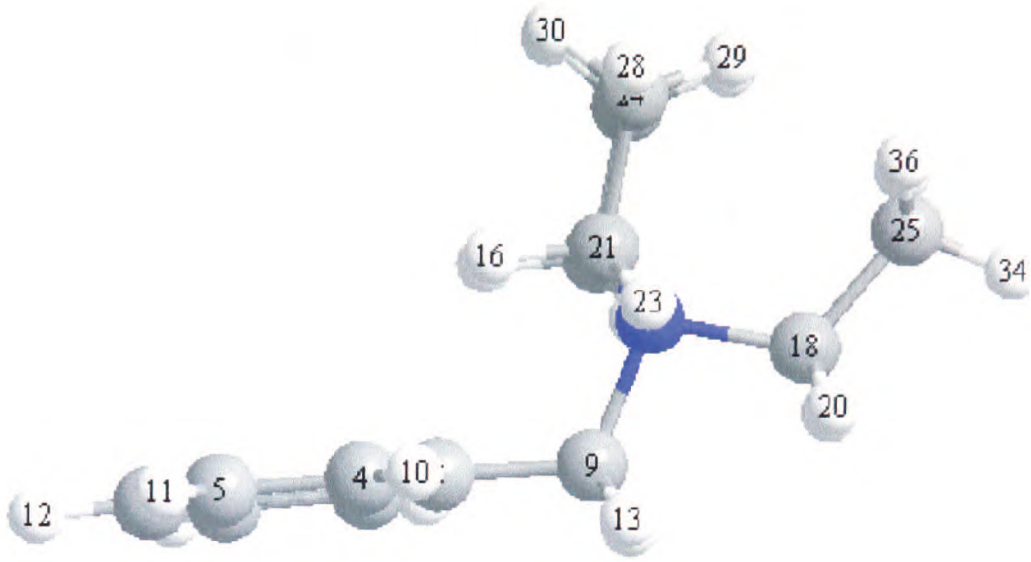

Figure 6. Triethyl ammoniumyl group.

Triethylammoniumyl group	
C(1) -0.230182	C(19) -0.224766
C(2) -0.222987	H(20) 0.268941
C(3) -0.105507	C(21) -0.225765
C(4) -0.223731	H(22) 0.269127
C(5) -0.230567	H(23) 0.258947
C(6) -0.221823	C(24) -0.621651
H(7) 0.274071	C(25) -0.630892
H(8) 0.246256	H(26) 0.258072
C(9) -0.230602	C(27) -0.621470
H(10) 0.246173	H(28) 0.251006
H(11) 0.273954	H(29) 0.239341
H(12) 0.279407	H(30) 0.238170
H(13) 0.282796	H(31) 0.250854
H(14) 0.282273	H(32) 0.239532
N(15) -0.733738	H(33) 0.237974
H(16) 0.302157	H(34) 0.258173
H(17) 0.305109	H(35) 0.238342
C(18) -0.215698	H(36) 0.238701

Table 6. Mulliken charges for triethyl ammoniumyl group.

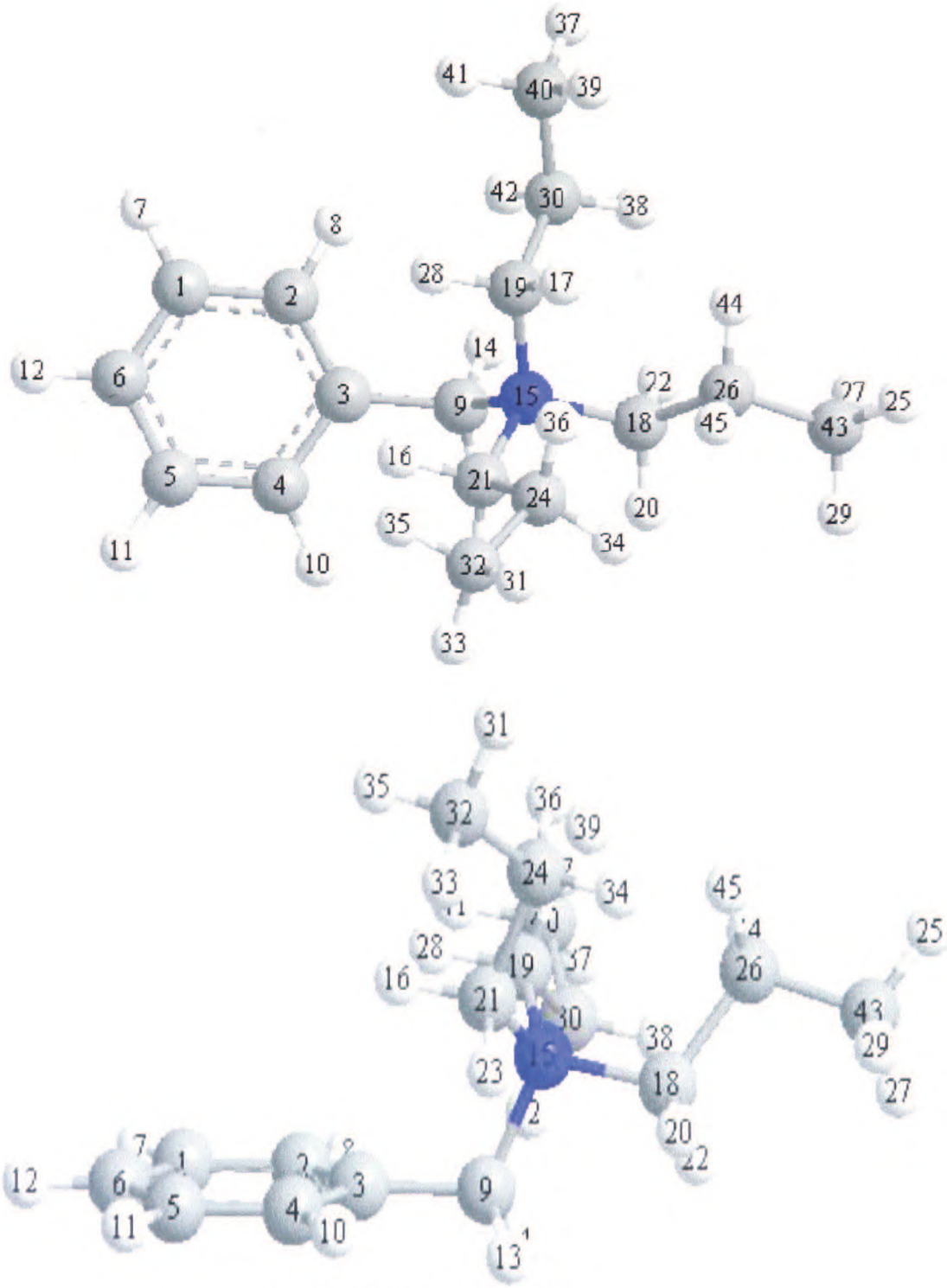

Figure 7. Tripropylammoniumyl group.

Tripropylammoniumyl group	
C(1) -0.231974	C(24) -0.473621
C(2) -0.226417	H(25) 0.241581
C(3) -0.113841	C(26) -0.487582
C(4) -0.215822	H(27) 0.212702
C(5) -0.231222	H(28) 0.285393
C(6) -0.222305	H(29) 0.213499
H(7) 0.271425	C(30) -0.481029
H(8) 0.254361	H(31) 0.240979
C(9) -0.222503	C(32) -0.573857
H(10) 0.244526	H(33) 0.213005
H(11) 0.272296	H(34) 0.233548
H(12) 0.277498	H(35) 0.214552
H(13) 0.279542	H(36) 0.230949
H(14) 0.286022	H(37) 0.241351
N(15) -0.752015	H(38) 0.237587
H(16) 0.293009	H(39) 0.214982
H(17) 0.274394	C(40) -0.577901
C(18) -0.184551	H(41) 0.214601
C(19) -0.192535	H(42) 0.230181
H(20) 0.264727	C(43) -0.577246
C(21) -0.186981	H(44) 0.235733
H(22) 0.265154	H(45) 0.252755
H(23) 0.255048	

Table 7. Mulliken charges for tripropyl ammoniumyl.

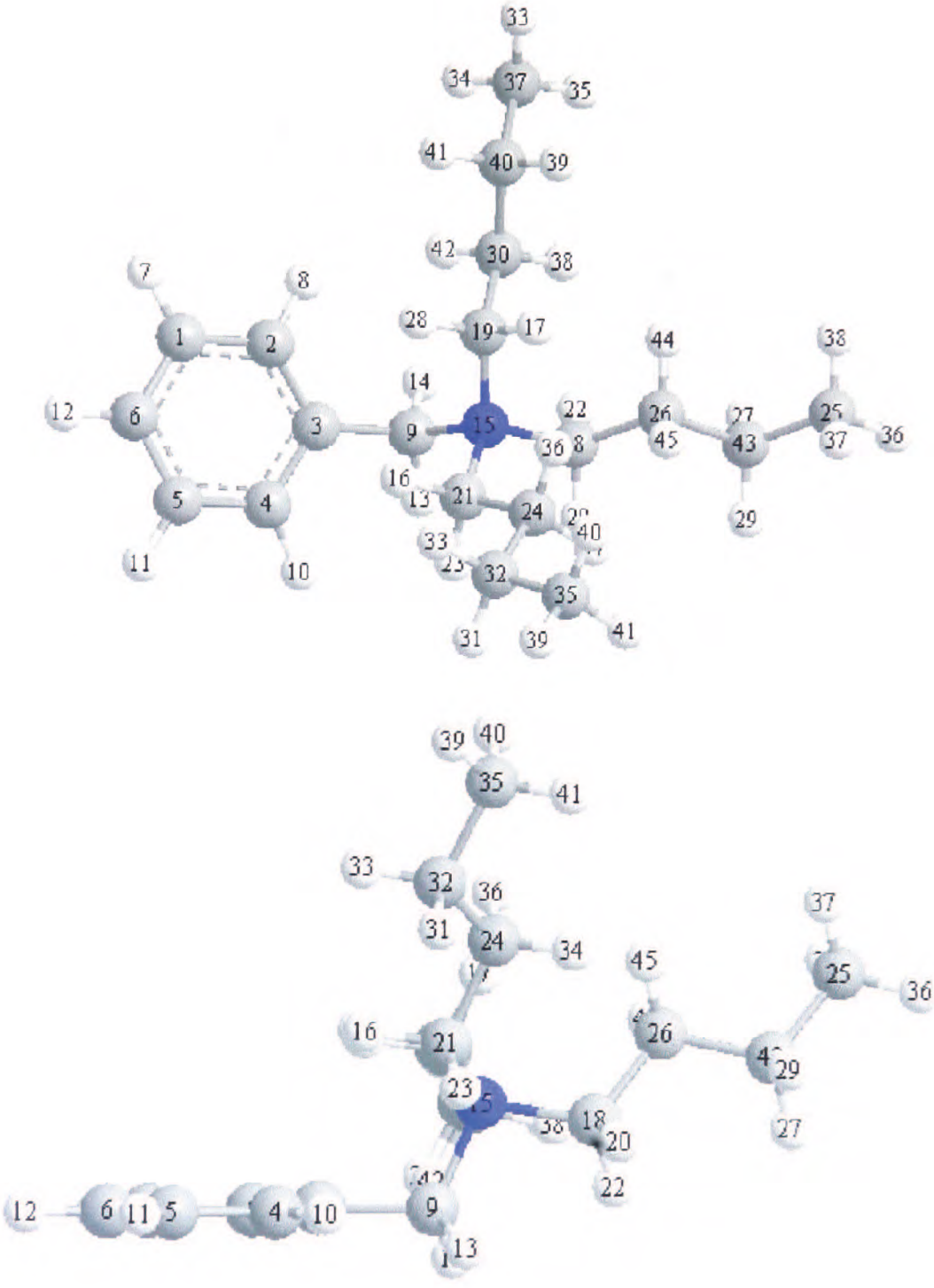

Figure 8. Tributyl ammoniumyl.

tributyl ammoniumyl	
C(1) -0.232137	H(28) 0.284425
C(2) -0.226081	H(29) 0.215412
C(3) -0.113438	C(30) -0.452790
C(4) -0.215924	H(31) 0.214792
C(5) -0.231304	C(32) -0.420377
C(6) -0.222445	H(33) 0.218163
H(7) 0.270618	H(34) 0.228982
H(8) 0.254799	H(35) 0.228680
C(9) -0.221777	H(36) 0.204545
H(10) 0.244315	C(37) -0.569207
H(11) 0.271541	H(38) 0.205960
H(12) 0.276684	H(39) 0.226181
H(13) 0.278584	H(40) 0.228706
H(14) 0.285436	H(41) 0.205311
N(15) -0.753751	C(42) -0.569382
H(16) 0.291197	H(43) 0.232601
H(17) 0.273863	H(44) 0.205379
C(18) -0.187635	H(45) 0.217057
C(19) -0.194860	H(46) 0.228003
H(20) 0.263655	C(47) -0.424955
C(21) -0.188626	H(48) 0.205272
H(22) 0.264213	H(49) 0.217682
H(23) 0.253630	H(50) 0.205342
C(24) -0.445236	H(51) 0.225930
C(25) -0.569292	C(52) -0.423963
C(26) -0.459656	H(53) 0.232007
H(27) 0.215345	H(54) 0.248524

Table 8. Mulliken charges for tributyl ammoniumyl.

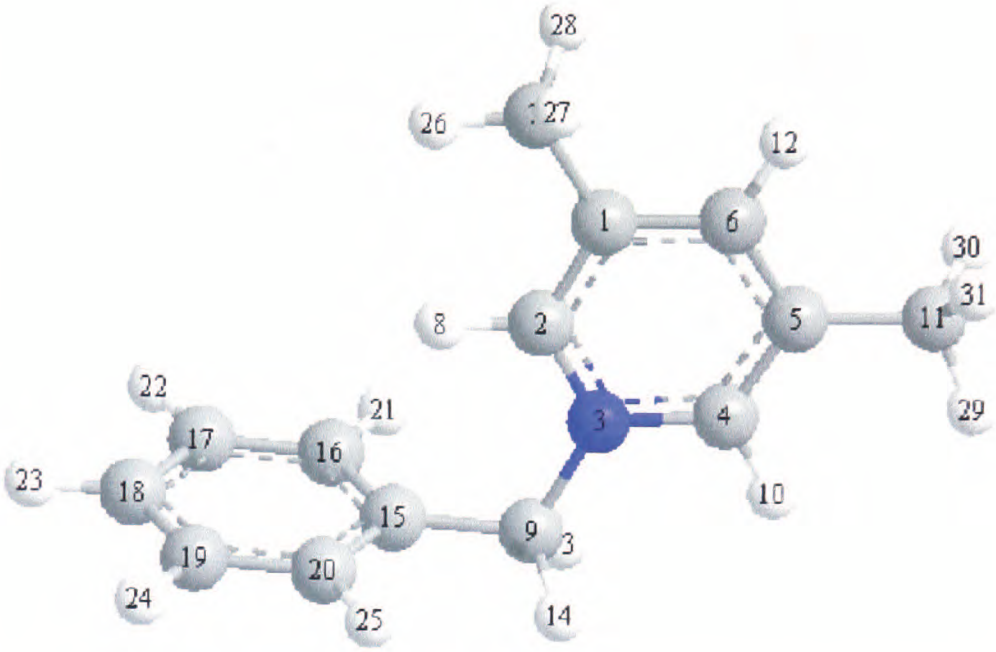

Figure 9. Dimethylpyridium

Dimethylpyridium	
C(1) -0.180168	C(17) -0.231171
C(2) 0.272976	C(18) -0.223109
N(3) -0.889321	C(19) -0.231182
C(4) 0.263075	C(20) -0.212317
C(5) -0.180555	H(21) 0.254304
C(6) -0.082604	H(22) 0.273555
C(7) -0.590071	H(23) 0.278223
H(8) 0.350262	H(24) 0.274257
C(9) -0.165505	H(25) 0.256268
H(10) 0.316582	H(26) 0.241577
C(11) -0.590924	H(27) 0.258729
H(12) 0.311854	H(28) 0.255585
H(13) 0.287967	H(29) 0.240354
H(14) 0.287919	H(30) 0.261211
C(15) -0.150885	H(31) 0.255353
C(16) -0.212238	

Table 9. Mulliken charges for dimethylpyridium.

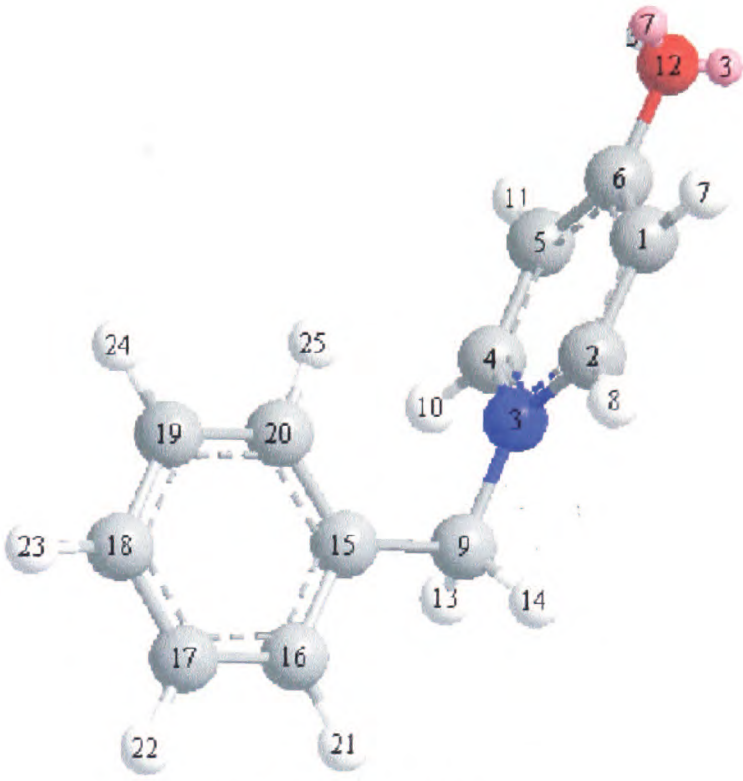

Figure 10. hydroxypyridinium.

hydroxypyridinium	
C(1) -0.332684	H(14) 0.286647
C(2) 0.257157	C(15) -0.095387
N(3) -0.893708	C(16) -0.222447
C(4) 0.262496	C(17) -0.220232
C(5) -0.378201	C(18) -0.230004
C(6) 0.516539	C(19) -0.219840
H(7) 0.341428	C(20) -0.226396
H(8) 0.347557	H(21) 0.251433
C(9) -0.178728	H(22) 0.274176
H(10) 0.343810	H(23) 0.273731
H(11) 0.311221	H(24) 0.266309
O(12) -0.687797	H(25) 0.228562
H(13) 0.287327	H(26) 0.437031

Table 10. Mulliken charges for hydroxypyridinium.

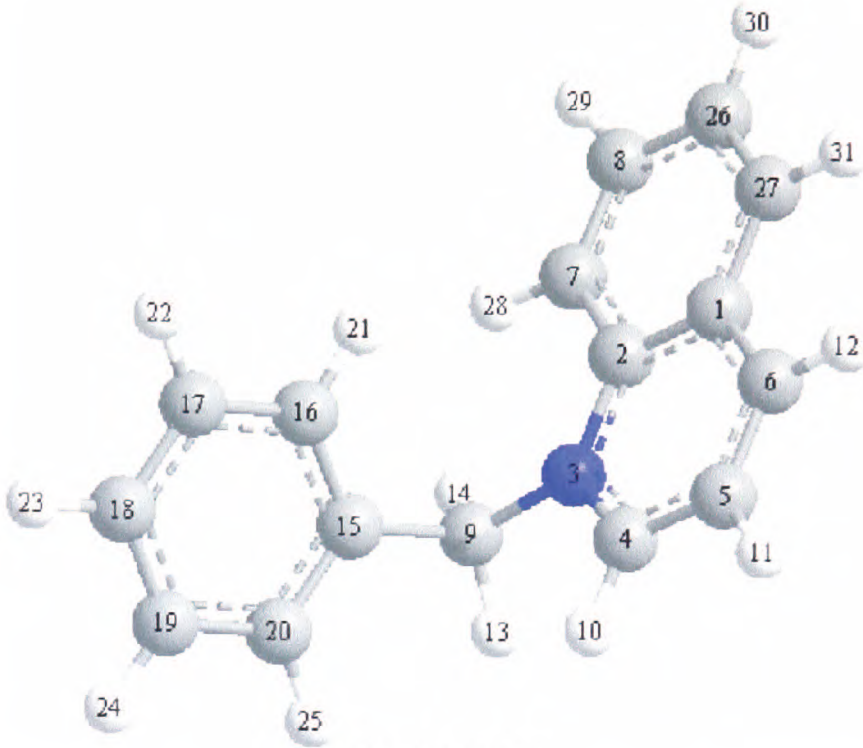

Figure 11. Quinolinium.

quinolinium	
C(1) -0.156473	C(17) -0.226161
C(2) 0.444726	C(18) -0.226140
N(3) -0.955260	C(19) -0.226345
C(4) 0.307199	C(20) -0.222103
C(5) -0.358580	H(21) 0.248331
C(6) -0.055524	H(22) 0.267005
C(7) -0.227608	H(23) 0.273188
C(8) -0.202138	H(24) 0.270946
C(9) -0.219908	H(25) 0.248067
H(10) 0.336902	C(26) -0.226873
H(11) 0.315554	C(27) -0.178754
H(12) 0.323632	H(28) 0.287995
H(13) 0.280956	H(29) 0.302572
H(14) 0.292404	H(30) 0.295984
C(15) -0.085644	H(31) 0.291983
C(16) -0.219934	

Table 11. Mulliken charges for Quinolinium